

Improving therapeutic approaches for the treatment of Non-small Cell Lung Cancer using an *ex-vivo* explant culture system

Thesis submitted for the degree of
Doctor of Philosophy
At the University of Leicester

By

Ellie Karekla (BSc. Hons. University of Leicester)

Department of Biochemistry

University of Leicester

2014

ABSTRACT

Improving therapeutic approaches for the treatment of Non-small Cell Lung Cancer using an *ex-vivo* explant culture system

Ellie Karekla

Lung Cancer is the leading cause of cancer death worldwide in both males and females. Non-small cell lung cancer (NSCLC) accounts for ~80-85% of lung cancers. NSCLC is a very heterogeneous disease, both genetically and histologically, and there is an increasing list of mutations and copy number alterations in cancer associated genes. Several drugs that could potentially improve lung cancer outcomes are in development and some have entered clinical trials. However, the current established preclinical models, particularly animal xenografts, are not always predictive of patient outcome and there has been a large attrition of clinical candidate drugs at the Phase III stage. The aim of this project was to establish a primary NSCLC explant culture system with the view to developing a better platform to test the efficacy of existing drugs as well as novel drug combinations.

The tissue architecture and tumour heterogeneity of individual NSCLC patients can be examined in an *ex-vivo* NSCLC explant culture system which maintains viability and proliferation in a short period of 24 hours + recovery (16-20 hours). Even though there is a moderate effect of cultivation, the *ex-vivo* NSCLC explant culture system can be used for assessing *in situ* drug responses over short periods. Responses of explants were assessed after treatment with cisplatin, MEK and PI3K inhibitors singly and in combination and TRAIL and ABT-737 singly and in combination in the presence or absence of cisplatin. This model points towards being more predictive of patient outcome in clinical studies than *in vitro* studies or animal models. The data show that the explant system has the potential to improve on current preclinical models for lung cancer or other solid cancers and help the drug development process achieve greater successes in the clinic. The model could provide a platform for personalising treatment to each patient and for identifying effective biomarkers for drug responses.

ACKNOWLEDGEMENTS

First and foremost, I would like to express my gratitude to my supervisors Prof Catrin Pritchard, Dr Howard Pringle and Prof Marion MacFarlane for their continued help, support and encouragement throughout the past four years.

I would especially like to thank Will Monteiro and Hilary Mashal for collecting the samples at Glenfield and putting up with my everyday phonecalls and emails asking about the samples.

I would also like to thank Angie, Linda and Janine for cutting thousands of slides for me during this project and for all their help and encouragement.

I have been running around between three different buildings during the span of this project and there are so many people that helped me along the way that I can't begin to thank them all.

To my friends Katerina, Maggie, Pooyeh, Ioanna, Stelios, Peter, Jo and Emma thank you for your continued support and friendship.

To my amazing boyfriend, Sam, I would like to say thank you for all your love and support, understanding and affection through all this time, especially at the end. I love you so much.

Finally, I am grateful to my parents for putting up with all my stress and always being a phonecall away whenever I needed them. I couldn't do it without you.

I would like to dedicate the thesis to my grandmother Ellie who I miss so much.

Table of Contents

Abstract	1
Acknowledgements	2
Abbreviations	8
List of Figures	14
List of Tables	19
1. Introduction	20
1.1 Lung Cancer	20
1.1.1 Incidence, Mortality and Survival Rates	20
1.1.2 Risk Factors	21
1.1.3 Types of Lung Cancer	22
1.1.4 Lung Cancer Diagnosis and Staging	24
1.1.5 Treatment of NSCLC	26
1.2 Genetics, Oncogenic Pathways and Targeted Treatments of NSCLC	27
1.2.1 Cancer is a genetic disease	27
1.2.2 NSCLC's genomic complexity	29
1.2.3 EGFR and Targeted Therapies	31
1.2.4 EML4-ALK and Targeted Therapies	33
1.2.5 RAS/RAF/MEK/ERK Pathway and Targeted Therapies	34
1.2.5.1 KRAS	34
1.2.5.2 BRAF	37
1.2.5.3 MEK	38
1.2.6 PI3K/AKT/mTOR Pathway and Targeted Therapies	40
1.2.6.1 PIK3CA	40
1.2.6.2 AKT	44
1.2.6.3 PTEN	45

1.2.6.4 MTOR	45
1.4 Cell Death Pathways	46
1.4.1 Caspases Are Central Executioners of Apoptosis	46
1.4.2 The Extrinsic Apoptotic Pathway	47
1.4.3 The Intrinsic Apoptotic Pathway	49
1.4.4 Targeting TRAIL	50
1.4.5 BCL-2 Inhibitors	51
1.5 Preclinical Models	52
1.5.1 Cell Lines	52
1.5.2 Mouse Models	53
1.5.3 3D culture models of human tumours	55
1.6 Aims and Objectives	57
2. Materials And Methods	59
2.1 Ex-vivo Explant Culture Model	59
2.1.1 Collection of Tissue	59
2.1.2 Processing of the tissue	59
2.1.3 Ex-vivo Explant Cultures	60
2.1.3.1 Tissue processing and treatment	60
2.1.3.2 Fixation and Embedding	63
2.1.3.3 Immunohistochemical staining	63
2.1.4 Analysis of Stained Sections	65
2.1.5 Representations of the Data	68
2.2 DNA Isolation and Genotyping	72
2.2.1 Extraction of genomic DNA from fresh tissue or cell lines	72
2.2.2 Extraction of genomic DNA from FFPE tissues	72
2.2.3 Quantification of DNA	73
2.2.4 Oligonucleotide primers and probes for mutation analysis	73
2.2.5 Quantitative PCR (qPCR)	76

2.3 Statistical Analysis	77
3. Patients' Demographics	78
3.1. Introduction	78
3.2. Results	78
3.2.1 Demographics	78
3.2.2 Smoking History	78
3.2.3 Histology	80
3.2.4 Mutation Analysis	82
3.3 Discussion	86
4. Development of An Explant Culture System For NSCLC Samples	88
4.1 Introduction	88
4.2 Aims and Objectives	88
4.3 Results	89
4.3.1 Staining	89
4.3.2 Analysis	91
4.3.3 Intrinsic rates of proliferation and apoptosis in ex-vivo explant cultures	93
4.3.4 Tumour Area Differences	96
4.3.5 Culture conditions	96
4.3.5.1 Example of low intrinsic proliferation case: LT33 adenocarcinoma	97
4.3.5.2 Example high intrinsic proliferation case: LT31 squamous	103
4.3.5.3 Proliferation of ex-vivo explant cultures is decreasing at increasing culture time	109
4.3.5.4 Cell Death of ex-vivo explant cultures is increasing at increasing culture time	110
4.3.5.5 The effect of varying concentrations of FCS in ex-vivo explant cultures	113
4.3.6. Comparison across explants from one tumour	120
4.3.7 Normal Lung Ex-vivo explant culture	121
4.4 Discussion	122

5. Testing The Response OF EX-vivo NSCLC explants To Cisplatin	127
5.1 Introduction	127
5.1.1 Cisplatin: Mode of action	127
5.2 Aims and objectives	128
5.3 Results	128
5.3.1 Dose responses to Cisplatin in 10 samples	128
5.3.1.1 Cisplatin sensitive example case	128
5.3.1.2 Cisplatin resistant example case	131
5.3.1.3 Summary of dose responses to cisplatin in 10 samples	134
5.3.2 Responses of ex-vivo explant cultures to 50 μ M of Cisplatin only	139
5.3.2.1 Correlation with clinical outcomes	142
5.3.3 Characterisation of samples by P53 expression status	143
5.3.3.1 Correlation with p21/ ^{CIP1}	146
5.3.3.2 Correlation of cisplatin response to p53 expression status	148
5.3.4 LA-ICP-MS element distribution mapping of Pt-treated explants	151
5.4 Discussion	153
6. Assessment of Responses to new agents: targeting mapk and pi3k signalling pathways	158
6.1 Introduction	158
6.2 Aims and Objectives	160
6.3 Results	160
6.3.1 Targeting PI3K	161
6.3.1.1 Example <i>PIK3CA</i> mutant case treated with LY294002	161
6.3.1.2 Dose responses to LY294002	166
6.3.1.3 Dose responses to GDC-0941	168
6.3.2 Targeting MEK	170
6.3.2.1 Example <i>PIK3CA</i> mutant case treated with PD184352	170

6.3.2.2 Dose responses to PD184352 _____	173
6.3.2.3 Dose responses to UO126 _____	175
6.3.3. Inhibiting PI3K and MEK simultaneously _____	176
6.3.3.1 Example PIK3CA mutant case treated with combinations of LY294002 and PD184352 _____	176
6.3.3.2 Dose responses to LY294002 in combination with PD184352 _____	179
6.3.3.3 Dose responses to GDC-0941 in combination with PD184352 _____	181
6.4 Discussion _____	183
7. Assessment of Responses to new agents: targeting non-oncogene addicted Cell Death pathways _____	187
7.1 Introduction _____	187
7.2 Aims and Objectives _____	188
7.3 Results _____	188
7.3.1 TRAIL responses in 12 samples _____	188
7.3.2 TRAIL responses in combination with cisplatin in 12 samples _____	190
7.3.4 Dose responses to ABT-737 in 10 samples _____	192
7.3.5 Dose responses to ABT-737 in combination with TRAIL in 10 samples _____	194
7.3.7 Dose responses to ABT-737 in combination with cisplatin in 4 samples _____	196
7.4 Discussion _____	198
8. Summary and Conclusions _____	202
Appendix _____	206
References _____	224

ABBREVIATIONS

A	Adenine
ABCB5	ATP-binding cassette sub-family B member 5
AC	Atypical Carcinoid
ADC	Adenocarcinoma
AKT	v-akt murine thymoma viral oncogene homolog
ALK	Anaplastic lymphoma kinase
APAF1	Apoptosis Protease Activating Factor-1
APC	Adenomatous polyposis coli
ARID1A	AT rich interactive domain 1A
ATM	Ataxia telangiectasia mutated
ATP	Adenosine triphosphate
BH	Bcl-2 homology domain
BRD3	Bromodomain containing 3
BSA	Bovine Serum Albumin
C	Cytosine
CBL	Casitas B-lineage Lymphoma
CDKN2A	Cyclin-dependent kinase inhibitor 2A
cFLIP	Cellular fllice-like inhibitory protein
CFTR	Cystic fibrosis transmembrane conductance regulator
CI	Confidence Intervals
c-KIT	v-kit Hardy-Zuckerman 4 feline sarcoma viral oncogene homolog
COSMIC	Catalogue of Somatic Mutations in Cancer-Sanger
COX2	Cyclooxygenase-2
CREBBP	CREB binding protein
CT	Computed Tomography
CTNNB1	Catenin (cadherin-associated protein), beta 1
DAB	3,3' – diaminobenzidine
DACH1	Dachshund family transcription factor 1

DcR	Decoy Receptor
DED	Death effector domain
DISC	Death-inducing signalling complex
DMEM	Dulbecco's modified Eagle's medium
DMF	Dimethylformamide
DMSO	Dimethyl sulfoxide
DNA	Deoxyribonucleic acid
DPX	with Xylene but free of carcinogenic Dibutyl phthalate
EDTA	Ethylenediaminetetraacetic acid
EGFR	Epidermal growth factor receptor
EML4	Echinoderm microtubule associated protein like
EP300	E1A binding protein p300
EPHA3	EPH receptor A3
EPHA7	Ephrin type-A receptor 7
ERBB4	v-erb-b2 avian erythroblastic leukemia viral oncogene homolog 4
ERK	Extracellular-signal-regulated kinase
FADD	Fas-associated protein with death domain
FBXW7	F-box/WD repeat-containing protein 7
FCS	Foetal Calf Serum
FDG	Fluoro-deoxy-glucose
FFPE	Formalin fixed paraffin embedded
FGFR4	Fibroblast growth factor receptor 4
FLT-3	Fms-related tyrosine kinase 3
GDC	GDC-0941
GDP	Guanosine diphosphate
GEMMs	Genetically Engineered Mouse Models
GOPC	Golgi-associated PDZ and coiled-coil motif-containing protein
GPCR	G protein-coupled receptors
Grb2	GTP-exchange complex growth factor receptor bound2
GTP	Guanosine triphosphate

H&E	Haematoxylin and Eosin
HBSS	Hank's Balanced Salt Solution
HCBS	Histology facility of the Core Biotechnology Services
HDAC	Histone deacetylase
HDRA	Histoculture drug response assay
HLA-A	Human leukocyte antigen A
IALT	International Adjuvant Lung Cancer Trial
IAPs	Inhibitors of Apoptosis
IARC	International Agency for Research on Cancer
IASLC	International Association for the study of Lung Cancer
IC50	Half maximal inhibitory concentration
ICGC	International Cancer Genome Consortium
IDC	Invasive Ductal Carcinoma
IHC	Immunohistochemistry
IMS	Industrial Methylated Spirit
KDR	Kinase insert domain receptor
KEAP1	Kelch-like ECH-associated protein 1
KRAS	Kirsten rat sarcoma viral oncogene homolog
LA-ICP-MS	Laser Ablation Inductively Coupled Plasma Mass Spectrometry
LY	LY294002
MAPK	Mitogen-activated protein kinase
MCTS	Multicellular tumour spheroids
MEK	Mitogen-activated protein kinase kinase
MGB	Minor groove binder
MLL	Myeloid/Lymphoid leukemia gene
MOMP	Mitochondrial outer membrane permeabilization
Mt	Mutant
mTOR	The mammalian target of rapamycin
MTT	3-(6)-2, 5-diphenyl tetrazolium bromide
NaCl	Sodium Chloride
NF1	Neurofibromin 1

NFE2L2	Nuclear factor (erythroid-derived 2)-like 2
NOD/SCID	Non-obese diabetic/severe combined immunodeficient
NOTCH1	Notch homolog 1, translocation-associated
NRAS	Neuroblastoma RAS viral (v-ras) oncogene homolog
NSCLC	Non-Small Cell Lung Cancer
NTC	No template control
OPG	Osteoprotegerin
OS	Overall Survival
PAK3	p21 protein (Cdc42/Rac)-activated kinase 3
P-AKT	Phospho-AKT
PARP	Poly ADP ribose polymerase
PBS	Phosphate Buffered Saline
PCR	Polymerase chain reaction
PCB	Paclitaxel, carboplatin, and bevacizumab
PD	PD184352
PDGFR	Platelet-derived growth factor receptor
PDK1	Phosphatidylinositol- dependent kinase 1
PDX	Patient derived xenograft
P-ERK	Phospho-ERK
PET-CT	Positron emission tomography- computed tomography
PFA	Paraformaldehyde
PFS	Progression Free Survival
PH	Pleckstrin homology domain
PI	Proliferation Index
PI3K	Phosphatidylinositol 3- Kinase
PIK3CA	Phosphatidylinositol-4,5-bisphosphate 3-kinase, catalytic subunit alpha
PIP3	Phosphatidylinositol (3,4,5) triphosphate
PLK1	Polo-like kinase
PPP2R1A	Protein phosphatase 2, regulatory subunit A, alpha
Pt	Platinum

PTEN	Phosphatase and Tensin homolog deleted on chromosome 10
qPCR	Quantitative real-time PCR
RB1	Retinoblastoma 1
RBM10	RNA binding motif protein 10
RELN	Reelin
RhTrail	Human Recombinant TRAIL
RNA	Ribonucleic Acid
RR	Response rate
RTK	Receptor tyrosine kinase
SABT	Stereotactic ablative body radiotherapy
SCC	Squamous Cell Carcinoma
SCLC	Small Cell Lung Cancer
SDS	Sodium dodecyl sulfate
SETD2	SET domain containing 2
SH2	Src homology 2 domain
SLIT2	Slit homolog 2 protein
SMAD4	SMAD family member 4
SMARCA4	SWI/SNF Related, Matrix Associated, Actin Dependent Regulator of Chromatin, Subfamily A, Member 4
SOS	Son of sevenless
STK11	Serine/Threonine Kinase 11
STK33	Serine/Threonine Kinase 33
T	Thymidine
TBK1	TANK-binding kinase 1
TBS	Tris-buffered saline
TNFR-I	Tumour necrosis factor receptor I
TNM system	Tumour Node Metastasis system
TP53	Tumour protein p53
TRAIL	TNF-related apoptosis-inducing ligand
TRAIL-R	TRAIL receptor
U2AF1	U2 Small Nuclear RNA Auxiliary Factor 1

UHL	University Hospitals of Leicester
VEGF	Vascular endothelial growth factor
WHO	World Health Organisation
WT	Wild-type

LIST OF FIGURES

Figure 1.1. The 20 most common causes of cancer deaths in the UK in 2011..	21
Figure 1.2. Histologic appearance of the most common lung cancer types.....	23
Figure 1.3. The most frequent genetic aberrations in adenocarcinoma and squamous cell carcinoma of the lung.....	31
Figure 1.4. Kaplan–Meier Curves for Progression-free Survival after Gefinitib treatment.....	32
Figure 1.5. The MAPK pathway and associated inhibitors.....	36
Figure 1.6. The PI3K Pathway and inhibitors for pathway components.....	43
Figure 1.7. Extrinsic and Intrinsic Apoptotic Pathway.....	48
Figure 2.1. Overview of the <i>ex-vivo</i> explant culture model.....	62
Figure 2.2. Analysis of stained sections.....	67
Figure 2.3. Separate graphs - 3 different graphs.....	68
Figure 2.4. Combined graph.....	69
Figure 2.5. Pooled cases Graph - two different graphs.....	70
Figure 2.6. Tumour area graph.....	71
Figure 2.7. The Taqman Principle.....	74
Figure 2.8. PCR Conditions.....	76
Figure 3.1. Sex ratio of patients, age group distribution and smoking history...	80
Figure 3.2. Histological categories of patients.....	81
Figure 3.3. Adenocarcinoma subcategories.....	81
Figure 3.4. Graphical representation of qPCR mutation analysis results.....	83
Figure 3.5. Mutation analysis in patient cohort (57/60).....	84
Figure 4.1. MNF116 stained sample example image.....	89
Figure 4.2. Image of Ki67 staining to assess proliferation.....	90
Figure 4.3. Image of cleaved PARP staining to assess apoptosis.....	90
Figure 4.4. Comparison of Immunoratio vs manual counting with Bland-Altman.....	91

Figure 4.5. 10x photomicrographs are not significantly different than 20x.....	92
Figure 4.6. Intrinsic rates of combined cell death, proliferation and separate necrosis of all the usable ex-vivo explant cultures set up (21).....	94
Figure 4.7. Intrinsic Rates of Ki67 staining across histologies.....	95
Figure 4.8. Intrinsic Rates of cell death across histologies.....	95
Figure 4.9. Proliferation and Cell Death of LT33 in varying FCS concentrations through culture time.....	98
Figure 4.10. Proliferation and Cell Death of LT31 in varying FCS concentrations through culture time.....	104
Figure 4.11. % Ki67 of tumour area of 5 NSCLC ex-vivo explants through culture time.....	109
Figure 4.12. The 5 NSCLC samples from figure 4.11 plotted together.....	110
Figure 4.13. % Cell Death of tumour area of 5 NSCLC ex-vivo explants through culture time.....	111
Figure 4.14. The 5 NSCLC samples from figure 4.13 plotted together.....	112
Figure 4.15. % Cell Death of tumour area of 5 NSCLC ex-vivo explant cultures in varying FCS concentrations at 24 + recovery.....	114
Figure 4.16. The 5 NSCLC samples from figure 4.15 plotted together.....	115
Figure 4.17. % Ki67 of tumour area of 5 NSCLC ex-vivo explant cultures in varying FCS concentrations at 24 + recovery.....	116
Figure 4.18. The 5 NSCLC samples from figure 4.17 plotted together.....	117
Figure 4.19. Box and whiskers plot of %Cell Death of tumour area in the uncultured tumour compared to 24 + recovery in 1%FCS media. (N=15).....	118
Figure 4.20. Box and whiskers plot of % Ki67 of tumour area in the uncultured tumour compared to 24+recovery in culture in 1%FCS media. (N=15).....	119
Figure 4.21.% Cell death and % proliferation per explants in an example case.....	120
Figure 4.22. Representative Images of H&E stain of an adjacent normal lung sample.....	121
Figure 5.1. Representative images of corresponding areas in H&E staining, Ki67 staining (Proliferation marker) and cleaved PARP staining (apoptosis marker) of LT92.....	129
Figure 5.2. LT92 dose response to cisplatin treatment.....	130

Figure 5.3. Representative images of corresponding areas in H&E staining, MNF116 (epithelial cell marker), Ki67 staining (Proliferation marker) and cleaved PARP staining (apoptosis marker) of LT33.....	132
Figure 5.4. LT33 dose response to cisplatin treatment.....	133
Figure 5.5. Fold Cell Death relative to control of 10 NSCLC <i>ex-vivo</i> explant cultures treated with doses of cisplatin.....	136
Figure 5.6. Fold Proliferation relative to control of 10 NSCLC <i>ex-vivo</i> explant cultures treated with doses of cisplatin.....	138
Figure 5.7. Induction of cell death relative to the carrier control upon 50 μ M cisplatin treatment in 19 NSCLC <i>ex-vivo</i> explants.....	141
Figure 5.8. Reduction of proliferation relative to the carrier control upon 50 μ M cisplatin treatment in 19 NSCLC <i>ex-vivo</i> explants.....	142
Figure 5.9. A p53 wild-type example (LT33) upon cisplatin doses.....	144
Figure 5.10. Examples of samples expressing constitutively high p53.....	145
Figure 5.11. Intrinsic Rates of Ki67 staining according to p53 IHC status.....	145
Figure 5.12. p21 ^{CIP1} expression in LT33 upon cisplatin doses.....	147
Figure 5.13. Induction of cell death and reduction of Ki67 score upon 50 μ M cisplatin treatment in 19 NSCLC <i>ex-vivo</i> explants stratified by p53 status.....	148
Figure 5.14. Comparison between IHC-wtp53 and IHC-mtp53 explants to fold responses and raw differences in response to 50 μ M cisplatin.....	150
Figure 5.15. LA-ICP-MS sampling of human lung cancer explant LT31 treated with 10 μ M cisplatin for 24h.....	152
Figure 6.1. RAS/RAF/MEK/ERK pathway activity can be inhibited using MEK inhibitors UO126 or PD184352. PI3K/AKT/mTOR pathway activity can be inhibited using PI3K inhibitors, LY294002 or GDC-0941.....	159
Figure 6.2. Examples of two cases demonstrating high levels of p-ERK (A) and p-AKT (B) respectively.....	161
Figure 6.3. Representative images of corresponding areas of LT16 (<i>PIK3CA</i> mutation positive) in H&E staining, Ki67 staining (proliferation marker) and cleaved PARP staining (apoptosis marker).....	163
Figure 6.4. Dose response of LT16 (<i>PIK3CA</i> mutation positive) to LY294002.....	164
Figure 6.5. P-Akt staining of LT16 (<i>PIK3CA</i> mutation positive) in increasing concentrations of LY294002.....	165
Figure 6.6. Fold cell death dose responses to LY294002 relative to control...	167

Figure 6.7. Fold proliferation dose responses to LY294002 relative to the carrier control.....	168
Figure 6.8. Fold cell death dose responses to GDC-0941 relative to control..	169
Figure 6.9. Fold proliferation dose responses to GDC-0941 relative to control.....	170
Figure 6.10. Representative images of corresponding areas of LT16 (<i>PIK3CA</i> mutation positive) in H&E staining, Ki67 staining (proliferation marker) and cleaved PARP staining (apoptosis marker).....	171
Figure 6.11. Dose response of LT16 (<i>PIK3CA</i> mutation positive) to PD184352.....	172
Figure 6.12. P-ERK staining of LT16 (<i>PIK3CA</i> mutation positive) in increasing concentrations of PD184352.....	173
Figure 6.13. Fold cell death dose responses to PD184352 relative to control.....	174
Figure 6.14. Fold proliferation dose responses to PD184352 relative to control.....	175
Figure 6.15. Fold cell death and fold proliferation to dose responses to UO126 relative to control.....	176
Figure 6.16. Representative images of corresponding areas of LT16 (<i>PIK3CA</i> mutation positive) in H&E staining, Ki67 staining (proliferation marker) and cleaved PARP staining (apoptosis marker).....	177
Figure 6.17. Dose responses of LT16 (<i>PIK3CA</i> mutation positive) to LY294002 in combination with PD184352.....	178
Figure 6.18. Fold cell death and proliferation dose responses to LY294002 in combination with PD184352 relative to control.....	180
Figure 6.19. Fold cell death and proliferation dose responses to GDC-0941 in combination with PD184352 relative to control.....	182
Figure 7.1. Fold Cell Death responses to 1 µg/ml of TRAIL relative to the carrier control.....	189
Figure 7.2. Fold Proliferation responses to 1 µg/ml of TRAIL relative to the carrier control.....	190
Figure 7.3. Fold Cell Death responses to 1 µg/ml of TRAIL, 50µM Cisplatin and combination of the two relative to the carrier control.....	191
Figure 7.4. Fold Proliferation responses to 1 µg/ml of TRAIL, 50µM Cisplatin and combination of the two relative to the carrier control.....	192

Figure 7.5. Fold Cell Death responses to increasing doses of ABT-737 relative to the carrier control.....193

Figure 7.6. Fold Proliferation responses to increasing doses of ABT-737 relative to the carrier control.....194

Figure 7.7. Fold Cell Death responses to increasing doses of ABT-737 in combination with TRAIL relative to the carrier control.....195

Figure 7.8. Fold Proliferation responses to increasing doses of ABT-737 in combination with TRAIL relative to the carrier control.....196

Figure 7.9. Fold Cell Death responses to 2 μ M and 10 μ M of ABT-737, 10 μ M cisplatin and combinations relative to the carrier control.....197

Figure 7.10. Fold Proliferation responses to 2 μ M and 10 μ M of ABT-737, 10 μ M cisplatin and combinations relative to the carrier control.....197

LIST OF TABLES

Table 1.1. Summary of the histological classification of Lung Tumours according to the World Health Organisation.....	24
Table 1.2. Stage groups of NSCLC.....	26
Table 2.1. Therapeutic agents used in this study.....	61
Table 2.2. Antibodies used in this study.....	65
Table 2.3. Primers and Probes used in this study.....	75
Table 2.4. Mutation Probes Controls and Annealing Temperature.....	77
Table 3.1 Patients' Characteristics.....	79
Table 3.2 Mutations found in patient cohort.....	85
Table 4.1. %Cell Death and % Ki67 values at 24 hours after recovery for 6 cases cultured in a range of FCS.....	113
Table 5.1. The responses of 10 samples treated with 1 μ M, 10 μ M and 50 μ M of Cisplatin for 24 hours after an initial recovery of 16-20 hours, shown as fold changes compared to each sample's carrier control.....	135
Table 5.2. A summary of information on explants set up from 19 samples and the corresponding patient information.....	140
Table 5.3. Correlation of cisplatin response to p53 expression status.....	149

1. INTRODUCTION

1.1 Lung Cancer

1.1.1 Incidence, Mortality and Survival Rates

Lung cancer is the second most commonly diagnosed cancer in the UK after breast cancer in women and prostate cancer in men. As stated by the Cancer Research UK website, around 43500 people are diagnosed every year with lung cancer in the UK. It is also the leading cause of cancer death in the UK (Figure 1.1) and worldwide. In fact, according to GLOBOCAN, a worldwide database of cancer incidence and mortality rates, it is estimated that ~1.59 million people died from lung cancer in 2012 in the world (IARC). The World Health Organization (WHO) estimates that lung cancer deaths worldwide will continue to escalate, mainly due to an increase in global tobacco use, especially in Asia (Dela Cruz *et al.*, 2011).

Lung cancer also has one of the worst survival rates with the overall five-year survival rate being dismal at ~10%. The major reasons for this low survival rate is the fact that about two thirds of the patients are diagnosed at late stages as a consequence of the lack of effective screening methods (Herbst & Bunn, 2003).

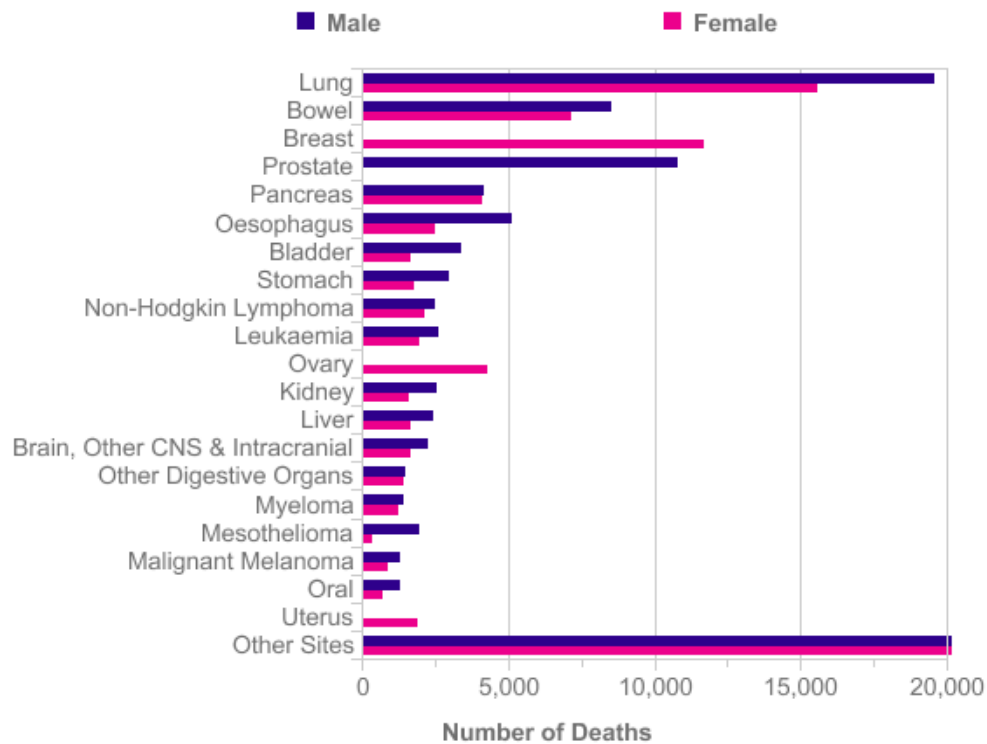


Figure 1.1. The 20 most common causes of cancer deaths in the UK in 2011. Lung cancer is the leading cause of death from cancer in both male and females. Taken from Cancer Research UK website. (<http://www.cancerresearchuk.org/cancer-info/cancerstats/mortality/cancerdeaths/#Twenty>)

1.1.2 Risk Factors

The link with lung cancer and tobacco smoke was established several decades ago (Doll & Hill, 1950). In fact, about 85% of lung cancers are caused by exposure to tobacco smoke carcinogens as reviewed in (Dela Cruz *et al.*, 2011; Hecht, 1999). Consequently lung cancer research was mainly focused on anti-tobacco campaigns and smoking cessation methods. This led to a decrease in the percentage of smokers but still there are about 1 billion smokers around the world which leaves tobacco smoke as the major driver of lung cancer (Hecht, 1999).

However, approximately 10% of lung cancer cases occur in patients who have never smoked. Other environmental factors such as occupational exposure to

agents like asbestos, heavy metals or diesel fumes, exposure to radon gas in our homes (Alberg *et al.*, 2013) and genetic susceptibility have been associated with carcinogenesis in the lungs (Herbst *et al.*, 2008).

1.1.3 Types of Lung Cancer

The two major forms of lung cancer are small-cell lung cancer (SCLC; Figure 1.2-C) which accounts for ~15-20% of the lung cancer cases and is usually a more aggressive disease, and non-small cell lung cancer (NSCLC) which accounts for ~80-85% of the cases and is the subject of this study.

NSCLC can be further divided into three histologically distinct subtypes: squamous cell carcinoma, adenocarcinoma, and large-cell lung cancer. In most countries, adenocarcinoma is the most common subtype of NSCLC with frequencies ranging from 35 to 45% (Walters *et al.*, 2013). However, in the UK squamous cell carcinoma is slightly more common with 27% compared to 25% of adenocarcinomas and 23% of large cell lung cancers (Walters *et al.*, 2013).

Squamous cell carcinoma (Figure 1.2-A) arises from bronchial epithelium and is characterised by keratinization and/or intercellular bridges depending on its differentiation. Squamous cell lung cancer is most commonly a central tumour.

Adenocarcinoma is characterised by glandular differentiation (Figure 1.2-B) or mucin production and it shows various different types of growth patterns such as acinar, papillary, micropapillary, lepidic and solid (Travis *et al.*, 2011). Adenocarcinoma arises most frequently in the periphery of the lungs. Large cell carcinoma (Figure 1.2-D) is a NSCLC that lacks the features of small cell, adenocarcinomas or squamous differentiation. Almost 50% of lung carcinomas show histologic heterogeneity and are comprised of more than one of the major types (Travis *et al.*, 2004). There are also many other different descriptions of histological types of lung cancer (see Table 1.1) but their frequency is low.

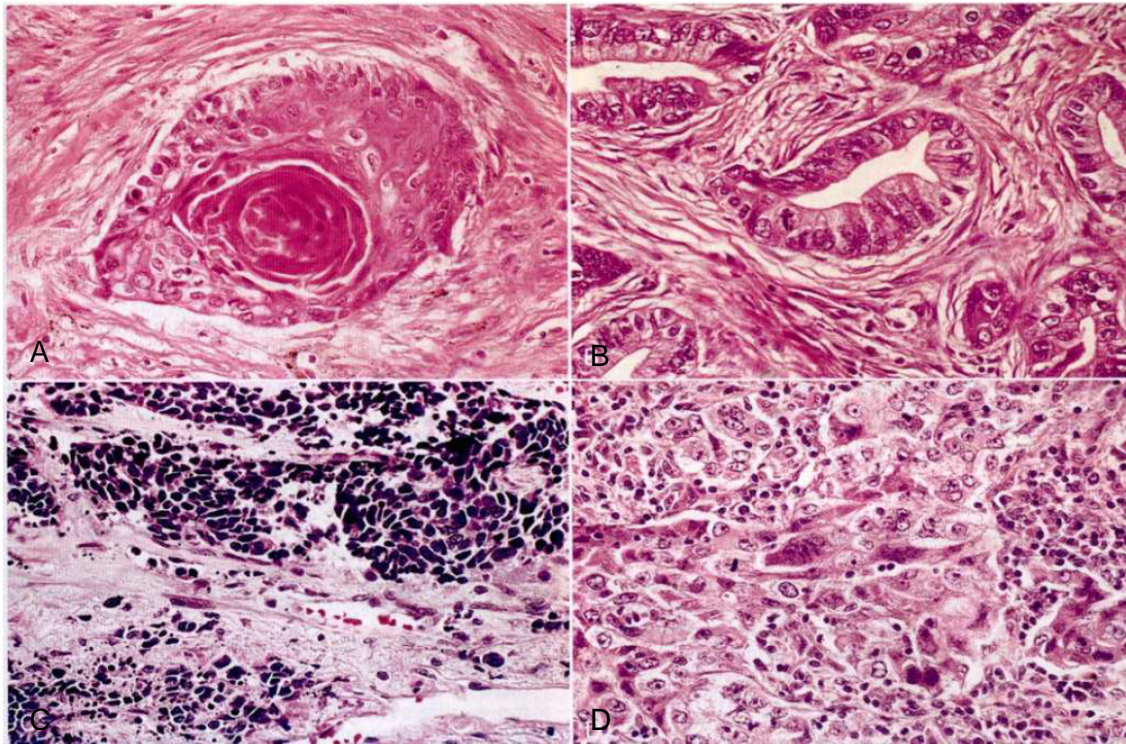


Figure 1.2. Histologic appearance of the most common lung cancer types. A) Well-differentiated squamous cell carcinoma showing keratinization. B) Adenocarcinoma with glandular differentiation. C) Small cell carcinoma with islands of small basophilic cells and necrosis. D) Large cell carcinoma. Taken from Robbins and Cotran pathologic basis of disease 7th Edition (Kumar *et al.*, 2005).

Table 1.1. Summary of the histological classification of Lung Tumours according to the World Health Organisation (WHO) (Travis et al., 2004; Travis et al., 2011).

Histological Classification of Lung Tumours	
Pre-invasive lesions	Squamous carcinoma in situ Atypical adenomatous hyperplasia Diffuse idiopathic pulmonary neuroendocrine cell hyperplasia
Benign epithelial tumours	Papillomas Adenomas
Malignant epithelial tumours	Squamous cell carcinoma Papillary Clear Cell Small cell Basaloid Adenocarcinoma Acinar Papillary Lepidic Micropapillary Solid Invasive mucinous adenocarcinoma Adenosquamous carcinoma Sarcomatoid carcinoma Large cell carcinoma Neuroendocrine Basaloid

1.1.4 Lung Cancer Diagnosis and Staging

Lung cancer symptoms usually do not appear until later stages of the disease and usually include a persistent cough, shortness of breath and bloody sputum. Once a patient is suspected of having lung cancer, there are a number of imaging tests and/or invasive procedures available to aid diagnosis.

Imaging techniques include a simple chest X-ray which usually does not pick up early stage tumours, computed tomography (CT) scanning which can determine tumour size and invasion, MRI and integrated positron emission tomography-CT (PET-CT) which usually uses Fluoro-deoxy-glucose (FDG). FDG is a radioactive glucose analogue and is used to detect cancer cells as these cells

have higher metabolic activity than surrounding normal cells and therefore they uptake FDG which makes it easier to visualise (Tsim *et al.*, 2010).

When the disease is more difficult to see, a number of invasive tests can be performed to confirm diagnosis, such as bronchoscopy, endobronchial ultrasound guided biopsy, CT-guided biopsy or surgical biopsy which can be mediastinoscopy or thoracoscopy.

There is no national lung cancer screening program as yet. Most patients are diagnosed at late stages and early disease is asymptomatic. A recent large screening trial in the US enrolled 50000 high risk patients to undergo lung cancer screening with either 3 annual low-dose spiral CTs or chest X-rays and showed reduced mortality in the CT group which aided early stage diagnosis (National Lung Screening Trial Research Team *et al.*, 2011). However, unfortunately the cost-effectiveness of a lung cancer screening program means it is not applicable as of yet.

An important prognostic factor in lung cancer, as with most cancers is the tumour stage. NSCLC classification is based on the TNM system (**T**umour **N**ode **M**etastasis) which dates back to 1944 and is used for staging the majority of epithelial tumours.

T describes the position and size of the tumour and it can range from T0 to T4.

N is used to describe whether the tumour cells have spread in the lymph nodes and it ranges from N0 to N3 depending on the spread.

M indicates whether the tumour has metastasised elsewhere in the body.

The stages of NSCLC can be classified as seen in Table 1.2 and they provide an important prognostic factor as well as information of which type of treatment would be appropriate for each patient. The TNM classification system was recently updated after the International Association for the study of Lung Cancer (IASLC) established the Lung cancer staging project which collected data on >100,000 patients diagnosed with lung cancer between 1990 and 2000 worldwide (Detterbeck *et al.*, 2009; Detterbeck *et al.*, 2013).

Table 1.2. Stage groups of NSCLC. Redrawn from (Detterbeck et al., 2009; Tsim et al., 2010).

Stage Groups	T	N	M	5-year survival
Ia	T1a,b	N0	M0	50-80%
Ib	T2a	N0	M0	47%
Ila	T1a,b	N1	M0	36%
	T2a	N1	M0	
	T2b	N0	M0	
Ilb	T2b	N1	M0	26%
	T3	N0	M0	
Illa	T1-3	N2	M0	19%
	T3	N1	M0	
	T4	N0,1	M0	
IIlb	T4	N2	M0	7%
	T1-4	N3	M0	
IV	T any	N any	M1a,b	2%

1.1.5 Treatment of NSCLC

According to the stage of the disease when diagnosed, patients can be offered one of the following treatments or combinations of them.

Surgical Treatment: If the patients are in the early stage of the disease (I, II or maximum of IIIa with minimal lymph node spread) and they are fit enough, they can have surgery with intent of complete response. Lobectomy is usually recommended over smaller resections such as wedge resection or segmentectomy (McCloskey *et al.*, 2013). When there is too much involvement, one of the two lungs can be completely resected (pneumonectomy). Patients are offered adjuvant chemotherapy after complete resection to ensure prevention of re-occurrence of the cancer. However, chemotherapy is not indicated in very early stage disease.

Radiotherapy: Patients with early stage (I or II) who are not fit for surgery can undergo stereotactic ablative body radiotherapy (SABR) (McCloskey *et al.*, 2013) where high dose radiation targets the tumour very precisely. Patients with late stage disease can be offered radiotherapy in combination with chemotherapy to treat the disease or to control the disease and alleviate symptoms that affect the quality of life.

Chemotherapy: Chemotherapy for NSCLC is usually cisplatin or carboplatin combined with at least one of the new generation drugs: vinorelbine, gemcitabine, paclitaxel, docetaxel or pemetrexed (Zarogoulidis *et al.*, 2013; Darlison, 2005) if the patient is fit enough to receive combination treatments, otherwise single treatments are considered.

The fact that many cancers are sensitive to chemotherapy drugs such as cisplatin which is a DNA cross-linker, is due to tumour cells already experiencing a high level of DNA damage stress to accommodate their huge mutation overload; therefore by adding an extra level of DNA stress, the cancer cells are unable to cope and this results in death. This phenomenon has been described as non-oncogene addiction (Luo *et al.*, 2009b); it describes the price the tumour cells need to pay for being abnormal and their dependency on stress pathways.

Targeted Therapies: Novel treatments for NSCLC have been mainly focused on EGFR small molecule inhibitors erlotinib/ gefitinib (Sharma *et al.* 2007; Mok *et al.*, 2009; Rosell *et al.* 2012) and crizotinib which targets tumours with ALK rearrangements and showed increased progression free survival amongst patients reviewed (Casaluce *et al.*, 2013; Gridelli *et al.*, 2014). The problem however is that for all of these drugs, resistance eventually develops. (These will be discussed in more detail below: sections 1.2.3 and 1.2.4).

1.2 Genetics, Oncogenic Pathways and Targeted Treatments of NSCLC

1.2.1 Cancer is a genetic disease

Decades of research have revealed that cancer is ultimately a disease resulting from changes occurring in the DNA sequence of the genomes of the cancer cells (Stratton *et al.*, 2009). Normally, cells are tightly regulated and there are many different mechanisms in place to check whether everything is running smoothly. However, damaging genetic changes accumulate as age increases or

as a result of harmful environmental exposures (e.g. smoking), that lead to the eventual uncontrollable growth of cells.

Hanahan and Weinberg in 2000 proposed that there are some generic hallmarks of cancer which include self-sufficiency in growth signals, evasion of growth suppressors and cell death, ability to replicate indefinitely, induction of angiogenesis and eventual tissue evasion and metastasis (Hanahan & Weinberg, 2000). The hallmarks of cancer were updated in 2010 to include avoiding immune destruction, deregulating cellular energetics, tumour promoting inflammation and genome instability and mutation (Hanahan & Weinberg, 2011). These capabilities are mainly acquired after somatic mutations have been developed in the cancer associated genes which include base substitutions, insertions or deletions of segments of DNA, rearrangements or copy number changes. Genes can also be altered by epigenetic mechanisms. The changes mainly occur in genes called oncogenes, which “drive” cancer initiation, maintenance and progression and tumour-suppressor genes which need to be de-activated if the cancer is to progress.

Oncogenes identified in cancer offer a great opportunity for the development of novel therapies since inhibitors that target them could potentially kill tumour cells that are addicted to the action of the specific oncogene (Luo *et al.*, 2009). Therefore by inhibiting the action of the oncogene-product, the cancer cell becomes vulnerable and dies.

The International Cancer Genome Consortium (ICGC) was launched in 2010 to coordinate large-scale cancer genome studies across the most common types of cancers to reveal the range of oncogenic mutations present in cancers and aid in the development of new cancer therapeutics (International Cancer Genome Consortium *et al.*, 2010; Stratton *et al.*, 2009; Bignell *et al.*, 2010).

1.2.2 NSCLC's genomic complexity

NSCLC is a complex group of diseases highlighted by the range of the evident histologic subtypes as discussed in 1.1.3. To add to this complexity, NSCLC is one of the most genomically diverse of all cancers, making it even more intricate to deal with. An excessive number of genes have been linked with NSCLC, suggesting personalised medicine would be the answer. In fact, NSCLC treatment has become the prototype for genetically tailored targeted therapy (Buettner *et al.*, 2013). This genetic complexity of NSCLC is also highlighted by the number of review articles published in the last few years discussing oncogenes involved and targeted therapies available (Heist *et al.*, 2012; Sanders & Albitar, 2010; Pao & Girard, 2011; Black & Morris, 2012; Raparia *et al.*, 2013; Tiwari *et al.*, 2011; Tiwari *et al.*, 2012; Pal *et al.*, 2010; Oxnard *et al.*, 2013; Reungwetwattana *et al.*, 2012; Bronte *et al.*, 2010; Sato *et al.*, 2007; Shames & Wistuba, 2014; Li *et al.*, 2013; Brandao *et al.*, 2012; Buettner *et al.*, 2013; Sharma *et al.*, 2007; Johnson *et al.*, 2012; Drilon *et al.*, 2012; Heist & Engelman, 2012; Herbst *et al.*, 2008).

Genomic studies in NSCLC have mainly been focused on the adenocarcinoma sub-type. The first large collaborative cancer genome study for lung adenocarcinoma was performed by Weir *et al.* where they analysed 371 tumours using dense single nucleotide polymorphism arrays and identified about 57 significantly recurrent events (Weir *et al.*, 2007). Amongst them, large-scale copy-number gain or loss of whole chromosome arms, 24 amplifications and 7 homozygous deletions were detected, emphasising the complexity of NSCLC.

In 2008 another large collaborative study sequenced the DNA of 623 genes known to be involved in cancer across 188 human lung adenocarcinomas and identified 26 genes that are mutated at high frequencies, suggesting their involvement in lung adenocarcinoma carcinogenesis (Ding *et al.*, 2008). Among those genes were: *KRAS*, *EGFR*, *TP53*, *STK11*, *NF1*, *APC*, *EPHA3*, *CDKN2A*, *ERBB4*, *KDR*, *FGFR4*, *RB1*, *PAK3*, *ATM* and *NRAS*.

An additional large study sequenced the genome of matched adenocarcinoma/normal DNA pairs from 183 patients (Imielinski *et al.*, 2012).

This was in addition to the already well-studied adenocarcinoma genome. Here a mean mutation rate of 12 events per megabase was identified and the previously reported genes were identified as mutated along with novel ones (Imielinski *et al.*, 2012). They identified the 25 most significantly mutated genes in the study as: *TP53*, *KRAS*, *EGFR*, *STK11*, *KEAP1*, *ATM*, *NF1*, *SMARCA4*, *ARID1A*, *BRAF*, *RBM10*, *SETD2*, *PIK3CA*, *CBL*, *FBXW7*, *PPP2R1A*, *RB1*, *SMAD4*, *CTNNB1*, *U2AF1*, *KIAA0427*, *PTEN*, *BRD3*, *FGFR3* and *GOPC* (Imielinski *et al.*, 2012). Copy number alterations were also identified in another 13 genes some of them included in the mutation set.

In a different study the genomic landscape of NSCLC in smokers and never smokers in 17 patients with various histologies was reported. They showed that smokers with lung cancer had more than 10-fold higher point mutations than never-smokers. They also identify some novel lung cancer genes, including *DACH1*, *CFTR*, *RELN* and *ABCB5*, on top of the previously implicated lung cancer genes such as *ALK*, *EGFR*, *KRAS*, *STK11* (Govindan *et al.*, 2012).

The first comprehensive genomic characterization of squamous lung cancers was published by the cancer genome atlas research network (Cancer Genome Atlas Research Network *et al.*, 2012). They used 178 squamous lung cancer samples and whole genome sequencing and found recurrent important mutations in 11 genes: *TP53* in 81% of the samples, *CDKN2A* in 15%, *PTEN* in 8%, *PIK3CA* in 16%, *KEAP1*, *MLL2*, *HLA-A*, *NFE2L2*, *NOTCH1* and *RB1* (Cancer Genome Atlas Research Network *et al.*, 2012).

Genomic analyses of SCLC, which is more strongly associated with smoking, identified an extremely high mutation rate of 7.4 ± 1 protein-changing mutations per million base pairs (Peifer *et al.*, 2012). In this study, recurrent mutations were identified in *TP53*, *RB1*, *CREBBP*, *EP300*, *MLL*, *PTEN*, *SLIT2* and *EPHA7* (Peifer *et al.*, 2012).

We can conclude that NSCLC is very heterogeneous in respect to histology and genomic complexity. In an effort to simplify things, most of the focus here will be placed on common driver oncogenic mutations identified in NSCLC, since they are the ones that have “druggable” targets. Figure 1.3 shows a summary of the

most frequent mutations present in adenocarcinomas and squamous cell carcinomas of the lung.

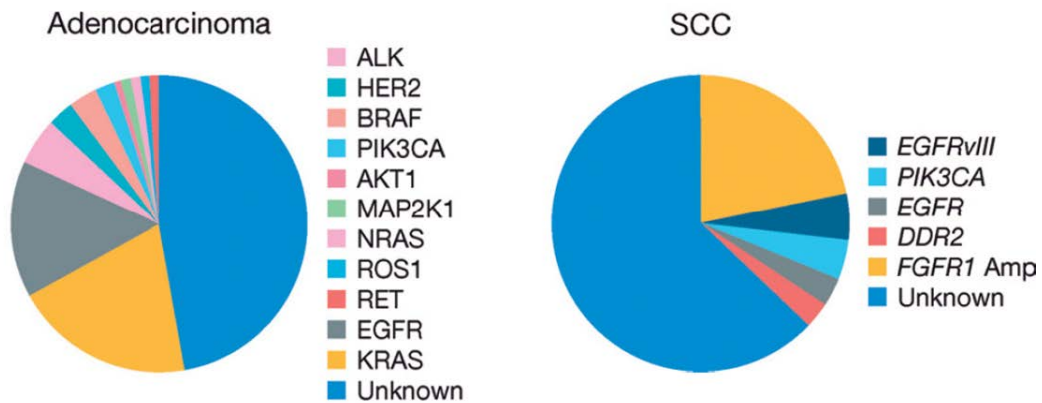


Figure 1.3. The most frequent genetic aberrations in adenocarcinoma and squamous cell carcinoma of the lung. Taken from (Li et al., 2013).

1.2.3 EGFR and Targeted Therapies

The epidermal growth factor receptor (EGFR) is a receptor tyrosine kinase (RTK) whose activation leads to the induction of multiple signal transduction pathways, such as the Ras-MAPK signal pathway and the PI3K/AKT pathway which lead to cellular proliferation. Activated EGFR also leads to induction of angiogenesis by increasing VEGF expression and tissue invasion and metastasis by interacting with components of the integrin pathway (Herbst & Bunn, 2003).

EGFR activating mutations in lung cancer are usually exon 19 deletions or the L858R point mutation (Rosell *et al.*, 2009). *EGFR* mutations are seen in ~10% of lung cancer patients from Northern America and Western Europe and in ~30-50% in patients of East Asian descent (Sharma *et al.*, 2007). The mutation correlates with the adenocarcinoma histology, never-smokers and females, usually of Asian origin (Yokoyama *et al.*, 2006; Rosell *et al.*, 2009).

EGFR protein overexpression which can be a result of high copy number or gene amplification is very common in NSCLC (>60%; Hirsch *et al.*, 2003). Studies on the prognostic value of EGFR amplification have shown conflicting results reviewed in (Kotsakis & Georgoulas, 2010). In general, EGFR amplification has not been predictive of response to EGFR inhibitors.

Gefitinib and erlotinib are the first generation of EGFR tyrosine kinase inhibitors that target the intracellular domain of EGFR, thereby blocking the downstream signalling of the receptor. They are orally bioavailable synthetic anilinoquinazoles (Reungwetwattana *et al.*, 2012). Clinical trial data show that gefitinib (Figure 1.4; Mok *et al.*, 2009) and erlotinib (Rosell *et al.*, 2012) improve the median survival rate of patients carrying an EGFR activating mutation by up to 12 months, with gefitinib showing better results (Pal *et al.*, 2010). Both of the drugs are approved for the treatment of advanced NSCLC. However, relapse eventually occurs and this is usually because drug resistance develops. The main reason for this is the secondary gatekeeper *EGFR* mutation T790M which confers resistance to EGFR inhibitors erlotinib and gefitinib (Engelman & Janne, 2008). Novel irreversible EGFR inhibitors that target T790M are identified and have been shown to be effective in murine lung cancer models (Zhou *et al.*, 2009).

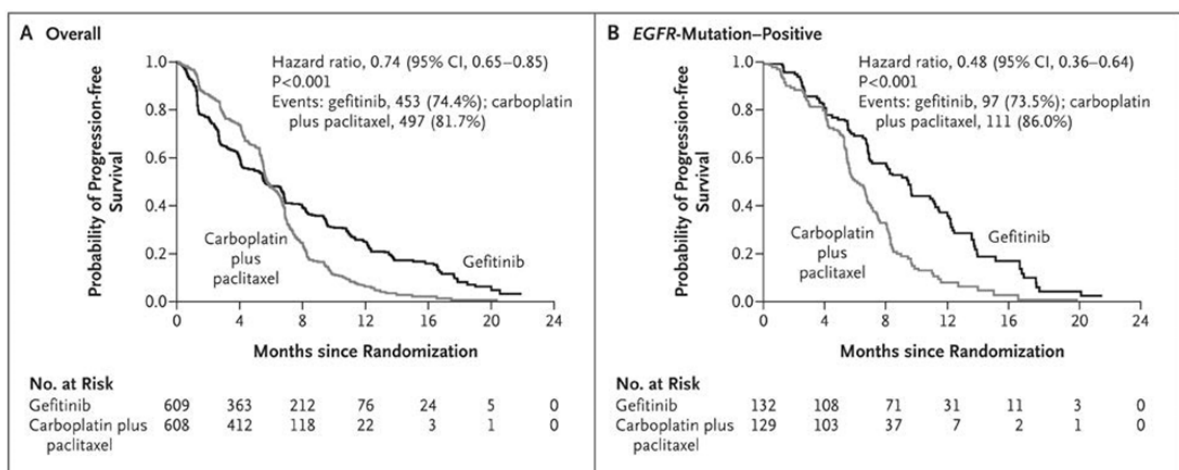


Figure 1.4. Kaplan–Meier Curves for Progression-free Survival after Gefitinib treatment. Kaplan–Meier curves for progression-free survival are shown for the overall population (A) and patients who were positive for the EGFR mutation (B). Taken from (Mok *et al.*, 2009).

1.2.4 EML4-ALK and Targeted Therapies

The translocation of two genes on the short arm of chromosome 2, the kinase domain of anaplastic lymphoma kinase (ALK) and the terminal portion of the echinoderm microtubule associated protein-like (EML4) was discovered in 2007 in Japanese patients with NSCLC (Soda *et al.*, 2007). Since then, EML4-ALK fusions have been observed in about 3-7% of NSCLC (Pao & Girard, 2011). This fusion gene causes irregular activation of oncogenic pathways such as MAP-Kinase and PI3-K pathways which lead to increased proliferation and inhibition of apoptosis. EML4-ALK translocations associate with the adenocarcinoma histology (predominantly of acinar type), light or no smoking history and a younger age (Bronte *et al.*, 2010).

Another novel targeted therapy that has been approved in lung cancer is crizotinib which targets ALK and several other kinases including MEK. This drug has been shown to be effective in the small subset of patients that carry the EML4-ALK translocation, showing an overall response rate of 57% (Heist & Engelman, 2012) and has recently been approved in the USA for patients with advanced ALK-positive NSCLC.

The identification and characterisation of these targets is already having a growing impact on the management of NSCLC and several clinical practise guidelines now recommend patients with an adenocarcinoma component should undergo genetic testing for *EGFR* mutations and ALK rearrangements.

1.2.5 RAS/RAF/MEK/ERK Pathway and Targeted Therapies

The RAS/RAF/MEK/ERK pathway is of high importance for developing NSCLC. Evidence comes from the high proportion of mutations found in components of the pathway in lung cancer and studies from mice.

RTKs such as EGFR, PDGFR (platelet-derived growth factor receptor) and many others, are stimulated after a growth factor or a cytokine binds on their extracellular domain (Figure 1.5). This leads to the recruitment of Src homology 2 (SH2) domain containing protein (Shc) to the intracellular domain of the RTK. SH2 protein recruits Grb2 (GTP-exchange complex growth factor receptor bound-2) and SOS (son of sevenless) which catalyse the activation of RAS by exchanging GDP to GTP. GTP-Ras recruits RAF to the membrane where it becomes activated. RAF then goes on to phosphorylate by its serine/threonine kinase activity, MEK1/2 kinases. These in turn, phosphorylate ERK1/2. Activated ERK1/2 serine/threonine kinases regulate a variety of targets (>600) (Steelman *et al.*, 2011) that control cell growth and differentiation.

1.2.5.1 KRAS

RAS genes encode a family of 21 KDa membrane bound guanosine triphosphate (GTP) - binding proteins comprised of KRAS, HRAS and NRAS.

KRAS is the most frequently mutated RAS family member in about 15-25% of NSCLC patients (Reungwetwattana *et al.*, 2012). The most common *KRAS* activating mutations are point mutations in codons 12 or 13 of exon 2. More specifically at 34G → T,C or A (49%) and 35G→T,C or A (43%) (<http://www.sanger.ac.uk/genetics/CGP/cosmic>). *KRAS* mutations are predominantly found in adenocarcinoma (~30%) rather than in squamous cell carcinoma (5%) and are more strongly associated with a history of smoking (Roberts *et al.*, 2010).

Although the identification of most oncogenes has led to the discovery of effective inhibitors, studies on *KRAS* have failed to identify clinically effective inhibitors.

One approach to treat KRAS-driven tumours is to target downstream signalling components such as RAF, MEK and PI3 Kinase. In fact, combined use of NVP-BEZ235 (a PI3K and mTOR inhibitor) and ARRY-142886 (MEK inhibitor) has been shown to synergistically act in shrinking KRAS-driven murine lung cancers (Engelman *et al.*, 2008). Another strategy for targeting KRAS is by using the concept of synthetic lethality whereby genes/gene products are identified that, when inhibited, result in cell death only when a mutant allele of another gene exists. One study using systematic RNA interference identified TBK1 to be selectively essential in cells with mutant *KRAS* and they showed that suppressing TBK1 specifically induced apoptosis in human cancer cell lines with oncogenic KRAS expression but not with WT KRAS (Barbie *et al.*, 2009). PLK1 (Luo *et al.*, 2009a) and STK33 (Scholl *et al.*, 2009) were also identified as KRAS synthetic lethal partners. These data suggest that inhibitors targeting PLK1 or TBK1, which are available, may provide treatment options for KRAS mutated NSCLC patients. However, this remains to be evaluated.

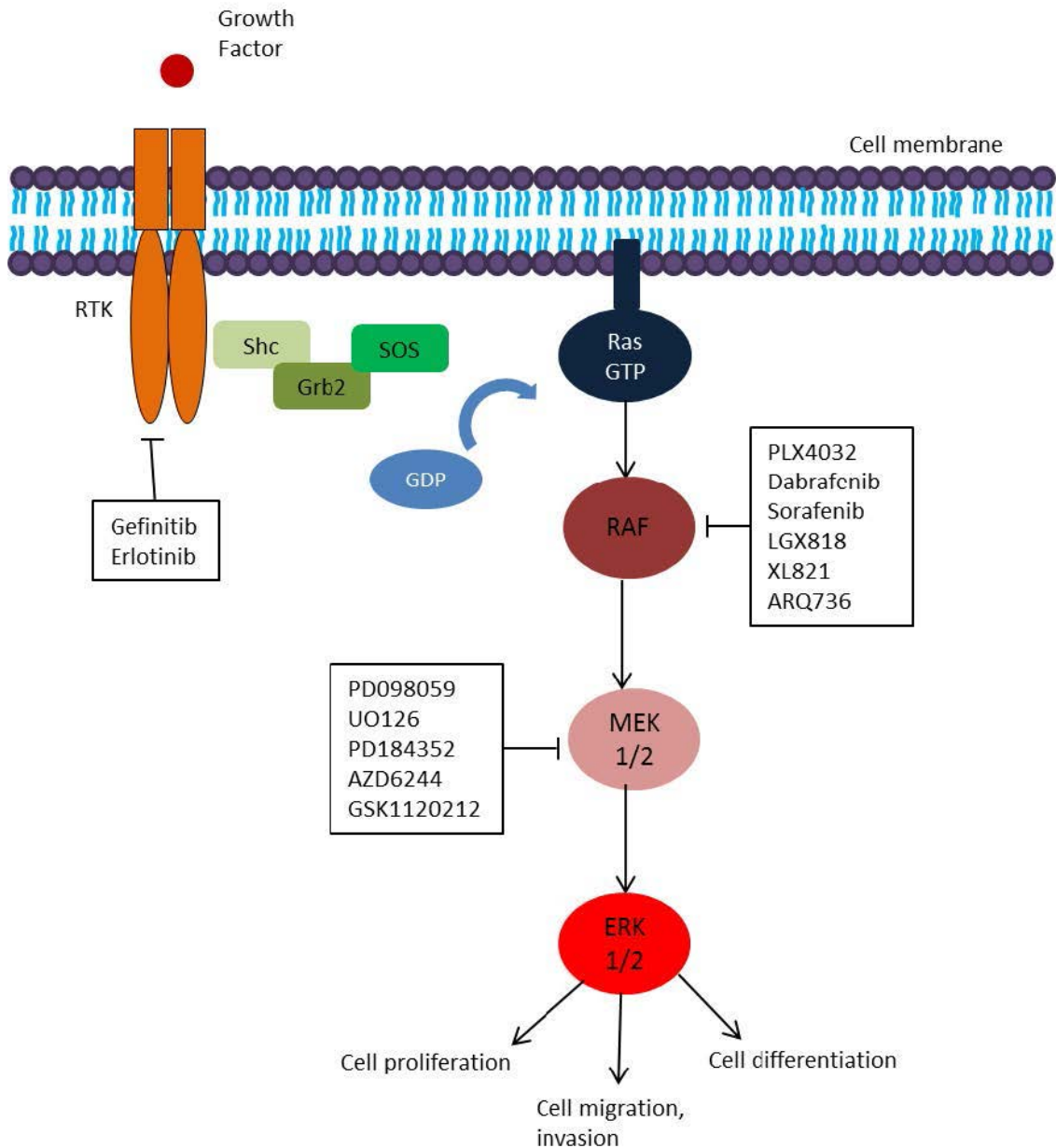


Figure 1.5. The MAPK pathway and associated inhibitors. Growth factor stimulation of RTK leads to the recruitment of SHC to the intracellular domain of the RTK. SHC then brings Grb2 and SOS which catalyse the activation of Ras by exchanging GDP to GTP. Activated RAS recruits RAF to the membrane where it becomes activated. RAF then phosphorylates MEK1/2 kinases. These in turn, phosphorylate ERK1/2. Activated ERK1/2 regulates a variety of targets which leads to cell proliferation, migration, invasion and differentiation. Inhibitors of pathway components are indicated in the boxes.

1.2.5.2 BRAF

The RAF serine threonine kinase family consists of three members: ARAF, BRAF and CRAF. *BRAF* mutations are found in ~7% of human cancers. Most frequently they are found in melanomas, being present in >90% samples (Davies *et al.*, 2002). The most common point mutation of *BRAF* is V600E which involves a 1799 A to T transversion, producing a valine to glutamine substitution at residue 600. This results in the constitutive activation of BRAF kinase activity. Interestingly, in NSCLC *BRAF* mutations are not very common occurring only in 1-3% of patients (Davies *et al.*, 2002; Pao & Girard, 2011) and the majority (~88% of the mutations) are not the most common V600E mutation but others including the G469A mutation in the G loop of the activation domain and the L597V mutation in the kinase domain (Minuti *et al.*, 2013). *BRAF* mutations are most commonly associated with the adenocarcinoma histology in NSCLC.

A number of BRAF inhibitors are currently in development. Vemurafenib (PLX4032) has shown remarkable activity in V600E positive melanoma patients in prolonging PFS (Progression Free Survival) and OS (Overall Survival) (Chapman *et al.*, 2011). A case study showed response with vemurafenib in one NSCLC patient who harboured the V600E-BRAF mutation (Gautschi *et al.*, 2012) suggesting further investigation in NSCLC.

A new BRAF kinase inhibitor dabrafenib developed by GlaxoSmithKline is undergoing a Phase II clinical trial (NCT01336634) in advanced stage NSCLC patients harbouring a *BRAF* mutation. Interim results of this phase II study show promise as they reported 40% RR (Response Rate) in a small cohort of patients (Planchard *et al.*, 2013).

Another drug, Sorafenib (BAY43-9006), was developed originally as a BRAF inhibitor, however it was discovered that it is actually a multi-kinase inhibitor of CRAF, BRAF, VEGF-1,2,3, PDGF- β , FGFR-1, c-KIT and FLT-3 (Wilhelm *et al.*, 2004). Sorafenib has been assessed in NSCLC mostly as an angiogenesis inhibitor. The ESCAPE phase III trial evaluated the efficacy and safety of sorafenib plus gemcitabine/cisplatin compared with a placebo in a cohort of 926 chemotherapy naïve patients with advanced non-squamous NSCLC but found

no significant differences in the survival between these two groups (Paz-Ares *et al.*, 2012). Another phase II trial selected patients with a *KRAS* mutation to be treated with sorafenib plus chemotherapy and showed more promising results (Dingemans *et al.*, 2013). Other BRAF inhibitors in development include LGX818 by Novartis, XL281 by Exelixis and ARQ736 which is a pan-RAF kinase inhibitor (Huang *et al.*, 2013).

1.2.5.3 MEK

MEK1/2 are serine threonine kinases downstream of BRAF that activate ERK1/2. *MEK1/2* mutations are not very common in cancer. One study reported point mutations identified in MEK1 at K57N in 2 out of 207 lung tumour samples and Q56P in 1 out of 85 NSCLC cell lines (Marks *et al.*, 2008). These mutations were mutually exclusive of other mutations in the MAPK pathway and they conferred increased activation of MEK and sensitivity to MEK inhibitor AZD6244 (Marks *et al.*, 2008). Despite MEK not being commonly mutated in cancer, it has been an attractive target in cancer therapy and multiple inhibitors have been developed and are being pursued in clinical trials.

The first specific MEK inhibitor described was PD098059, which was identified in a compound library screen and was found to inhibit MEK with an IC₅₀ of ~10 µmol/L (Dudley *et al.*, 1995). The compound U0126 was identified in a library screen for inhibitors of AP-1 transactivation and was shown to directly inhibit MEK1 and MEK2 specifically (Favata *et al.*, 1998). Although PD098059 and U0126 have been extremely useful in studying MAPK signalling *in vitro*, they did not carry on to the clinic because of their poor pharmacological characteristics (Friday & Adjei, 2008).

The first MEK inhibitor to proceed to clinical testing was PD184352 (also known as CI-1040) which was identified as a better candidate after PD098059 with improved pharmacological characteristics (Friday & Adjei, 2008). PD184352 selectively inhibited MEK1 in a non-competitive way in respect to ATP suggesting a different binding site for the inhibitor. Crystal structures of CI-1040 bound to MEK with ATP showed that there is an inhibitor binding pocket close

to the ATP binding site (Ohren *et al.*, 2004). This also explains the high degree of specificity identified in different MEK inhibitors. CI-1040 entered an open-label, phase II study to assess the antitumor activity and safety in 67 patients with breast cancer, colon cancer, NSCLC, and pancreatic cancer (Rinehart *et al.*, 2004). The drug was generally well tolerated but did not demonstrate enough promise for further development.

Instead, PD0325901, a second generation MEK inhibitor with improved pharmacologic properties was developed (Rinehart *et al.*, 2004). PD0325901 completely suppressed tumour growth in BRAF mutant xenografts. However RAS mutant tumours were only partially inhibited (Solit *et al.*, 2006). PD0325901 entered a Phase II study on heavily pre-treated NSCLC patients and failed to show any objective responses. It was concluded that patients in future clinical trials with MEK inhibitors should be refined more carefully according to their genetics and that combinations with other inhibitors could be beneficial since MEK inhibitors only cause growth arrest on their own (Haura *et al.*, 2010).

ARRY-142886 (AZD6244 or selumetinib) is another potent, selective MEK inhibitor with an IC₅₀ of 14 nmol/L against purified MEK1 (Yeh *et al.*, 2007). ERK1/2 phosphorylation was inhibited in several cell lines and growth suppression of several cell lines containing *BRAF* and *RAS* mutations was observed, with no effect on a normal fibroblast cell line (Yeh *et al.*, 2007). ARRY-142886 given orally to human colon and pancreatic mouse xenograft models was capable of inhibiting both ERK1/2 phosphorylation and growth (Yeh *et al.*, 2007). Early phase I studies of AZD6244 showed that it is well tolerated and shows target inhibition (Adjei *et al.*, 2008). Phase II studies showed that even though AZD6244 has clinical activity in patients with advanced NSCLC, there is no advantage as a monotherapy over standard chemotherapy at least in an unselected population and it was proposed that further development of the drug in NSCLC should focus on *BRAF* or *RAS* mutation-positive patients and/or combination regimens (Hainsworth *et al.*, 2010). In fact, there are a number of current ongoing clinical trials in NSCLC testing combinations of AZD6244 with erlotinib (NCT01229150 clinicaltrials.gov) and other drugs in selected populations of patients. One phase II study assessed selumetinib plus

docetaxel in previously treated patients with advanced KRAS-mutant NSCLC and showed promising activity, although there were a higher number of adverse effects than monotherapies (Jänne *et al.*, 2013).

There are a few other MEK inhibitors that have entered the clinic including GSK1120212 or Trametinib that has high potency, selectivity, and long circulating half-life (Gilmartin *et al.*, 2011).

1.2.6 PI3K/AKT/mTOR Pathway and Targeted Therapies

This pathway is an important survival pathway that is constitutively activated in most cancers including NSCLC (LoPiccolo *et al.*, 2008). Phosphatidylinositol 3-Kinase (PI3K) becomes activated after RTK stimulation. PI3K phosphorylates PIP₂ to PIP₃ (phosphatidylinositol (3,4,5) triphosphate) at the cell membrane (Figure 1.6). PIP₃ then recruits PDK1 (phosphatidylinositol-dependent kinase 1) and AKT to the membrane where PDK1 activates AKT. Activated AKT results in protection from apoptosis and increased proliferation by targeting a wide variety of substrates including mTOR which is involved in regulation of translation. PTEN (Phosphatase and Tensin homolog deleted on chromosome 10) negatively regulates the pathway by converting PIP₃ back to PIP₂.

1.2.6.1 PIK3CA

PI3K is a lipid kinase which is a heterodimer composed of a catalytic subunit (P110) and a regulatory subunit (P85), which is activated by RTKs or G protein-coupled receptors (GPCR). As already mentioned, when activated, it converts the plasma membrane lipid PIP₂ to PIP₃. *PIK3CA*, the gene that encodes the main catalytic subunit of the PI3 Kinase (p110 α) is a gene that is found to be frequently mutated or amplified in human cancers, for example mutations are found in 19% of colon cancer and 27% of breast cancers (Downward, 2008).

In a study with Chinese patients *PIK3CA* amplification was found to be associated with smoking history and to be more common in squamous cell carcinoma rather than adenocarcinoma (Ji *et al.*, 2011). In another two studies with Japanese patients, *PIK3CA* mutations were found in ~3-4% of patients (Kawano *et al.*, 2006; Okudela *et al.*, 2007) and copy number gains in 18.3% (Okudela *et al.*, 2007) and again the prevalence was higher in squamous cell carcinoma (Okudela *et al.*, 2007; Kawano *et al.*, 2006). Also an association with the male sex and smoking history was reported (Okudela *et al.*, 2007). In general, in NSCLC, *PIK3CA* mutations are most frequently found at Glu 542 and Glu 545 of exon 9 and they are frequently found in both adenocarcinomas as well as squamous cell cancers (Pao & Girard, 2011).

Multiple PI3K inhibitors are in development. One of the first inhibitors of PI3K was LY294002 which was developed from quercetin and has an IC₅₀ 1.4µM for PI3K (Vlahos *et al.*, 1994). LY294002 along with wortmannin have been used widely in the laboratory setting and have been shown to induce anti-proliferative effects in many studies; however they have high levels of toxicity, poor pharmacological properties and lack of specificity which prevented their progression to the clinic (Heavey *et al.*, 2014). In fact, even though LY294002 is one of the most widely used PI3K inhibitors (Ihle & Powis, 2010), it was found to inhibit a range of other substrates, such as mTOR, casein kinase 2, DNA-PK, GSK3 and several others suggesting its use to study PI3K signalling should be stopped (Gharbi *et al.*, 2007).

More specific inhibitors that target the catalytic domain p110 of class IA PI3K have been developed and have been explored clinically in lung cancer.

GDC-0941 is a selective and highly orally bioavailable (Salphati *et al.*, 2011) inhibitor of class IA PI3Ks that binds competitively to the ATP binding site of PI3K and has an IC₅₀ of 0.003µM for p110α (Folkes *et al.*, 2008). A preclinical study using NSCLC cell lines and xenograft models showed the combination of GDC-0941 with paclitaxel, erlotinib, or a MAPK inhibitor had greater effects on cell viability than PI3K inhibition alone (Spoerke *et al.*, 2012). A Phase Ib trial evaluating GDC-0941 in combination with paclitaxel and carboplatin, with or

without bevacizumab, in patients with NSCLC is ongoing (NCT00974584). Partial responses have been observed in 8/18 patients (Besse *et al.*, 2011).

A Phase I study with combination dosing of XL518 and GDC-0941 was generally well tolerated and decreases in tumour burden were seen in some patients including some with NSCLC (Shapiro *et al.*, 2011). Another phase I study of GDC-0941 in combination with erlotinib in patients with advanced solid tumours is ongoing (NCT00975182).

BKM120 (Novartis) is a highly specific orally bioavailable pan-class I PI3K inhibitor with activity against the most common somatic *PIK3CA* mutations (Maira *et al.*, 2012). BKM120 was tested in a panel of 353 cell lines and showed preferential inhibition of tumour cells bearing *PIK3CA* mutations and exhibited tumour growth inhibition in xenograft models (Maira *et al.*, 2012). In a recent Phase I study, once-daily BKM120 of 100 mg/d demonstrated a safe and well tolerated profile, clear evidence of target inhibition, and preliminary antitumor activity in patients with advanced cancer (Bendell *et al.*, 2012). BKM120 is currently being investigated in patients with NSCLC in a number of Phase I and II clinical trials singly and in combination with mTOR inhibitors, standard chemotherapy drugs, with MEK inhibitors and others (Beck *et al.*, 2014; Papadimitrakopoulou, 2012).

There is a plethora of other PI3K inhibitors currently being investigated clinically and preclinically showing promising indications, including XL147, PX-866 and BYL-719 (Beck *et al.*, 2014). Furthermore, because the catalytic domains of PI3K p110 subunit and mTOR are structurally similar, there are small molecule inhibitors that can target both proteins; examples of these in current clinical development include XL765, BEZ235, GSK2126458 and GDC-0980 (Papadimitrakopoulou, 2012).

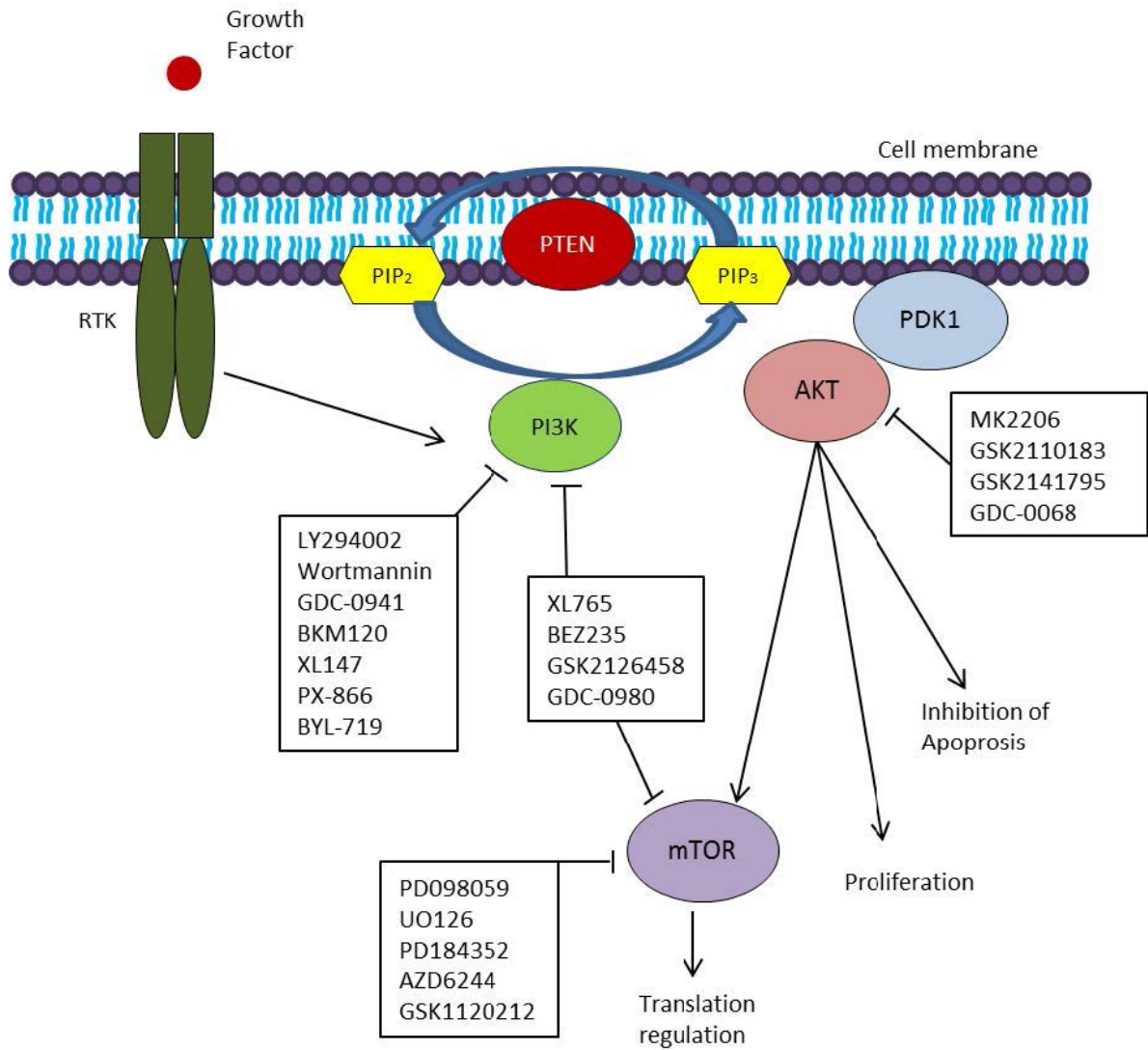


Figure 1.6. The PI3K Pathway and inhibitors for pathway components. PI3K is activated by RTKs and converts PIP₂ to PIP₃ which leads to activation of AKT by PDK1. AKT has multiple targets including mTOR which is involved in the regulation of translation. AKT activation leads to proliferation and inhibition of apoptosis. Inhibitors are shown in boxes. XL765, BEZ235, GSK2126458 and GDC-0980 are dual specificity inhibitors of both PI3K and mTOR.

1.2.6.2 AKT

There are three members of the AKT family (AKT1, AKT2 and AKT3) which are broadly expressed serine/threonine kinases that have a central catalytic domain, a PH domain and a short regulatory domain (Vivanco & Sawyers, 2002). AKT is activated by recruitment to the plasma membrane and direct binding through the PH domain with PIP₃ and phosphorylation at Thr308 by PDK1 and Ser473 by PDK2 (Vivanco & Sawyers, 2002).

AKT was found to be phosphorylated and thus activated in more than 50% of NSCLCs in a range of early stage and late stage tumours suggesting activation of the PI3K/AKT pathway is an early event in lung tumourigenesis (Balsara *et al.*, 2004). A somatic mutation (E17K) that constitutively activates *AKT1* has been found in 1.9% NSCLC patients with squamous histology (Malanga *et al.*, 2008). Further studies have failed to identify more *AKT1* mutations (Do *et al.*, 2010). Nevertheless, a number of AKT inhibitors are in development.

One of the most promising compounds is MK-2206 (Merck, Whitehouse Station, NJ) which is an oral allosteric AKT inhibitor with high potency against purified recombinant human AKT1 (IC₅₀ = 5 nmol/L), AKT2 (IC₅₀ = 12 nmol/L) and AKT3 (IC₅₀ = 65 nmol/L) (Hirai *et al.*, 2010; Yap *et al.*, 2011). MK-2206 was shown to inhibit phosphorylation at both Thr308 and Ser473 residues of AKT and demonstrated *in vitro* and *in vivo* antitumor activity as a single agent and enhanced the preclinical activity of chemotherapeutic drugs and other molecular targeted therapies (Hirai *et al.*, 2010). A phase I study of MK-2206 in patients with advanced solid tumours exhibited minor responses and a well-tolerated profile of the drug (Yap *et al.*, 2011). MK-2206 is currently being tested in combination with erlotinib in a phase II study in patients with advanced NSCLC (NCT01294306) and with chemotherapeutic drugs.

Other oral AKT inhibitors in clinical development include GSK2110183, GSK2141795 and GDC-0068 (Papadimitrakopoulou, 2012).

1.2.6.3 PTEN

PTEN, originally isolated as a tumour suppressor gene in breast cancer, is a dual specificity phosphatase that shows activity against lipid and protein substrates (Vivanco & Sawyers, 2002). Its main function is to negatively regulate the PI3K pathway by dephosphorylating PIP₃ to PIP₂.

Mutations that inactivate *PTEN* have been observed in NSCLC (Forgacs *et al.*, 1998). In another study PTEN protein expression was reduced or lost in 74% (86/117) (Marsit *et al.*, 2005) of tumours suggesting inactivation of *PTEN* is a common event in NSCLC.

1.2.6.4 MTOR

mTOR (the mammalian target of rapamycin), a direct target of AKT, is a serine/threonine kinase that regulates protein synthesis by activating p70 S6 kinase (RSK), a translational activator and by inhibiting 4E-BP1, a translational repressor (Vivanco & Sawyers, 2002). mTOR is activated in more than 50% of NSCLCs (Balsara *et al.*, 2004). Several mTOR inhibitors are currently being investigated in the clinical setting; examples include everolimus, temsirolimus and ridaforolimus. Everolimus was examined in a phase I study in combination with chemotherapeutic drug pemetrexed and showed to be generally well tolerated (Vansteenkiste *et al.*, 2011). However increased toxicities were observed from the combination. A phase II study investigated the combination of Everolimus with Gefinitib (an EGFR inhibitor) but failed to reach the pre-specified response threshold to pursue further study (Price *et al.*, 2010). Nonetheless, there was no stratification of the patients according to pathway activation which might explain the poor response rate.

1.4 Cell Death Pathways

Programmed Cell Death or Apoptosis was first described as a series of morphological changes by Kerr et al in 1972. They observed plasma membrane disruption, nuclear and cytoplasmic condensation, formation of apoptotic bodies and engulfment by nearby cells (Kerr *et al.*, 1972). All this happens in a period of 30-120 minutes (Wyllie *et al.*, 1980).

Inhibition of apoptosis is one of the hallmarks of cancers and this allows cells that carry considerable genomic alterations to survive (Hanahan & Weinberg, 2000). There are two apoptotic pathways; the intrinsic and the extrinsic pathway (Figure 1.7). Targeting the apoptotic machinery of tumour cells could potentially be used to treat cancers cells selectively. In fact, a number of compounds that target apoptotic pathways are in clinical trials for NSCLC and other tumour types (Pore *et al.*, 2010).

1.4.1 Caspases Are Central Executioners of Apoptosis

Caspases are a family of cysteine proteases which are synthesised as inactive zymogens and are the central executioners which bring about the morphological characteristics of apoptosis (Hengartner, 2000). Caspases require specific cleavage at aspartate residues to become activated (Cohen, 1997).

Based on their function they can be classified into two groups; the initiator caspases and the effector caspases. Initiator caspases (Caspase -2,-8,-9 and -10) usually possess a death effector domain (DED), have long prodomains and act upstream to transmit the apoptotic signal by interacting with adaptor molecules (Jin & El-Deiry, 2005). The effector caspases (-3, -6, and -7) are characterised by short prodomains and they are activated by the initiator caspases and execute the downstream steps of apoptosis by cleaving multiple substrates (>100) including cytoskeletal proteins, cellular DNA repair proteins, structural proteins (Jin & El-Deiry, 2005) and PARP (Poly-ADP-Ribose Polymerase (Tewari *et al.*, 1995).

1.4.2 The Extrinsic Apoptotic Pathway

The extrinsic or death receptor pathway is triggered via members of the death receptor superfamily such as Fas/CD95, tumour necrosis factor receptor I (TNFR-I) or TRAIL receptor (TNF-related apoptosis-inducing ligand) which after ligand binding they induce receptor clustering. This ligand-receptor complex recruits FADD (Fas-associated protein with death domain (Chinnaiyan *et al.*, 1995) and procaspase-8 to the cell membrane causing caspase-8 activation in a complex named the death-inducing signalling complex (DISC) (Pennarun *et al.*, 2010). Caspase-8 then cleaves the executioner procaspase 3 which becomes activated and the apoptotic program begins. cFLIP (Cellular fllice-like inhibitory protein), a non-functional procaspase-8 homologue, can compete with procaspase 8 for FADD binding and this can lead to suppression of apoptosis (Pennarun *et al.*, 2010).

Caspase-8-mediated cleavage of Bid, a pro-apoptotic Bcl-2 family member, results in its translocation to the mitochondria, where it promotes cytochrome c exit and converges the two pathways together under certain conditions (Hengartner, 2000).

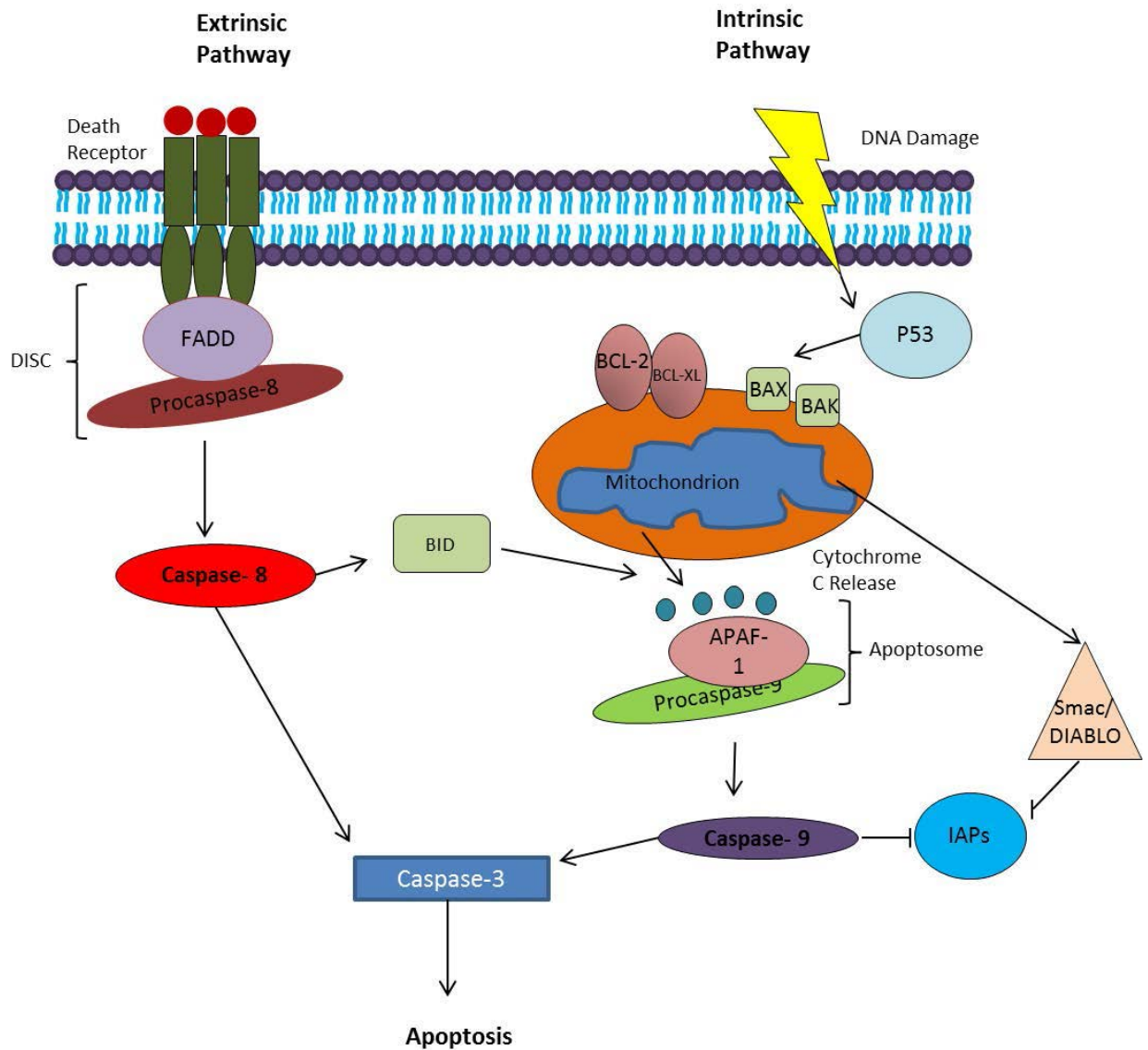


Figure 1.7. Extrinsic and Intrinsic Apoptotic Pathway. The extrinsic pathway is activated through death receptor stimulation at the plasma membrane and subsequent formation of DISC and activation of caspase which leads to apoptosis. The intrinsic pathway is triggered through various conditions such as DNA damage and it signals through the mitochondria with cytochrome c release and the formation of the apoptosome which leads to caspase activation.

1.4.3 *The Intrinsic Apoptotic Pathway*

The intrinsic pathway is activated by various conditions such as growth factor deprivation, hypoxia and DNA damage which can be imposed for example by chemotherapeutic drugs. The central actor in this pathway is cytochrome c which normally resides in the space between the inner and outer mitochondrial membranes. When apoptosis is initiated, the mitochondrial outer membrane becomes permeabilized (MOMP) and cytochrome c spills out in the cytosol. MOMP is mainly controlled by Bcl-2 family members (Jin & El-Deiry, 2005).

The Bcl-2 family is comprised of both anti- and pro-apoptotic proteins and they all contain at least one Bcl-2 homology (BH) domain. They can be divided into three groups. The anti-apoptotic members, such as Bcl-2, Bcl-XL, Bcl-w and Mcl-1 are characterized by four short BH domains and C-terminal hydrophobic tail, which localizes the proteins to the outer surface of mitochondria (Hengartner, 2000; Jin & El-Deiry, 2005). The second group consists of Bcl-2 family members with pro-apoptotic activity and 3 BH domains; this includes Bax and Bak. The third group consists of pro-apoptotic BH3-only proteins such as Bad, Bid, Noxa and Puma. Interactions amongst the BCL-2 family members determine whether apoptotic thresholds are exceeded and MOMP takes place.

When cytochrome c is released into the cytosol it induces the formation of the apoptosome by binding to Apoptosis Protease Activating Factor-1 (APAF1) and procaspase-9. This leads to the activation of caspase-9 and subsequent activation of apoptosis by activation of the effector caspase-3. Another protein which is released from the mitochondria is Smac/DIABLO which acts to neutralise the inhibitory activity of IAPs on the caspases and promotes apoptosis (Jin & El-Deiry, 2005).

The intrinsic apoptotic pathway can be initiated by p53 by activating Bax (Gottlieb & Oren, 1998).

1.4.4 Targeting TRAIL

TRAIL exists as a type II membrane protein or in a soluble form and was originally discovered from its homology to other TNF family members (Wiley *et al.*, 1995). There are five receptors that bind TRAIL in humans, TRAIL-R1 (DR4), TRAIL-R2 (DR5), DcR1, DcR2 and OPG. Only binding of TRAIL to DR4 and DR5 elicits the formation of DISC and subsequent activation of the extrinsic apoptotic pathway (Almasan & Ashkenazi, 2003). DcR1, DcR2 and OPG are decoy receptors that lack functional cytoplasmic domains and are therefore incapable of inducing apoptosis. However they can bind to TRAIL and inhibit downstream signalling (Ashkenazi, 2002).

TRAIL receptor targeting agents represent an attractive therapeutic approach since they promote apoptosis selectively in tumour cells but not normal cells (Walczak *et al.*, 1999; Ashkenazi *et al.*, 1999). This is probably because of a number of factors including increased expression of decoy receptors on normal cells and increased expression of DR4 and DR5 on tumour cells (Emmett, 2011). Notably, TRAIL-induced tumour killing is independent of p53 status which is inactivated in the majority of NSCLC (Stegehuis *et al.*, 2010). TRAIL receptor targeting agents have been developed and include agonistic monoclonal antibodies directed at DR4 and/or DR5 and recombinant human soluble TRAIL. These have been examined in NSCLC. Approximately 50% of NSCLC cell lines tested, show resistance to apoptosis by TRAIL receptor targeting agents (reviewed in Stegehuis *et al.*, 2010). Combination treatments can sensitize TRAIL induced apoptosis. Recombinant TRAIL or DR5 directed antibody combined with chemotherapeutic drugs has been shown to inhibit tumour growth in orthotopic mouse models of lung cancer (Jin *et al.*, 2004; Jin *et al.*, 2008). Other combination treatments reported to synergise with TRAIL in inducing tumour cell death in NSCLC include bortezomib (Voortman *et al.*, 2007; Luster *et al.*, 2009), a novel thymidylate synthase inhibitor trifluorothymidine (Azijli *et al.*, 2014) and many others such as HDAC inhibitors (Stegehuis *et al.*, 2010).

Phase I and II clinical trials using TRAIL targeted agents are underway. RhTrail was tested in combination with paclitaxel, carboplatin and bevacizumab in a Phase Ib study in 24 NSCLC patients where it was shown to be well tolerated

and have a response of 58% in the study population (Soria *et al.*, 2010). However, a subsequent Phase II study with the same compound in 213 patients did not improve outcomes in unselected patients with previously untreated advanced or recurrent NSCLC (Soria *et al.*, 2011).

Another study evaluated the efficacy, safety, and pharmacokinetics of conatumumab (a DR5 agonistic antibody) combined with paclitaxel-carboplatin as first-line treatment for advanced NSCLC in 172 patients. Although the combination was well tolerated, again the addition of conatumumab did not improve outcomes of this cohort of unselected patients (Paz-Ares *et al.*, 2013). In general TRAIL targeted agents have limited toxicity in patients and therefore in theory they could be exploited with a number of combination therapies such as the targeting of oncogenes.

1.4.5 BCL-2 Inhibitors

Interfering with Bcl-2 and other anti-apoptotic family members is another strategy which can help to restore the sensitivity of cancer cells to pro-apoptotic signals. Two main strategies have been employed; antisense oligonucleotides that inhibit anti-apoptotic family members and small molecule inhibitors (Pore *et al.*, 2010). The second strategy is more promising. These small molecule inhibitors are designed to bind the hydrophobic groove of anti-apoptotic Bcl-2 proteins in place of BH3-only proteins; they are so called BH3-mimetics (Kang & Reynolds, 2009).

ABT-737, one of the most promising BH3 mimetics, was discovered using nuclear magnetic resonance (NMR)-based screening, parallel synthesis and structure-based design and was found to be an inhibitor of the anti-apoptotic proteins Bcl-2, Bcl-xL and Bcl-w, with a high affinity (Oltersdorf *et al.*, 2005). ABT-737 showed efficacy in lymphoma and small-cell lung carcinoma lines and in animal models (Oltersdorf *et al.*, 2005; Hann *et al.*, 2008). Synergistic interactions between ABT-737 and TRAIL have also been observed in tumour cell lines including NSCLC (Song *et al.*, 2008).

ABT-263 is an oral derivative of ABT-737 with improved pharmacological properties which showed complete tumour regressions when administered

orally in xenograft models of SCLC and acute lymphoblastic leukaemia (Tse *et al.*, 2008). Phase I studies of ABT-263 in SCLC and other solid cancers showed a safe and well tolerated profile of the drug and some encouraging data with one SCLC patient having stable disease for more than 2 years (Gandhi *et al.*, 2011). Phase II studies of ABT-263 as monotherapy has shown limited activity in SCLC and it was suggested that future studies should focus on combination treatments (Rudin *et al.*, 2012). Results from a recent Phase I study combining ABT-263 with gemcitabine showed stable disease in 54% of the patients and the combination to be generally well tolerated with a favourable safety profile in patients with advanced solid tumours (Cleary *et al.*, 2014).

1.5 Preclinical Models

Critical reviews on drug development rates from 1964 to 2000 estimated less than 11% success rate in bringing a drug to the market in the US and Europe (Astashkina *et al.* 2012). As a result, millions of pounds have been wasted in the drug development process because the current preclinical models simply fail to accurately predict drug performance *in vivo*.

1.5.1 Cell Lines

It has been shown that tumour derived cell lines maintain the genomic features of primary tumours (Sharma *et al.*, 2010) and can be potentially useful in drug screening. The CMT1000 platform is a human tumour cell line platform that includes ~1200 cell lines and is being used to study the genetic basis for sensitivity to anticancer drugs that are either already approved or under investigation. Using this platform it became evident that genetically defined cancer subsets, regardless of the tissue of origin, associate with specific kinase inhibitors (Sharma *et al.*, 2010; McDermott *et al.*, 2007).

There are more than 200 established lung cancer cell lines that have made a substantial contribution to translational research (Gazdar *et al.*, 2010). For example it has been shown, using cell lines, that sensitivity to an ALK inhibitor

correlated with ALK-activating chromosomal translocations which have a 3-7% frequency in NSCLC (McDermott *et al.*, 2008).

Cell lines have obvious advantages such as their widespread availability, the ease of culturing and the fact they represent a pure population of tumour cells (Gazdar *et al.*, 2010). Nevertheless, testing drugs in cultured cell lines is not the best way to reflect the situation with *in vivo* tumours. Cell lines growing on a monolayer on a plastic dish have little similarities with physiological conditions.

1.5.2 Mouse Models

Most of the pharmaceutical industries assess the efficacy of novel drugs on human tumour xenografts established from human tumour cell lines on mice. One of the problems with these models is the inability to represent the tumour heterogeneity evident in cancer patients (Heyer *et al.*, 2010; Daniel *et al.*, 2009) resulting in poor predictive capability. This is emphasised by the fact that many candidate anticancer agents that show great potential in xenograft models, have been disappointing in the clinic. This topic was recently reviewed by Mak and colleagues (Mak *et al.*, 2014). Noteworthy examples include drugs TGN1412 (humanized agonistic anti-CD28 monoclonal antibody developed for the treatment of immunological diseases and certain cancers) and IPI-926 (Hedgehog pathway antagonist) both of which showed great potential in xenograft models but failed to do so in human trials (Mak *et al.*, 2014). In fact, TGN1412 caused catastrophic systemic organ failure in patients; even though it was administered at a dose 500 times lower than that found safe in animal studies (Mak *et al.*, 2014).

Novel approaches for modelling cancer in mice (reviewed in (Malaney *et al.*, 2014; Khaled & Liu, 2014; Heyer *et al.*, 2010; Hayes *et al.*, 2014) include patient derived xenografts (PDXs) which are based on the transfer of primary tumours directly from the patient into a non-obese diabetic/severe combined immunodeficient (NOD/SCID) mouse (Siolas & Hannon, 2013). Tumours can be engrafted heterotopically (implantation into the subcutaneous flank of a mouse) or orthotopically (direct grafting to the mouse organ of

choice). Orthotopic PDX models, even though more challenging to create, show better predictability of clinical outcome (Siolas & Hannon, 2013).

In a pilot study of advanced cancer patients, PDX models from 14 patients were used to test 63 drugs (Hidalgo *et al.*, 2011). Nine out of eleven patients that were given the PDX identified regimens, showed durable partial remission reflecting a high correlation between drug activity in the model and clinical outcome (Hidalgo *et al.*, 2011). Another PDX study from NSCLC patients showed consistent results with clinical trials, when PDX models with *EGFR* activating mutations showed response to gefinitib whereas *KRAS* mutants were resistant (Zhang *et al.*, 2013). Nonetheless, PDX models are very costly and take a long time to set up (Siolas & Hannon, 2013). Another problem with PDX models is the lack of tumour cell interactions with the innate immune system since they are implanted into immunodeficient mice (Siolas & Hannon, 2013).

To this end, Genetically Engineered Mouse Models (GEMMs) have a fully functional immune system and they mimic spontaneous tumourigenesis (Heyer *et al.*, 2010; Singh *et al.*, 2012). Treatment of chimeric GEMMs of NSCLC with an *EGFR* mutation or a *KRAS* mutation with an EGFR inhibitor resulted in near complete tumour regression and no response to the treatment, respectively, accurately reflecting previous clinical observations (Zhou *et al.*, 2010).

There is a new concept stated as a “Co-clinical Trial” which refers to trials that are conducted simultaneously in GEMMs and human patients as part of Phase I/II trials for drug development (Nardella *et al.*, 2011). A co-clinical trial of lung cancer has already shown promising results and identified predictive genetic biomarkers (Chen *et al.*, 2012). In this study, GEMMs were used to conduct a co-clinical trial which mirrored an ongoing human clinical trial in patients with *KRAS*-mutant lung cancers to determine if the MEK inhibitor selumetinib (AZD6244) increases the efficacy of docetaxel, a standard of care chemotherapy (Chen *et al.*, 2012). It was previously shown that concomitant loss of tumour suppressors TP53 or LKB1 impaired the response of *KRAS*-mutant cancers to docetaxel monotherapy. Therefore, the combination treatment on GEMMs with mutated *KRAS*, *KRAS*+TP53 and *KRAS*+LKB1 was tested and it was found that the addition of selumetinib provided substantial

benefit for mice with lung cancer caused by *KRAS* and *KRAS* and *TP53* mutations, but mice with *KRAS* and *LKB1* mutations had primary resistance to this combination therapy (Chen *et al.*, 2012).

To conclude, there are some exciting new mouse models that have shown better predictability of drug response in cancer. However, these models are quite expensive to set up plus require laborious and time-consuming procedures. Furthermore, we have to keep in mind that we are ultimately dealing with a different species and it should not necessarily be implied that information found using mice models will always accurately translate to humans.

1.5.3 3D culture models of human tumours

Three-dimensional culture models of human tumours provide an easier, less expensive and less time-consuming approach to preclinical modelling since they can reliably reflect tumour growth *in vivo* (Pampaloni *et al.*, 2007). There are various 3D culture systems being evaluated for this purpose such as multicellular tumour spheroids (MCTS), *ex vivo* tissue slices (Vaira *et al.*, 2010) and HDRA (histoculture drug response assay; Hoffman, 1993).

MCTS systems offer an evolving tool to model the heterogeneity and microenvironmental aspects of *in vivo* tumour growth and they have been shown to have greater chemotherapeutic resistance than the same cells in monolayer cultures (Fennema *et al.*, 2013), which reflects the situation in the clinic. A novel 3D co-culture model using NSCLC cell lines in combination with lung fibroblasts has allowed the investigation of tumour-stroma interactions and has the potential to be used in the cancer drug discovery field since they can be grown in an automated way (Amann *et al.*, 2014).

One other promising technique is the culturing of *ex vivo* tissue slices. Such models have been long known and have been used for studying the toxicities of many compounds such as the herbicide paraquat for example in a lung slice system (Parrish *et al.*, 1995). Tissue slices used to be prepared by a mechanical slicing apparatus to produce slices of identical dimensions in order to have constant rates of nutrient and gas diffusion and were placed on a grid in

a plate (Parrish *et al.*, 1995). This technique was improved for use in analysing anticancer agents on tissue slices of human tumours. For example one study used precision cut tissue slices of surgically resected hepatocellular carcinoma to analyse the effects of COX2 inhibition (Kern *et al.*, 2006).

A different, more recent study reported using various human tumour tissues, immediately after harvesting from surgery, to cut tumour slices and culture up to 120h with no significant decrease in proliferating cells as assessed by Ki-67 immunostaining after fixing the tissues. The effect of a PI3K inhibitor LY294002 on some of the samples was examined and showed dose dependent tumour inhibition (Vaira *et al.*, 2010).

In a different culture approach, one study from 1986 showed human tumours (64/89) obtained immediately after surgery could grow *in vitro* for long periods (up to >100 days) and still maintain their *in vivo* properties such as tissue organisation, preservation of differentiated function as well as growth of multiple types of cells from a single tumour (Freeman & Hoffman, 1986). In this study, specialised collagen gel from pigskin was used to culture tumour fragments of ~1mm³ (Freeman & Hoffman, 1986).

Researchers began optimising this technique further to use in drug testing and it was subsequently called HDRA (Vescio *et al.*, 1987; Vescio *et al.*, 1991). One study reported 86% accuracy *in vitro* of predicting drug resistance *in vivo* when using various chemotherapeutic drugs (Vescio *et al.*, 1991). In 1995, a correlative clinical trial with 107 advanced gastric cancer and 109 advanced colorectal cancer patients took place. From them, 208/216 (96.3%) were evaluated by HDRA with an MTT endpoint (Furukawa *et al.*, 1995). After surgery, 38 patients were evaluated for comparison of the effects of chemotherapy in the HDRA with clinical outcome. Twenty-nine patients treated with drugs that were shown to be ineffective in the HDRA, and all 29 cases showed clinical chemoresistance (Furukawa *et al.*, 1995). In nine patients treated with drugs shown to be effective in the HDRA, six showed clinical response and three showed arrest of disease progression (Furukawa *et al.*, 1995). Therefore they reported a correlation rate of HDRA to clinical drug sensitivity response of 92.1% (35/38 patients).

A number of studies followed up with this technique in NSCLC and most of them showed good predictability rates (Yoshimasu *et al.*, 2005; Yoshimasu *et al.*, 2003; Tanahashi *et al.*, 2008; Yoshimasu *et al.*, 2007; Hayashi *et al.*, 2009). One of the disadvantages with this technique is the end point used to assess drug response, the MTT (3-(6)-2, 5-diphenyl tetrazolium bromide) assay as this requires enzymatic digestion of tissue.

Pirnia *et al.* used a modified version of the HDRA with 20 NSCLC patient tumour samples whereby they cultured tumour tissue fragments for up to 120h and treated them with mitomycin C, taxotere and cisplatin (Pirnia *et al.*, 2006). In their technique they used Alamar blue to assess the drug responses which allows cytotoxicity to be measured without processing the tissue cultures. They were able to fix and analyse the samples with immunohistochemistry (Pirnia *et al.*, 2006).

Professor MacFarlane's group (MRC Toxicology Unit, Leicester) recently used *ex-vivo* explant cultures with IHC as an end point to examine the response of breast carcinomas *in situ* to the cytotoxic ligand TRAIL, and found that primary explants were more predictive than tumour-derived cell line cultures (Twiddy, D., *et al.*, 2010-poster abstract). They found that most of the tumour cell lines were sensitive to TRAIL-induced apoptosis whereas Invasive Ductal Carcinoma (IDC), which is the most common breast cancer form, required the addition of an appropriate sensitizing agent such as doxorubicin for apoptosis to occur (Twiddy, D., *et al.*, 2010-poster abstract).

1.6 Aims and Objectives

The aim of this PhD was to establish a primary NSCLC explant culture system based on the previous breast cancer explant culture system established by Prof. MacFarlane's laboratory (Twiddy, D., *et al.*, 2010-poster abstract) to test the efficacy of existing drugs as well as novel drug combinations. This was combined with stratification by tumour genotype and analysis of the signalling pathway output, with the aim of identifying predictive biomarkers.

The specific objectives of the project by chapters are:

Chapter 3. Patients' Demographics

- Age, Sex, Stage of Disease, Mutation status.

Chapter 4. Development of an explant culture system for NSCLC samples

- Evaluation of the best way to analyse data and to present the results.
- Optimisation of the explant model for NSCLC samples by testing different foetal calf serum (FCS) concentrations and assessing varying culture times.

Chapter 5. Testing the response of *ex-vivo* NSCLC explants to cisplatin.

- Correlate responses to clinical information on patient outcomes if possible.
- Test whether response to cisplatin correlates with p53 expression.
- Confirmation of cisplatin accumulation in explants by LA-ICP-MS.

Chapter 6. Assessment of responses to new agents: Targeting MAPK and PI3K signaling pathways.

- Determine the responses of explants to PD184352 (MEK inhibitor) and LY294002 or GDC401 (PI3K inhibitor) singly and in combination.
- Correlate response to mutations in key components of the pathway including *KRAS*, *EGFR*, *BRAF* and *PI3K*.
- Determine effect of inhibitors on pathway outputs by assessing P-ERK and P-AKT staining.
- Correlate responses to available clinical data on clinical trials with these agents in the literature.

Chapter 7. Assessment of responses to new agents: Targeting non-oncogene addicted cell death pathways.

- Determine the responses of explants to TRAIL and ABT-737, singly and in combination, and in the presence and absence of cisplatin.
- Correlate responses to available clinical data on clinical trials with these agents in the literature.

2. MATERIALS AND METHODS

2.1 *Ex-vivo* Explant Culture Model

2.1.1 *Collection of Tissue*

NSCLC tumour and adjacent normal samples were collected from consented patients undergoing lung surgery at Glenfield hospital by Will Monteiro and Hilary Marshall (Department of Infection, Immunity and Inflammation, University of Leicester) under the supervision of pathologist Dr Salli Muller with Ethical Approval (UHL 10402- Molecular and Functional Mechanisms of Human Lung Disease, PI: Prof A. Wardlaw) (see appendix for ethics documentation). The patients had no prior exposure to chemotherapy. Surgical segments were taken from patients that had an excised tumour greater than 3cm in diameter and they were sampled from the centre of the tumour to avoid risking any surgical margin diagnosis by pathology. The tissue was kept in Hank's Balanced Salt Solution (HBSS) media on ice and was collected fresh, shortly after the surgery had taken place. The samples were transferred to the MRC Toxicology Unit and were processed in a specified Primary Cell Culture Facility in a Class II Hood. A total number of 60 samples were collected throughout this project. A table summarising the patients' details can be found in the Appendix.

A detailed paper trail was kept for each sample for ethical reasons (see appendix for example of form completed for each sample).

2.1.2 *Processing of the tissue*

Samples were cut into fragments, portions were weighed, recorded and kept in appropriate storage conditions for eventual generation of protein lysates, RNA extracts and DNA extracts. A portion was also fixed in 4% PFA (4% [w/v] paraformaldehyde, 80mM Na_2HPO_4 , 20mM NaH_2PO_4) for histological examination and a portion was used to set up *ex-vivo* explant cultures whenever possible, as described below. The tissue fragments stored for

eventual generation of protein (kept at -80°C) and RNA (kept in 1ml RNA later® at -20°C) from the samples was not used for this project but were stored for future research.

2.1.3 Ex-vivo Explant Cultures

The *ex-vivo* explant culture model for NSCLC (see Figure 2.1 for an illustrative overview of the model) was based on previous work on breast explant cultures by Professor McFarlane's group (Twiddy et al., 2010-poster abstract).

2.1.3.1 TISSUE PROCESSING AND TREATMENT

Samples were cut using two skin graft blades (Fisher Scientific, UK) on a dental wax surface (Agar Scientific, UK) into small fragments of approximately 2-3 mm³. The explants were placed in fresh culture media [DMEM (GIBCO, supplemented with 4.5 g/L Glucose and L-Glutamine) + 1% (v/v) FCS + 1% pen/strep]. Nine explants were randomly selected and placed on a Millipore organotypic culture insert disc of 0.4µm using forceps, which was floated on 1.5 ml of media in 6 well plates. The explants were then left to recover at 37°C and 5% CO₂ overnight (see Figure 2.1). The following day, 1.5 ml of fresh media was added in newly labelled 6-well plates and different drugs at various concentrations were added to each well (see Table 2.1 for a list of therapeutic agents used in this study) in a volume of 1.5µl. The culture inserts containing the explants were carefully transferred into the new 6-well plates containing the drugs using forceps. The explants were then incubated for a period of 24 hours, 48 hours or 72 hours at 37°C and 5% CO₂.

Table 2.1. Therapeutic agents used in this study.

Drug	Final concentration	Source	Constituted in	Storage
LY294001	10,20,50 μ M	New England Biolabs, USA #9901	DMSO	-20 °C
GDC-0941	5,10,20 μ M	Selleck Chemicals, USA (s1065)	DMSO	-20 °C
UO126	5,10,20 μ M	Cell Signalling, USA #9903	DMSO	-20 °C
PD184352	5,10,20 μ M	Dr Simon Cook, Babraham Institute, UK	DMSO	Room temperature
TRAIL	1 μ g/ml	Prof Marion McFarlane, MRC Toxicology Unit, UK	DMSO	-80 °C
ABT-737	2,10 μ M	Selleck Chemicals, USA (s1002)	DMSO	-20 °C
Cisplatin	1,10,50 μ M	Sigma-Aldrich, UK (P4394)	DMF	Room temperature
Sorafenib	5,10,20 μ M	Prof. Richard Marais, Institute of Cancer Research, UK	DMSO	Room temperature

Tissue processing and Treatment



Fixation and Embedding



Immunohistochemical staining



Figure 2.1. Overview of the ex-vivo explant culture model. Tissue processing and treatment: Samples were collected fresh after surgical excision from Glenfield hospital. They were taken to the MRC Toxicology Unit and processed in a class II hood. Samples were cut into small pieces of about 2-3mm³ with skin graft blades on a dental wax surface. 9 fragments were randomly selected and put on 0.4µm Millipore discs which were floated on 1.5 ml of media in 6-well plates. The tissue explants were left to recover overnight. They were then treated with various drugs for a period of time. Fixation and embedding: The tissue fragments were fixed in 4% PFA, embedded in wax and processed for H&E staining. Immunohistochemical staining: IHC was performed on sections of samples with various antibodies, using the Novolink Polymer Detection System™.

2.1.3.2 FIXATION AND EMBEDDING

After the treatment, the culture inserts containing the explants were carefully washed with PBS (Phosphate Buffered Saline) and transferred into new 6-well plates containing 1ml of 4% PFA. A few drops of the fixative were also put on top of each culture insert. The fragments were left in the solution for 20 hours. The explants were then carefully transferred onto sponges (rectangular 25x31mm, Fisher Scientific, UK) which were pre-soaked in 70% Ethanol, placed in cassettes (Electron Microscopy Sciences, UK) and kept in a container in 70% (v/v) Ethanol until the end of each experiment. They were then transferred to the Histology facility of the Core Biotechnology Services (HCBS) located at the Department of Cancer Studies, RKCSB, University of Leicester where the explants were carefully embedded into paraffin. Care was taken to ensure orientation of the explants was intact (see Figure 2.1). It was arranged such that the side that was closest to the media on the culture discs was placed down into the wax.

Lung tissue explant sections were cut from formalin fixed paraffin embedded (FFPE) blocks by the HCBS staff and placed on untreated slides into 4µm slices using a microtome and Haematoxylin and Eosin (H&E) stained using an automated machine by HCBS.

2.1.3.3 IMMUNOHISTOCHEMICAL STAINING

Lung explant sections were cut from the FFPE blocks into sections of 4 µm and mounted onto vectabond-treated slides (VectorLabs, UK) by HCBS. After air-drying in a 37 °C incubator overnight, the slides were ready to use. To facilitate de-waxing, the sections were put in a plastic rack and heated to 65 °C for 10 minutes and then immersed in xylene twice for 3 minutes each time. Next, they were rehydrated in 99% IMS twice for 1 minute, 95% (v/v) IMS for a further minute and soaked in slow-running tap water for 5 minutes. The rehydrated slides were immersed in a 500ml microwavable plastic container in 1x Citrate Buffer (10mM Sodium Citrate, pH 6.0) and microwaved for 20 minutes at 750W. The slides were then allowed to cool down for 20-40 minutes. The Novolink™ Polymer Detection system (Nakane & Pierce, 1966; Tsutsumi *et al.*, 1995) kit

supplied by Leica Microsystems (Milton Keynes, UK) was used for all the immunohistochemical staining of slides in this study.

Following the antigen retrieval, slides were placed on a tray and incubated in peroxidase blocking solution [3–4% (v/v) Hydrogen peroxide] for 5 minutes to neutralise any endogenous peroxidase activity. Samples were then washed in TBS (Tris-buffered saline, pH 7.6) twice for 3 minutes each time. Next, a protein blocking solution (0.4% Casein in phosphate-buffered saline, with stabilizers, surfactant, and 0.2% Bronidox L as a preservative) was added onto each section for 5 minutes to reduce non-specific binding, followed by two washes in TBS for 3 minutes each time. The diluted antibody solutions were added onto the slides (~100µl per slide) and incubated overnight at 4 °C. The primary antibodies used (Table 2.2) were diluted in blocking solution made with 3% Bovine Serum Albumin (BSA), 0.1% (v/v) Triton X-100 (Fisons, UK) in TBS to provide the highest quality of specific binding of the antibodies on the tissue. A no primary antibody control slide was included each time.

After incubation with each primary antibody, the slides were washed in TBS twice for 3 minutes, incubated with post primary blocking solution [Rabbit anti mouse IgG (<10 µg/mL) in 10% (v/v) animal serum in TBS/0.09% ProClin™ 950] for 30 minutes and washed again in TBS twice for 3 minutes. The post primary block solution is used to detect mouse immunoglobulins by rabbit anti-mouse antibodies. The slides were then incubated with the Novolink Polymer [Anti-rabbit Poly-HRP-IgG (<25µg/mL) containing 10% (v/v) animal serum in TBS/0.09% ProClin™ 950] for 30 minutes. The polymer recognises rabbit immunoglobulins and therefore detects any post primary and any tissue bound rabbit primary antibodies. The polymer creates HRP-linker (horse-radish peroxidase) antibody conjugates which can be visualised when the sections are incubated with the Novolink DAB substrate buffer and DAB chromogen (1.74% w/v 3, 3'- diaminobenzidine, in a stabilizer solution). The reaction with the peroxidase produces a brown precipitate allowing visualisation of the staining. After washing in water, the sections were counter-stained with haematoxylin for 30 seconds and after serial dehydrating of the slides (95% IMS, 99% IMS and xylenes), they were mounted onto coverslips using DPX mounting solution. The

result of the staining was viewed under a LEICA DM 2500 microscope and photographed with a LEICA DFC 420 camera.

Table 2.2. Antibodies used in this study

Antibody	Species	Dilution	Source
Phospho-Akt (ser473)	Rabbit (monoclonal)	1:100	Cell Signaling #4060S
Phospho-p44/42 Mapk	Rabbit (polyclonal)	1:400	Cell Signaling #9101S
Cleaved PARP [E51]	Rabbit (monoclonal)	1:6000	Abcam ab32064
Ki-67 Clone MIB-1	Mouse (monoclonal)	1:2000	DAKO M7240
Cytokeratin Clone MNF116	Mouse (monoclonal)	1:5000	DAKO M0821
P53 (DO1)	Mouse (monoclonal)	1:1000	Gift from David Lane
P21 [EA10]	Mouse (monoclonal)	1:50	Abcam ab16767

2.1.4 Analysis of Stained Sections

For quantifying the results of the nuclear staining with cleaved PARP and Ki-67 antibodies, images of the tumour explants in each slide were taken at 10x magnification (see Figure 2.2.A for illustration). Adobe Photoshop CS5.1 was used to photo-merge each image of each explant together (see Figure 2.2.B for illustration- File> Automate> Photomerge> Layout=Reposition/Blend images together) using overlapping images of each explant. Each picture represented one tumour explant fragment of which the tumour area was measured using ImageJ (Schneider *et al.*, 2012). Areas of necrosis (contiguous or overlapping cells with cleaved parp staining) were measured separately and were excluded from the tumour area. Also, as far as possible, stroma cells or inflammatory cells were removed from the pictures using ImageJ (see Figure 2.2.C for illustration). The ratio of the labelling index was analysed using ImmunoRatio (Tuominen *et al.*, 2010) which is a publicly available ImageJ plug-in for quantitative image analysis (see Figure 2.2.D for illustration). The parameters of the program were adjusted depending on the exposure of the images (blue

threshold adjustment ranged from 0 to -40 and brown threshold adjustment ranged from +10 to -30).

Finally, one additive number was obtained which represented all the staining from one slide and also had taken into account the area of the tumour cells for each explant on the slide. Because the tumour content and size of each explant is different, a bias could be introduced if the tumour area was not introduced in the calculations. Therefore the labelling index ratio of each explant on the slide was multiplied by its area to obtain a number from each available explant for each particular condition/treatment, which, when added together, represented all the staining in each slide.

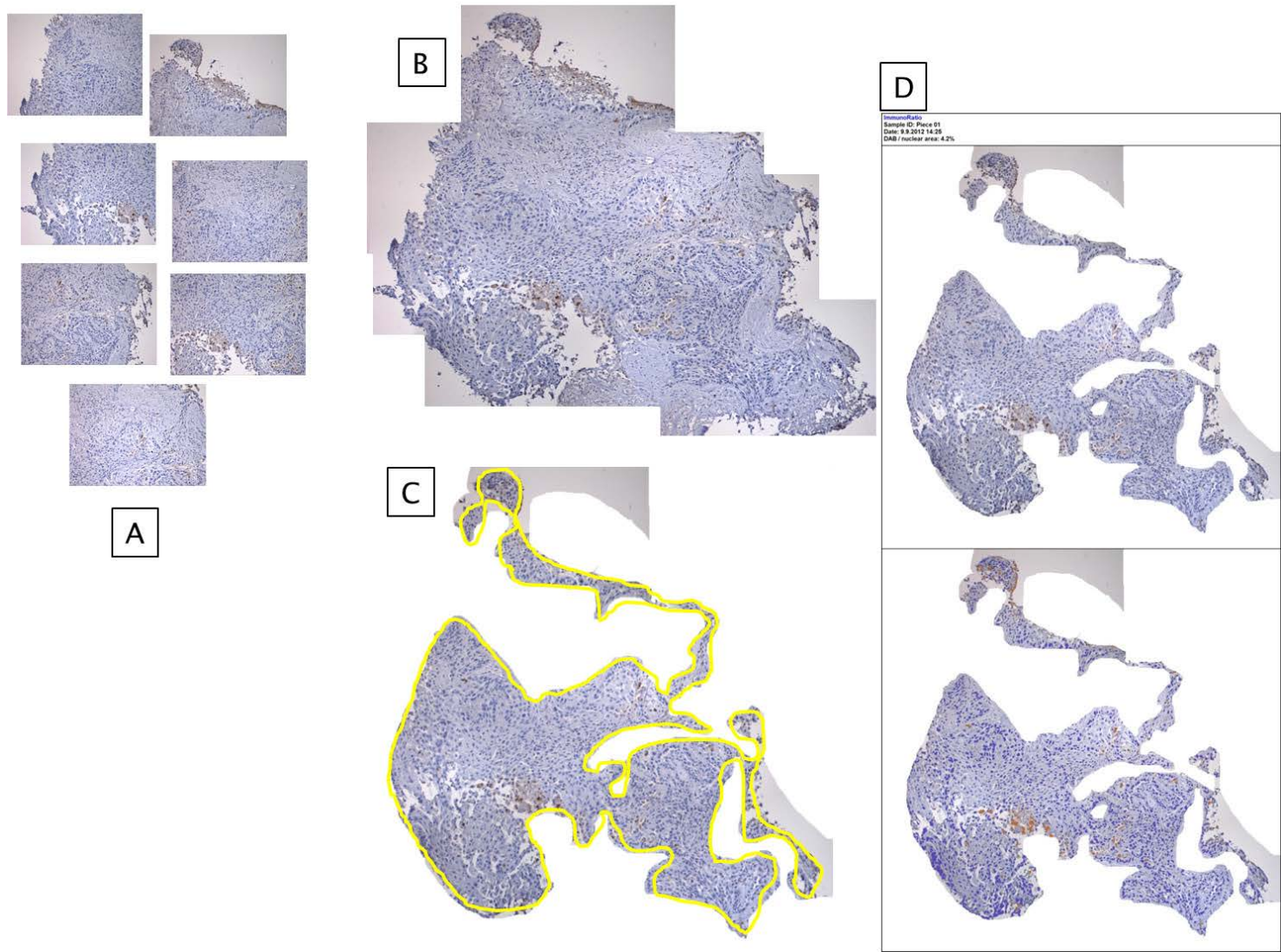


Figure 2.2. Analysis of stained sections. A) Pictures of the staining were taken at 10x magnification. B) Images from each piece were photo-merged together using Adobe Photoshop CS5.1. C) Stroma and inflammatory cells were removed from the image as far as possible and the tumour area was measured using Image J. D) The staining of the tumour cells was quantified with ImmunoRatio.

2.1.5 Representations of the Data

Three different ways were used to present data and graphs were created in GraphPad Prism 6.0 or Microsoft Office Excel 2010.

A) Separate graphs. Three different graphs (see Figure 2.3 for a graphic example).

There are three separate graphs for three separate variables in this type of representation:

- Ki67: each point on the graph represents all the staining of tumour cells from each explant.
- Apoptosis: each point on the graph represents all the nuclear cleaved PARP staining of tumour cells from each explant.
- Necrosis: each point on the graph represents all the necrotic area as a percentage of the total from each explant.

In this type of representation, we can see the intra-tumour differences between tissue fragments from one condition.

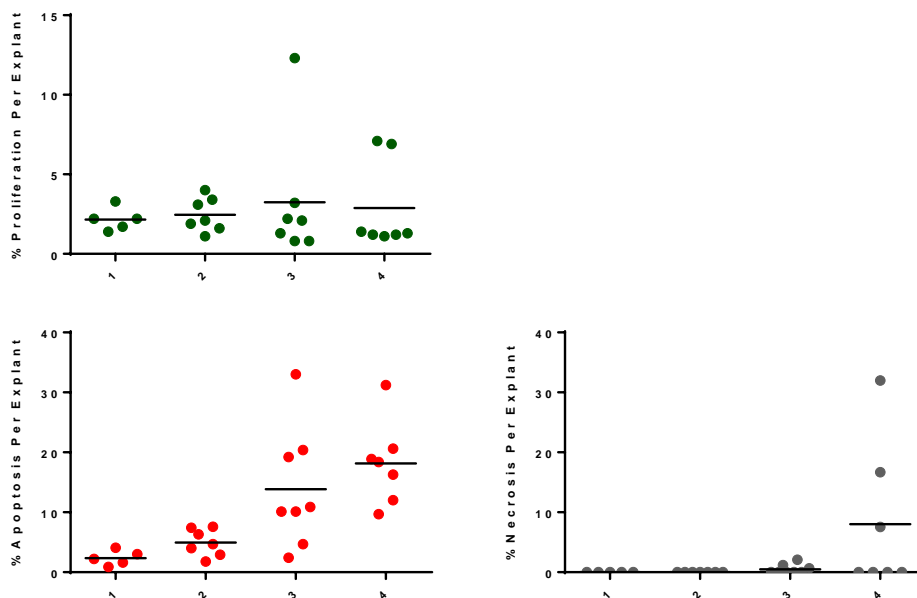


Figure 2.3. Separate graphs - 3 different graphs.

B) Combined graph (see Figure 2.4 for a graphic example). This graph contains three variables:

- Ki67: This value represents the percentage of the Ki67 positive tumour cells out of all tumour cells present in each condition/slide; added together taking into consideration the tumour area.
- Cleaved PARP: This value represents the percentage of the cleaved PARP nuclear stained positive tumour cells out of all tumour cells present in each condition/slide added together taking into consideration the tumour area.
- Necrosis Area: Represents areas judged necrotic as a measure of cleaved PARP leakage from each slide.

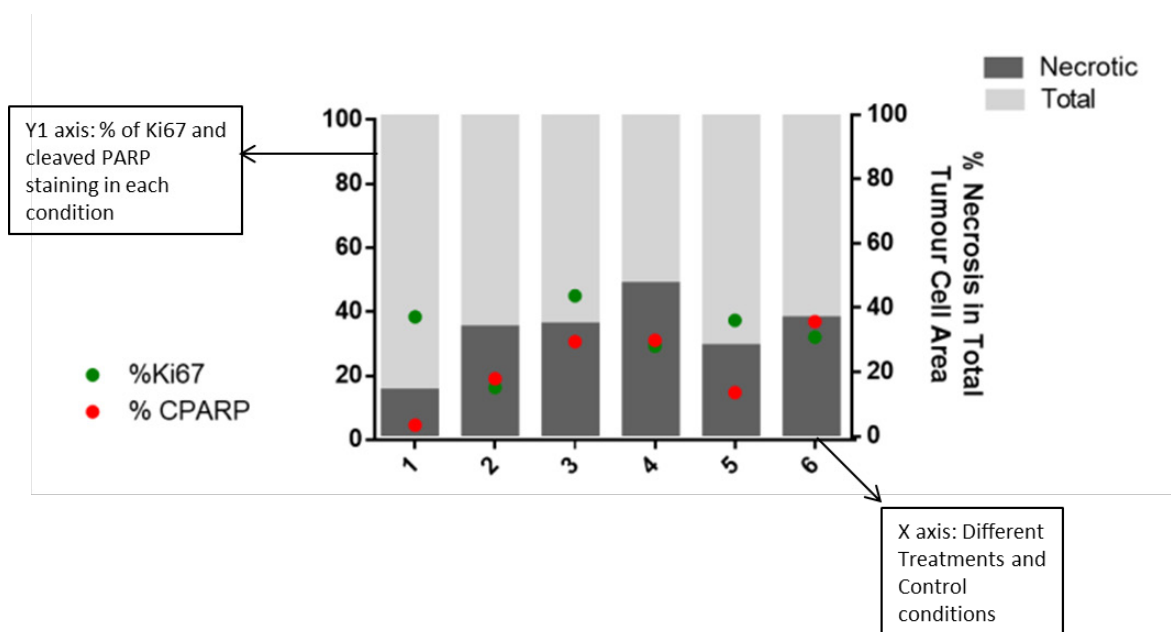


Figure 2.4. Combined graph.

C) Pooled cases Graph - two different graphs (see Figure 2.5 for an example).

To simplify the response from one treatment across a range of samples the apoptosis can be combined with necrosis to give one value for cell death.

$$\text{Cell Death} = \text{Apoptotic Area (Area for cleaved PARP x \% cleaved PARP staining)} + \text{Necrotic Area}$$

There are two variables: Ki67 and Cell Death in two separate graphs

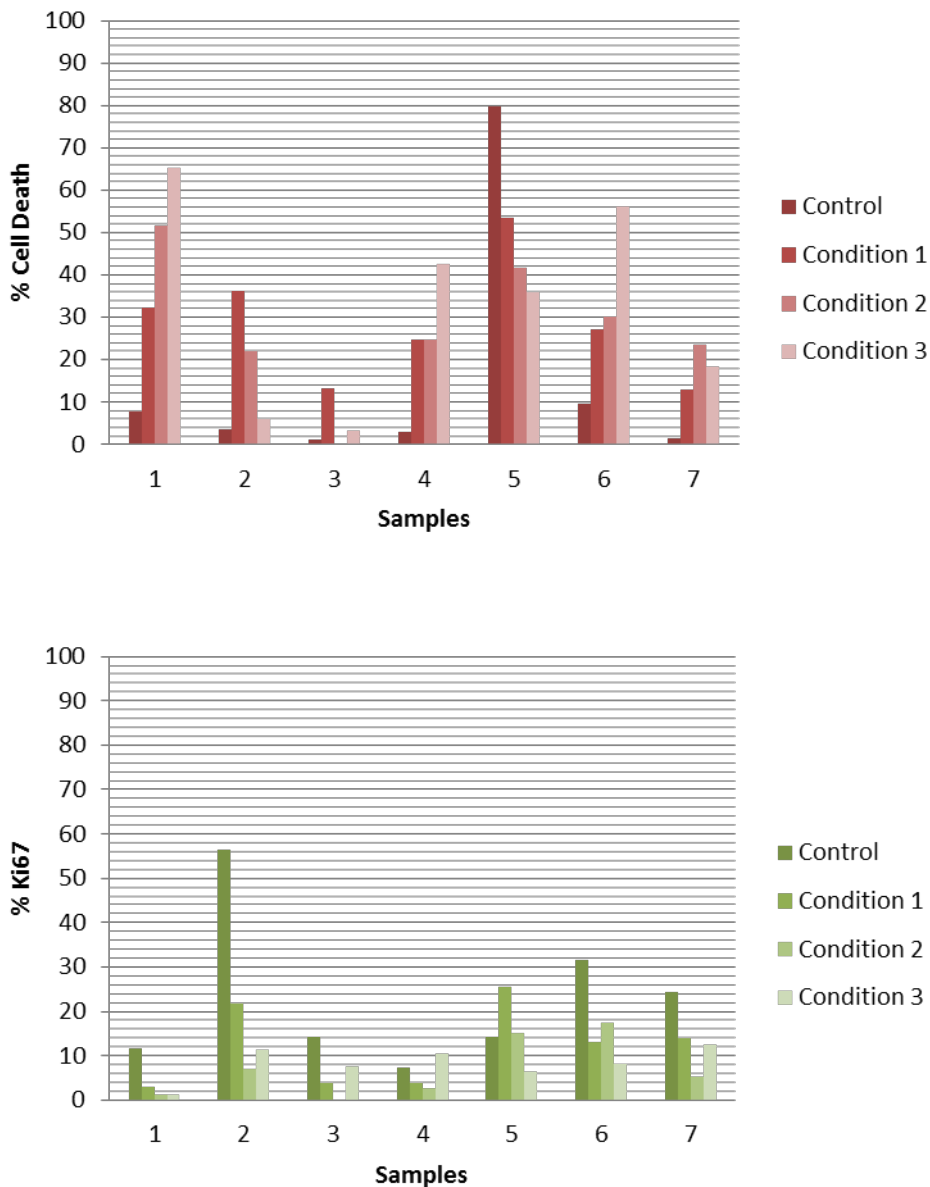


Figure 2.5. Pooled cases Graph - two different graphs.

D) Area Graph (see Figure 2.6 for an example)

The area of the tumour between conditions is sometimes different and it should be represented to show how powerful an observation is.

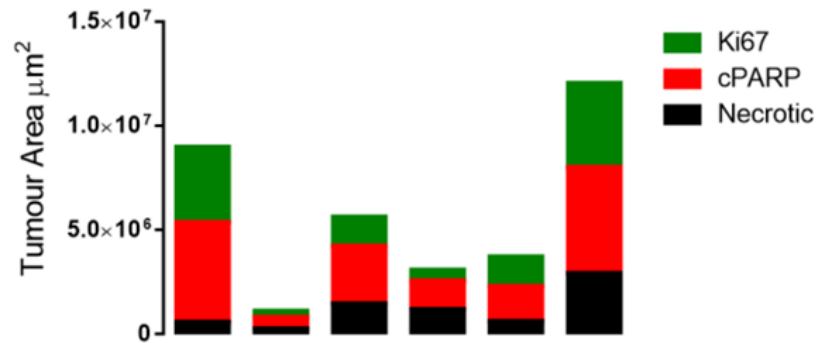


Figure 2.6. Tumour area graph. The tumour area used to measure the Ki67 and cleaved PARP staining is shown in green and red respectively. The necrotic area measured is shown in black.

2.2 DNA Isolation and Genotyping

2.2.1 *Extraction of genomic DNA from fresh tissue or cell lines*

Purification of genomic DNA was achieved by extraction with phenol: chloroform: isoamyl alcohol (25:24:1) solution according to the manufacturer's instructions (Sigma-Aldrich, UK). Lung tissue was lysed in 0.05M Tris pH8/0.1% SDS buffer (+ 0.5mg/ml Proteinase K) overnight at 60°C. An equal volume of phenol: chloroform: isoamyl alcohol (25:24:1) was added to the samples and then centrifuged at 13,000 rpm for 5 minutes. The upper layer containing DNA was carefully pipetted and transferred into new microcentrifuge tubes. An equal volume of chloroform: isoamyl alcohol (24:1) was added to the samples to wash the phenol out and the samples were centrifuged at 13,000 rpm for 5 minutes. The upper layer containing DNA was carefully pipetted and transferred into new microcentrifuge tubes. The DNA was precipitated by adding one-tenth volume of 1 M NaCl and three volumes of ice cold absolute ethanol. Resultant solutions were mixed briefly by hand for a few seconds. The samples were then centrifuged for 10 min and after carefully removing the supernatant, the DNA pellets were washed in 70% (v/v) ethanol. Finally, the DNA pellets were centrifuged again, air-dried and re-suspended in 150 µl of 1×TE (Tris at pH 9.0, EDTA) and stored at 4°C.

2.2.2 *Extraction of genomic DNA from FFPE tissues*

FFPE tissue sections were de-waxed and rehydrated using the same method as described in 2.2.1. Tissues were carefully scraped off the slide using a pipette tip and they were re-suspended in 500 µl Tris pH8/0.1% SDS + 25 µl of Proteinase K (10mg/ml) and digested at 56°C for three days. 25 µl of Proteinase K were added each day to assist protein digestion. The same method described in 2.2.1 was then used to extract the DNA using the phenol-chloroform method. Some differences were introduced because of the small amounts of DNA present in FFPE tissues. At the step where the precipitation of DNA occurs by adding the NaCl and ethanol, the tubes were left to incubate at -20°C overnight to increase the amount of precipitated DNA to the maximum. The samples were

then centrifuged at 13000rpm for 15 minutes at 4°C and again washed with 70% (v/v) ethanol and re-centrifuged. The pellets were air-dried and re-suspended in 50µl of TE.

2.2.3 Quantification of DNA

The concentration of DNA was determined using the NanoDrop Spectrophotometer ND-1000 (NanoDrop Technologies, USA). 1µl of DNA was loaded onto the pedestal and absorbance was measured at A260 and A280 nm. The purity of the samples was verified by comparing the absorbance values at 260 and 280 nm with pure DNA having an A260/280 anticipated ratio of ~1.8.

2.2.4 Oligonucleotide primers and probes for mutation analysis

All primers and probes were designed in house using web-based programs such as Primer 3 and the Primer Express version 3.0 from Applied Biosystems. The primers (Sigma-Aldrich, UK) were used at a working concentration of 10 pm/µl. The probes (Applied Biosystems, USA) were Taqman® and were designed to recognise common point mutations in some key genes as found in the Catalogue of Somatic Mutations in Cancer (COSMIC-<http://cancer.sanger.ac.uk/cancergenome/projects/cosmic/>) database. Most of the primers and probes used in this study (Table 2.3) were designed and validated by past members of Dr Howard Pringle's lab, Department of Cancer Studies, University of Leicester. The primers and probes for the EGFR exon 19 deletions were designed according to this study (Endo *et al.*, 2005) and they were intended to identify some of the most common deletions of exon 19 of *EGFR* according to the COSMIC database.

The probes were labelled with different reporter dyes at their 5' end, the wild-type probes were VIC™ labelled and the mutant probes were FAM™ labelled. Each probe also had a minor groove binder (MGB) and a non-fluorescent quencher at their 3' end. The MGB increases the stability of the probes (Afonina *et al.*, 1997). The Taqman principle (Figure 2.7) is that on an intact probe, the quencher prevents the reporter dye to fluorescence. When the probe hybridizes

to the target sequence, DNA polymerase extends from the primer to the probe and cleaves it with its 5' nuclease activity. This separates the quencher and the dye, resulting in fluorescence by the reporter dye. Therefore, the fluorescence signal generated in a PCR reaction is proportional to the amount of product formed.

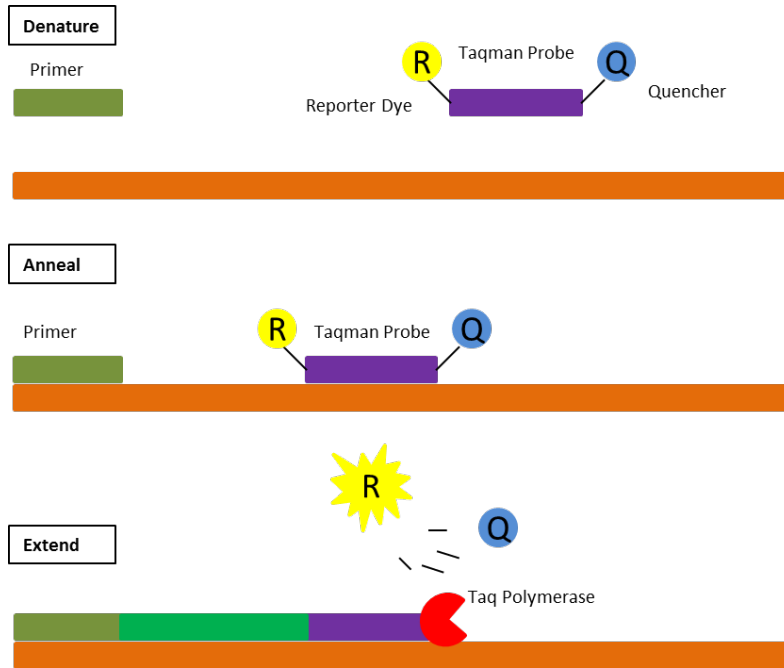


Figure 2.7. The Taqman Principle.

Table 2.3. Primers and Probes used in this study.

Mutation	Description	Sequence	Label
PIK3CA G1663A	Forward	5'-GCAATTTCTACACGAGATCCTCTCT-3'	None
	Reverse	5'-CATTTTAGCACTTACCTGTGACTCCAT-3'	None
	Wild-type	5'-TGAAATCACTAAGCAGGA-3'	VIC
	Mutant probe	5'-ATCACTGAGCAGGAGAA-3'	FAM
PIK3CA A3140G	Forward	5'-CAAGAGGCTTTGGAGTATTTTCATG-3'	None
	Reverse	5'-TGTTTAATTGTGTGGAAGATCCAATC-3'	None
	Wild-type	5'-ATGCACGTCATGGTG-3'	VIC
	Mutant probe	5'-ATGCACATCATGGTGG-3'	FAM
BRAF V600E	Forward	5'-TCATGAAGACCTCACAGTAAAAATAGGT-3'	None
	Reverse	5'-ATCCAGACAACCTGTTCAAACCTGATG-3'	None
	Wild-type	5'-TAGCTACAGTGAAATC-3'	VIC
	Mutant probe	5'-TAGCTACAGAGAAATC-3'	FAM
KRAS	Forward	5'-AGGCCTGCTGAAAATGACTGA-3'	None
	Reverse	5'-TGTATCGTCAAGGCACTCTTGC-3'	None
	Wild-type	5'-CTACGCCACCAGCTC-3'	VIC
34G>T,C,orA	Mutant probe	5'-TACGCCACDAGCTC-3'	FAM
35G>T,C,orA	Mutant probe	5'-TACGCCADCAGCTC-3'	FAM
38G>A	Mutant probe	5'-CTACGTCACCAGCTC-3'	FAM
EGFR exon 19	Forward	5'-CCCAGAAGGTGAGAAAGTTAAAATTC-3'	None
	Reverse	5'-AGCAGAACTCACATCGAGGATT-3'	None
	Wild-type	5'-AGGAATTAAGAGAAGCAACATCT -3'	VIC
Del2235-2249, Del2236-2250	Mutant probe	5'- CTATCAARACATCTCCG-3'	FAM
Del2240-2254	Mutant probe	5'- ATCAAGGAATCTCCGAAAGC-3'	FAM
Del2240-2257, Del2239-2256	Mutant probe	5'- CTATCAAGGAAYCGAAAGC -3'	FAM
EGFR T2573G	Forward	5'-AACACCGCAGCATGTCAAGA- 3'	None
	Reverse	5'-CCGCACCCAGCAGTTTG-3'	None
	Wild-type	5'- ACAGATTTTGGGCTGG- 3'	VIC
	Mutant probe	5'- CAGATTTTGGGCGGG- 3'	FAM

2.2.5 Quantitative PCR (qPCR)

The primers and probes were used to test for mutations in DNA from the lung samples. Each PCR reaction was set-up on ice and consisted of: 3 μ l DNA (10ng/reaction), 5 μ l TaqMan Genotyping Master Mix (Applied Biosystems, UK), 0.6 μ l of forward and reverse primers; 0.2 μ l of wild-type probe (VIC) and 0.2 μ l of mutant probe (FAM) and 0.4 μ l of sterile Ultra Pure H₂O, making up a total reaction volume of 10 μ l. Each sample was performed in duplicate. In addition to the samples, a positive control for mutated or wild-type DNA (Table 2.4) was included for each probe set on every plate, along with a no template control (NTC) to assess whether genomic DNA contamination occurred during the PCR set-up. Plates were spun at 3000rpm for 30 seconds before the reaction. All reactions were performed on the Step-One thermal cycler (Applied Biosystems, USA) in the conditions shown in Figure 2.8. PCR reactions consisted of 40 cycles of 15 seconds denaturation at 95 °C and annealing and extension temperature for 1 minute. This temperature step varied between different probes according to each probes' annealing temperature (Table 2.4).

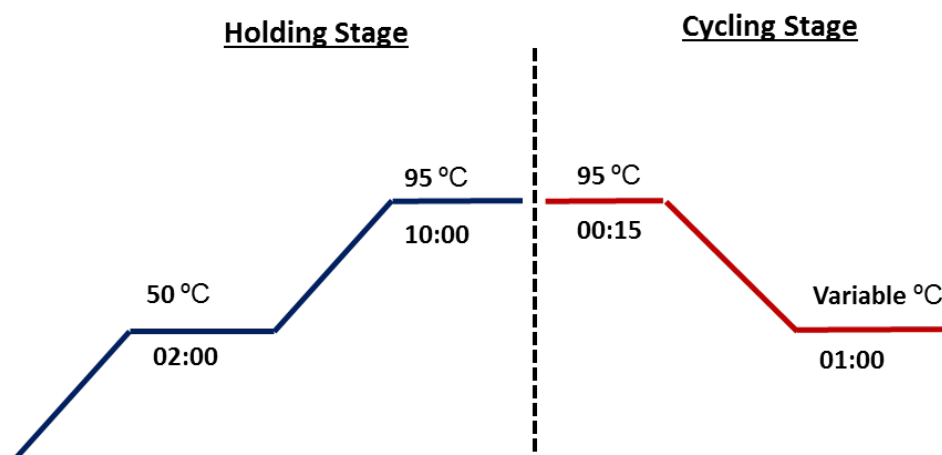


Figure 2.8. PCR Conditions.

Table 2.4. Mutation Probes Controls and Annealing Temperature.

Gene	Mutation/ Deletion	Positive Control	Wild-Type Control	Annealing Temperature
KRAS	34G>T, C or A	H358	Tonsil	63 °C
	35G>T, C or A	SW480	Tonsil	61 °C
	38G>A	HCT116	Tonsil	64 °C
PIK3CA	G1633A	MCF7	Tonsil	60 °C
	A3140G	HCT116	Tonsil	62 °C
EGFR	T2573G	H1975	Tonsil	57 °C
	Del2235-2249, Del2236-2250	HCC827	Tonsil	61 °C
	Del2240-2254	EGFR19D2 +ve	Tonsil	63 °C
	Del2240-2257, Del2239-2256	EGFR19D3 +ve	Tonsil	62 °C
BRAF	T1799A	Skme15	Tonsil	60 °C

2.3 Statistical Analysis

For statistical analysis of the IHC results, for unpaired samples the Mann-Whitney non parametric test was used. For paired samples, the Wilcoxon matched paired rank test was used when comparing two values only and the Friedman test was used when comparing more than two values. Correlations were investigated by Spearman's rho test. Trend analysis for matched samples was investigated by Page's L non-paramateric test manually using an excel spreadsheet from MRC (<http://imaging.mrc-cbu.cam.ac.uk/statswiki/FAQ/pagesL>). All other statistics were performed in GraphPad Prism 6.0. P values of <0.05 were considered statistically significant.

3. PATIENTS' DEMOGRAPHICS

3.1. Introduction

This chapter summarises the demographic data, histology and mutation status of the patients' samples. All the information regarding the patients was taken from the official histopathology report submitted for each patient by consultant pathologists working at Leicester Hospitals, unless otherwise stated.

3.2. Results

From March 2010 to November 2013, 60 tumour samples were collected from consented patients undergoing lung surgery at Glenfield Hospital in Leicester. *Ex-vivo* explant culture models were set up, when possible, immediately after surgery. For samples not collected on the same day as surgery, explants were not derived but the samples were processed for histological examination and DNA extraction.

3.2.1 *Demographics*

There were 34 male patients and 26 female patients giving a ratio of 57% and 43% respectively (see Table 3.1 and Figure 3.1). The median age of the patients was 71; with a range of 43 to 85 years old (see Table 3.1 and Figure 3.1). The majority of the patients were between 60 and 79 (75%).

3.2.2 *Smoking History*

Smoking history is known for 44 out of the 60 patients (see Table 3.1 and Figure 3.1). From these 44 only 3 patients were recorded as non-smokers. The rest were either ex-smokers (25/44) or current smokers (15/44).

Table 3.1 Patients' Characteristics.

Characteristic	Number (N = 60)	Usable explants (N=21)
Sex		
Male	34	11
Female	26	10
Age		
Median	71	70
Range	43-85	54-85
Age Groups		
40-49	1	0
50-59	7	2
60-69	19	8
70-79	26	8
80-89	7	3
Smoking History		
ex-smoker	25	10
smoker	15	2
non-smoker	3	1
unknown	16	8
Histology		
Adenocarcinoma	28	9
Squamous Cell Carcinoma	24	10
Large Cell Carcinoma	3	0
Adenosquamous	2	0
Atypical carcinoid tumour	2	2
Metastatic colorectal	1	0
Stages TNM		
pT1, pN0, pMx	1	0
pT1a, pN0, R0	1	1
pT1b, pN0, R0	3	2
pT2, pN0, pMx, R0	4	2
pT2, pN2b, pMX, R0	1	0
pT2a, pN0, pMx, R0	11	4
pT2a, pN1, pM1a, R0	1	0
pT2a, pN1, pMX, R0	3	1
pT2a, pN2, pMX, R0	4	0
pT2b, pN0, pMX, R0	5	1
pT2b, pN1, pMX	5	2
pT2b, pN1, pM1a	1	0
pT2b, pN2, pMx, R0	1	0
pT3, pN0, pMx	6	3
pT3, pN1, pMx	3	2
pT3, pN2, pMX	4	2
pT4, pN1(mi), pM1, Rx	1	0
pT4, pN1	1	0
Unclear from histopathology report	4	1
Stage groups*		
IA	5	3
IB	15	6
IIA	9	2
IIB	6	2
IIIA	17	6
IIIB	2	1
IV	3	0
Unknown**	3	1

*Stage groups were given according to the classification of TNM shown in Table 1.2.

**Unknown: could not be deduced because of insufficient information from histopathology reports.

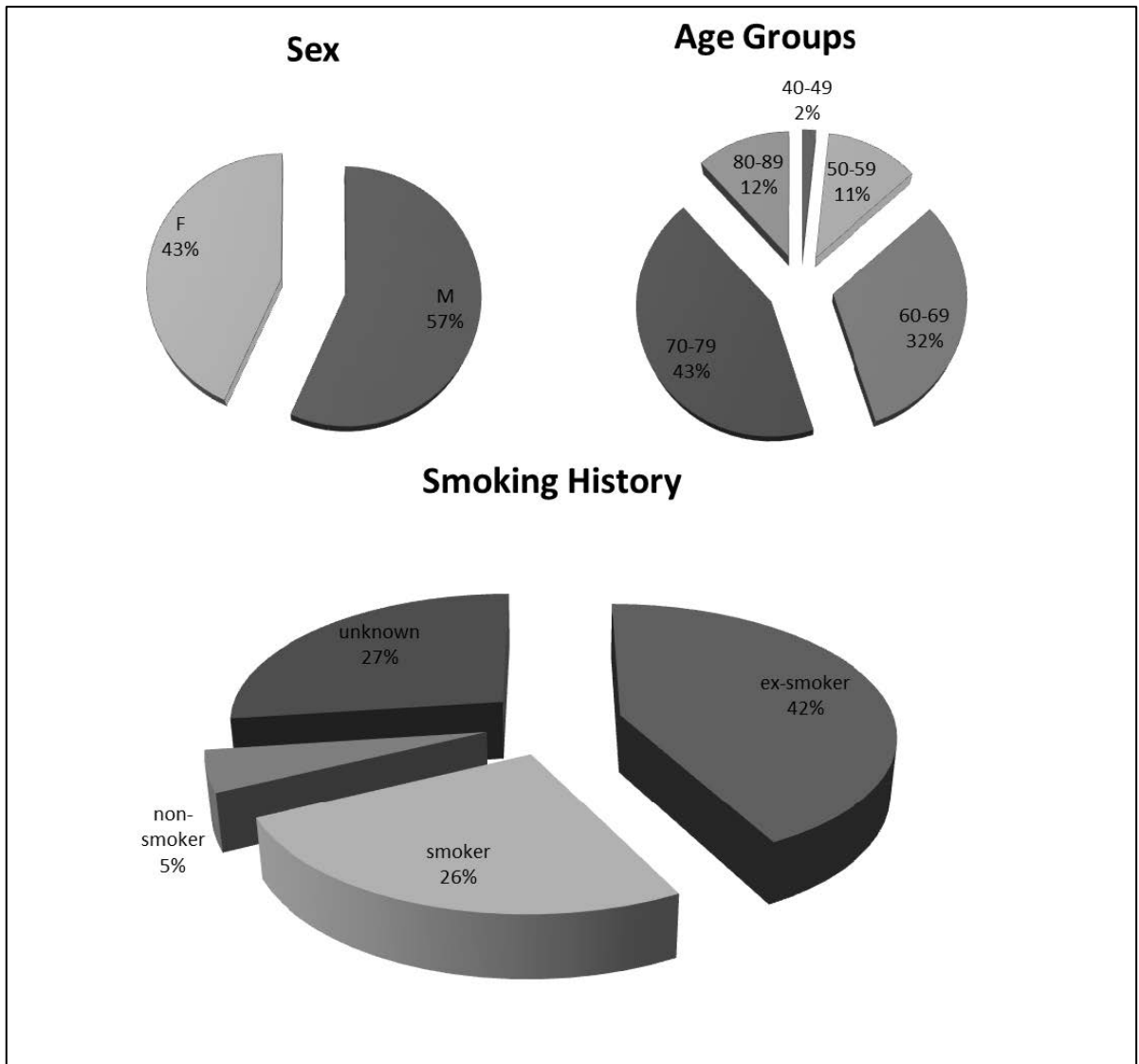


Figure 3.1. Sex ratio of patients, age group distribution and smoking history.

3.2.3 Histology

The majority of the patients fit into the adenocarcinoma or squamous cell carcinoma categories (see Table 3.1 and Figure 3.2) with 47% being adenocarcinoma (28/60) and 40% squamous cell carcinoma (22/60). There were three patients with Large Cell carcinoma histology, two patients with atypical carcinoid tumours and two patients with adenosquamous histology. One of the patients had metastatic colorectal cancer in their lungs.

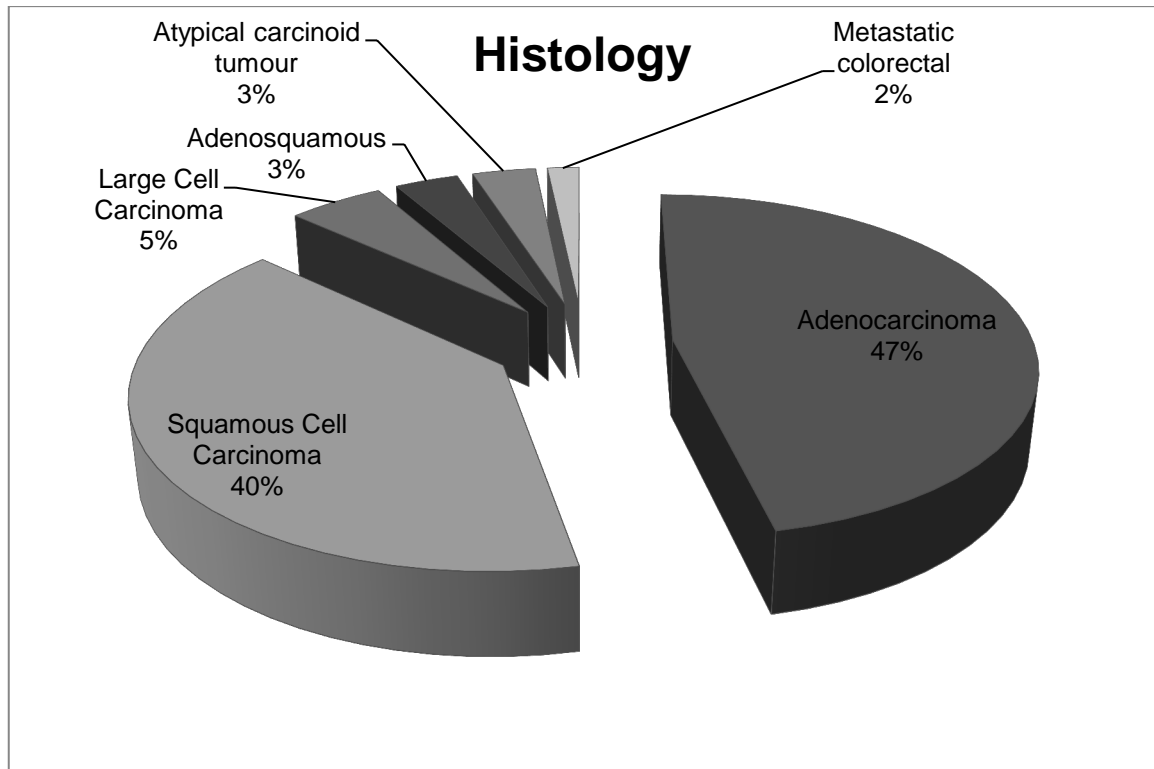


Figure 3.2. Histological categories of patients.

Adenocarcinoma histology can be further subcategorised into 5 different patterns: lepidic, acinar, solid, papillary and micropapillary. In this instance the majority of the histopathology reports did not categorise samples to their specific patterns (53%). Of the ones known, 18% were acinar adenocarcinomas, 11% lepidic, 11% mixed type, 3% papillary and 4% solid adenocarcinomas (see Figure 3.3).

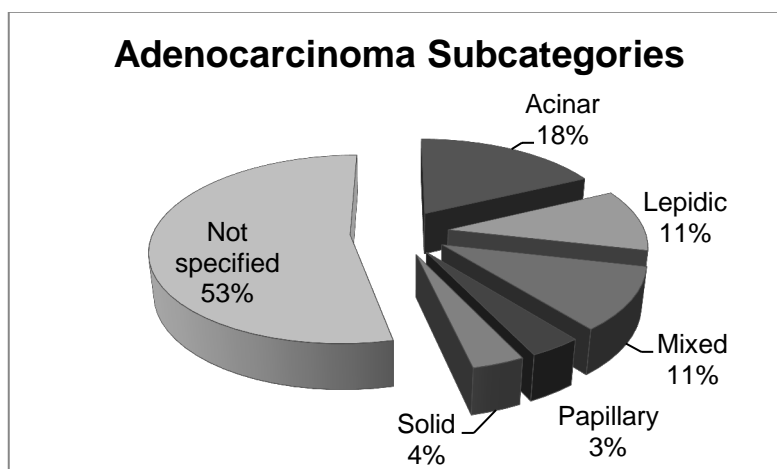


Figure 3.3. Adenocarcinoma subcategories.

3.2.4 Mutation Analysis

DNA was extracted from the majority of the samples (57/60) and mutation analysis by qPCR was performed for some point mutations in *KRAS*, *PIK3CA*, *EGFR* and *BRAF* genes (see section 2.2.4 & 2.2.5 for details). The mutation analysis was done in collaboration with Callum Rhakit. Figure 3.4 shows a representative example of the qPCR results. Each sample was always compared to a mutant and a wild-type DNA control. LT1 has clearly amplified both the WT and mutant probes indicating to have a heterozygous *PIK3CA* G1633A mutation status (Figure 3.4). The ΔCT shows that only a proportion of the DNA is mutated (Figure 3.4).

Out of the 57 tumours tested, 15 were found positive (see Table 3.3 for details); 9 had *PIK3CA* mutations, 4 *KRAS* and 2 *EGFR* mutations (see Figure 3.5).

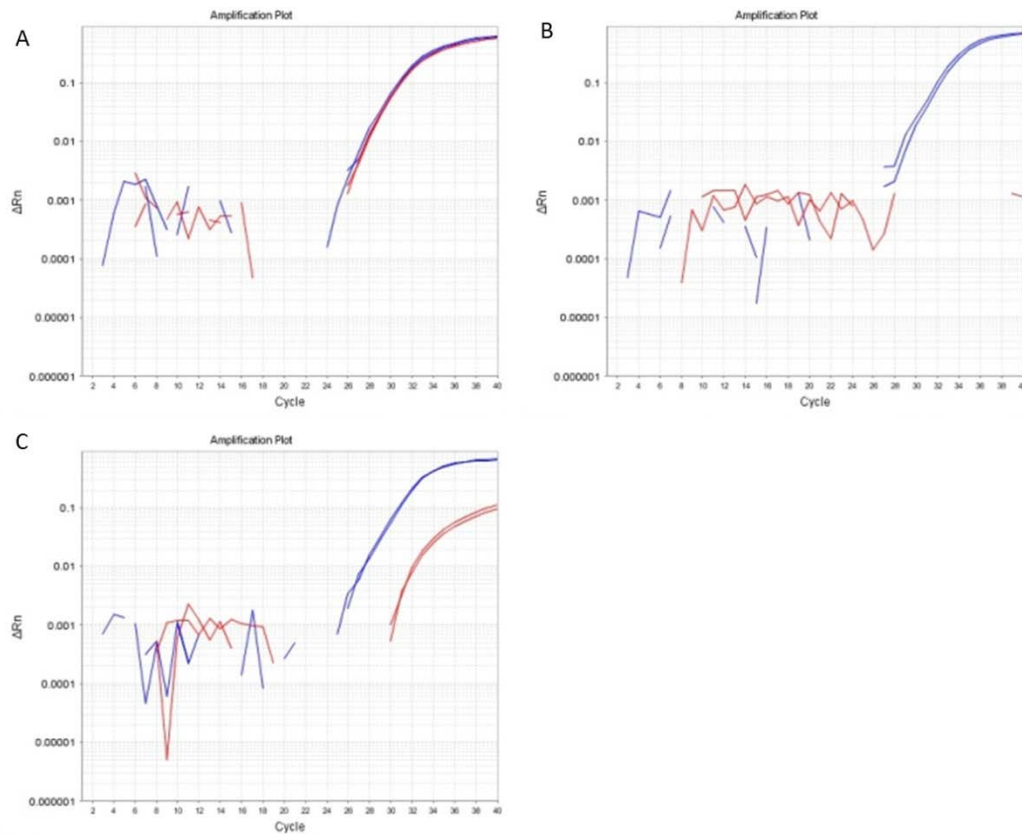


Figure 3.4. Graphical representation of qPCR mutation analysis results. The graphs show the amplifications of the mutant (red) and wild-type (blue) Taqman® probes in ΔRn per PCR cycle. Rn is the reporter signal normalized to the fluorescence signal of a passive reference dye. ΔRn is Rn minus the baseline. A) Positive mutant control DNA (PIK3CA G1633A) from MCF7 breast cancer cell line. B) Wild type control DNA from HCT116 colorectal cell line. C) DNA from lung tumour sample LT1 showing amplification of the PIK3CA G1633A probe.

Categorising the mutations by histology showed that the only mutation found in the squamous cell carcinoma histology was the *PIK3CA* with a frequency of 21% (see Figure 3.4). In contrast in samples with adenocarcinoma histology, a range of different mutations was present with *KRAS* being the most common (14%), *PIK3CA* (11%) and *EGFR* (7%).

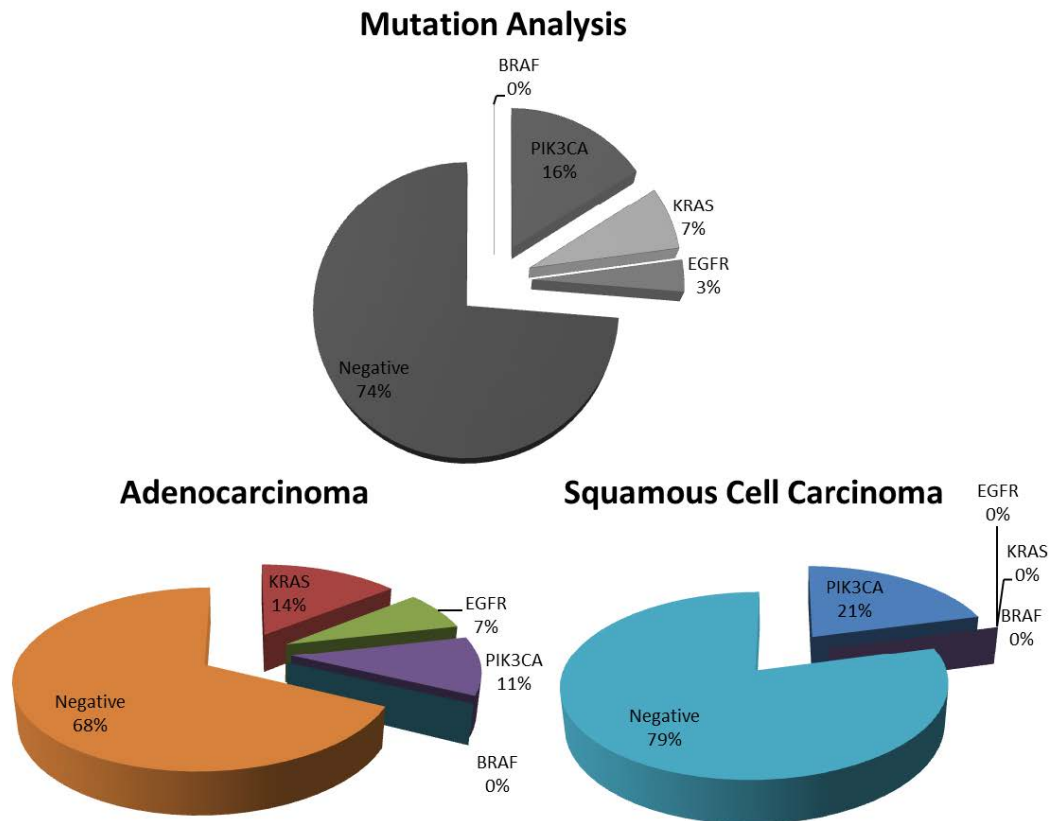


Figure 3.5. Mutation analysis in patient cohort (57/60).

The majority of the patients with identified mutations were classified as smokers or ex-smokers (13/15) with only 2/15 having an unknown status (see Table 3.3 for details).

Table 3.2 Mutations found in patient cohort.

Sample	Histology	Positive Mutation	Smoking History	Sex
LT4	Adenocarcinoma	KRAS 35G>T,C or A	Ex-smoker	F
LT9	Adenocarcinoma	KRAS 34G>T, C or A	Ex-smoker	F
LT51	Adenocarcinoma	KRAS 34G>T, C or A	Smoker	F
LT83	Adenocarcinoma	KRAS 34G>T, C or A	Ex-smoker	M
LT16	Adenocarcinoma	PIK3CA G1633A	Ex-smoker	F
LT21	Adenocarcinoma	PIK3CA G1633A	Ex-smoker	M
LT36	Adenocarcinoma	PIK3CA A3140G	Unknown	M
LT41	Adenocarcinoma	EGFR L858R	Smoker	F
LT49	Adenocarcinoma	EGFR L858R	Ex-smoker	M
LT2	Squamous cell carcinoma	PIK3CA G1633A	Ex-smoker	F
LT35	Squamous cell carcinoma	PIK3CA G1633A	Smoker	M
LT92	Squamous cell carcinoma	PIK3CA G1633A	Unknown	F
LT23	Squamous cell carcinoma	PIK3CA A3140G	Ex-smoker	M
LT38	Squamous cell carcinoma	PIK3CA A3140G	Ex-smoker	M
LT1	Adenosquamous	PIK3CA G1633A	Smoker	M

3.3 Discussion

Sixty patient samples were collected during the span of this project from consented patients undergoing lung surgery at Glenfield hospital. The majority of the patients were recorded as current or former smokers (41 out of 44 known smoking histories; Figure 3.1). This is in line with the strong link between tobacco smoke and lung cancer that has been established several years ago (Doll & Hill, 1950). Furthermore, the age distribution among the patients (see Figure 3.1) comes in agreement with Cancer Research UK statistics stating lung cancer occurs in 9 out of 10 people aged 60 or more. Also there is a comparable number of female to male patients with 43% and 57% respectively, mirroring the general trend of the increase of female patients with lung cancer which reflects smoking patterns between sexes. It has been revealed that the number of female smokers has been slightly increasing while male smoker population has been decreasing over the past years (Cancer Research UK).

The most common histological category of NSCLC among the 60 patients is adenocarcinoma with a frequency of 47% (28/60). In most countries, adenocarcinoma is the most common subtype of NSCLC with frequencies ranging from 35 to 45% (Walters *et al.*, 2013). However, it has been recorded that in the UK squamous cell carcinoma is slightly more common with 27% compared to 25% of adenocarcinomas and 23% of large cell lung cancers (Walters *et al.*, 2013). This is not the case with our patient cohort that shows adenocarcinoma to be more common (47%) to squamous cell carcinoma (40%) and large cell carcinoma which was only identified in 3 patients giving it a frequency of 5% (Figure 3.2). This could be a result of the small population size of 60 patients.

The mutation analysis has identified *PIK3CA* point mutations G1633A and A3140G to be the most common in this study with a frequency of 16% across all samples (Figure 3.5) which is higher than that previously reported in a number of studies so far which state an incidence of only ~3-4% (Ji *et al.*, 2011, Kawano *et al.*, 2006, Okudela *et al.*, 2007, Samuels *et al.*, 2004). This is followed by *KRAS* point mutations with a frequency of 7% and *EGFR* point mutation L858R at 3% across all samples. Distributing the mutations according to the two main

histology categories (Figure 3.5), adenocarcinoma and squamous cell carcinoma, shows differences between the frequencies of the mutations. Firstly, *PIK3CA* mutations are the only ones identified in squamous cell carcinoma with a frequency of 21%. The prevalence has been recorded as higher in squamous cell carcinoma (Okudela et al., 2007; Kawano et al., 2006) however, the frequencies reported for *PIK3CA* mutations in both squamous cell carcinoma (~5 and ~12%) and adenocarcinomas (~2-3% and ~4-5%; Li et al, 2013; Heist & Engelman, 2012, respectively) are significantly lower than in this study.

In samples with adenocarcinoma histology, mutations of *KRAS* (14%), *PIK3CA* (11%) and *EGFR* (7%) were identified. The adenocarcinoma histology has been linked with more mutations in a number of genes compared to squamous cell carcinoma histology. *KRAS* has been found to be frequently mutated in 15-30% of NSCLC patients and is predominantly found in adenocarcinoma (Roberts et al., 2010; Reungwetwattana et al., 2012). *EGFR* mutation frequencies identified in this study (7% in adenocarcinomas) are more or less in agreement with reports that they are seen in ~10% of lung cancer patients from Northern America and Western Europe and in ~30-50% in patients of East Asian descent (Sharma et al., 2007).

To conclude, *PIK3CA* has been identified to be far more commonly mutated than reported, in our study. Nevertheless, it should be kept in mind that the number of samples analysed in this study (57) is very small in comparison with the published literature therefore more samples are required to compose statistically significant conclusions.

4. DEVELOPMENT OF AN EXPLANT CULTURE SYSTEM FOR NSCLC SAMPLES

4.1 Introduction

Three-dimensional culture models of human tumours provide an easier, less expensive and less time-consuming approach to preclinical modelling in animal models, since they can reliably reflect tumour growth *in vivo* (Pampaloni et al., 2007). Professor MacFarlane's group (MRC Toxicology Unit, Leicester) recently used *ex-vivo* explant cultures with IHC as an end point to examine the response of breast carcinomas *in situ* to the cytotoxic ligand, TRAIL and found that primary explants were more predictive of patient outcome than tumour-derived cell line cultures (Twiddy, D., et al., 2010- poster abstract). Based on this, the aim of my PhD was to develop the model further and establish the best conditions for NSCLC with the objective to test the efficacy of existing drugs as well as novel drug combinations.

4.2 Aims and Objectives

- Evaluation of the best way to analyse data and to present the results.
- Optimisation of the explant model for NSCLC samples by testing different foetal calf serum (FCS) concentrations and assessing varying culture times.

4.3 Results

4.3.1 Staining

In some of the NSCLC cases, the histology was complex resulting in difficulties in identifying the tumour cells from the stroma in H&E stains. Thus, the DAKO antibody clone MNF116 which reacts with cytokeratins 5, 6, 8, 17 and probably also 19 was used to detect cells of epithelial origin (see Figure 4.1) since it stains human epithelial tissue from simple glandular to stratified squamous epithelium.

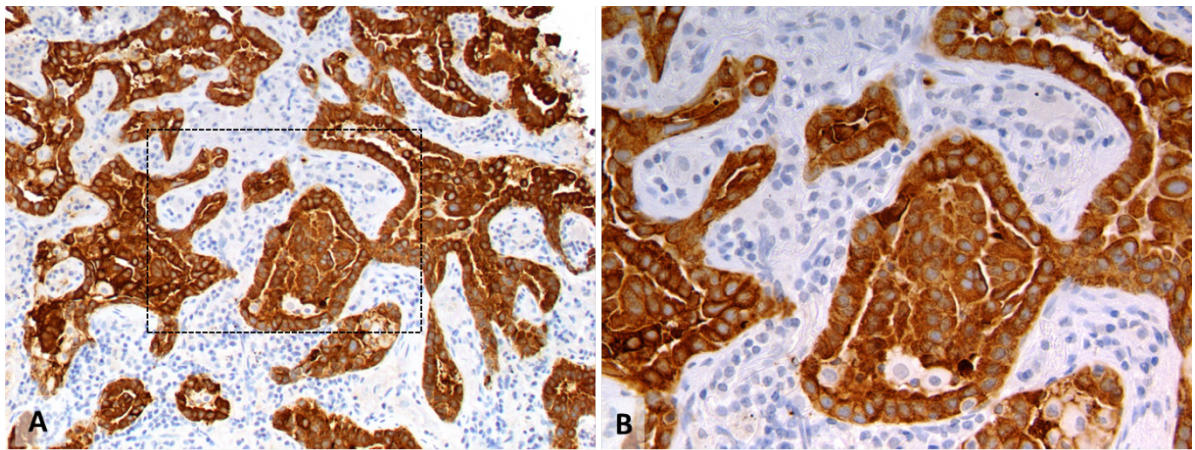


Figure 4.1. MNF116 stained sample example image. MNF116 (epithelial cell marker) was used to identify tumour areas in difficult samples. A) Low power view (x20) of MNF116 staining in an explant case. B) Higher power magnification (x40) of a stained area.

All the samples were stained with Ki67 as a proliferation marker (Figure 4.2) and cleaved PARP as an apoptosis marker. The latter was also used as a necrosis marker as indicated by contiguous or overlapping cells with cleaved PARP staining (see Figure 4.3).

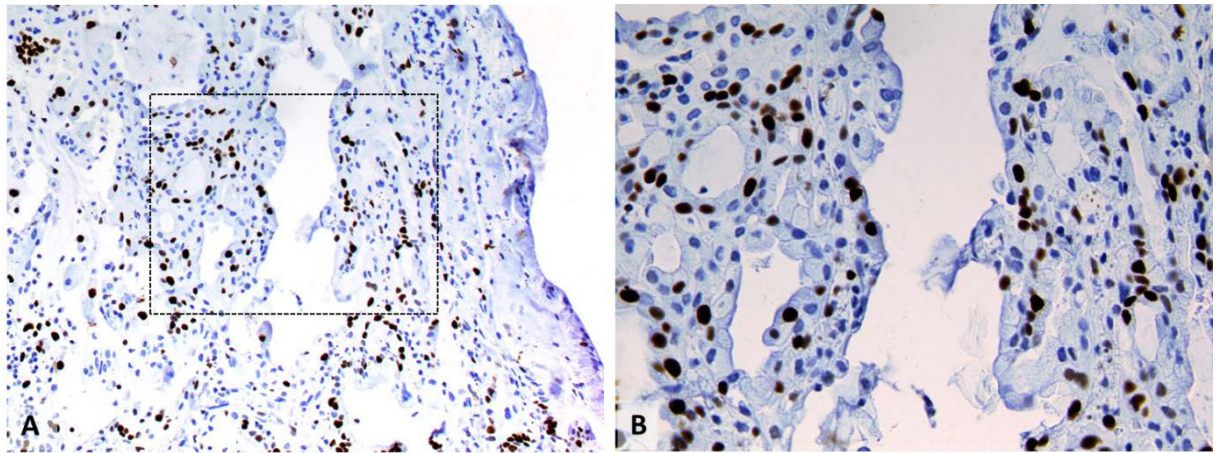


Figure 4.2. Image of Ki67 staining to assess proliferation. A) Low power view (x20) of Ki67 staining in an explant case. B) Higher power magnification (x40) of a stained area.

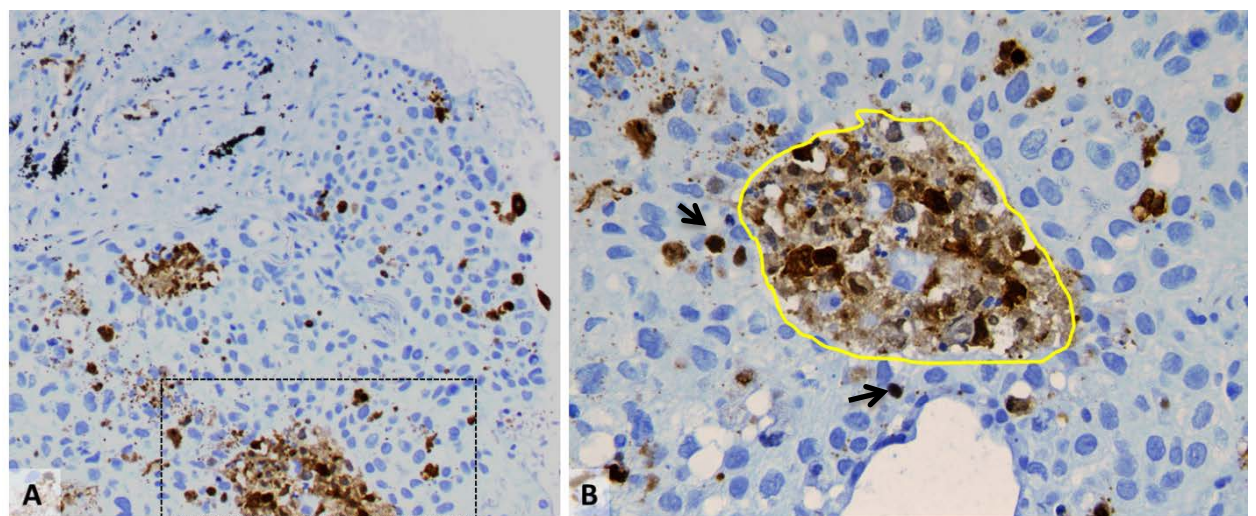


Figure 4.3. Image of cleaved PARP staining to assess apoptosis. A) Low power view (x20) of cleaved PARP staining in an explant case. B) Higher power magnification (x40) of a stained area. Black arrows indicate to cells undergoing apoptosis. Area circled in yellow represents an example area that was measured as necrotic.

4.3.2 Analysis

A substantial amount of time was spent in the optimisation of the assay conditions and in developing the best analysis method. Automatic scanning equipment was not available to us and therefore an approach was used based on the Immunoratio software which is a publicly available software as an Image J plugin developed by Tuominen, V.J. et al (Tuominen *et al.*, 2010). To validate this method of counting, the Immunoratio values from 30 images representing three different cases stained with either cleaved PARP or Ki67 were compared with the corresponding manual count values. Figure 4.4 shows the Bland-Altman graph of Immunoratio vs manual counting or difference plot, which is a graphical method to compare two measurement techniques (Bland & Altman, 1986). In this graphical method the differences between the two techniques are plotted against the averages of the two techniques and all the points but one are within the limits of agreement (From -17.69 to 12.74; Figure 4.4). From this result, and the correlation coefficient (0.96; P Value <0.0001) between the two techniques, it was concluded that Immunoratio is not statistically different from manual counting and this gave us confidence to use it for analysing the cases.

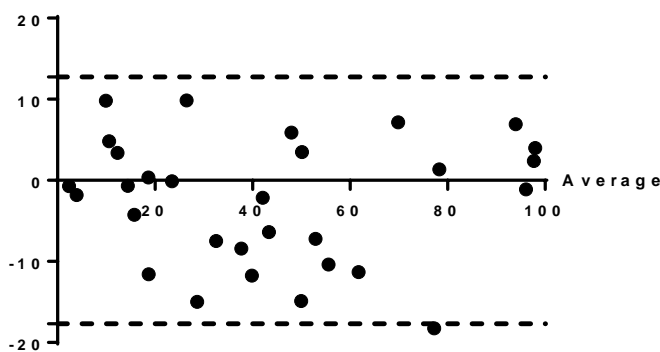


Figure 4.4. Comparison of Immunoratio vs manual counting with Bland-Altman. 30 different images of areas that were stained with either cleaved PARP or Ki67 from three different cases were counted manually and the same images were counted using the Immunoratio software. The differences between the two techniques are plotted against the averages of the two techniques. The dotted lines represent the 95% confidence intervals of the limits of agreement (From -17.69 to 12.74). The correlation coefficient between the two methods is 0.96 (P Value <0.0001).

The possibility of using images taken with the 10x objective instead of the 20x objective was assessed in order to decrease the amount of time spent on taking the images and their subsequent analysis, by analysing corresponding images at 10x and 20x magnifications (Figure 4.5). Comparison between the measurements of tumour areas using Image J taken with the two different objectives, 10x and 20x, showed high correlation (Spearman correlation = 0.99; $P < 0.0001$). Furthermore, comparison between the ImmunoRatio % labelling index of images taken with the two different objectives also showed high correlation (Spearman correlation = 0.81; $P < 0.0001$). Therefore it was decided to switch to taking the images at 10x magnification in order to increase time efficiency.

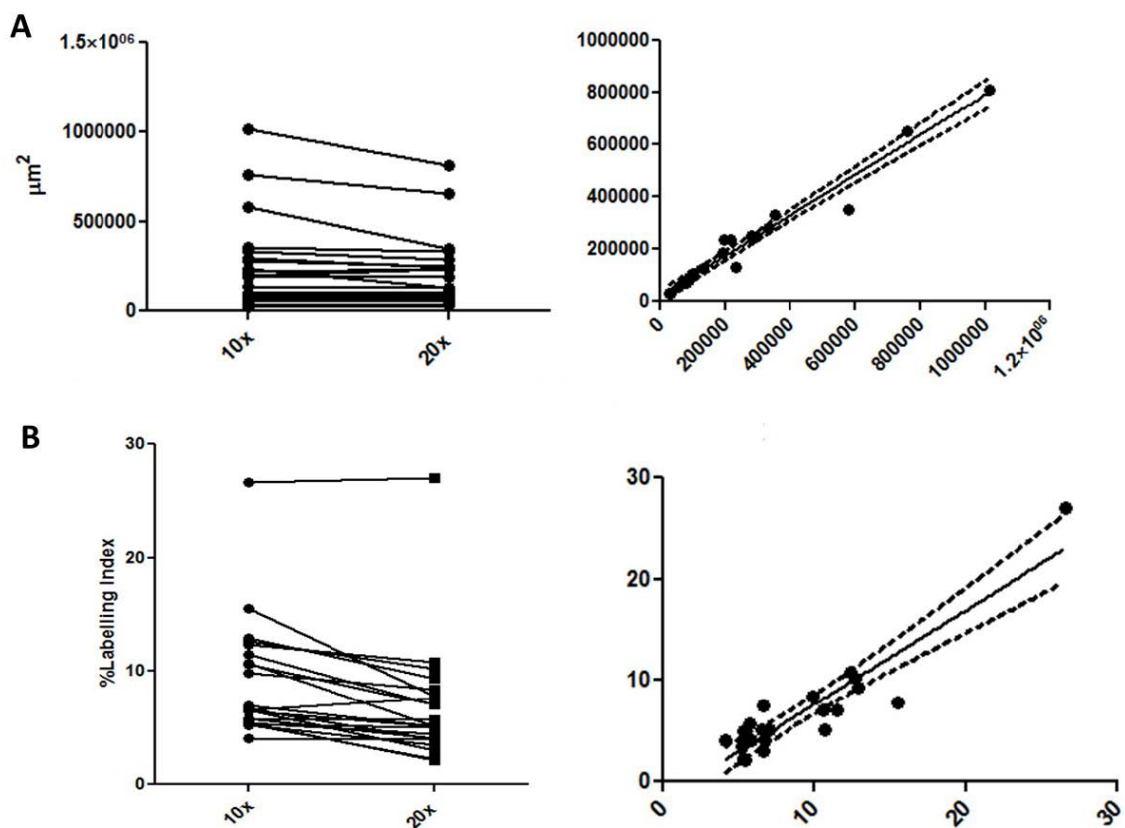


Figure 4.5. 10x photomicrographs are not significantly different than 20x. A) Comparison between the measurements of tumour areas using Image J taken with different objectives (10x and 20x). Spearman correlation = 0.99 ($P < 0.0001$). B) Comparison between the ImmunoRatio % labelling index of images taken with different objectives (10x and 20x). Spearman correlation = 0.81 ($P < 0.0001$).

Therefore, the final analysis method for quantifying the results was to take the images at 10x magnification from the entire slide, stitch each image together with Adobe Photoshop, measure the tumour area using Image J and then find the ratio of the labelling index using ImmunoRatio (Tuominen et al, 2010).

This resulted in the following measurements from the analysis of each case:

- % Apoptosis (labelling index of cleaved PARP)
- % Proliferation (labelling index of Ki67)
- Tumour Area Undergoing Apoptosis (in μm^2)
- Tumour Area Undergoing Proliferation (in μm^2)
- Area Undergoing Secondary Necrosis (in μm^2)

4.3.3 Intrinsic rates of proliferation and apoptosis in ex-vivo explant cultures

A total of 34 *ex-vivo* explant cultures were set up using various conditions, during the duration of this project. 23 of 34 were analysed fully whereas the remaining 11 of the cultures had problems that regarded them as not usable for further analysis. For example, 9 of these had levels of high necrosis in both the uncultured and cultured controls. This reflects poor quality of the samples with intrinsic necrosis which makes them unsuitable for culture. One case proved to be viable in the uncultured control but not in the cultured controls. Therefore in this case the sample did not survive the culture. And in the last of the 11 cases not analysed, the tissue was lost while cutting slides from the paraffin embedded explants for H&E staining, due to technical problems.

From the 23 analysed cases, one of the cases proved to have high background intrinsic necrosis (more than 60%) and another had high background necrosis in the controls, therefore it was decided not to include them in the results. Consequently, 12 tumour samples out of 34 (~35%) were too necrotic for analysis by this approach. If we include the one case that did not survive the

culture, 13 cases in total out of 34 (~38%) failed to be cultured as explant cultures.

The intrinsic rates of cell death or proliferation as assessed by cleaved PARP and Ki67 staining in uncultured samples were variable among the 21 viable cases as were levels of necrosis. These data are summarised in Figure 4.6. All the samples show low intrinsic cell death and low levels of inherent necrosis. The variability is more evident on Ki67 staining where three groups of proliferation can be seen; high, medium and low (Figure 4.6).

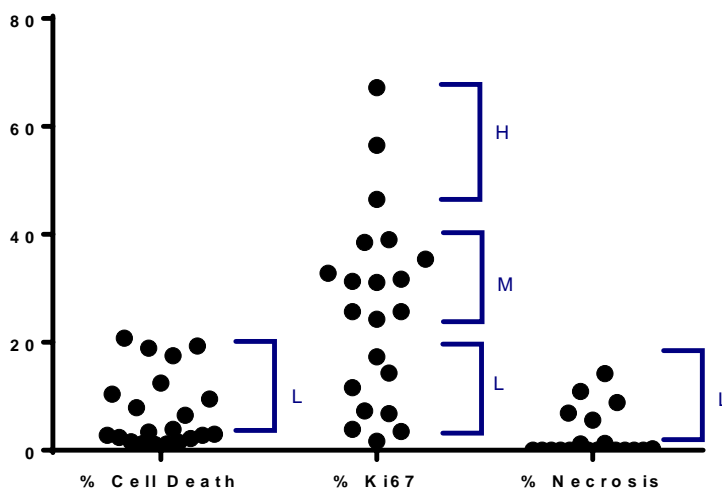


Figure 4.6. Intrinsic rates of combined cell death, proliferation and separate necrosis of all the usable ex-vivo explant cultures set up (21). H= High, M= Medium, L= Low. Each circle represents one sample.

When looking at the proliferation rates according to histology, squamous cell carcinoma ex-vivo explant cultures showed higher rates of intrinsic proliferation than either adenocarcinomas or atypical carcinoid tumours (Figure 4.7). This result was not significant with a Mann Whitney test (Mann-Whitney U=27.00; P=0.15) because of the low number of the cases; however the difference is clearly visible on the graph (Figure 4.7). There was no difference in intrinsic cell death rates across histologies (Figure 4.8).

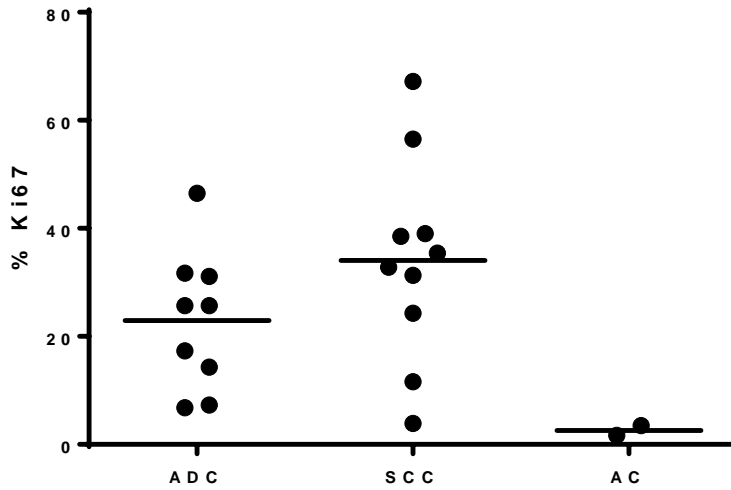


Figure 4.7. Intrinsic Rates of Ki67 staining across histologies. Each circle represents one sample. ADC= Adenocarcinoma, SCC= Squamous Cell Carcinoma, AC= Atypical Carcinoid.

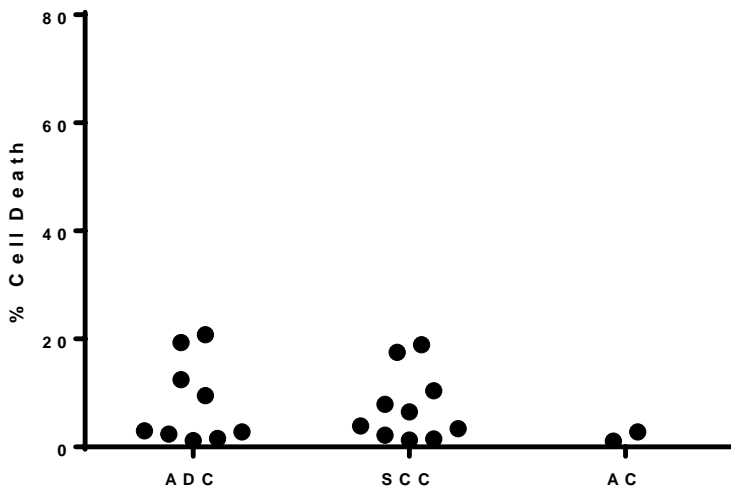


Figure 4.8. Intrinsic Rates of cell death across histologies. Each circle represents one sample. ADC= Adenocarcinoma, SCC= Squamous Cell Carcinoma, AC= Atypical Carcinoid.

4.3.4 Tumour Area Differences

Tumour area differences were observed between individual explants within a given tumour as well as across tumours. An initial set of 9 explants was routinely set up for each different culture condition per sample. These explants were embedded in paraffin after processing, but, in some cases some of the explants were lost at this stage, due to their tiny size. There were 128 explants from the uncultured controls of the 21 usable explant cultures. The average tumour area per control explant was 0.44 mm² (SD=0.66 mm²; range= 0.002 - 4.42 mm²; median=0.22 mm²) and the average number of explants with tumour areas per control slide was 6.09 (SD=2.19; range= 1 - 11; median=6). However, the number of total explants initially set up per uncultured control was higher than nine in most cases.

In contrast there were 1802 explants that were cultured in 403 conditions from the 21 usable explant cultures. The average tumour area per cultured explant was 0.35 mm² (SD=0.46 mm²; range= 90.5 µm² - 4.89 mm²; median=0.19 mm²) and the average number of explants with tumour areas per control slide was 4.47 (SD=1.99; range= 1 - 9; median=4).

4.3.5 Culture conditions

To establish the best culture conditions for NSCLC a set of 6 lung tumour explants was used to test various FCS concentrations in DMEM media (0, 0.5, 1, 2.5 and 5% FCS) and varying culture time (24, 48 and 72 hours). One of the six samples was very small and explants could only be set-up for the 24 + recovery culture time.

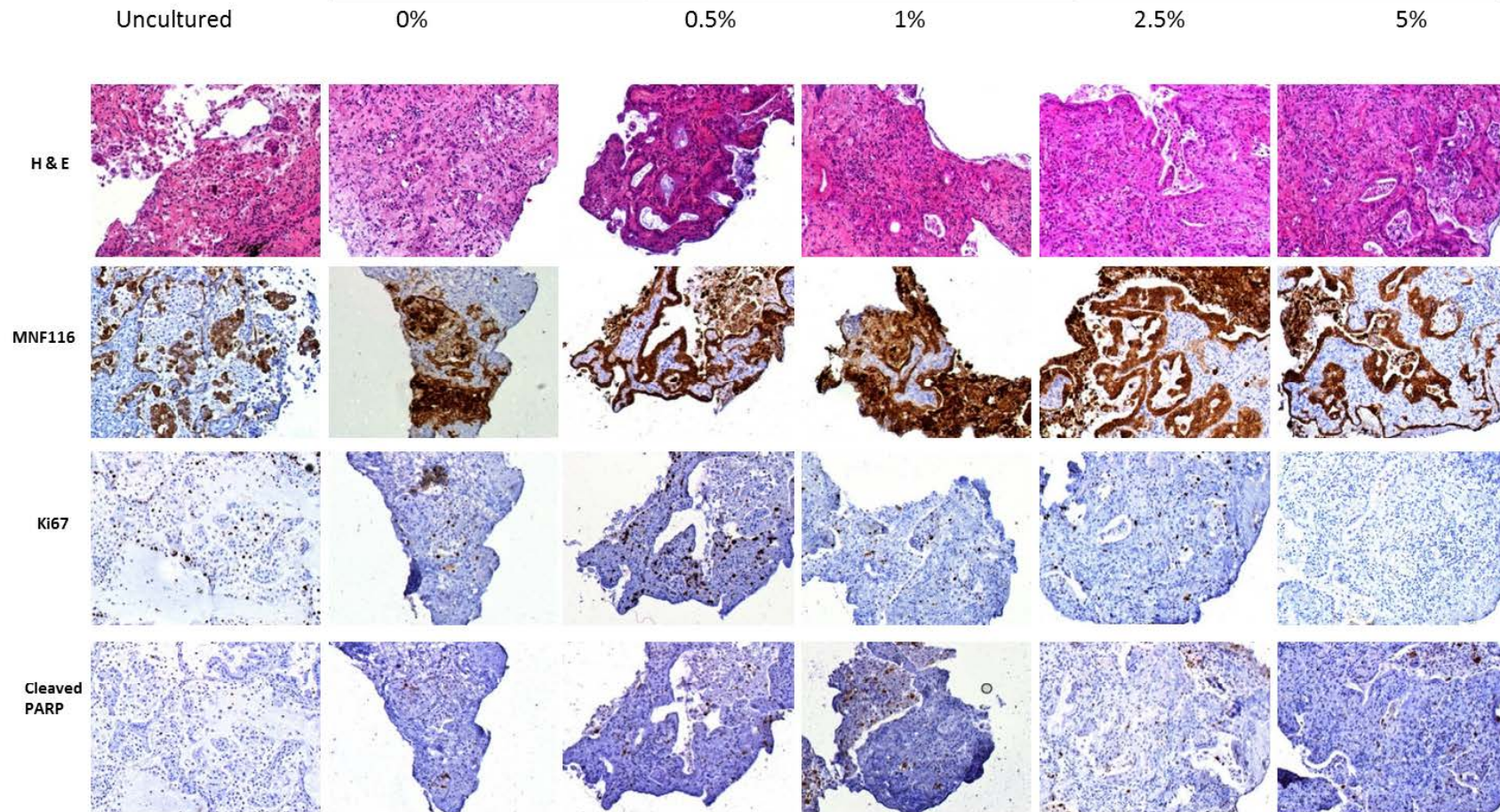
Examples of an intrinsic low proliferation sample, LT33 (Figure 4.9) and an intrinsic high proliferation sample, LT31 (Figure 4.10) are represented.

**4.3.5.1 EXAMPLE OF LOW INTRINSIC PROLIFERATION CASE: LT33
ADENOCARCINOMA**

LT33 had low intrinsic proliferation and low intrinsic cell death. This stayed the same across the different FCS concentrations and across the different culture times of 24 + recovery (Figure 4.9A &D), 48 + recovery (Figure 4.9B &E) and 72 + recovery (Figure 4.9C &F). At 48 hours the 1% FCS point and at 72 hours the 0.5% and 5% FCS points are missing as, unfortunately, the tissue in some of the paraffin embedded samples was lost during processing with the microtome.

A **LT33**

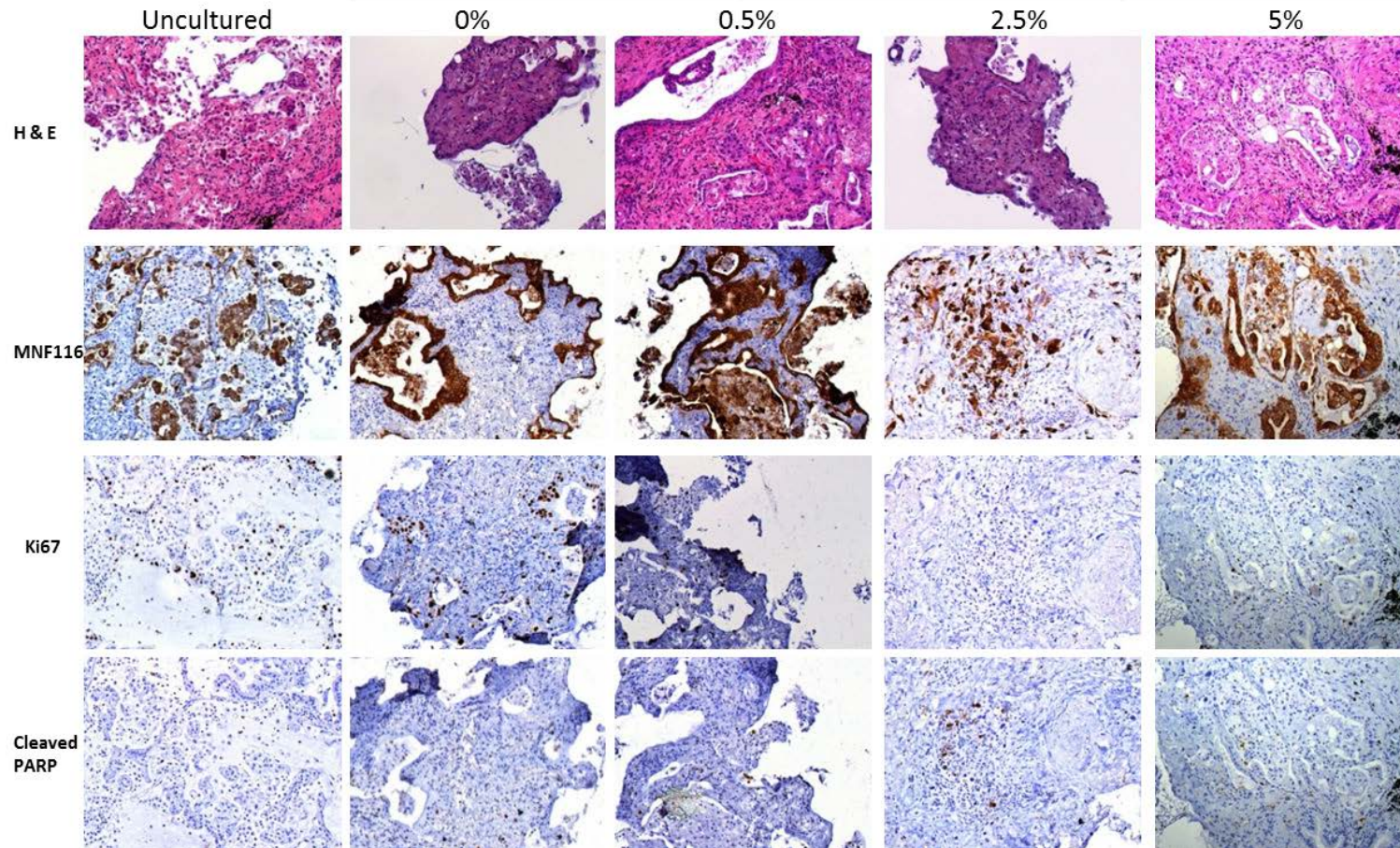
%FCS 24 hours after recovery



B

LT33

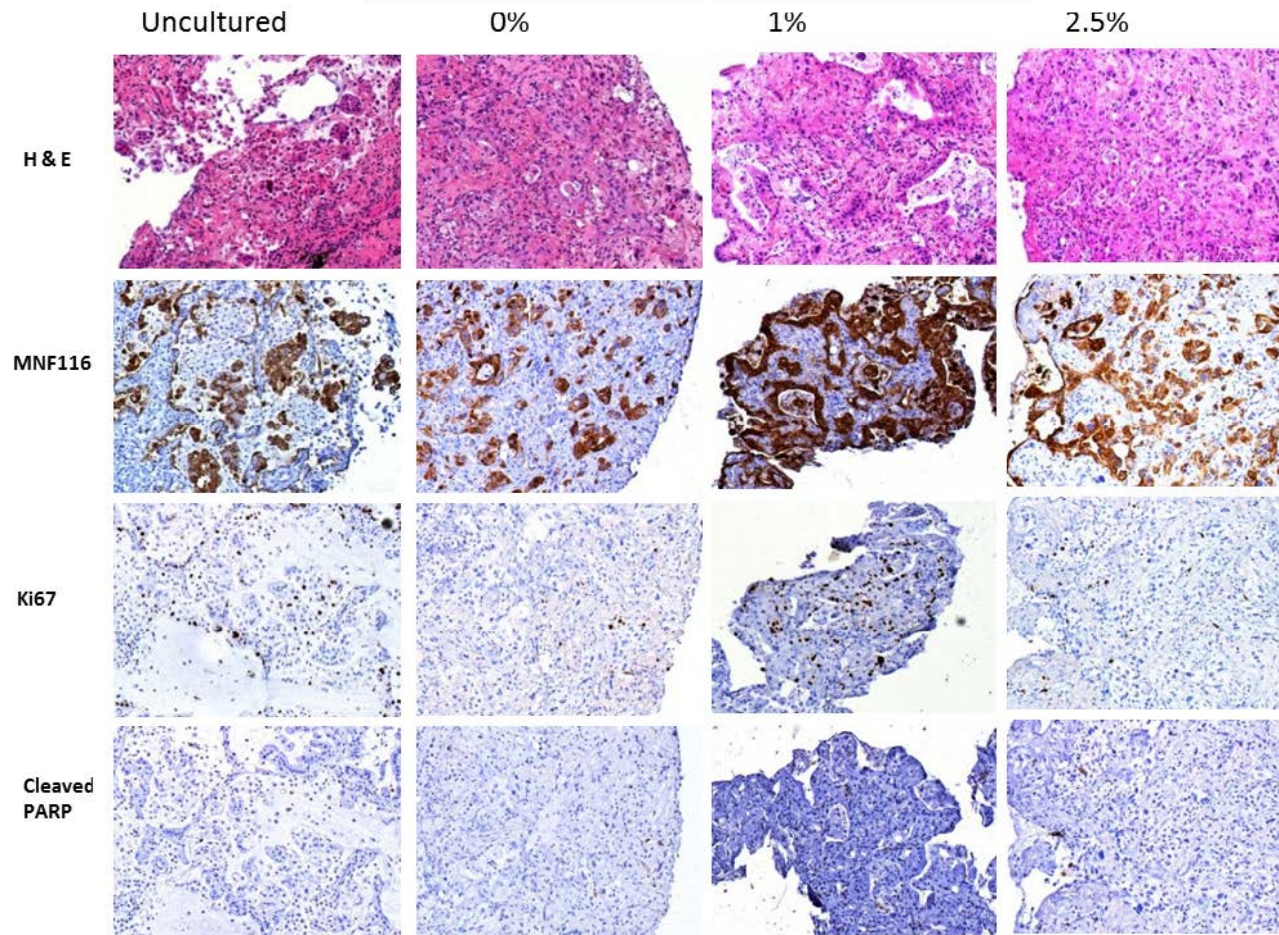
%FCS 48 hours after recovery

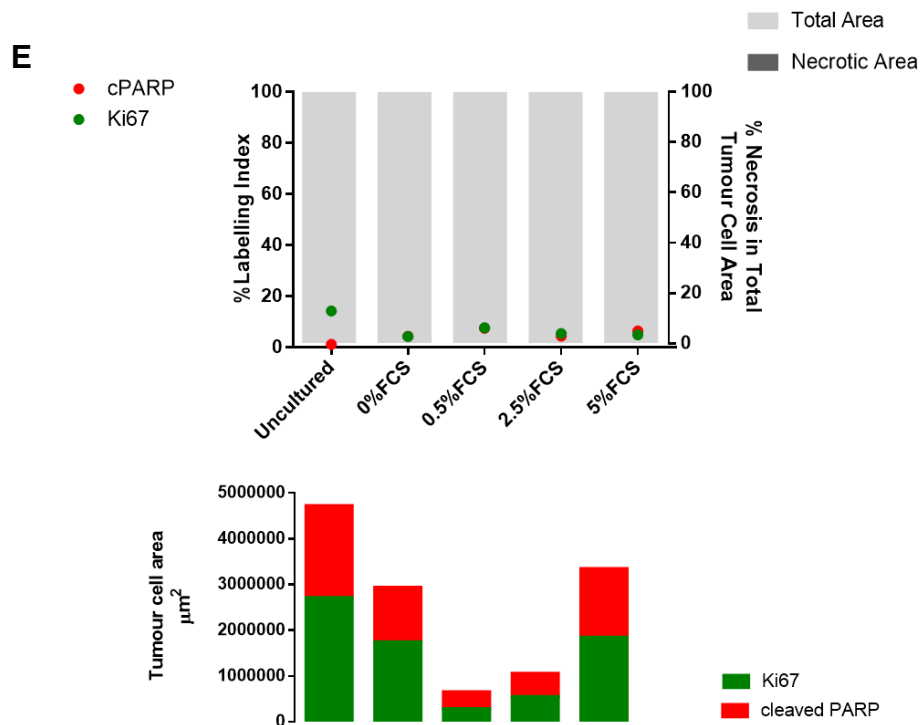
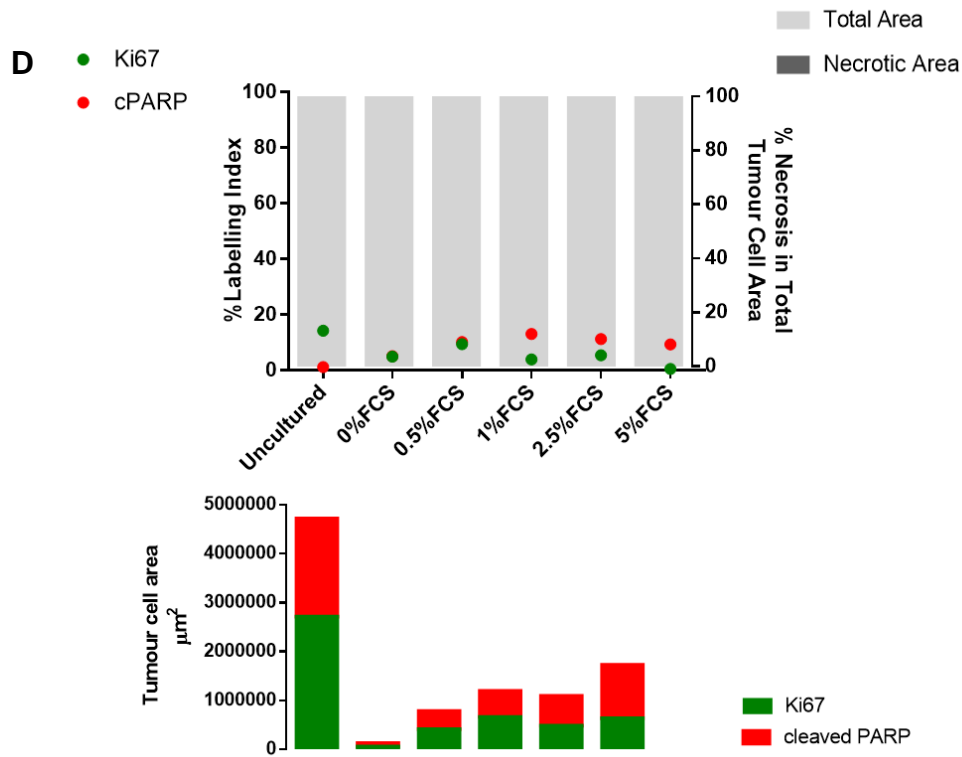


C

LT33

%FCS 72 hours after recovery





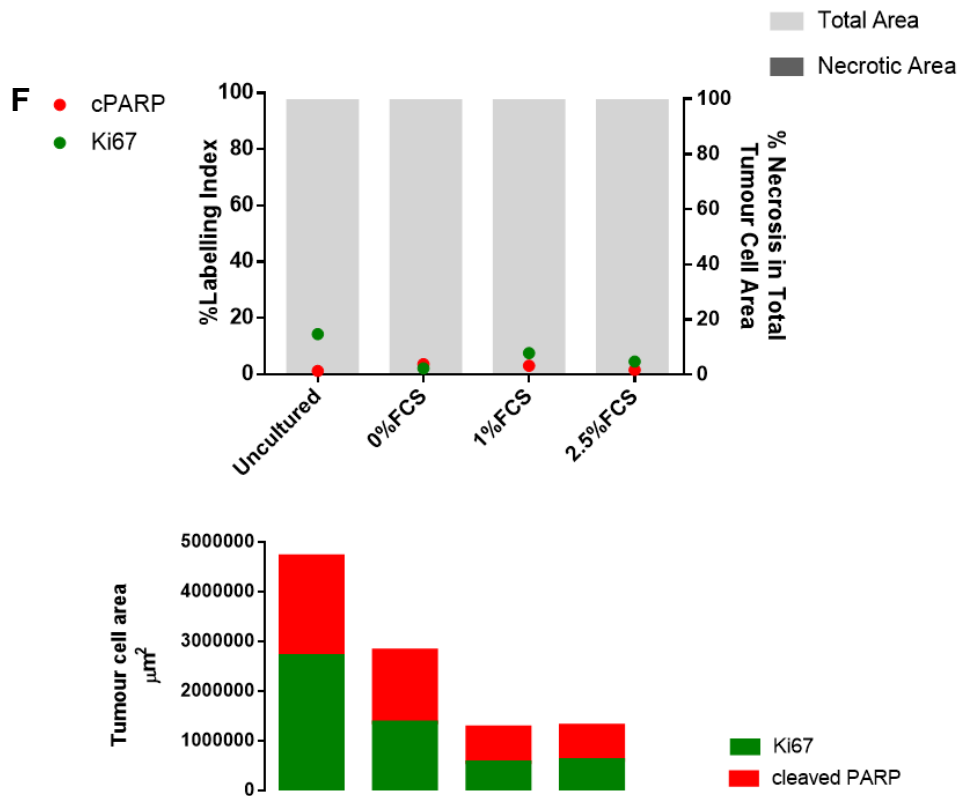


Figure 4.9. Proliferation and Cell Death of LT33 in varying FCS concentrations through culture time. A-C) Representative images of corresponding areas in H&E staining, MNF116 (epithelial cell marker), Ki67 staining (proliferation marker) and cleaved PARP staining (apoptosis marker). A) 24 + recovery in culture B) 48 + recovery in culture and C) 72 + recovery in culture. D-F) Each point represents an additive number which characterises all the staining from each slide and also takes into account the area of the tumour cells for each explant on the slide. The red dot represents the percentage of cells that have a nucleus stained with cleaved PARP out of all the tumour cells present in the slide and similarly the green dot represents the Ki67 labelling index. The dark grey bars behind show the percentage of the area that was undergoing secondary necrosis as decided by cleaved PARP leakage out of the total area (light grey). It shows the proliferation (Ki67-green) and the apoptosis (cPARP-red) or the secondary necrosis (dark grey) of LT33 undergoing culture with varying serum concentrations for 24 (D), 48 (E) and 72 (F) hours after the initial recovery period. Lower graph. This graph represents the exact values of the tumour areas used for Ki67 analysis (green bar), cleaved PARP analysis (red bar) and secondary necrosis so we can compare each condition with the amount of tumour cells present.

4.3.5.2 EXAMPLE HIGH INTRINSIC PROLIFERATION CASE: LT31 SQUAMOUS

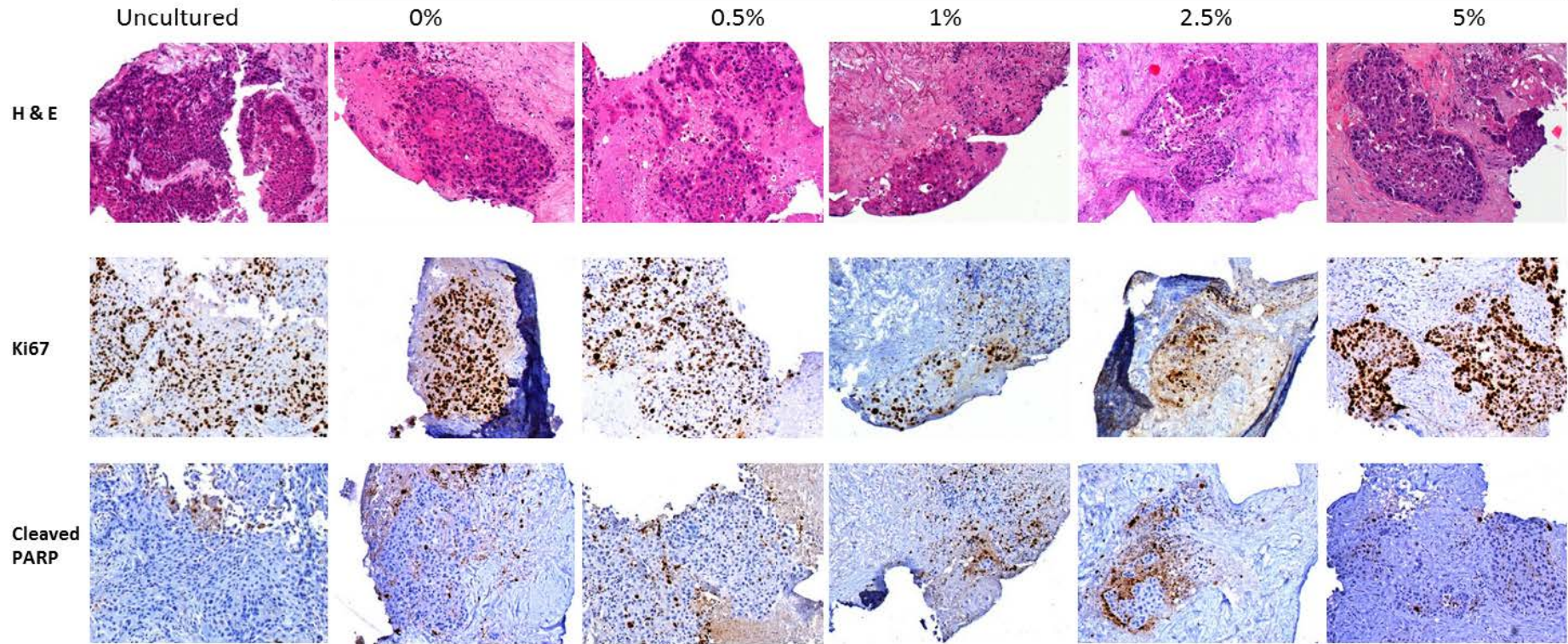
LT31 had high intrinsic proliferation and low cell death. At 24 hours after recovery (Figure 4.10A & D) the best FCS concentration for LT31 seemed to be 0% or 0.5% FCS, since these conditions retained the proliferation levels and had low cell death while 5% FCS, although retaining proliferation had increased necrosis. 1% and 2.5% FCS show increased cell death rates compared to the control. However, the values are based on smaller tissue areas and therefore might not be as accurate.

At 48 hours after recovery (Figure 4.10B & E) the best FCS concentration seemed to be 2.5% FCS and 5% FCS, with the latter showing increased necrosis. At 72 hours after recovery (Figure 4.10C & F) the proliferation is significantly decreased in all of the FCS concentrations and cell death appears to be increased at 0% FCS. The 5% point is missing as, unfortunately, the tissue in some of the paraffin embedded samples was lost during processing with the microtome.

A

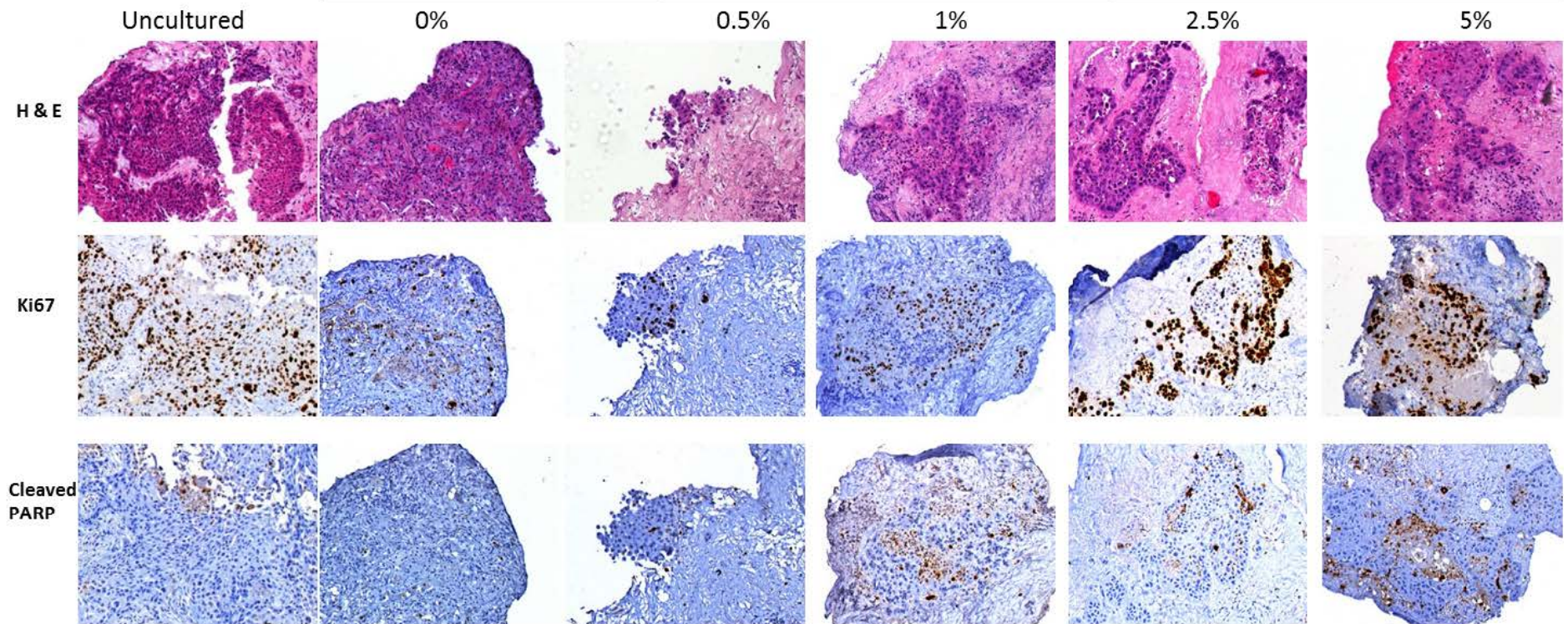
LT31

%FCS 24 hours after recovery



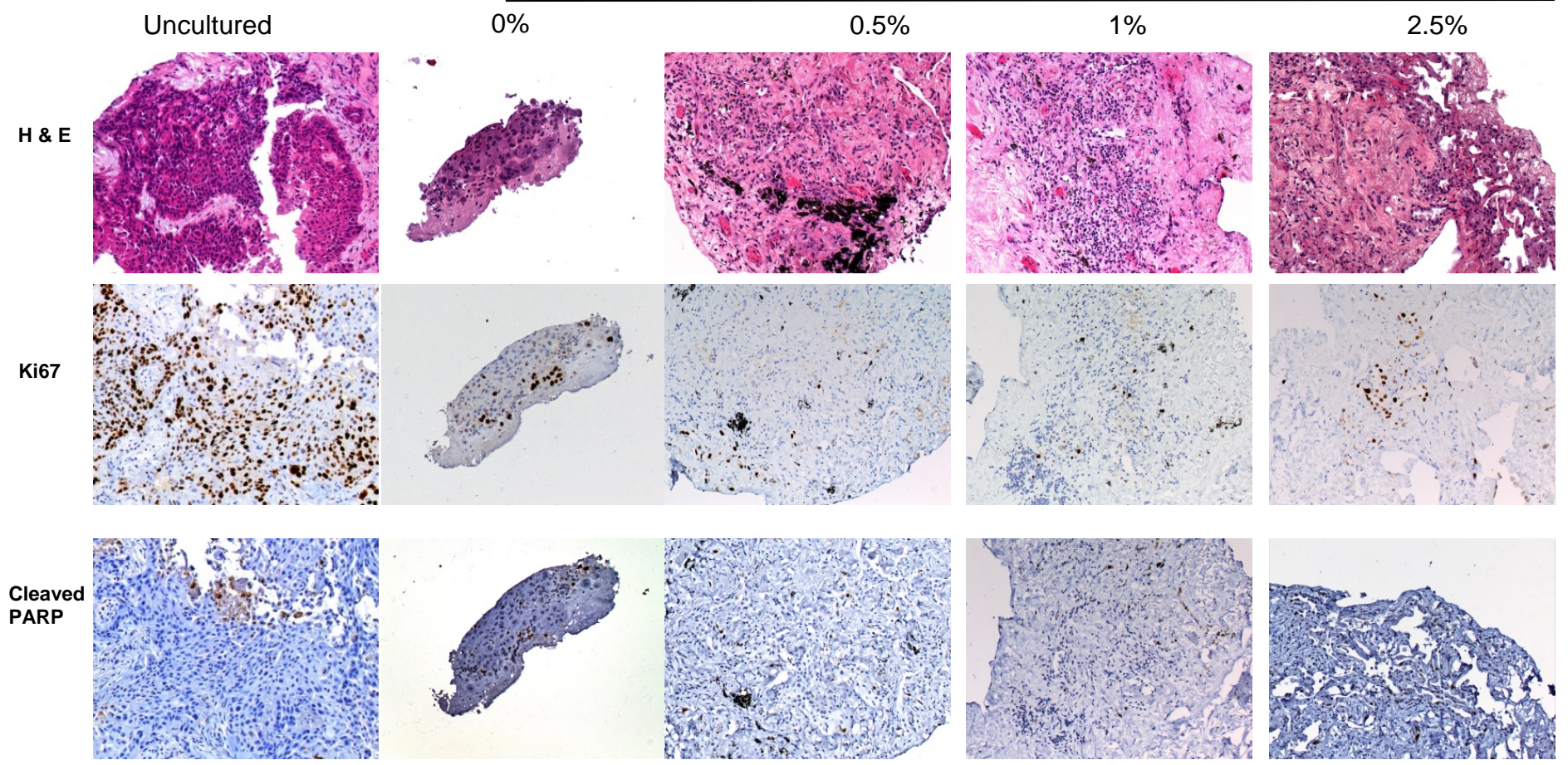
B
LT31

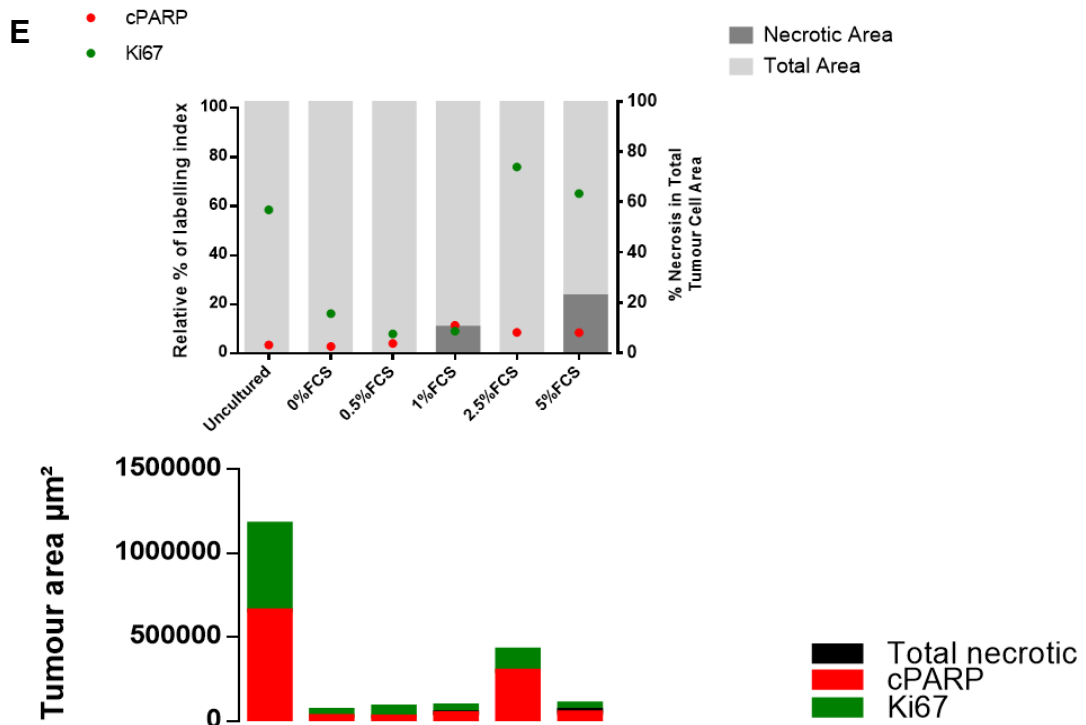
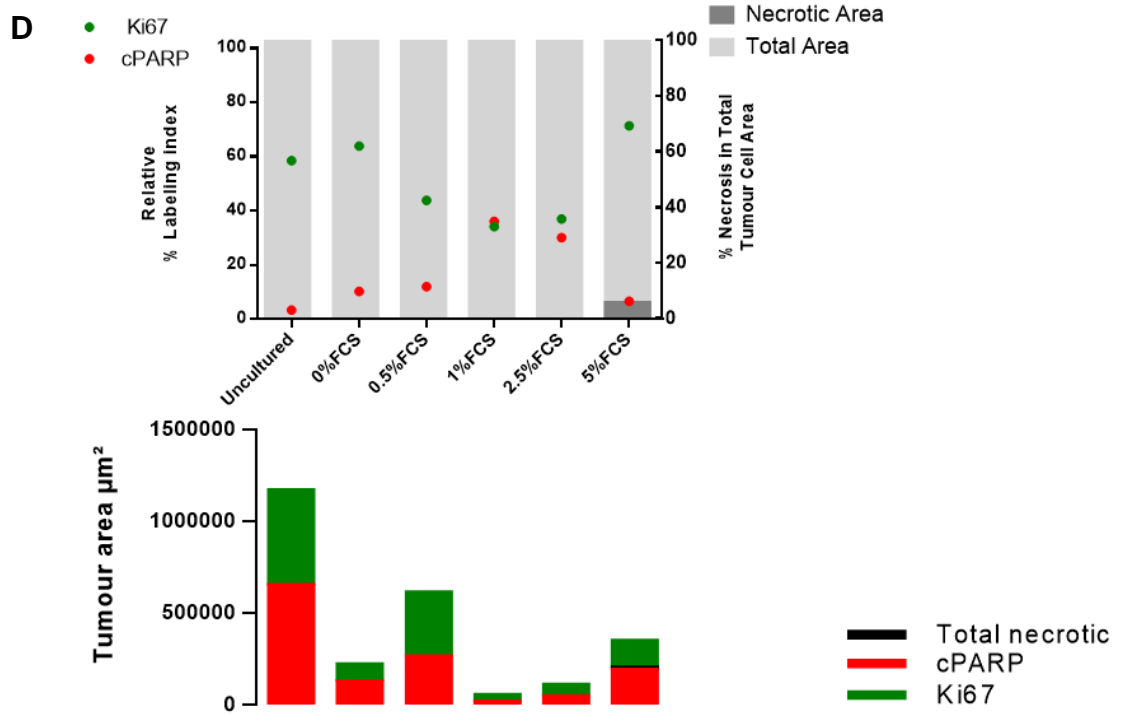
%FCS 48 hours after recovery



C
LT31

%FCS 72 hours after recovery





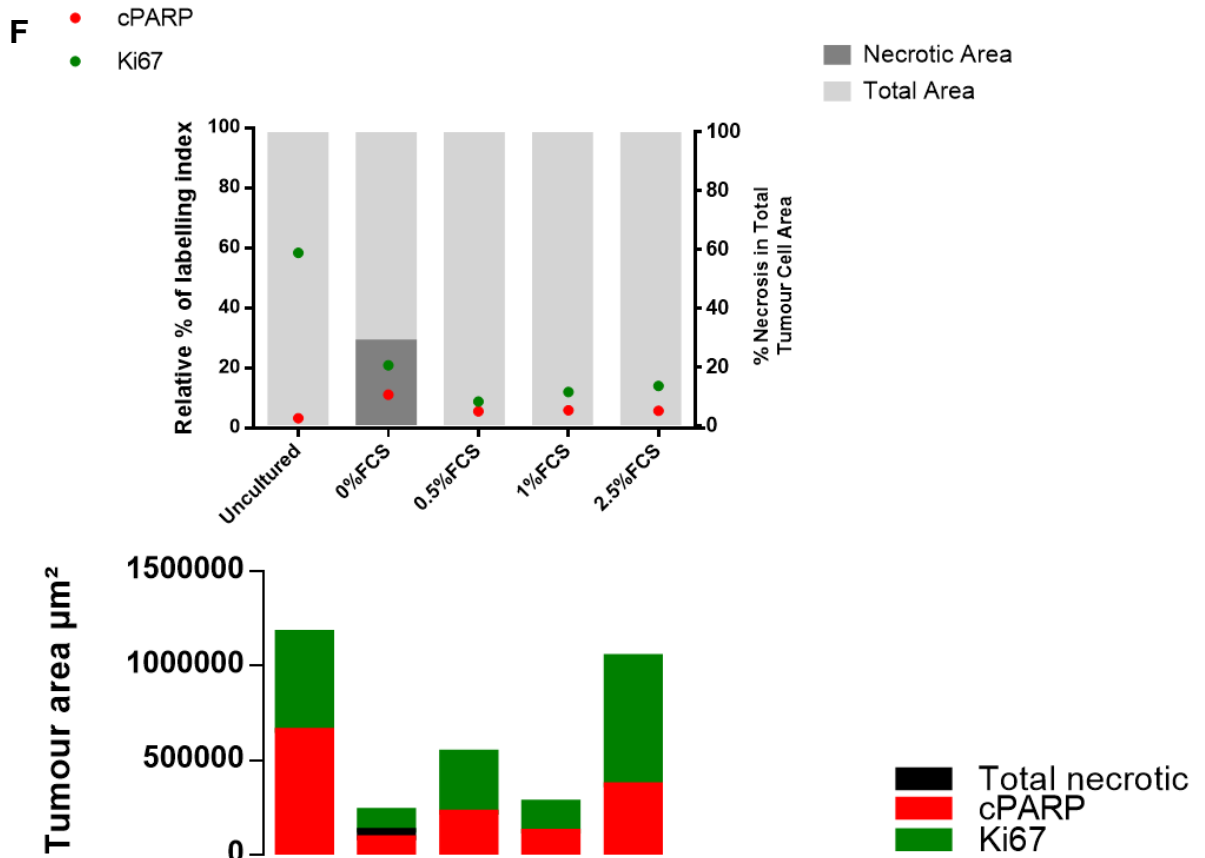


Figure 4.10. Proliferation and Cell Death of LT31 in varying FCS concentrations through culture time. A-C) Representative images of corresponding areas in H&E staining, Ki67 staining (proliferation marker) and cleaved PARP staining (apoptosis marker). A) 24 + recovery in culture B) 48 + recovery in culture and C) 72 + recovery in culture. D-F) Each point represents an additive number which characterises all the staining from each slide and also takes into account the area of the tumour cells for each explant on the slide. The red dot represents the percentage of cells that have a nucleus stained with cleaved PARP out of all the tumour cells present in the slide and similarly the green dot represents the Ki67 labelling index. The dark grey bars behind show the percentage of the area that was undergoing secondary necrosis as decided by cleaved PARP leakage out of the total area (light grey). It shows the proliferation (Ki67-green) and the apoptosis (cPARP-red) or the secondary necrosis (dark grey) of LT31 undergoing culture with varying serum concentrations for 24 (D), 48 (E) and 72 (F) hours after the initial recovery period. Lower graph. This graph represents the exact values of the tumour areas used for Ki67 analysis (green bar), cleaved PARP analysis (red bar) and secondary necrosis so we can compare each condition with the amount of tumour cells present.

4.3.5.3 PROLIFERATION OF EX-VIVO EXPLANT CULTURES IS DECREASING AT INCREASING CULTURE TIME

5 *ex-vivo* explant cultures were used to test the effect of culture time of 24, 48 and 72 hours after an initial recovery period of 16-20 hours. The % Ki67 staining of the tumour area of the individual cases can be seen in Figure 4.11. Most of the cultures showed a decrease in proliferation at increasing culture time.

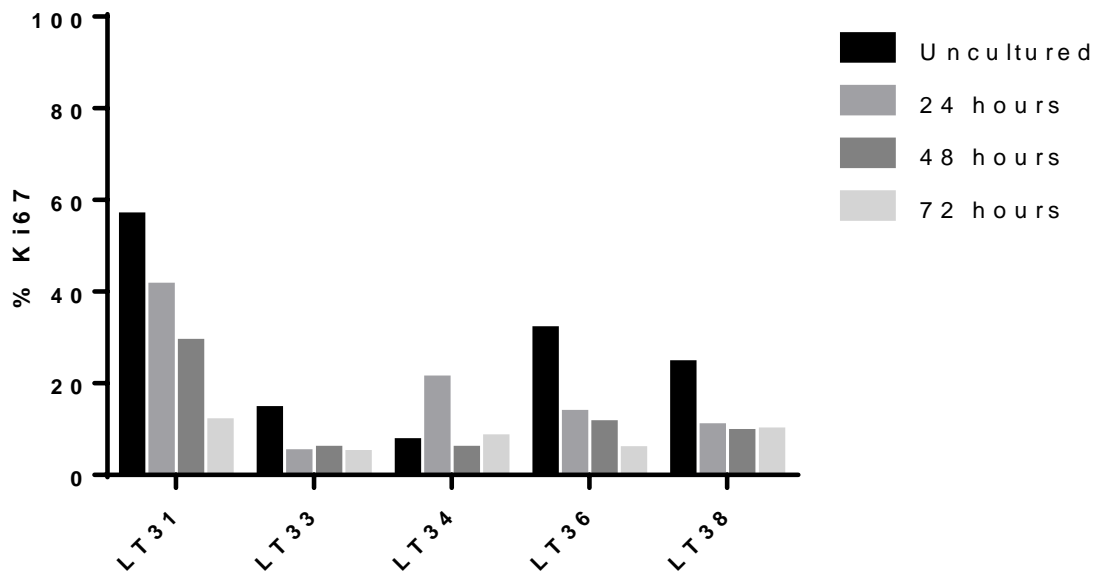


Figure 4.11. % Ki67 of tumour area of 5 NSCLC *ex-vivo* explants through culture time. The Ki67 staining values from each sample are the uncultured tumour in its native state, 24 hours, 48 hours and 72 hours of culture after an initial recovery of 16-20 hours. The values for each sample are the average of explants from the same sample, cultured in different FCS concentrations (0, 0.5, 1, 2.5 and 5% FCS).

When we combined the 5 cases as mean % Ki67 + 95% CI (Figure 4.12) we could see a clear decrease in proliferation with increasing culture time. Statistical analysis with a Friedman test showed only the 72 hour time point to be significantly different from the uncultured control (Friedman statistic: 8.3; $P=0.04$). However, when we applied a Page's L nonparametric trend test, a negative trend was evident with increasing culture time (L statistic =143; $P=0.01$), suggesting *ex-vivo* explant cultures are more proliferative in short term culture.

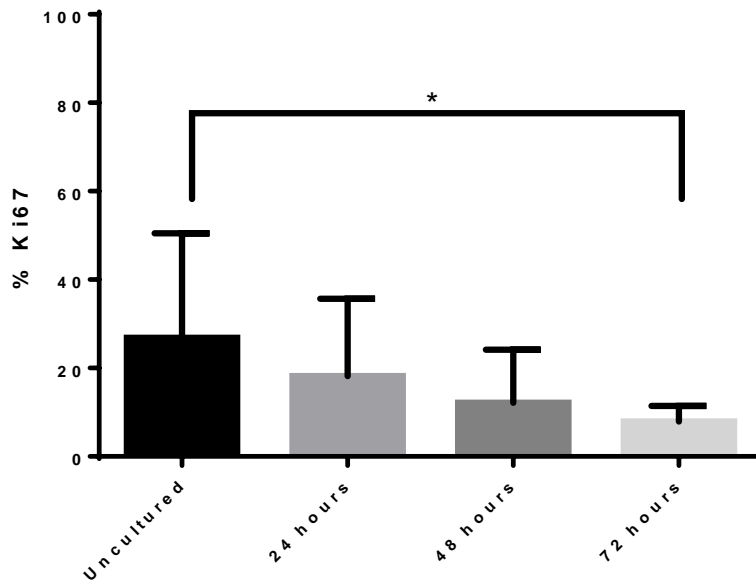


Figure 4.12. The 5 NSCLC samples from figure 4.11 plotted together. Data are expressed as mean %Ki67 values + 95% CI (Confidence Intervals). A Friedman test identified 72 hours to be statistically significantly different from the Uncultured (* P= 0.04; Friedman statistic: 8.3). Page's L nonparametric trend test showed a negative trend with increasing culture time (P=0.01; L statistic =143).

4.3.5.4 CELL DEATH OF EX-VIVO EXPLANT CULTURES IS INCREASING AT INCREASING CULTURE TIME

The same 5 *ex-vivo* explant cultures were analysed for cell death. The % cell death of the tumour area of the individual cases can be seen in Figure 4.13. All of the cultures showed an increase in cell death at increasing culture time.

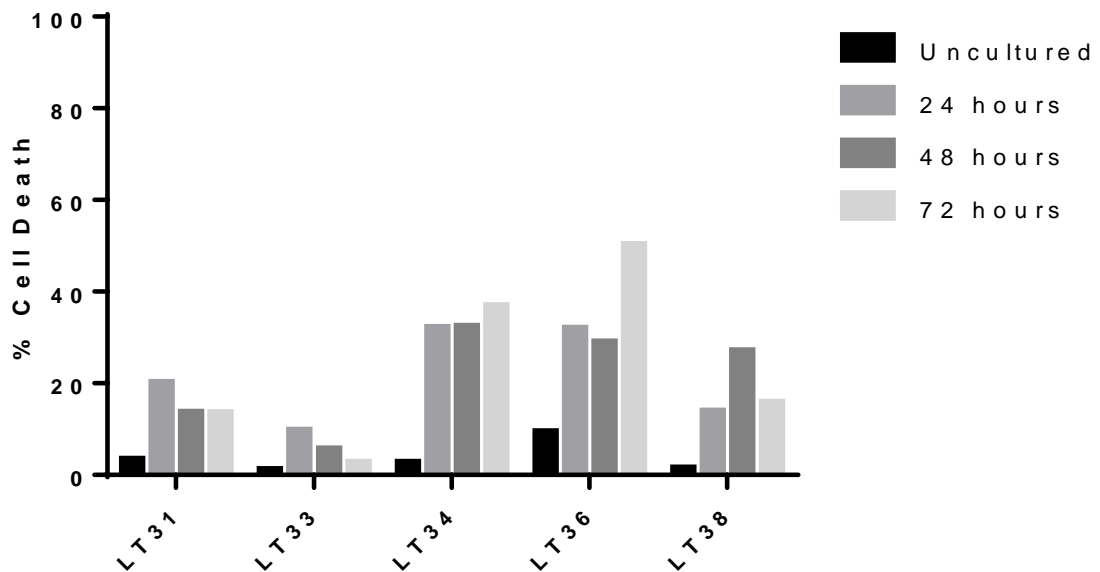


Figure 4.13. % Cell Death of tumour area of 5 NSCLC ex-vivo explants through culture time. The % Cell Death values from each sample are the uncultured tumour in its native state, 24 hours, 48 hours and 72 hours of culture after an initial recovery of 16-20 hours. The values for each sample are the average of explants from the same sample, cultured in different FCS concentrations (0, 0.5, 1, 2.5 and 5% FCS).

When we combined the 5 cases as mean % Cell Death + 95% CI (Figure 4.14) a clear increase of cell death could be seen with culture which was significant at 24, 48 and 72 hours (Friedman statistic: 9; $P=0.04$ for all culture times). From Figure 4.14 the 24 and 48 hour culture point did not look different. However, when we applied a Page's L nonparametric trend test, a positive trend was evident with increasing culture time (L statistic= 140; $P=0.05$), suggesting ex-vivo explant cultures are more viable in short term culture.

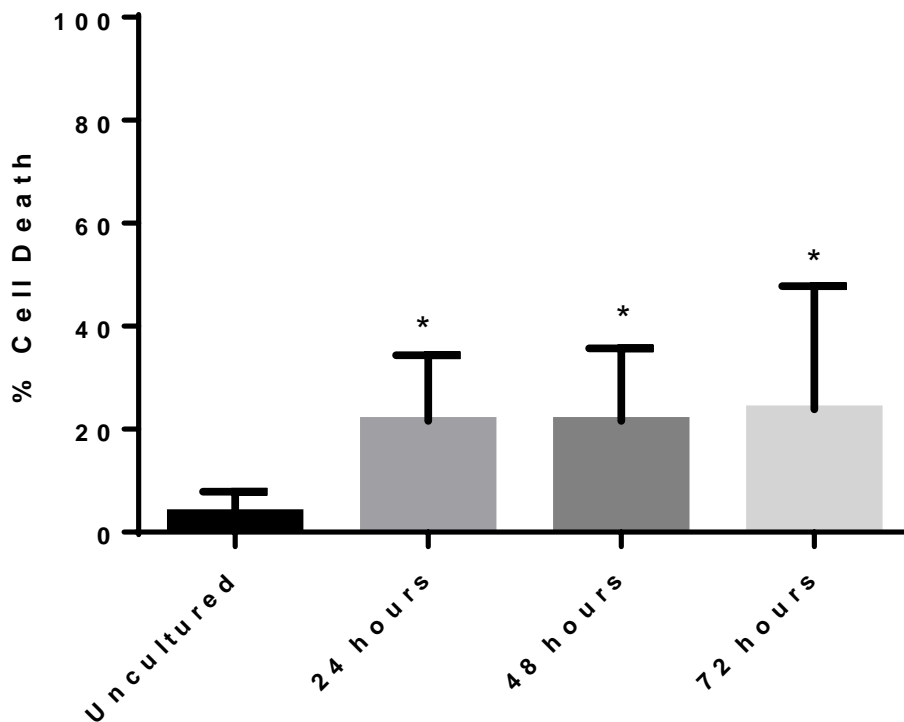


Figure 4.14. The 5 NSCLC samples from figure 4.13 plotted together. Data are expressed as mean %Cell Death values + 95% CI. A Friedman test identified 24, 48 and 72 hours to be statistically significantly different from the Uncultured (* P= 0.04 for all culture times; Friedman statistic=9) but not between them. Page's L nonparametric trend test showed a positive trend with increasing culture time (L statistic=140; P=0.05).

From these experiments, it was decided that the best culture time for the *ex-vivo* explant cultures is 24 hours after recovery.

4.3.5.5 THE EFFECT OF VARYING CONCENTRATIONS OF FCS IN EX-VIVO EXPLANT CULTURES

Next, we wanted to test whether different FCS concentrations are important in the proliferation and cell death of the samples. To do this, we used 5 samples which were cultured in 0, 0.5, 1, 2.5 and 5% FCS for 24 hours after recovery. Table 4.1 provides the percentages of cell death and proliferation values for tumour areas across the different FCS concentrations and the uncultured control which shows the values of the staining in the tumour in its native form.

Table 4.1. %Cell Death and % Ki67 values at 24 hours after recovery for 5 cases cultured in a range of FCS.

24 Hours After Recovery						
%Cell Death	Uncultured	0 % FCS	0.5 % FCS	1 % FCS	2.5 % FCS	5 % FCS
LT31	3.4	10.3	12.0	36.1	30.1	12.6
LT32	12.5	15.9	12.8	20.7	10.7	15.4
LT33	1.2	5.2	10.2	13.1	11.3	9.4
LT36	9.5	30.4	37.8	27.2	37.7	26.9
LT38	1.5	11.8	10.9	12.9	20.4	13.7
24 Hours After Recovery						
%Ki67	Uncultured	0 % FCS	0.5 % FCS	1 % FCS	2.5 % FCS	5 % FCS
LT31	56.5	57.3	38.6	21.9	25.9	62.4
LT32	46.5	47.8	65.7	53.2	53.7	68.8
LT33	14.3	4.9	9.4	4.0	5.5	0.6
LT36	31.7	14.1	12.2	13.1	11.8	15.9
LT38	24.3	5.9	7.4	14.0	13.5	11.8

Figure 4.15 shows the cell death values from the Table 4.1 plotted in a graph for all 5 cases. In most of the cases there was no evident difference between the different FCS concentrations. What was apparent was the small but consistent increase of cell death compared to the uncultured control.

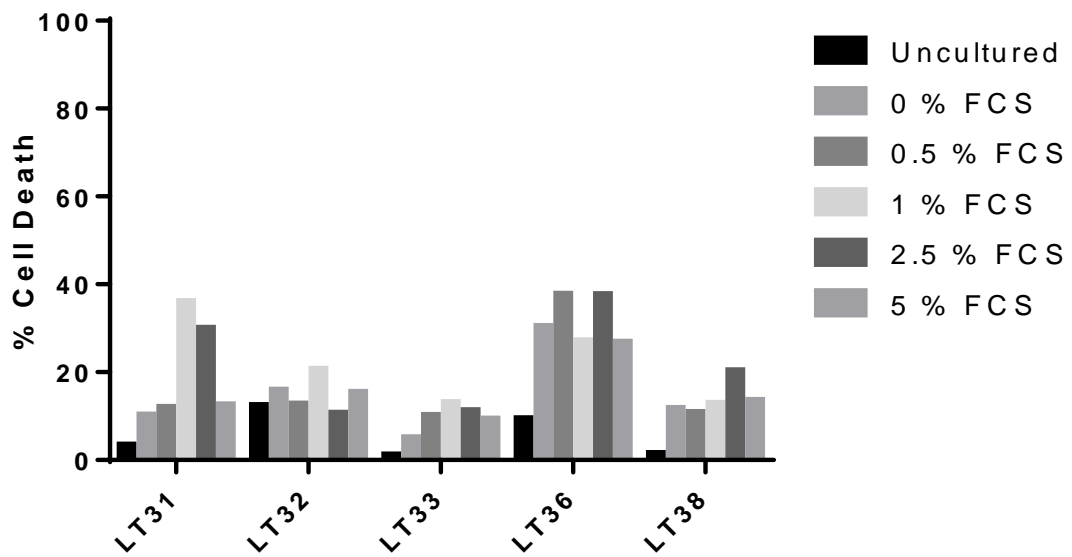


Figure 4.15. % Cell Death of tumour area of 5 NSCLC ex-vivo explant cultures in varying FCS concentrations at 24 + recovery. The % Cell Death values from each sample are the uncultured tumour in its native state, compared with explants from the same tumour cultured in varying FCS concentrations (0, 0.5, 1, 2.5 and 5% FCS) for 24 hours after an initial recovery of 16-20 hours.

When we expressed the values of the 5 cases as mean % cell death + 95% CI (Figure 4.16), the FCS concentrations did not show a statistically significant difference amongst each other.

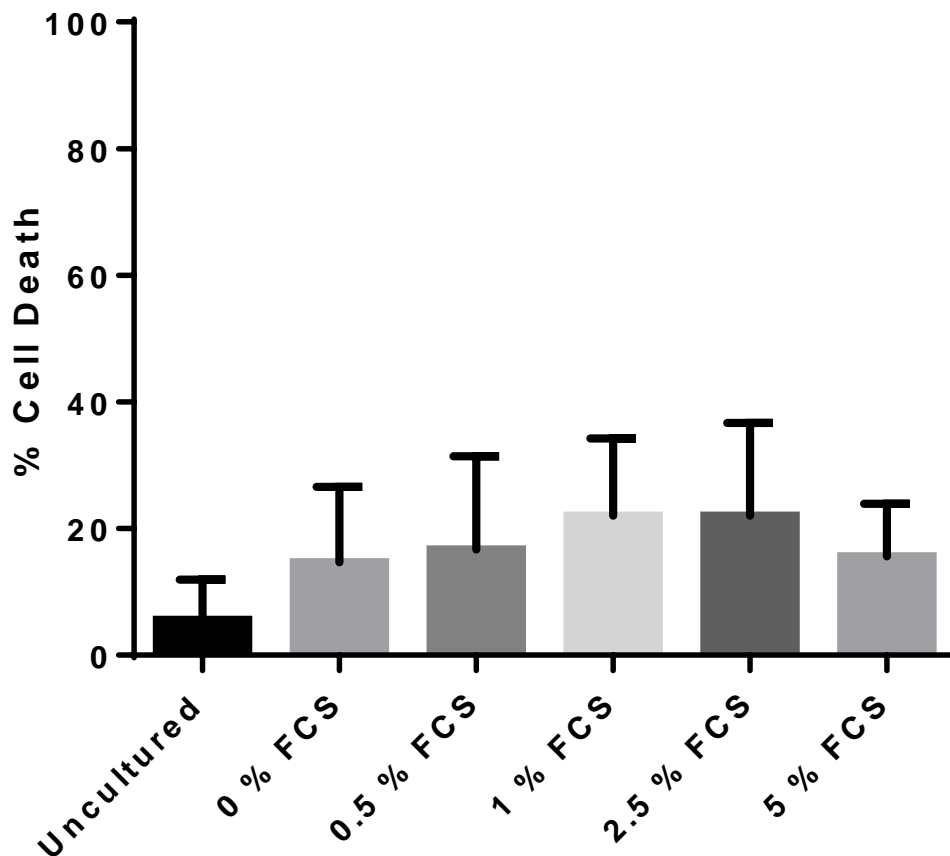


Figure 4.16. The 5 NSCLC samples from figure 4.15 plotted together. Data are expressed as mean %Cell Death values + 95% CI. A Friedman test identified none of the FCS concentrations to be statistically significantly different from each other.

Figure 4.17 shows the Ki67 values from the Table 4.1 plotted in a graph for all 5 cases. In most of the cases there was no evident difference between the different FCS concentrations.

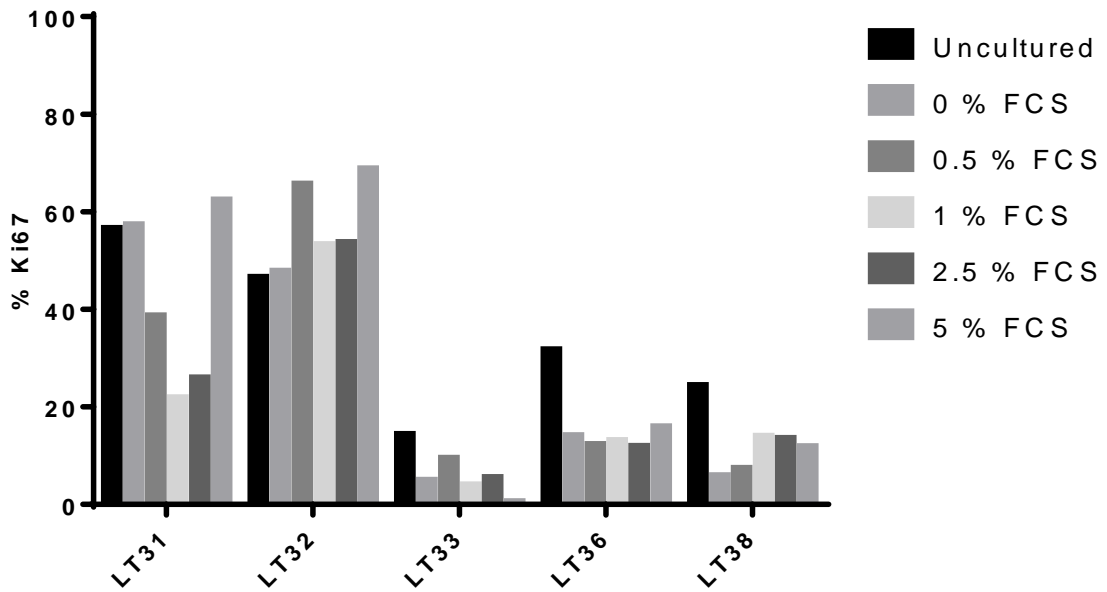


Figure 4.17. % Ki67 of tumour area of 5 NSCLC ex-vivo explant cultures in varying FCS concentrations at 24 + recovery. The % Ki67 values from each sample are the uncultured tumour in its native state, compared with explants from the same tumour cultured in varying FCS concentrations (0, 0.5, 1, 2.5 and 5% FCS) for 24 hours after an initial recovery of 16-20 hours.

In fact, when we expressed the values of the 5 cases as mean % Ki67 + 95% CI (Figure 4.18), the FCS concentrations did not show a statistically significant difference amongst each other.

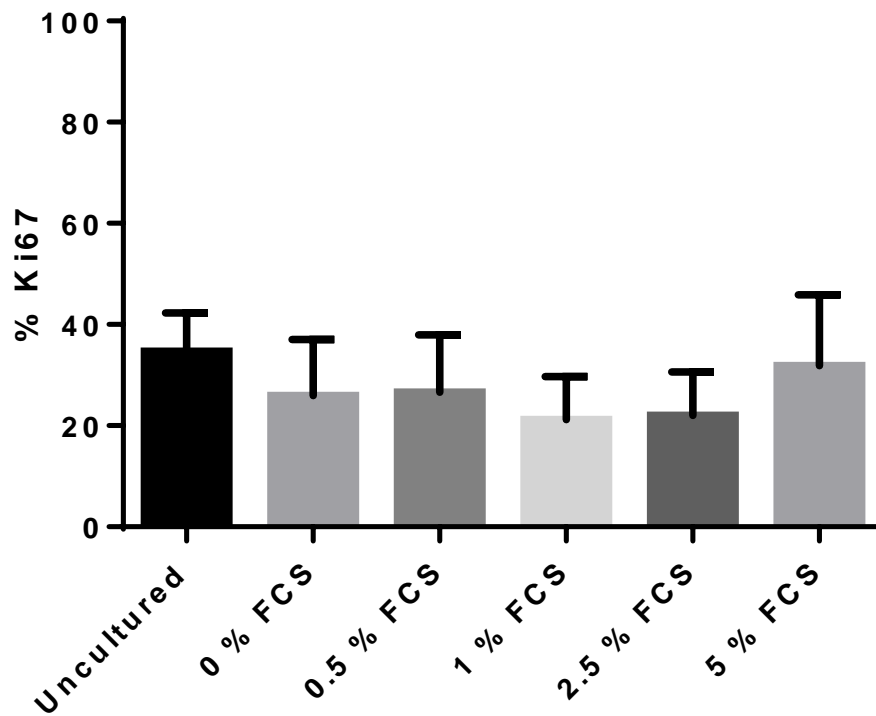


Figure 4.18. The 5 NSCLC samples from figure 4.17 plotted together. Data are expressed as mean %Ki67 values + 95% CI. A Friedman test identified none of the FCS concentrations to be statistically significantly different from each other or the Uncultured.

From these experiments, it was decided that FCS is probably not such an important factor for the culture of *ex-vivo* explants since the differences between FCS concentrations were so marginal in both the cell death and proliferation values. We decided to carry on with the 1%FCS in the media since most of the drug treatments were already done in that concentration.

Figure 4.19 and Figure 4.20 show the comparison of the uncultured and the 24 hours in culture after the recovery period between the rest of the analysed *ex-vivo* explant cultures. The cell death was increased by about 10-15% compared to the control (Figure 4.19) and the proliferation was decreased by about 5% compared to the native tumour (Figure 4.20).

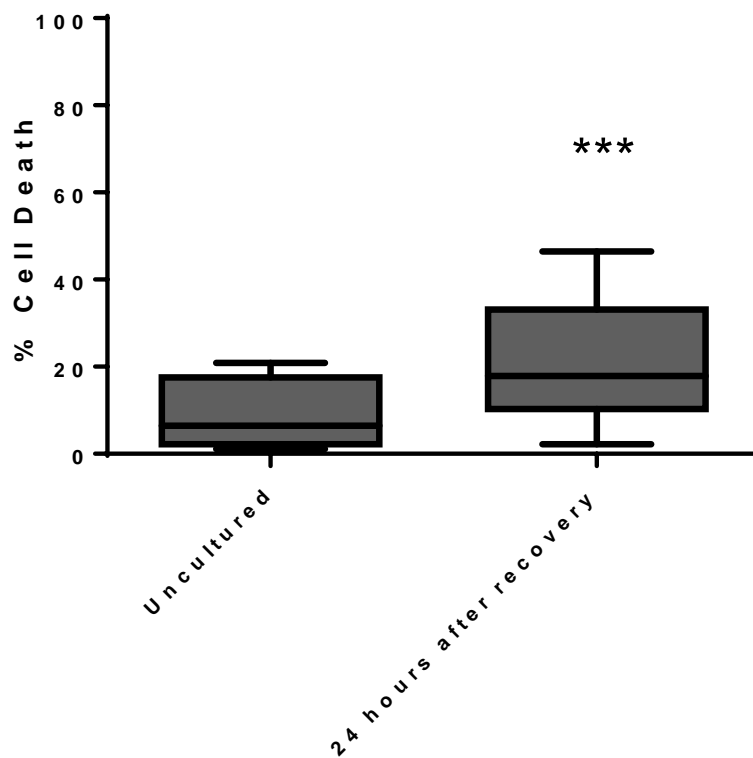


Figure 4.19. Box and whiskers plot of %Cell Death of tumour area in the uncultured tumour compared to 24 + recovery in 1%FCS media. (N=15). The box extends from the 25th to 75th percentiles. The line in the middle of the box is plotted at the median. The whiskers go down to the smallest value and up to the largest. A Wilcoxon matched paired rank test shows 24 hours in culture after recovery to be statistically significant from the uncultured ($P < 0.0001$).

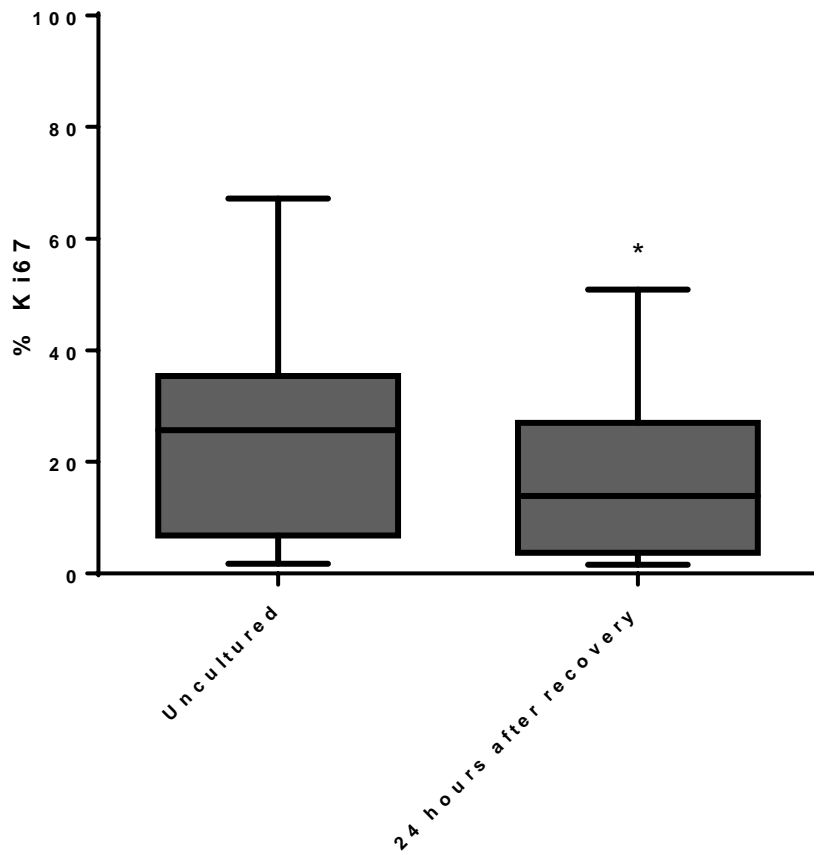


Figure 4.20. Box and whiskers plot of % Ki67 of tumour area in the uncultured tumour compared to 24+recovery in culture in 1%FCS media. (N=15). The box extends from the 25th to 75th percentiles. The line in the middle of the box is plotted at the median. The whiskers go down to the smallest value and up to the largest. A Wilcoxon matched paired rank test shows 24 hours in culture after recovery to be statistically significant from the uncultured (P=0.02).

4.3.6. Comparison across explants from one tumour

Thus far, the results have been presented as a single value per condition. However, if we plot the values from each explant from one tumour we can see heterogeneity between different explants from the same tumour. A representative example is shown in Figure 4.21. In this instance, the cell death values per explant seem to be more variable than the proliferation values which appear to be tighter.

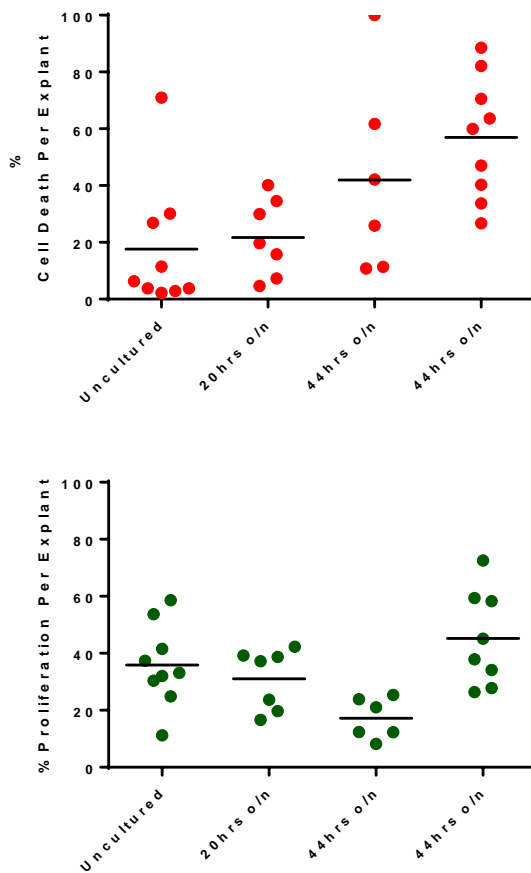


Figure 4.21. % Cell death and % proliferation per explants in an example case. Upper graph: Percentage Cell death as measured by cleaved PARP staining at different culture times. Each red circle represents one explant and the line represents the mean value between explants. Lower graph: Percentage proliferation as measured by ki67 staining at different culture times. Each green circle represents one explant and the line represents the mean value between explants.

4.3.7 Normal Lung Ex-vivo explant culture

Adjacent normal lung was used to set up *ex-vivo* explant cultures. An example of a culture over a 0-72 hour period is shown in Figure 4.22. The integrity of the culture was assessed by H&E staining. During increasing culture periods the integrity of the normal lung parenchyma was lost but cells remained viable.

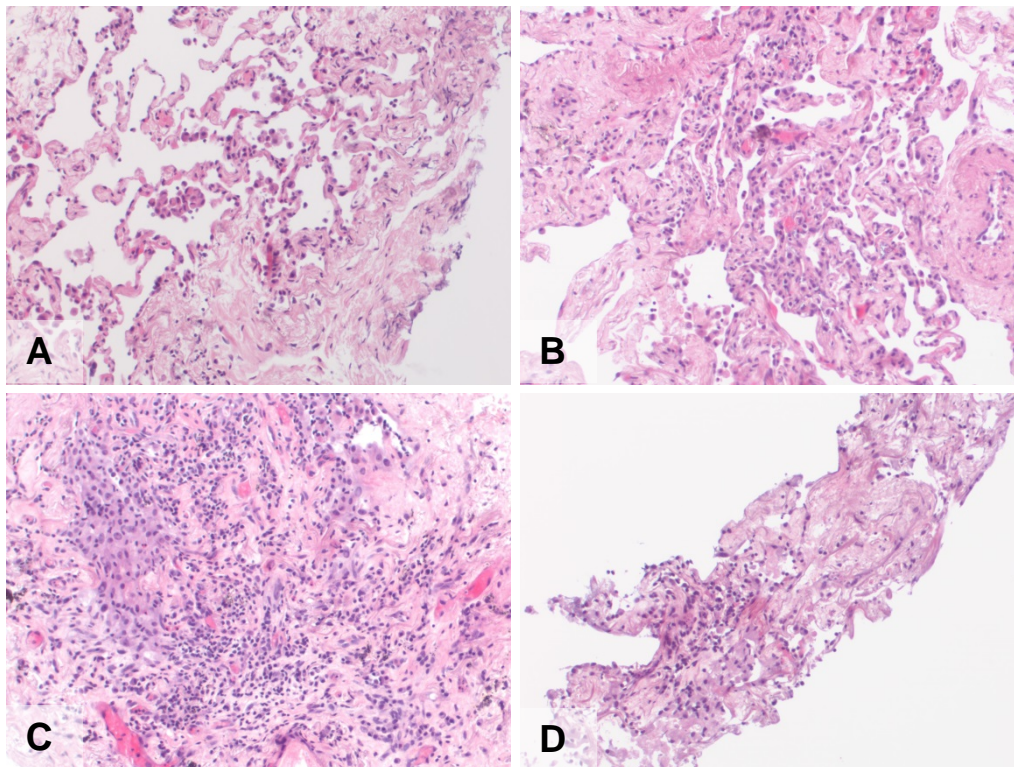


Figure 4.22. Representative Images of H&E stain of an adjacent normal lung sample. A) The uncultured control and explants cultured for 24 + recovery (B), 48+ recovery (C) and 72 hours + recovery (D).

4.4 Discussion

Cleaved PARP is an established marker of apoptosis as it is a product of effector caspases -3 and -7 (Soldani & Scovassi, 2002) and has been used as a marker of apoptotic cell death in numerous studies (Mallon *et al.*, 2011; Hoefflich *et al.*, 2012; Romano *et al.*, 2012; Iljin *et al.*, 2009). A cleaved PARP antibody has been chosen over cleaved caspase-3 to measure apoptotic cell death as a result of previous experiments by Shambhavi Naik (Prof MacFarlane's group) that showed cleaved PARP to be more stable in detecting apoptotic cells and to have good sensitivity in IHC.

Apoptosis should always terminate with the elimination of a cell undergoing apoptosis by a scavenger cell (Silva, 2010). When the clearance of apoptotic cells becomes insufficient as a result of a problem with the availability of phagocytes or the apoptotic load is simply too big, secondary necrosis is activated at the end of the full apoptotic program which leads to an autolytic disintegration of the cells (Silva, 2010). In our study we used cleaved PARP leakage as an indication of secondary necrosis (Figure 4.3). In secondary necrosis, features of apoptosis and necrosis exist such as apoptotic markers and membrane shredding (Silva, 2010). Therefore, markers of apoptosis such as cleaved PARP used in this study are released from the cells and areas of dark brown staining can be regarded as necrotic.

The Ki67 antibody (Gerdes *et al.*, 1983; Gerdes *et al.*, 1984) which detects a nuclear antigen expressed in all the states of the cell cycle (G1,S,G2 and M phase) but is absent in G0 cells was used to mark proliferating cells. This antibody is also routinely used in diagnostic laboratories to define the proliferation index of certain tumours as it has a prognostic value in certain cancers. In NSCLC the predictive value of Ki-67 labelling index has been controversial. A recent review by Jakobsen and colleagues reported no consensus on the prognostic role of Ki67 among 28 studies from 2000 to 2012 (Jakobsen & Sørensen, 2013). A recent study assessed the Ki67 proliferation index retrospectively by immunohistochemistry in a cohort of 1065 NSCLC in association with clinicopathological data including outcome and therapy (Warth

et al., 2014). Here they reported that the Proliferation Index (PI) differed significantly according to histology with SCC showing a mean (52.8%) twice as high as ADC (25.8%) which is in agreement with our findings (Figure 4.7). As far as the prognostic value is concerned, they reported opposing effects of PI on overall survival. A high PI in ADCs was a negative prognostic indicator in a stage-independent manner whereas high PI in SCC subtypes was associated with better survival (Warth *et al.*, 2014).

The fact that about a third of the surgically resected cases we obtained proved to be unusable due to poor viability of the controls reflects the quality of the samples obtained. Solid tumours often exhibit highly necrotic areas as a result of hypoxia. Most of the samples we received from Glenfield hospital come from the middle of the tumour in order to preserve the edges for pathology examinations; but unfortunately the middle is usually the most necrotic part of the tumour. Better selection of appropriate areas of tissue with tumour areas is needed. Current PhD students Wen-Jing Liao and Dr. Esraa Al Dujaily have found all the recent cases studied for NSCLC explants to be viable. Other studies have reported culture problems in about 10-30% of samples (Singh *et al.*, 2002; Vescio *et al.*, 1990).

The high occurrence of unusable samples led us to introduce a frozen section check on the quality of the sample, before setting up the *ex-vivo* explant cultures. However, this method was only instigated towards the end of this project, therefore some of the earlier explants proved unusable.

Figure 4.21 shows that there is heterogeneity between different explants from a single tumour. Tumours are heterogeneous in their nature and histopathology. The fact that our model shows heterogeneity between explants reflects the *in vivo* situation more accurately and areas within a tumour will react differently to treatments. By dissecting a tumour sample into tiny fragments and randomly collecting nine explant pieces for each condition, we can capture the heterogeneity of the tumour. This would not be the case when using tissue slices (Kern *et al.*, 2006; Vaira *et al.*, 2010) for example, where you would see more uniform results because the tissue is sliced from the same exact area or in cell lines and organoid cultures derived from tumours.

Differences in tumour area were observed across samples and this could be resolved by introducing additional duplicates of the conditions in order to ensure that sufficient tumour area is covered across each condition. We felt it was important to provide a measure of the total tumour area that was assessed for each condition but ultimately this value was not taken into account in determining the effectiveness of a response to a drug.

In similar studies working with IHC endpoint explant cultures, scientists have reported the use of different approaches for quantifying responses for example by counting at least 50 cells from three different areas (van der Kuip *et al.*, 2006), or they measure 3 random 40x fields from each of three tissue slices per condition (average 97 nuclei per field; (Maund *et al.*, 2014). For the way we have assessed response, introducing duplicates or triplicates of the conditions should resolve any issues with tumour area differences. However, this would be extremely challenging in the analysis of multiple tumour explants and so introducing a slide scanner and specific software for accurately counting the staining and automation of the procedure would be a great advantage.

In this study, the best culture time was identified to be 24 hours after recovery after Page's L nonparametric trend test showed a negative trend of Ki67 staining with increasing culture time (Figure 4.12, $P=0.01$) and a positive trend of cell death with increasing culture time (Figure 4.14, $P=0.05$). However, the cell death values for the 48 and 72 hour time points we examined were not very different from the 24 hour time point, suggesting that culturing *ex-vivo* explants for a period of up to 72 hours is not detrimental.

In fact most of the other studies described in the literature have used tissue cultures for 4-7 days (Hayashi *et al.*, 2009; Pirnia *et al.*, 2006; Vaira *et al.*, 2010) and report maintenance of viability similar to their controls. Nevertheless, to my knowledge no group has published extensive data on the viability of the tissue cultures through time or any other factor. We also have one *ex-vivo* explant tissue culture that was kept for one week in culture and showed no increase of cleaved PARP levels compared to the uncultured control (data not shown), although there was some decrease of Ki67 levels. One would argue that, by prolonging the culture of the tissue, the situation would no longer mirror the *in*

vivo situation as the tumour explants would start adapting to the culture conditions and outgrow their original counterparts. Therefore the original tissue architecture of the patient's tumour would gradually fade. By keeping the culture time at 24 hours following an initial recovery of the explants, this should provide enough time to observe whether a drug treatment has a response or not and also keeps the tissue architecture intact, representing the original tumour. Therefore the decision was made to use 24 hour time points after 16-20 hours recovery.

Following the decision for the time the *ex-vivo* explant cultures should stay in culture, we wanted to study the effect of varying concentrations of FCS of the media. We chose to test a range of 0, 0.5, 1, 2.5 and 5% FCS since previous experiments on breast *ex-vivo* explant cultures showed that higher FCS led to a decrease in tumour survival (Shambhavi Naik, Professor Marion MacFarlane, MRC Toxicology Unit). From our experiments comparing the cell death percentages amongst 5 samples (Figure 4.16) and the proliferation values (Figure 4.18) showed no significant differences amongst the range of FCS concentrations in the samples, suggesting that varying FCS does not make an important contribution to the survival of the explants.

Most of the published literature on three dimensional explant cultures report using 10% FCS in the media (Pirnia et al., 2006; Hayashi et al., 2009; Furukawa et al., 2000) or even 20% (Vaira et al., 2010; Furukawa et al., 1995). However, in our previous experience with breast cancer, higher FCS led to decreased tumour survival (Shambhavi Naik- Professor MacFarlane's group). The fact that most of the other groups use such a high concentration of FCS and still report good viability, suggests that the variability of whether a sample will survive or not in culture comes from the variability of the tumour samples and that adding FCS or not in the media does not make a significant contribution. The presence or absence of FCS was also reported not to influence morphology and survival in human glioma cell lines and glioma biopsy primary cultures (Clavreul et al., 2009).

Taking all these into consideration, it was decided that 1% FCS was reasonable to use since most of the drug treatments were already done in that concentration, consisted with the breast cancer studies.

Looking at the comparison between the uncultured controls and the same samples cultured for 24 hours after recovery of all the viable *ex-vivo* explant cultures that were set up, there is an evident effect of cultivation. The cell death percentages are somewhat increased (Figure 4.19) and the proliferation percentages are slightly decreased (Figure 4.20). This was also shown in a study using NSCLC samples to set up a short term tissue culture model with a 16 hour time point (Lang *et al.*, 2007). They also show that the viability, proliferation and apoptosis of the tissues were mildly affected by cultivation (Lang *et al.*, 2007). One would expect to see a moderate effect of cultivation since the tumour samples are being taken out of their original environment and are subjected to vigorous cutting and changes of the original conditions. This however, does not mean we cannot use the *ex-vivo* explant culture system to test treatments.

To conclude, our findings indicate that an *ex-vivo* explant culture system for NSCLC that was developed from a model established by Professor MacFarlane's group with breast cancer samples can be used to test various treatments for NSCLC. NSCLC show some intrinsic heterogeneity but this can be accounted for in the method used for data analysis. Viability and growth of the tumour cells can be maintained in short term culture.

5. TESTING THE RESPONSE OF *EX-VIVO* NSCLC EXPLANTS TO CISPLATIN

5.1 Introduction

In order to begin to assess whether our *ex-vivo* explant culture system is predictive of patient response we chose to use one of the most potent anticancer agents, cisplatin which shows significant clinical activity against a variety of solid tumours. In fact, cisplatin-based combination treatment has been the most effective systemic chemotherapy for NSCLC having a ~30% response rate in NSCLC treatment (Ardizzoni *et al.*, 2007). Most of the patients we collected samples from were in the early stages (I-III) of NSCLC since they were given surgical treatment. The majority of these patients would have received adjuvant chemotherapy after their surgery to either kill any remaining tumour or, in case of complete resection, to reduce the risk of recurrence. Therefore if these patients were treated with cisplatin and we had the clinical information of their response, we potentially could correlate the results with the cisplatin response from our *ex-vivo* explant culture system. We tested cisplatin responses in a total of 19 samples and the data are shown here.

5.1.1 *Cisplatin: Mode of action*

Cisplatin reacts with nucleophilic N7-sites of purine bases in DNA and forms intrastrand DNA adducts (Eastman, 1987). The DNA damage induced by cisplatin is recognised by various proteins that activate several signal transduction pathways. Amongst these are p53, p73, ATR and MAPK (Siddik, 2003). This could either lead to DNA damage induced apoptosis or cell cycle arrest. The latter is linked with resistance as it gives time for the cell to repair the damage. In fact, a major limitation of cisplatin based chemotherapy is the multiple ways for developing resistance to the drug. Resistance mechanisms include reduced drug uptake, increased drug inactivation by metallothioneine and

glutathione, increased DNA repair, activation of the PI3-K/Akt pathway, loss of p53 function, overexpression of anti-apoptotic Bcl-2, and interference with caspase activation (Siddik, 2003).

5.2 Aims and objectives

- Test cisplatin responses in *ex-vivo* explant cultures of NSCLC.
- Correlate responses to clinical information on patient outcomes if possible.
- Test whether response to cisplatin correlates with p53 expression.
- Confirmation of cisplatin accumulation in explants by LA-ICP-MS.

5.3 Results

5.3.1 Dose responses to Cisplatin in 10 samples

Dose responses to cisplatin (1 μM , 10 μM and 50 μM) were tested and analysed in 10 tumour samples by cleaved PARP and Ki67 staining of tumour cells. Some samples demonstrated resistance to cisplatin treatment where others were sensitive. An example of a sample with sensitive responses of the explants to cisplatin is shown in Figure 5.1 and 5.2 and an example of a resistant sample is shown in Figure 5.3 and 5.4.

5.3.1.1 CISPLATIN SENSITIVE EXAMPLE CASE

LT92 had low intrinsic cell death and medium Ki67 staining. LT92 showed a response to cisplatin at the concentrations of 10 μM and 50 μM , with an increase in cell death of ~55% and ~90% respectively, compared to the carrier control (Figures 5.1 and 5.2).

LT92

24 hours after recovery

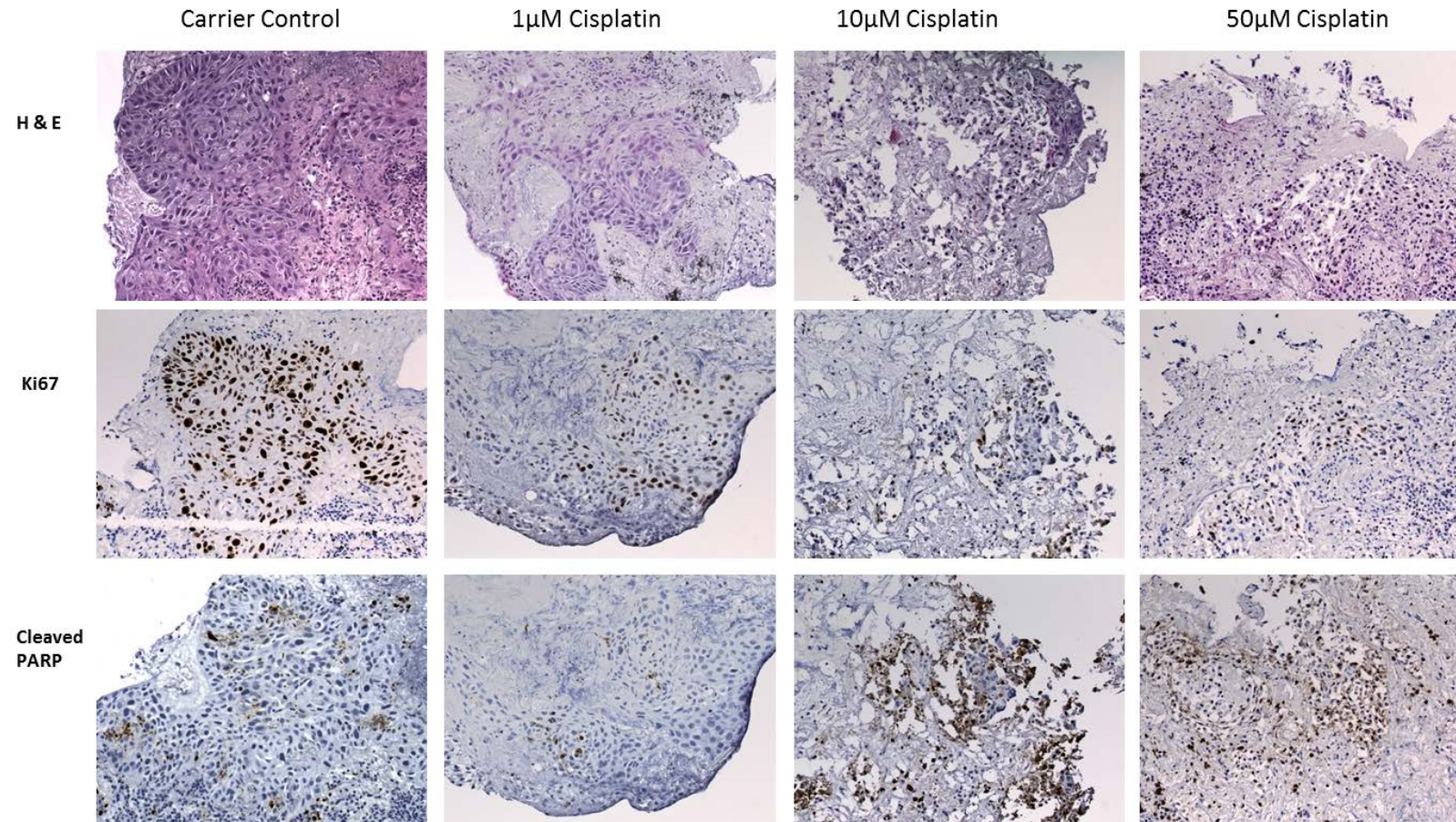


Figure 5.1. Representative images of corresponding areas in H&E staining, Ki67 staining (Proliferation marker) and cleaved PARP staining (apoptosis marker) of LT92.

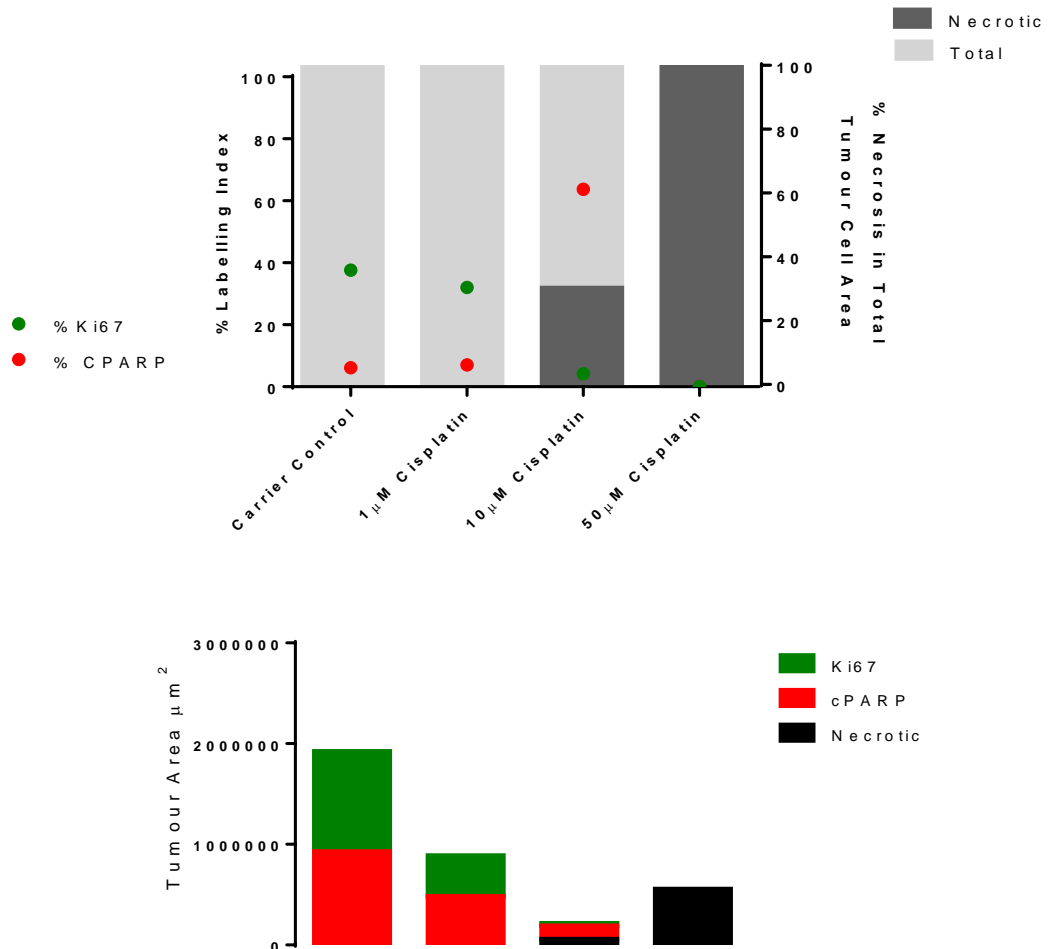


Figure 5.2. LT92 dose response to cisplatin treatment. Upper graph. Each point represents an additive number which characterises all the staining from each slide and also takes into account the area of the tumour cells for each explant on the slide. The red dot represents the percentage of cells that have a nucleus stained with cleaved PARP out of all the tumour cells present in the slide and similarly the green dot represents the Ki67 labelling index. The dark grey bars behind show the percentage of the area that was undergoing secondary necrosis as decided by cleaved PARP leakage out of the total area (light grey). It shows the proliferation (Ki67-green) and the apoptosis (cPARP-red) or the secondary necrosis (dark grey) of LT92 undergoing culture with the carrier alone and with increasing cisplatin concentrations (1 μ M, 10 μ M and 50 μ M) for 24 hours after the initial recovery period. Lower graph. This graph represents the exact values of the tumour areas used for Ki67 analysis (green bar), cleaved PARP analysis (red bar) and secondary necrosis so we can compare each condition with the amount of tumour cells present.

5.3.1.2 CISPLATIN RESISTANT EXAMPLE CASE

LT33 had low intrinsic proliferation and low intrinsic cell death. LT33 showed no response to cisplatin to either concentrations of 1 μM , 10 μM or the very high 50 μM , since no increase in cell death or reduction in proliferation was observed in comparison to the carrier control (Figures 5.3 and 5.4) suggesting LT33 is resistant to cisplatin treatment.

LT33

24 hours after recovery

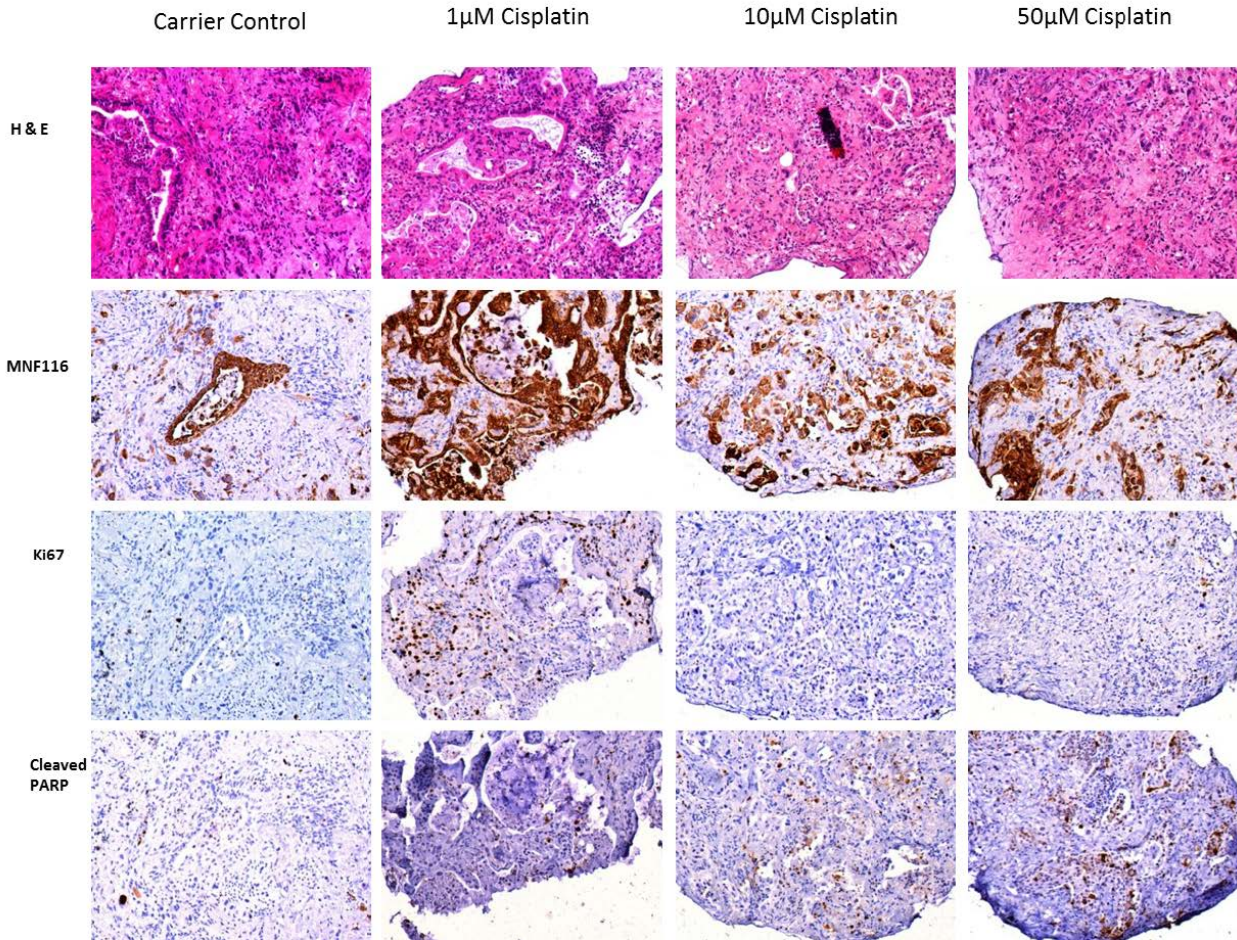


Figure 5.3. Representative images of corresponding areas in H&E staining, MNF116 (epithelial cell marker), Ki67 staining (Proliferation marker) and cleaved PARP staining (apoptosis marker) of LT33.

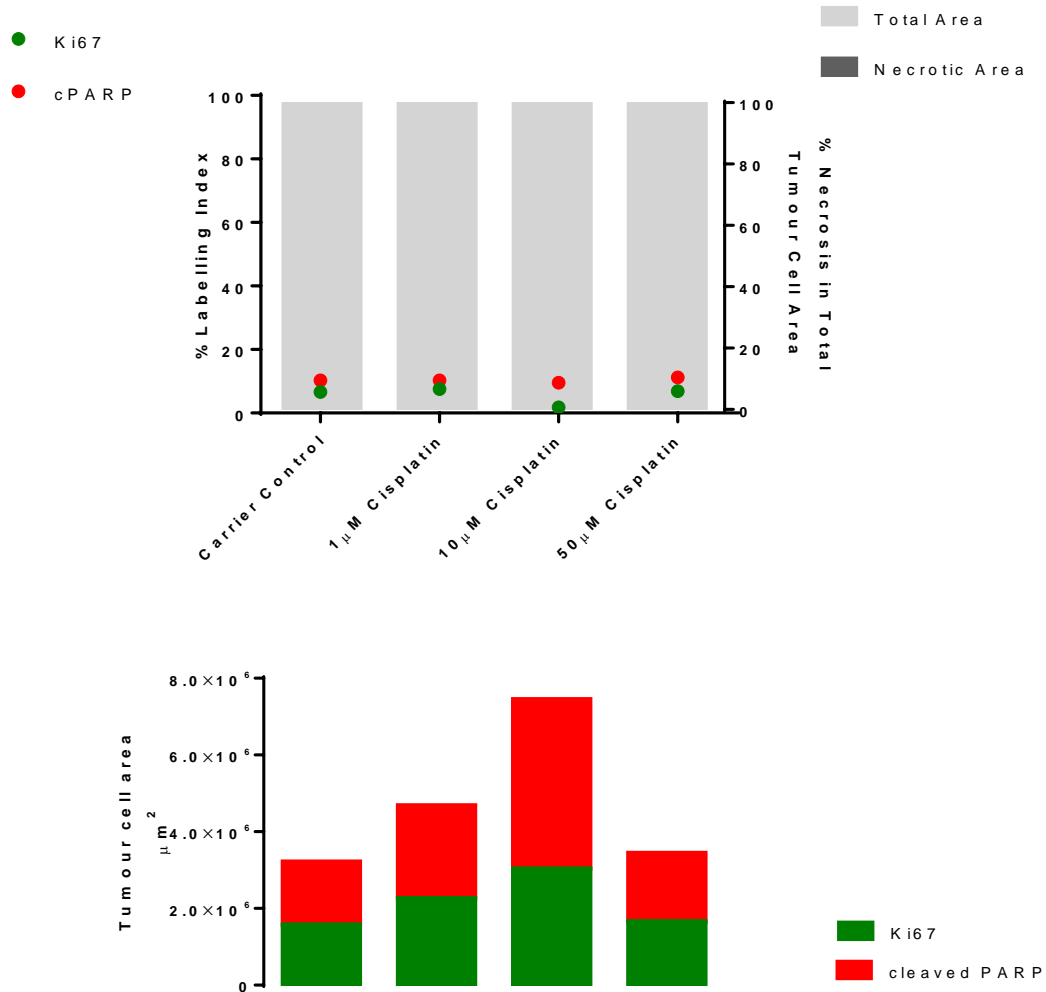


Figure 5.4. LT33 dose response to cisplatin treatment. Upper graph. Each point represents an additive number which characterises all the staining from each slide and also takes into account the area of the tumour cells for each explant on the slide. The red dot represents the percentage of cells that have a nucleus stained with cleaved PARP out of all the tumour cells present in the slide and similarly the green dot represents the Ki67 labelling index. The dark grey bars behind show the percentage of the area that was undergoing secondary necrosis as decided by cleaved PARP leakage out of the total area (light grey). It shows the proliferation (Ki67-green) and the apoptosis (cPARP-red) or the secondary necrosis (dark grey) of LT33 undergoing culture with the carrier alone and with increasing cisplatin concentrations (1 μ M, 10 μ M and 50 μ M) for 24 hours after the initial recovery period. Lower graph. This graph represents the exact values of the tumour areas used for Ki67 analysis (green bar), cleaved PARP analysis (red bar) and secondary necrosis so we can compare each condition with the amount of tumour cells present.

5.3.1.3 SUMMARY OF DOSE RESPONSES TO CISPLATIN IN 10 SAMPLES

The cleaved PARP and Ki67 staining of tumour cells were quantified for the 10 samples and normalised against each case's carrier control to take out the variability between cases and to be able to see the treatment effects only. A summary of the fold responses relative to the control is shown in Table 5.1 and Figures 5.5 for fold cell death and 5.6 for fold proliferation.

Table 5.1. The responses of 10 samples treated with 1 μ M, 10 μ M and 50 μ M of Cisplatin for 24 hours after an initial recovery of 16-20 hours, shown as fold changes compared to each sample's carrier control.

Sample	Concentration of Cisplatin	Fold cell death compared to control (=1)	Fold proliferation compared to control (=1)
LT31	1 μ M	0.88	0.49
	10 μ M	0.53	0.22
	50 μ M	6.47	0.00
LT33	1 μ M	1.00	1.14
	10 μ M	0.93	0.27
	50 μ M	1.09	1.04
LT34	1 μ M	0.85	1.52
	10 μ M	1.07	0.87
	50 μ M	2.07	0.10
LT36	1 μ M	0.62	0.96
	10 μ M	1.03	1.18
	50 μ M	1.35	0.37
LT38	1 μ M	2.70	1.24
	10 μ M	1.37	1.70
	50 μ M	6.11	1.01
LT83	1 μ M	0.91	0.67
	10 μ M	0.85	0.96
	50 μ M	4.46	0.51
LT84	1 μ M	0.65	1.58
	10 μ M	1.30	0.86
	50 μ M	2.18	0.00
LT88	1 μ M	2.72	7.13
	10 μ M	8.80	0.05
	50 μ M	9.49	0.00
LT89	1 μ M	1.04	2.20
	10 μ M	0.79	1.56
	50 μ M	1.42	1.19
LT92	1 μ M	1.15	0.84
	10 μ M	6.98	0.19
	50 μ M	16.39	0.00

Some of the explants showed cell death dose responses with increasing concentrations of cisplatin (LT92, LT88) whereas in others there was not a clear dose response.

At the concentration of 1 μM of cisplatin, out of the 10 samples, tested LT38 and LT88 (2/10 cases: 20%) showed a 3-fold cell death response relative to their controls (Figure 5.5). At the concentration of 10 μM of cisplatin, LT88 and LT92 (2/10 cases: 20%) showed a 9-fold and a 7-fold cell death response respectively. At the very high concentration of 50 μM of cisplatin, 5/10 samples showed a response (50%). Three of these samples showed a 4-7 fold cell death response (LT83, LT34 and LT38), whereas LT88 and LT92 showed > 9-fold cell death response (Figure 5.5).

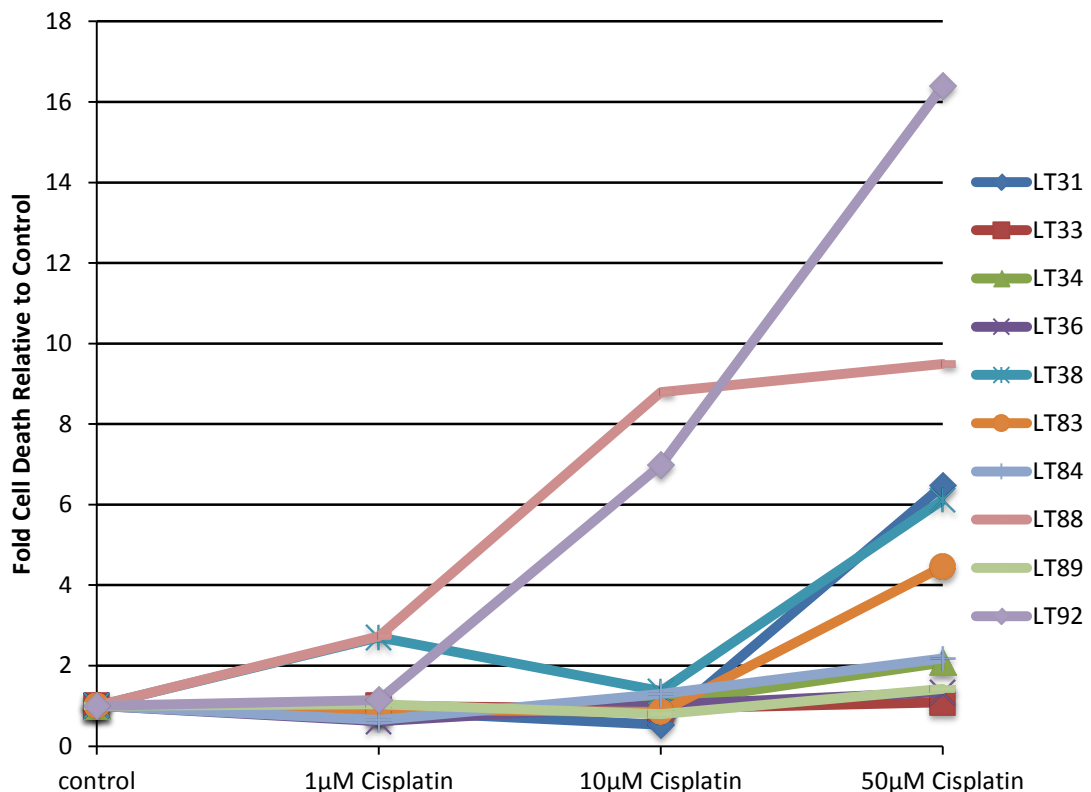


Figure 5.5. Fold Cell Death relative to control of 10 NSCLC *ex-vivo* explant cultures treated with doses of cisplatin. The % Cell Death values from each sample were determined from cleaved PARP staining for the carrier control compared with explants from the same tumour cultured in increasing cisplatin concentrations (1 μM , 10 μM and 50 μM) for 24 hours after an initial recovery of 16-20 hours. The value for each treatment was divided by the carrier control to give the fold change.

In assessing proliferation, some of the samples gave a slight increase of proliferation (1-2 fold) with low doses of cisplatin, although in one case this was 7-fold (Figure 5.6). The increase at 1 μM of Cisplatin is completely anomalous and is difficult to explain since some of these samples showed a cell death response at 1 μM (LT88). It is highly unlikely that any concentration of cisplatin would be inducing proliferation, given previous data on the drug. This raises the possibility that the increase arises from the variability of proliferation rates across the samples or loss of tissue during processing which could skew the data. By introducing duplicates or triplicates for the conditions we could increase the tumour area and be more certain of the results; however this depends on the amount of sample initially given from the surgery, which tends to be quite small.

Nonetheless, figure 5.6 shows that most of the samples treated with increasing doses of cisplatin show decrease in proliferation, especially from 10 μM to 50 μM . Because of the variability of Ki67 staining and quantitation our analysis would suggest we should focus on the cleaved PARP staining and the cell death data, rather than Ki67 proliferation.

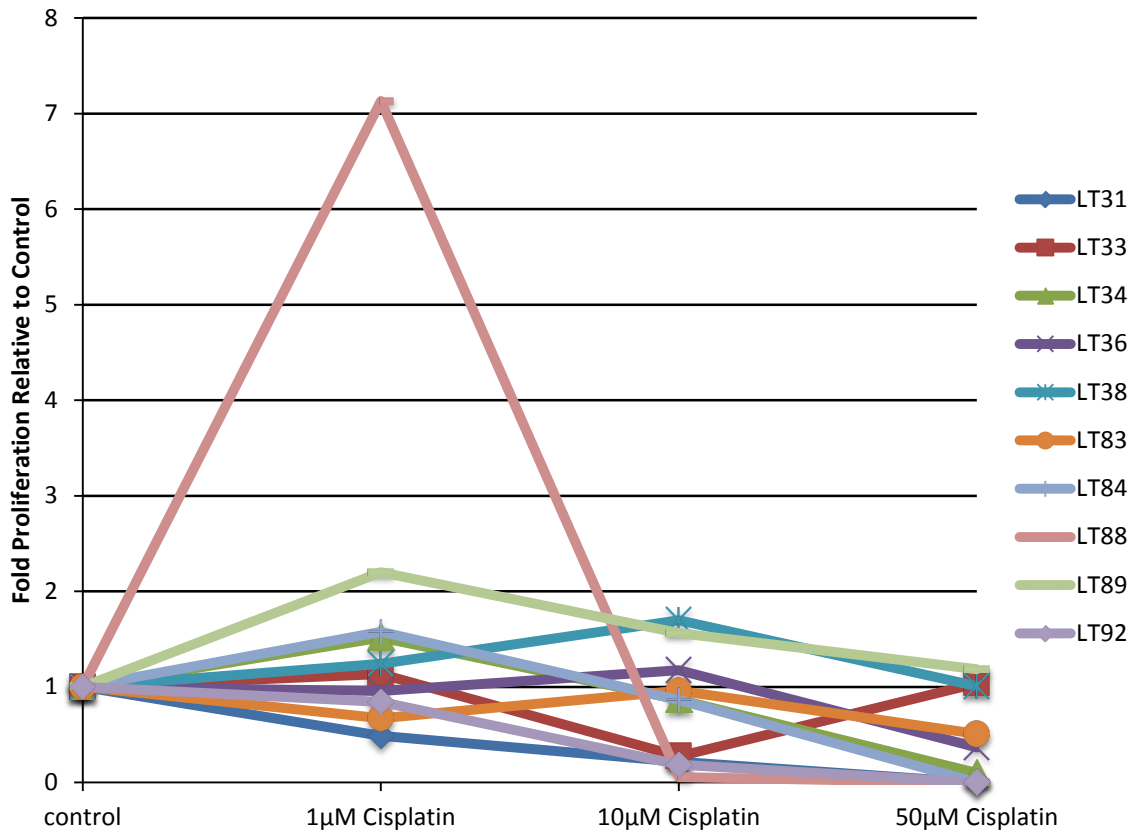


Figure 5.6. Fold Proliferation relative to control of 10 NSCLC *ex-vivo* explant cultures treated with doses of cisplatin. The % Proliferation values from each sample were determined from Ki67 staining for the carrier control compared with explants from the same tumour cultured in increasing cisplatin concentrations (1 µM, 10 µM and 50 µM) for 24 hours after an initial recovery of 16-20 hours. The value for each treatment was divided by the carrier control to give the fold change.

5.3.2 Responses of ex-vivo explant cultures to 50 µM of Cisplatin only

We obtained an additional nine samples that were treated with 50 µM of cisplatin only. Data from these were combined with the 50 µM treatment of the previous 10 samples, giving a total of 19 samples (Table 5.2). 7 (LT92, LT14, LT88, LT22, LT31, LT38 and LT83) out of the 19 samples (36.8%) showed response to 50 µM of cisplatin by more than 4-fold increase in cell death relative to the control (Figure 5.7). Two samples (LT32 and LT18) showed a 3-fold increase of cell death and another two (LT84 and LT34) showed a 2-fold increase of cell death. 8 out of the 19 samples did not respond at all.

Looking at the proliferation results in Figure 5.8, then 7 out of 19 samples showed strong suppression of proliferation (LT14, LT31, LT84, LT18, LT92, LT88 and LT34). Five samples showed no change of proliferation at all and some of them actually showed a small increase of proliferation, which again is probably reflective of variation between different tumour areas in a sample. These five samples also did not respond to the drug in terms of cell death changes (Figure 5.7). The rest 7 of the samples showed variable decreases of proliferation ranging from 0.3 to 0.7 of the control.

A four-fold increase of cell death would be a reasonable cut-off of sensitivity in a very high concentration of a drug. In this case, 7 out of 19 samples show response (36.8) (Figure 5.7). In fact 5 of these 7 samples also showed complete lack of proliferation (Figure 5.8).

5 of the 7 samples that responded to cisplatin were squamous cell cancers of the lung and 2 were adenocarcinomas (see Table 5.2).

Table 5.2. A summary of information on explants set up from 19 samples and the corresponding patient information. Patients with no death date are considered still alive. Samples highlighted in red were considered to respond by more than 4 fold increase of cell death at 50 μ M of cisplatin.

Code	fold cell death relative to control	fold proliferation relative to control	Histology	Death	Age	Sex	Group stage
LT89	1.42	1.19	Atypical carcinoid tumour		85	F	IB
LT33	1.09	1.04	Adenocarcinoma		79	F	IIIA
LT15	0.89	0.98	Atypical carcinoid tumour		54	M	IIIA
LT83	4.46	0.51	Adenocarcinoma	08/10/2013	70	M	IIB
LT22	7.82	0.52	Adenocarcinoma		65	M	IB
LT32	3.20	0.70	Adenocarcinoma		55	M	IB
LT16	1.26	1.45	Adenocarcinoma	26/04/2012	69	F	IIIA
LT38	6.11	1.01	Squamous cell carcinoma		76	M	IIA
LT20	1.50	0.45	Adenocarcinoma		77	F	IIIB
LT34	2.07	0.10	Adenocarcinoma		65	F	IIIA
LT27	1.56	0.53	Adenocarcinoma		60	M	IIIA
LT23	1.30	0.32	Squamous cell carcinoma		81	M	IIIA
LT36	1.35	0.37	Adenocarcinoma	01/05/2012	61	M	IB
LT18	3.10	0.01	Squamous cell carcinoma	05/06/2011	84	M	IA
LT14	10.01	0.00	Squamous cell carcinoma		65	F	IA
LT31	6.47	0.00	Squamous cell carcinoma		74	F	IB
LT84	2.18	0.00	Squamous cell carcinoma		75	F	Unknown
LT88	9.49	0.00	Squamous cell carcinoma		68	F	IA
LT92	16.39	0.00	Squamous cell carcinoma		62	F	IIB

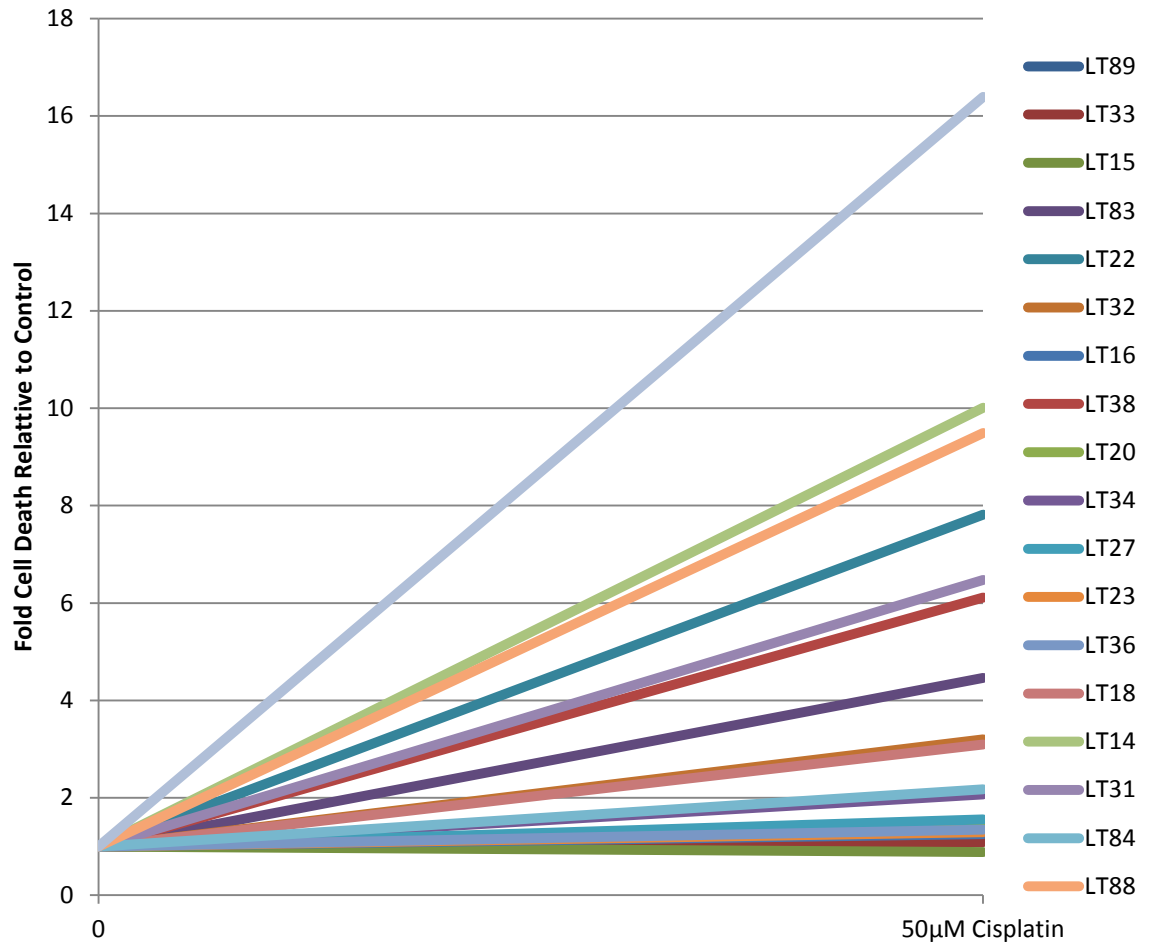


Figure 5.7. Induction of cell death relative to the carrier control upon 50 µM cisplatin treatment in 19 NSCLC *ex-vivo* explants. Cultures were incubated with or without cisplatin for 24 hours after an initial recovery period of 16-20 hours and analysed for cell death (cleaved PARP IHC positivity of cancer cells). Treatments were divided by each sample's control to calculate the fold difference.

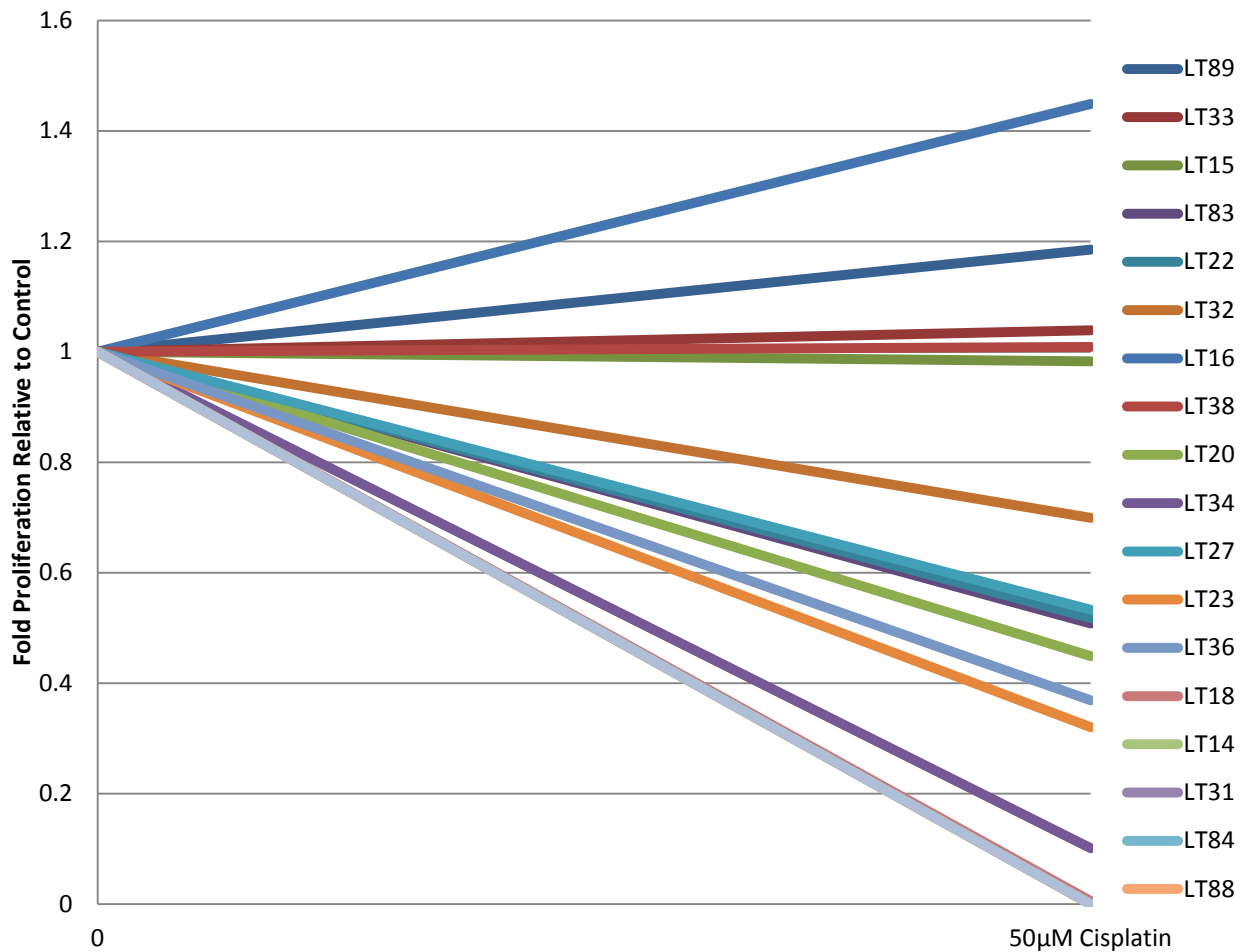


Figure 5.8 Reduction of proliferation relative to the carrier control upon 50 μ M cisplatin treatment in 19 NSCLC *ex-vivo* explants. Cultures were incubated with or without cisplatin for 24 hours after an initial recovery period of 16-20 hours and analysed for proliferation (Ki67 IHC positivity of cancer cells). Treatments were divided by each sample's control to calculate the fold difference.

5.3.2.1 CORRELATION WITH CLINICAL OUTCOMES

Unfortunately thus far, we do not have all the clinical information of the patients for which we set up *ex-vivo* explant cultures from tumours. Post-op therapy information was only provided for patient from LT34 (2 cycles of cisplatin/vinorelbine) and therefore we had to assume that most patients should have been treated with a cisplatin based combination therapy since it is the most commonly used drug in the clinic for NSCLC. The only clinical data we were provided with thus far is the death date of patients (Table 5.2). From this it is evident that 6/7 patients who showed a response to cisplatin in our *ex-vivo* explant model (more than 4-fold increase of cell death at 50 μ M) are still alive.

The exemption is patient LT83 who died exactly 21 days after the surgery took place, which suggests he might have died of complications from the surgery rather than being related to the chemotherapy he received (Table 5.2).

In contrast, two patients died after 6 months and 1 year from the surgery date, LT16 and LT36. These two patients showed no response to cisplatin treatment in our *ex-vivo* explant system (Table 5.2) even at the high 50 μ M dose. Thus 2/12 non-responders in explants have died.

5.3.3 Characterisation of samples by P53 expression status

The 19 *ex-vivo* NSCLC explant cultures that were treated with cisplatin were analysed for p53 protein expression by immunohistochemistry. According to their p53 immunostaining characteristics, the tumour samples could be divided into 3 categories: 1) In 9 of 19 cases (47%), we found constitutively low (less than 20% of cancer cells) or undetectable p53 levels in cancer cell nuclei in untreated samples and an accumulation of p53 in the cancer cells upon cisplatin treatment (Figure 5.9 for representative example). This suggests these samples carry wild-type *TP53* since under normal conditions p53 is not present at noticeable levels in the cell. However, upon various types of cellular stresses, p53 becomes stabilized and rapidly accumulates within the nucleus. 2) In 9 of 19 samples (47%) we found constitutively high p53 levels in the cancer cell compartment (Figure 5.10), with no further p53 accumulation after cisplatin treatment. This suggests *TP53* is mutated in these samples as p53 proteins produced by missense mutations are regularly very stable, as a result of escaping post-translational mechanisms that otherwise promote rapid p53 degradation (Schmid *et al.*, 2012). 3) In one case LT92, p53 protein was completely undetectable in cancer cell nuclei both without and with cisplatin treatment suggesting that *TP53* is probably deleted. In all, we can say that according to p53 IHC, 47% of the samples tested were IHC-wtp53 (9/19) and 53% were IHC-mtp53 (10/19, either missense mutation or deletion). Of these 10 IHC-mtp53 samples, 3 were adenocarcinomas and 7 were squamous cell carcinomas.

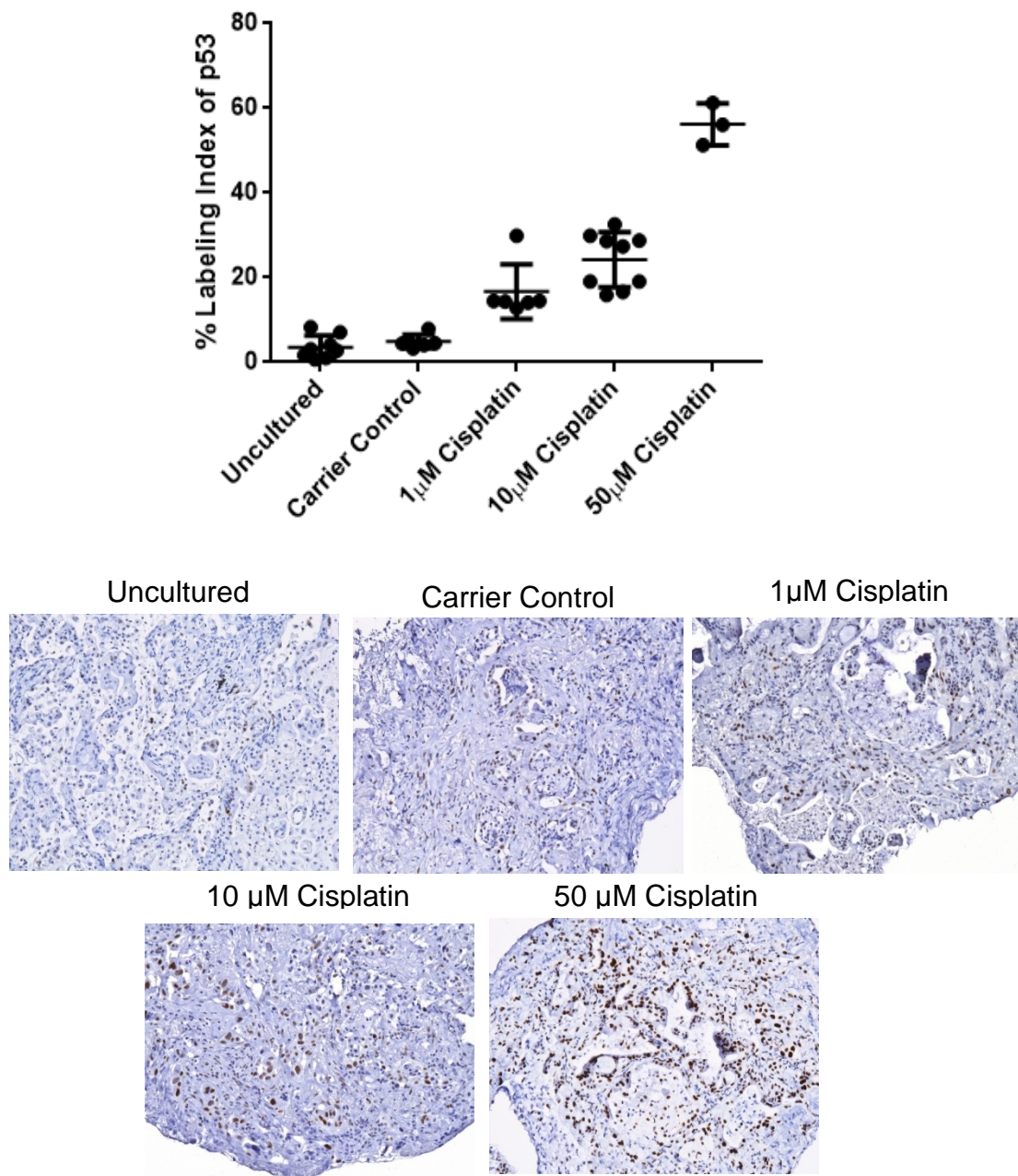


Figure 5.9 A p53 wild-type example (LT33) upon cisplatin doses. Quantification of nuclear p53 staining on tumour cells. The upper graph shows the accumulation of p53 during increasing doses of the drug, cisplatin (Test for linear trend $*P < 0.0001$). The bottom panel shows representative pictures of the p53 staining.

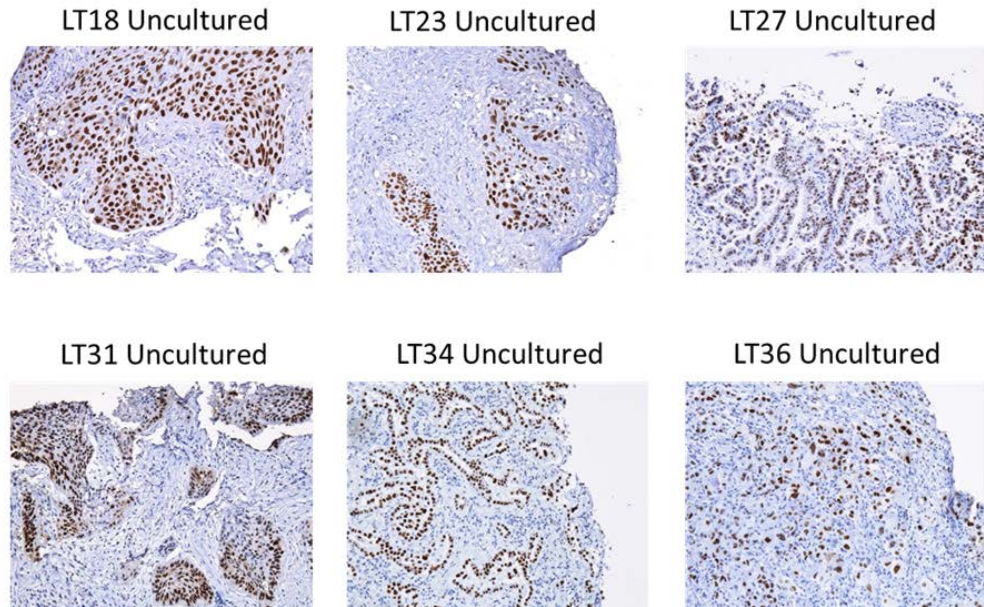


Figure 5.10 Examples of samples expressing constitutively high p53.

Interestingly, tumours harbouring IHC-mtp53 had a significantly ($P < 0.05$) higher intrinsic rate of Ki67-positivity in cancer cells of the native tumour compared with IHC-wtp53 tumours (Fig. 5.11). This is probably because most of them were squamous cell carcinomas and as mentioned in section 4.3.3 this subclass has higher intrinsic proliferation rates.

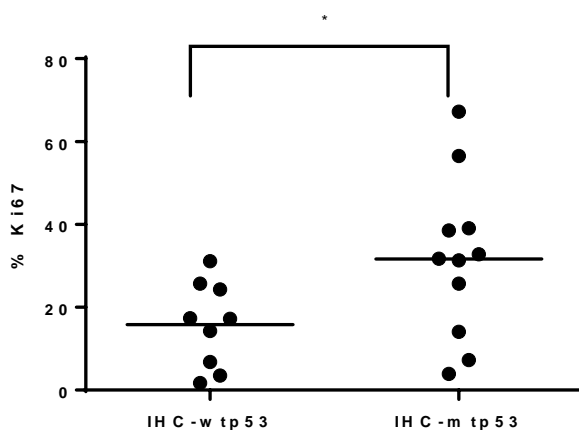


Figure 5.11 Intrinsic Rates of Ki67 staining according to p53 IHC status. Each circle represents one sample. Mann Whitney test between IHC-wtp53 and IHC-mtp53 showed significant difference (P value= 0.02).

5.3.3.1 CORRELATION WITH P21/^{CIP1}

We wanted to test whether IHC-wtp53 increase upon increasing concentration of cisplatin correlates with p21/^{CIP1} induction in the explants. Due to time restrains we could only test this in 3 IHC-wtp53 samples. A representative example is shown in Figure 5.12 for LT33 (p53 accumulation shown in Figure 5.9). We can observe p21/^{CIP1} induction upon increasing concentrations of cisplatin suggesting wt p53 signals through p21/^{CIP1}.

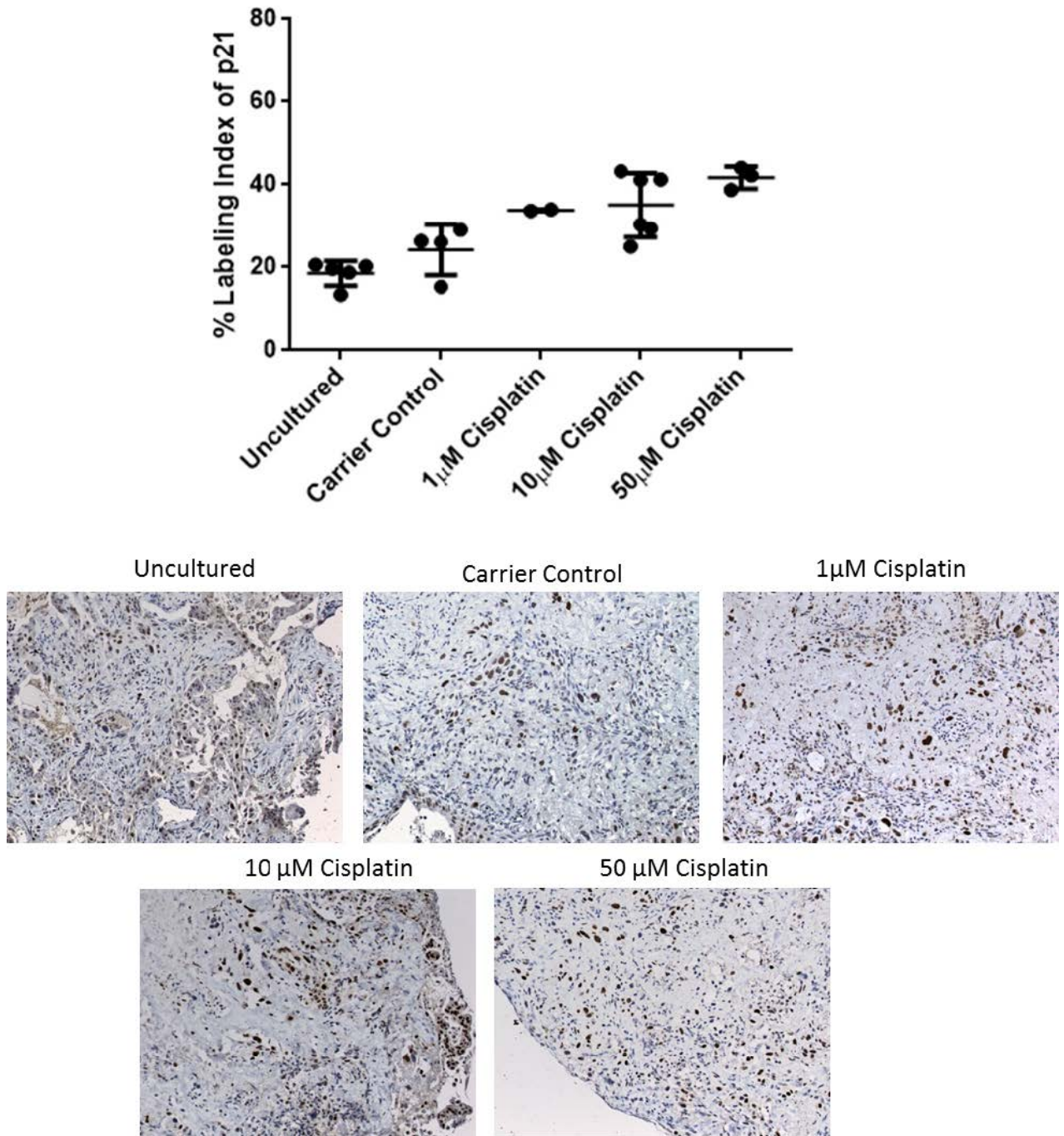


Figure 5.12. p21^{CIP1} expression in LT33 upon cisplatin doses. Quantification of nuclear p21 staining on tumour cells is shown in the upper graph during increasing doses of the drug, cisplatin (Test for linear trend *P< 0.0001). The bottom panel shows representative pictures of the p21 staining.

5.3.3.2 CORRELATION OF CISPLATIN RESPONSE TO P53 EXPRESSION STATUS

Re-plotting the responses of the 19 samples treated with 50 μ M of cisplatin according to their IHC p53 status (Table 5.3; Figure 5.13), showed that out of the 7 samples that showed more than 4-fold cell death increase: 4 had IHC-mtp53 and 3 had IHC-wtp53. From these, samples that were IHC-mtp53 seemed to show higher fold cell death responses and fold decreases in proliferation than the IHC-wtp53 sensitive samples. In general, IHC-mtp53 samples show higher fold decreases in proliferation with 50 μ M of cisplatin than IHC-wtp53. This probably reflects the high intrinsic proliferation of those samples since most of the IHC-mtp53 samples are squamous cell cancers of the lung (Figure 5.13).

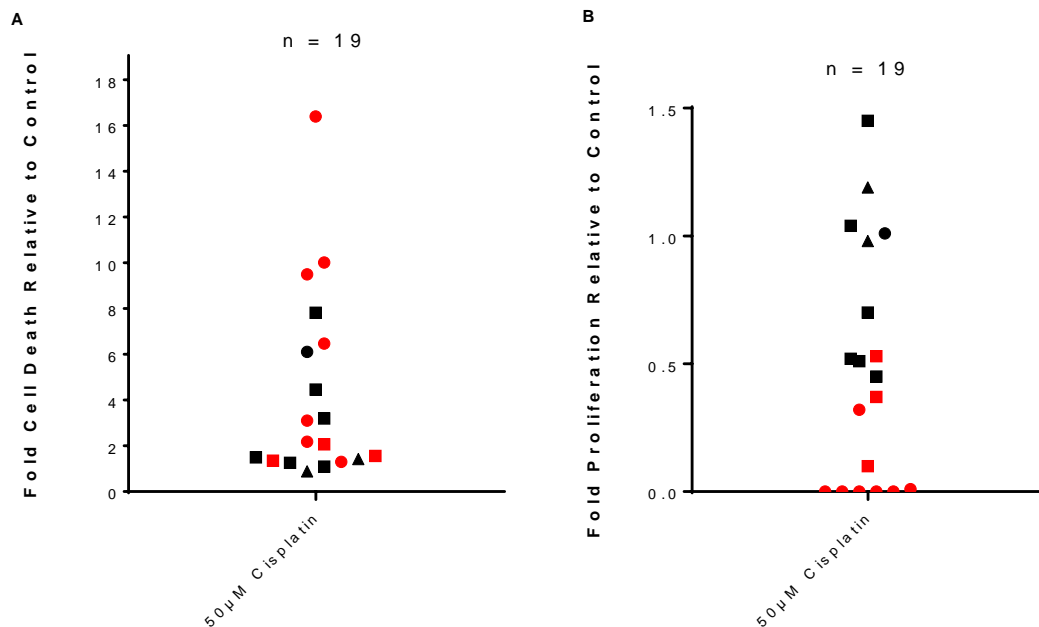


Figure 5.13. Induction of cell death and reduction of Ki67 score upon 50 μ M cisplatin treatment in 19 NSCLC *ex-vivo* explants stratified by p53 status. Red indicates IHC-mtp53 and black are IHC-wtp53 samples. Squares are ADC, circles SCC and triangles AC. A) Induction of fold cell death relative to controls in samples and B) Reduction of fold proliferation relative to controls in samples.

Table 5.3. Correlation of cisplatin response to p53 expression status. Shown here the fold cell death and fold proliferation relative to control after 50 μ M of cisplatin treatment, the raw cell death difference from the control, the raw proliferation difference from the control, the p53 IHC status and histology from 19 samples.

Code	fold cell death relative to control	fold proliferation relative to control	Cell death raw difference from control	Proliferation raw difference from control	p53 IHC	Histology
LT89	1.42	1.19	1.49	3.53	IHC-wtp53	AC
LT33	1.09	1.04	0.94	14.30	IHC-wtp53	ADC
LT15	0.89	0.98	-1.41	1.73	IHC-wtp53	AC
LT83	4.46	0.51	14.59	17.31	IHC-wtp53	ADC
LT22	7.82	0.52	29.94	6.81	IHC-wtp53	ADC
LT32	3.2	0.7	27.50	46.51	IHC-wtp53	ADC
LT16	1.26	1.45	8.80	31.08	IHC-wtp53	ADC
LT38	6.11	1.01	40.43	24.32	IHC-wtp53	SCC
LT20	1.5	0.45	18.05	25.67	IHC-wtp53	ADC
LT34	2.07	0.1	30.37	7.28	IHC-mtp53	ADC
LT27	1.56	0.53	21.58	25.71	IHC-mtp53	ADC
LT23	1.3	0.32	15.21	39.04	IHC-mtp53	SCC
LT36	1.35	0.37	22.15	31.69	IHC-mtp53	ADC
LT18	3.1	0.01	67.21	67.17	IHC-mtp53	SCC
LT14	10.01	0	90.01	38.5	IHC-mtp53	SCC
LT31	6.47	0	84.56	56.54	IHC-mtp53	SCC
LT84	2.18	0	54.05	32.79	IHC-mtp53	SCC
LT88	9.49	0	89.47	3.94	IHC-mtp53	SCC
LT92	16.39	0	93.90	31.28	IHC-mtp53	SCC

Separating the responses to cisplatin to IHC-wtp53 and IHC-mtp53 revealed significant differences (Figure 5.14). The fold proliferation reduction of IHC-mtp53 samples was significantly higher than IHC-wtp53 samples ($***P=0.0002$; Mann-Whitney $U=3$; Median of IHC-mtp53 group: 0.005 vs Median of IHC-wtp53 group: 0.98; Figure 5.14A). The fold cell death increases were not statistically significant between the two groups ($P=0.21$). However comparing the raw difference between the %cell death values of treated and control explants, showed that IHC-mtp53 samples had significantly higher cell death induction than IHC-wtp53 samples ($**P=0.004$; Mann-Whitney $U=11$; Median of IHC-mtp53 group: 14.59 vs Median of IHC-wtp53 group: 60.63; Figure 5.14D).

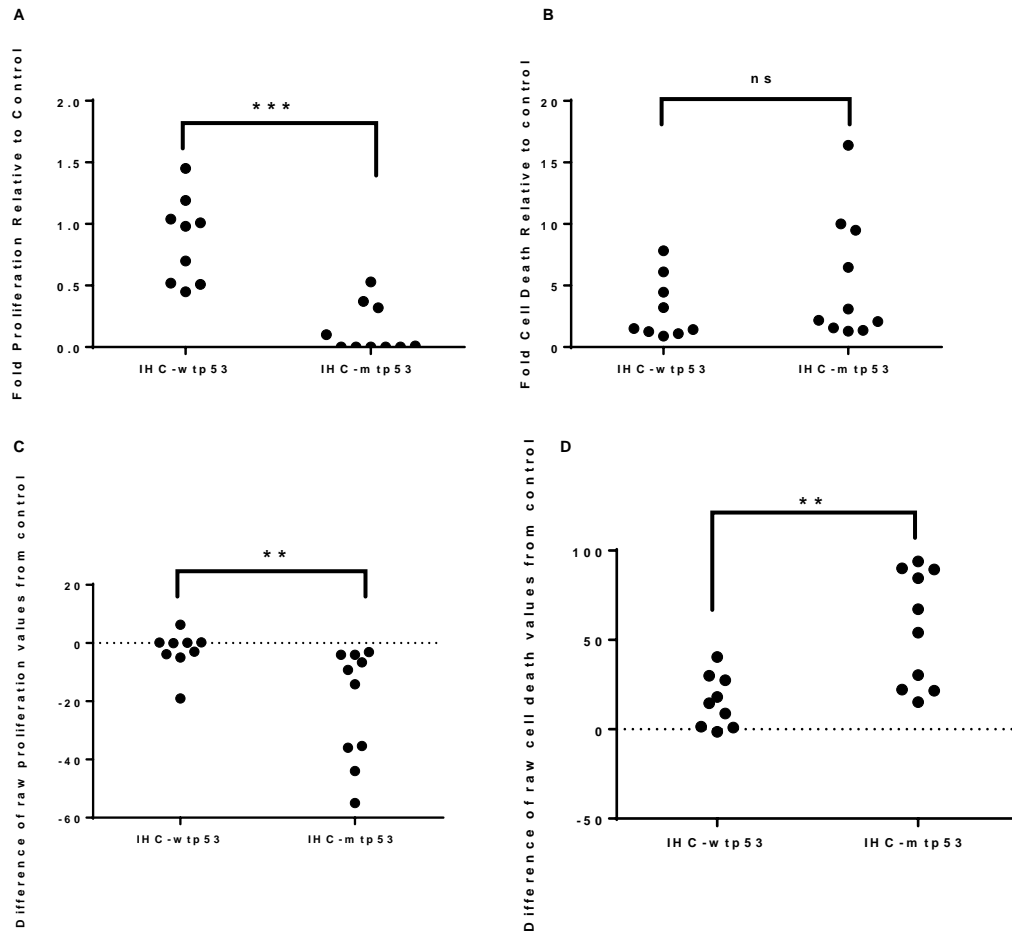


Figure 5.14. Comparison between IHC-wtp53 and IHC-mtp53 explants to fold responses and raw differences in response to 50 μ M cisplatin. A) Fold proliferation responses relative to control in IHC-wtp53 and IHC-mtp53 to 50 μ M cisplatin. Mann Whitney test between the two groups revealed significant differences (**P= 0.0002; Mann-Whitney U=3). B) Fold cell death responses relative to control in IHC-wtp53 and IHC-mtp53 to 50 μ M cisplatin. Mann Whitney test between the two groups revealed no significant differences (P=0.21). C) Differences between the raw %proliferation values between treated and control in IHC-wtp53 and IHC-mtp53 to 50 μ M cisplatin. Mann Whitney test between the two groups revealed significant differences (**P= 0.003; Mann-Whitney U=10). D) Differences between the raw %cell death values between treated and control in IHC-wtp53 and IHC-mtp53 to 50 μ M cisplatin. Mann Whitney test between the two groups revealed significant differences (**P= 0.004; Mann-Whitney U=11).

5.3.4 LA-ICP-MS element distribution mapping of Pt-treated explants

One thing we wanted to make sure of was whether the cisplatin is actually getting into the explants so that lack of response could not be attributed to inaccessibility of drug. One proof comes from IHC-wtP53 sample in Figures 5.9 and 5.12 where we can see an accumulation of p53 and p21, respectively, with increasing concentrations of cisplatin in one example case, suggesting that the drug is causing a DNA damage response in the tumour cells.

In addition, we collaborated with Professor Barry Sharp's group from Loughborough University that work with Laser Ablation Inductively Coupled Plasma Mass Spectrometry (LA-ICP-MS) which can be used to study the spatially-resolved distribution of elements (Zayed *et al.*, 2011). They were able to resolve the distribution of platinum (Pt) in our cisplatin treated slides with this method and we could therefore visualise where cisplatin is located in a sample. Due to time constraints we only have the LA-ICP-MS Pt distribution information for one sample thus far, LT31 treated with 10 μ M of cisplatin. LT31 (IHC-mtP53) showed no response at 10 μ M cisplatin but did show a response at 50 μ M. Figure 5.15 shows LT31 treated with 10 μ M of cisplatin and not responding to the treatment (Figure 5.15 D for cell death). As we can see from the Pt distribution from the LA-ICP-MS (Figure 5.15E), there is Pt depletion in areas corresponding to tumour cells but is present all around the tumour areas in the stroma cells suggesting that cisplatin is delivered through our *ex-vivo* NSCLC culture system. Another metal, Zinc, was used as a control (Figure 5.15F). Zinc distribution is similar across the tumour tissue slide.

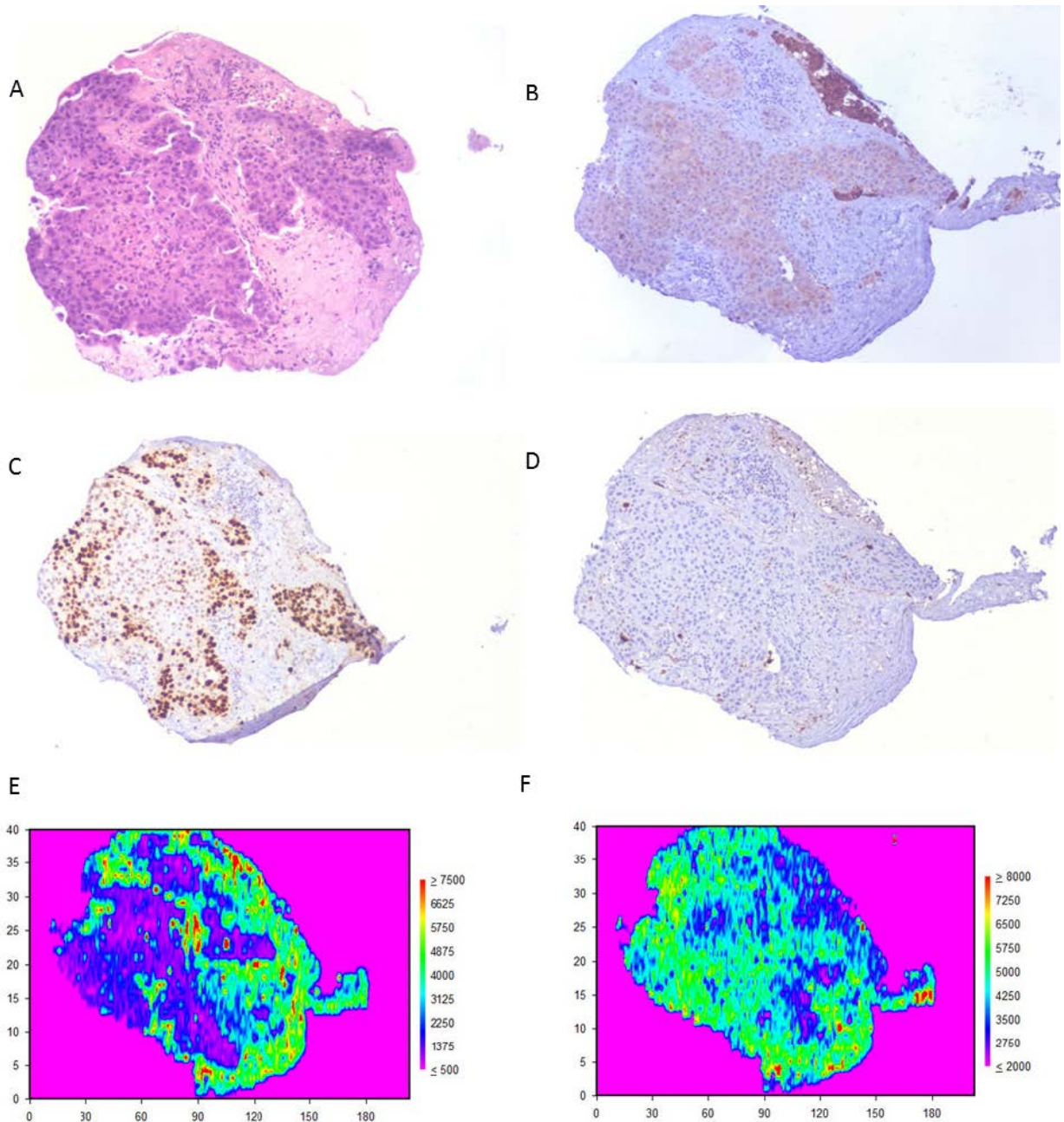


Figure 5.15. LA-ICP-MS sampling of human lung cancer explant LT31 treated with 10 μ M cisplatin for 24h. Photomicrographs showing: A) H & E stained tumour section, B) Pan Cytokeratin immunohistochemical (IHC) staining (tumour marker), C) Ki67 IHC staining (proliferation marker), D) cPARP IHC staining (cell death marker). LA-ICP-MS sampling (Data provided by Dr John Pugh) for the same section showing distribution for :- E) Platinum F) Zinc.

5.4 Discussion

The peak plasma concentration of cisplatin reported in the literature is variable. One study on 17 patients with advanced breast cancer treated with 100 mg/m² described a peak plasma platinum concentration of 3.91 µg/ml ± 1.41 (Ostrow *et al.*, 1980). Another study comparing the pharmacokinetics of cisplatin and two other drugs reported peak plasma platinum concentration of 3.09 µg/ml after 30 minute intravenous injection of 80mg/m² cisplatin (Sasaki *et al.*, 1989). One other study comparing different infusion times of 100 mg/m² cisplatin given in rapid, 3hr and 24hr infusion times reported plasma platinum levels of 8.62 µg/ml, 1.96 µg/ml and 0.27 µg/ml respectively (Vermorken *et al.*, 1982). In a different study working with paediatric patients with solid tumours they investigated the pharmacokinetics of free platinum in 12 children receiving cisplatin (75-120 mg/m²) with different infusion times and found plasma platinum concentrations of 13.5 +/- 4.97 µg/ml in patients treated with 100 mg/m² cisplatin (Erdlenbruch *et al.*, 2001). Another study reported peak concentration of total platinum of 49 µmolar per litre (van Hennik *et al.*, 1987) in patients treated with 100 mg/m² cisplatin, which corresponds to ~15 µg/ml.

Therefore, there is a range of peak plasma platinum concentrations reported from patients treated with 100 mg/m² cisplatin, from as low as 0.27 µg/ml to as high as 13.5 +/- 4.97 µg/ml. Differences in the infusion times of cisplatin or in the time intervals the plasma measurements took place, could account for this range. It can be confusing however when you are trying to determine the clinically relevant concentrations of drugs to use in experiments. In our study we chose to use 1 µM, 10 µM and 50 µM of cisplatin which correspond to 0.3 µg/ml, 3 µg/ml and 15 µg/ml, respectively. This allows for us to assess whether there is a dose response of the tumours.

Other studies using similar models to ours reported using a range of cisplatin concentrations. One study using tumour explants with autoradiography as an end point to screen for tumour drug sensitivity, described 1.5 µg/ml of cisplatin and 24 hr exposure to be therapeutically relevant according to peak plasma concentrations in patients (Vescio *et al.*, 1987). They also used a 10x

concentration and showed response in 14/27 explants, whereas the 1x concentration was only active in 7/29 (Vescio *et al.*, 1987). When they tried using higher concentrations, there was an increase of false-positive cases (Vescio *et al.*, 1991). In a different study using *ex-vivo* explants of NSCLC, they described 10 µg/ml of cisplatin to be clinically relevant and reported 5/9 samples to respond to this concentration after 120h treatment (Pirnia *et al.*, 2006).

The majority of studies have been based on HDRA (histoculture drug response assay) with the MTT assay as an endpoint and, using a massive 20 µg/ml of cisplatin, there was a high correlation between the assay and patients (Yoshimasu *et al.*, 2007; Furukawa *et al.*, 1995; Ariyoshi *et al.*, 2003; Fujita *et al.*, 2009; Furukawa *et al.*, 1992). In fact, Furukawa *et al.* discussed that the doses of drugs they used are supra-pharmacological but there was a high *in vitro* - *in vivo* correlation and they argued that the optimal cut-off drug concentrations should be determined independently with each assay and each end point used (Furukawa *et al.*, 1992).

In our study if we used 1 µM of cisplatin (0.3 µg/ml) as a cut-off value then we had two responders out of the ten samples tested at that concentration which gives a percentage of 20% response to cisplatin (Table 5.1, Figures 5.5). If we take 10 µM of cisplatin (3 µg/ml) as a cut-off value then 2/10 cases showed a response which also gives a percentage of 20% response to cisplatin. If we take 50 µM of cisplatin (15 µg/ml) as a cut-off value then 7/19 cases showed a response which gives a percentage of 36.8% response to cisplatin. The reported response rate to cisplatin-based treatment is 30% in NSCLC (Ardizzoni *et al.*, 2007), suggesting the explant system is broadly consistent with patient response. What we can definitely conclude is that we had 12/19 samples that showed no response even at 50 µM of cisplatin in our *ex-vivo* explant culture model system. We would argue that these patient's tumours would be intrinsically resistant to cisplatin treatment and this could have implications in choosing the right treatment for patients. Indeed two out of the twelve patients for whom we set up *ex-vivo* explant cultures from that did not respond, died after 6 months and 1 year from the surgery date, suggesting they would not have responded very well to post-op chemotherapy.

Because of the variability of Ki67 staining and quantitation we focused on the cleaved PARP staining and the cell death data, rather than Ki67 proliferation in assessing responders to cisplatin treatment. In low doses of the drug we observed increases in proliferation compared to the control in some cases (Figure 5.6). This observation most likely reflects the intrinsic proliferation variability evident in different regions of the tumours and the number of tumour cells present for analysis; larger areas should average this out. Another possibility is that because of tumour heterogeneity, different regions of the tumour respond differently to drugs. For example, *BRAF* mutated cells showed decreased proliferation to treatment with a *BRAF* inhibitor whereas *KRAS* mutated cells showed increases in proliferation (Heidorn *et al.*, 2010).

TP53 mutations are associated more with the squamous histology in NSCLC (Jin *et al.*, 2010; Le Calvez Florence *et al.*, 2005) and this is in agreement with our study too where 7/10 IHC-mtp53 samples were squamous cancers. However, we should be careful since studies report that IHC is not as sensitive as sequencing to predict *TP53* mutation status (Greenblatt *et al.*, 1994) and that discrepancies exist. Nevertheless, there are studies reporting high correlation between IHC and *TP53* mutation status (Ma *et al.*, 2014; Tsao *et al.*, 2007; Scoccianti *et al.*, 2012; Schmid *et al.*, 2012).

From the 7 samples that responded to treatment at 50 μ M of cisplatin, 5 of the samples were of the squamous histology and two were adenocarcinomas. This is consistent with one study which addressed whether histology predicts survival of advanced NSCLC patients treated with cisplatin-based chemotherapy and found no correlation in 1139 patients (Hoang *et al.*, 2013). Four of the 7 samples showed intrinsically high expression of p53 by IHC suggesting they carried a mutation and three of them showed IHC-wtp53 characteristics.

Multiple reports have addressed the question as to whether *TP53* mutations in NSCLC tumours have a prognostic value in predicting response to chemotherapy. The results are controversial, with some suggesting a negative prognostic effect, some a positive prognostic effect, and others showing no effect (Toyooka *et al.*, 2003). One report evaluated the predictive value of

mutations in *TP53*, in the International Adjuvant Lung Cancer Trial (IALT), a randomized trial of adjuvant cisplatin-based chemotherapy against observation and found that *TP53* mutations are not significant predictors of outcome in their trial of cisplatin-based chemotherapy in 524 patients (Ma *et al.*, 2014). In another study on 253 NSCLC patients, 132 (52%) were positive for p53 protein overexpression (Tsao *et al.*, 2007). Untreated p53-positive patients had significantly shorter overall survival than did patients with p53-negative tumours. However, these p53-positive patients also had a significantly greater survival benefit from adjuvant chemotherapy compared with patients with p53-negative tumours. On the other hand, they found that mutations in *TP53* or *RAS* genes were neither prognostic for survival nor predictive of a differential benefit from adjuvant chemotherapy (Tsao *et al.*, 2007). Therefore they suggest that p53 IHC positivity but not *TP53* mutations are associated with greater survival benefit from adjuvant chemotherapy.

Oppositely, the presence of a mutant p53 genotype was highly indicative of resistance to induction chemotherapy with cisplatin ($p < 0.002$) in a 35 NSCLC patient study (Kandioler *et al.*, 2008). In bladder cancer, a retrospective analysis of patients treated with adjuvant therapy found that patients with *TP53* mutation as assessed by IHC had increased sensitivity to treatment with DNA damaging agents cisplatin and doxorubicin, and had more benefit from adjuvant chemotherapy (Cote *et al.*, 1997). In this regard it was shown here, that IHC-mtp53 samples show higher fold proliferation reductions and higher cell death differences compared to the control in response to cisplatin treatment than IHC-wtp53 samples (Figure 5.14), agreeing with the notion that patients who are IHC-mtp53 have greater responses to cisplatin than IHC-wtp53.

Some groups have demonstrated that disruption of p53 function sensitizes tumour cells to cisplatin instead of making them resistant, as would be expected (Schmid *et al.*, 2012). These cells have an apoptotic dysfunction and one possibility has to do with p21^{CIP1} elimination. The increased sensitivity to cisplatin in such cases may be credited to a loss in the contributory role of p21^{CIP1} in G2/M arrest, resulting in premature entry into mitosis, with cell death being the final outcome (Schmid *et al.*, 2012). There is also a p53 independent

way of inducing cisplatin cytotoxicity which involves p73, which can also be induced by cisplatin to mediate apoptosis (Schmid *et al.*, 2012).

The evidence suggests that there are multiple possible mechanisms associated with cisplatin cytotoxicity and p53 is not the only pathway involved. Unfortunately, there are also multiple ways of developing resistance to cisplatin such as decreased intracellular drug accumulation and/or increased drug efflux, drug inactivation by increased levels of cellular thiols, processing of drug-induced damage by increased nucleotide excision-repair activity and decreased mismatch-repair activity, alterations in drug target, and evasion of apoptosis (Florea & Busselberg, 2011). In fact the LA-ICP-MS data from LT31 which was not responsive to 10 μ M of Cisplatin (Figure 5.15) and was IHC-mtP53 suggest decreased intracellular drug accumulation in the tumour cells as the method of resistance in this particular example.

Our results indicate that dose responses of cisplatin were achievable in some of the *ex-vivo* explant cultures of NSCLC. In responding samples, increasing cell death with increasing concentrations of the drug could be observed (Figure 5.5) or decreasing proliferation with increasing concentrations of the drug (Figure 5.6). Our data show that more than half of the samples are resistant to the drug which is consistent with known response in the clinic. This model could potentially be used to predict patient responses to drugs. We can also use the model to test the expression of proteins of interest. In this respect, we could test the expression of p53 and correlate with responses to cisplatin and found that IHC-mtp53 samples are more sensitive to cisplatin treatment than IHC-wtp53 samples. Overall it is encouraging that we can observe dose responses with cisplatin, that we can identify responders and non-responders and there may be some correlation with patient outcome.

6. ASSESSMENT OF RESPONSES TO NEW AGENTS: TARGETING MAPK AND PI3K SIGNALLING PATHWAYS

6.1 Introduction

After establishing the culture conditions of *ex-vivo* NSCLC explants and confirming the utility of the model to test drug responses of tumours *in situ*, we wanted to use the model to test targeted therapies and combinations that could improve therapeutic approaches for the treatment of NSCLC.

As discussed in depth in the general introduction section 1.2, cancer is a disease that arises from genetic alterations that give rise to the capabilities associated with tumours. These competences or generic hallmarks of cancer include self-sufficiency in growth signals, evasion of growth suppressors and cell death, ability to replicate indefinitely, induction of angiogenesis and eventual tissue evasion and metastasis (Hanahan & Weinberg, 2000). These capabilities are mainly acquired after somatic mutations have been acquired in cancer associated genes, i.e. tumour suppressor genes and oncogenes.

Oncogenes identified in cancer offer a great opportunity for the development of novel therapies since inhibitors that target them could potentially kill tumour cells that are addicted to the specific oncogene (Luo *et al.*, 2009b). Therefore by inhibiting the action of the oncogene-product or downstream effects, the cancer cell can become vulnerable and die. This has already been exploited in NSCLC with the introduction of EGFR and ALK inhibitors that are having a growing impact on the management of NSCLC and have improved outcomes of patients carrying *EGFR* mutations and *ALK* rearrangements. However, there are only a small percentage of patients associated with these mutations and lung cancer is a complex genetic disease, with many different genetic alterations identified.

Targeting two of the most common cancer-associated pathways, the RAS/RAF/MEK/ERK pathway and the PI3K/AKT/mTOR pathway, could potentially be useful in NSCLC as there is a high proportion of mutations found in components of these pathways in lung cancer and in all cancers in general. Therefore, we chose to use inhibitors targeting proteins downstream of both pathways (Figure 6.1), mainly MEK inhibitors (UO126 or PD184352) and PI3K inhibitors (LY294002 or GDC-0941).

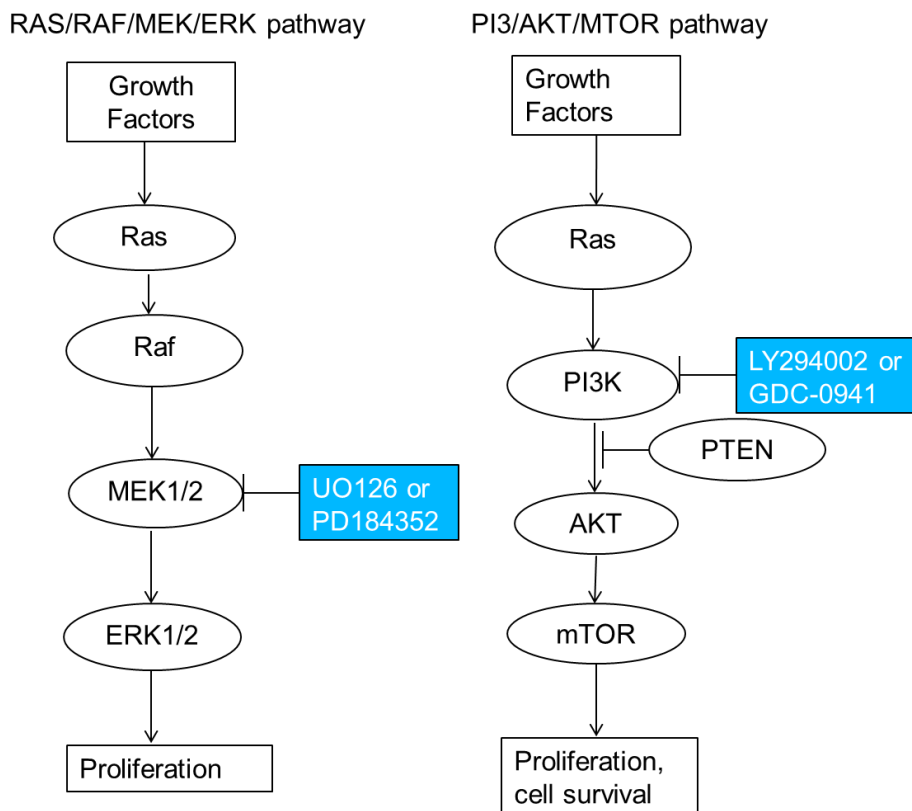


Figure 6.1 RAS/RAF/MEK/ERK pathway activity can be inhibited using MEK inhibitors UO126 or PD184352. PI3K/AKT/mTOR pathway activity can be inhibited using PI3K inhibitors, LY294002 or GDC-0941.

6.2 Aims and Objectives

- Determine the responses of explants to PD184352 or UO126 (MEK inhibitors) and LY294002 or GDC401 (PI3K inhibitors) singly and in combination.
- Correlate response to mutations in key components of the pathway including *KRAS*, *EGFR*, *BRAF* and *PIK3CA*.
- Determine effect of inhibitors on pathway outputs by assessing P-ERK and P-AKT staining.
- Correlate responses to available clinical data on clinical trials with these agents in the literature.

6.3 Results

Overall 10 *ex-vivo* explant NSCLC cultures were tested for their response to MEK and PI3K inhibitors and combinations. In three of these samples a *PIK3CA* point mutation was identified through qPCR analysis of the samples' DNA (see chapter 3-section 3.2.4). The other eight samples carried none of the mutations we tested for in *KRAS*, *BRAF*, *EGFR* or *PIK3CA*. Despite the lack of these mutations, the majority of NSCLC samples had high levels of p-ERK or p-AKT in the original tumour (Figure 6.2) suggesting one or both of the RAS/RAF/MEK/ERK and/or PI3K/AKT/mTOR pathways are activated, likely by mutations in genes other than the ones we tested by qPCR (chapter 3 - Table 3.2).

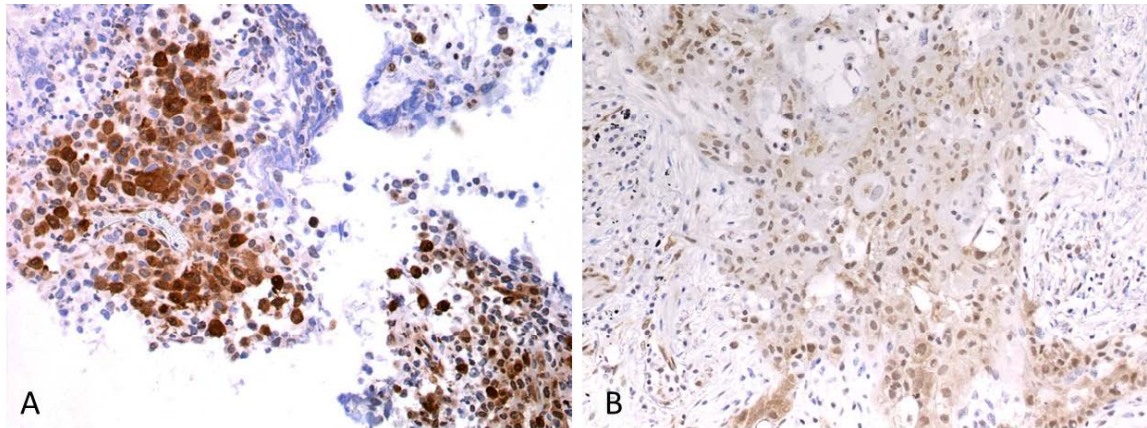


Figure 6.2. Examples of two cases demonstrating high levels of p-ERK (A) and p-AKT (B) respectively. None of the 10 mutations in *KRAS*, *BRAF*, *EGFR* or *PIK3CA* we tested by qPCR were positive for these tumours.

6.3.1 Targeting PI3K

Initially, six *ex-vivo* NSCLC explant cultures were treated with increasing doses of LY294002. However, LY294002 is not particularly specific for PI3K and is not a drug that is given to patients as it is not bioavailable. Therefore, we decided to switch to a more clinically relevant PI3K inhibitor, GDC-0941, and had time to test the responses of another four explant cultures.

6.3.1.1 EXAMPLE *PIK3CA* MUTANT CASE TREATED WITH LY294002

LT16 tested positively for the *PIK3CA* point mutation G1633A. This adenocarcinoma sample had some intrinsic cell death from the uncultured tumour and a slight increase in cell death was observed as a result of culture as can be seen by comparison to the carrier control. Nevertheless, LT16 showed a slight response to LY294002 in comparison to the carrier control (Figure 6.3 and Figure 6.4). The concentrations of 10 μ M and 50 μ M seemed to show a better response than 20 μ M of LY294002. A slight reduction in proliferation was also observed in comparison to the carrier control (Figure 6.3 and Figure 6.4). Even

though LT16 had a *PIK3CA* mutation, the p-AKT expression without any treatment was quite low (Figure 6.5 A). Nonetheless, treatment with 10, 20 and 50 μ M of LY294002 resulted in completely negative p-AKT expression (Figure 6.5 B, C and D), suggesting the inhibition of PI3K was successful even at the lowest LY294002 dose. However the cell death increase was small and the effect on proliferation minimal.

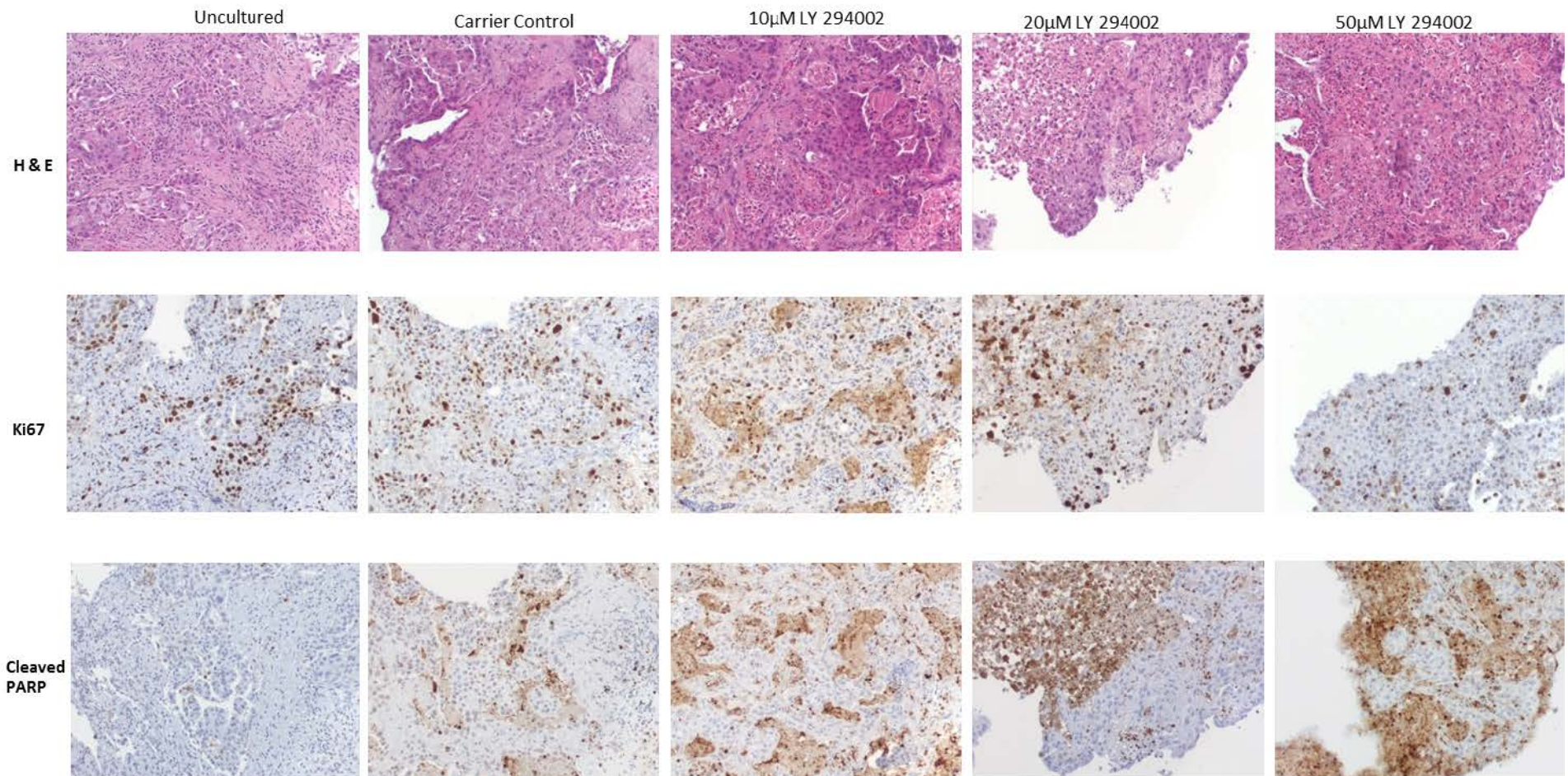


Figure 6.3. Representative images of corresponding areas of LT16 (*PIK3CA* mutation positive) in H&E staining, Ki67 staining (proliferation marker) and cleaved PARP staining (apoptosis marker).

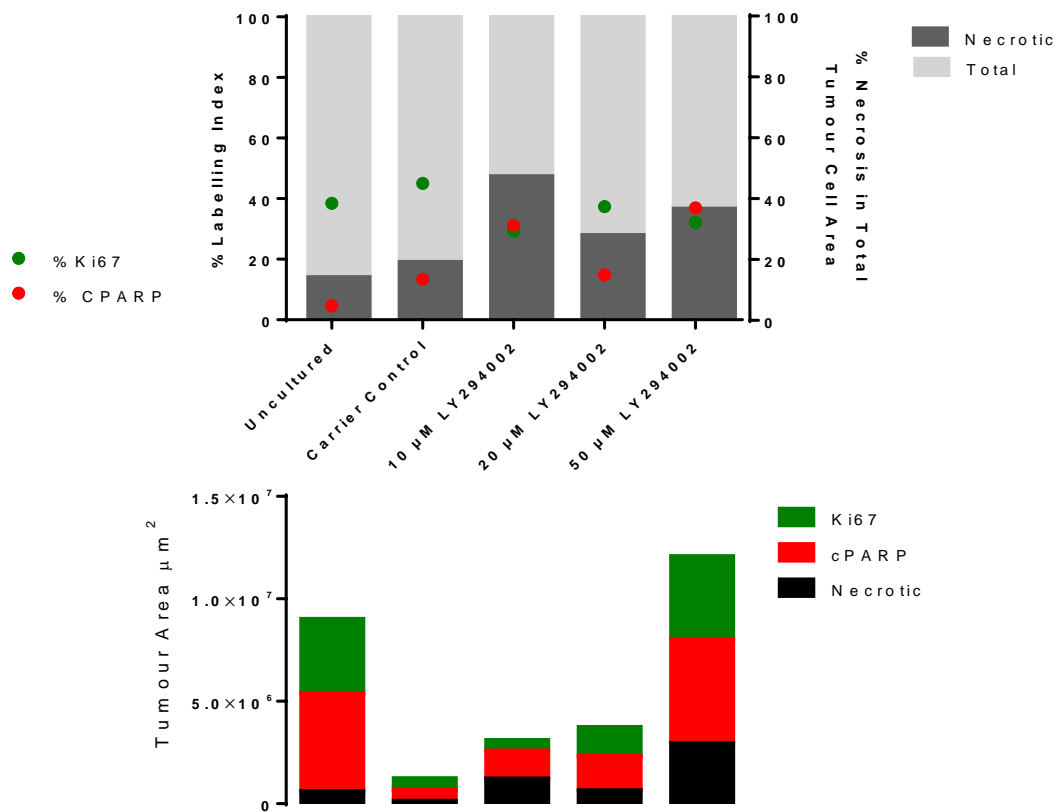


Figure 6.4. Dose response of LT16 (*PIK3CA* mutation positive) to LY294002. Upper graph. Each point represents an additive number which characterises all the staining from each slide and also takes into account the area of the tumour cells for each explant on the slide. The red dot represents the percentage of cells that have a nucleus stained with cleaved PARP out of all the tumour cells present in the slide and similarly the green dot represents the Ki67 labelling index. The dark grey bars behind show the percentage of the area that was undergoing secondary necrosis as decided by cleaved PARP leakage out of the total area (light grey). It shows the proliferation (Ki67-green) and the apoptosis (cPARP-red) or the secondary necrosis (dark grey) of LT16 undergoing culture with the carrier alone and with increasing LY294002 concentrations (10 µM, 20 µM and 50 µM) for 24 hours after the initial recovery period. Lower graph. This graph represents the exact values of the tumour areas used for Ki67 analysis (green bar), cleaved PARP analysis (red bar) and secondary necrosis so we can compare each condition with the amount of tumour cells present.

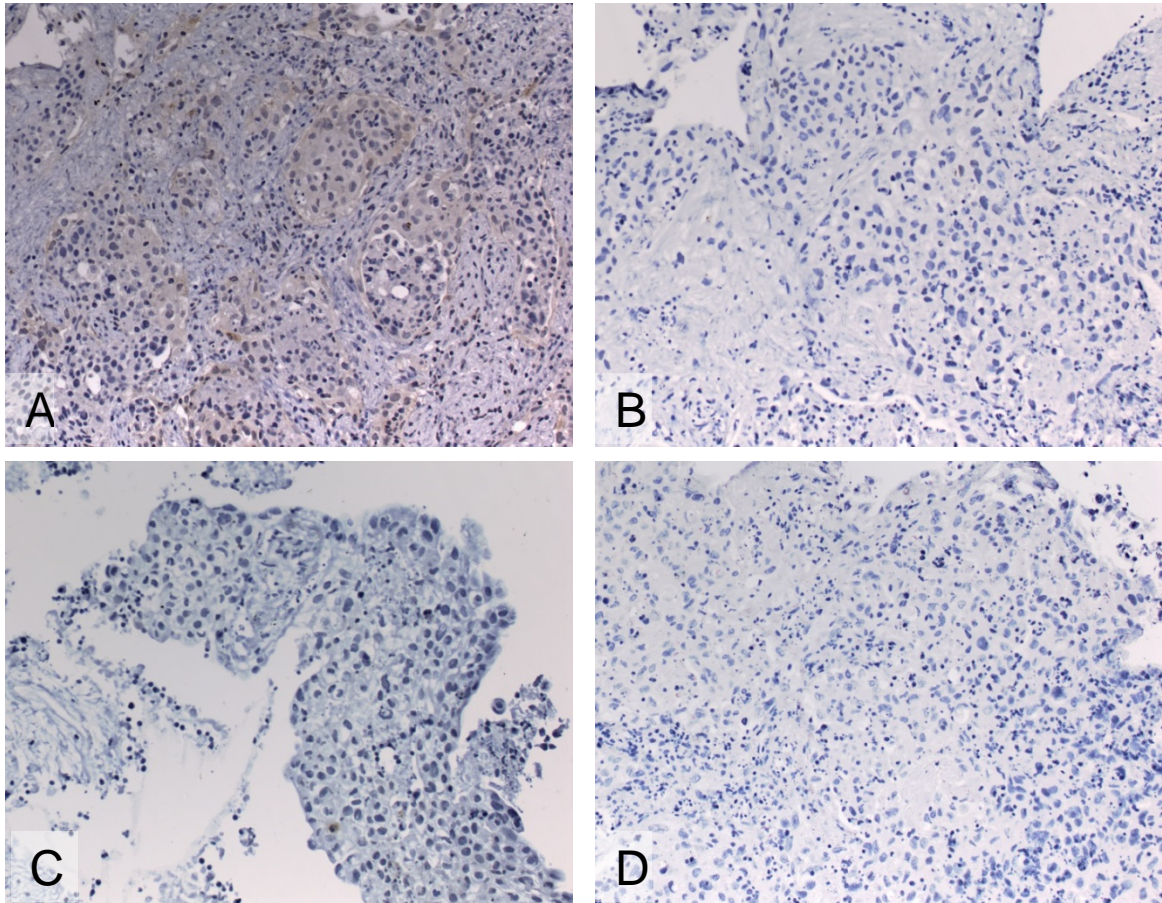


Figure 6.5. P-Akt staining of LT16 (*PIK3CA* mutation positive) in increasing concentrations of LY294002. A) P-Akt expression of the LT16 Carrier control. P-Akt expression of LT16 treated with LY294002 B) 10 μ M, C) 20 μ M and D) 50 μ M of LY294002.

6.3.1.2 DOSE RESPONSES TO LY294002

Six *ex-vivo* NSCLC explants were treated with increasing doses of LY294002. Three of the explants were adenocarcinomas and the other three were squamous cell carcinomas. The responses can be seen in Figure 6.6 for fold cell death and Figure 6.7 for fold proliferation. The responses were variable. The majority of samples showed a very small dose response with increasing concentrations of the drug, except LT20 which only showed a 1.5 fold increase at the highest 50 μ M dose. LT22 showed a 4-fold increase of cell death at 10 μ M, which reached more than 7-fold at 20 μ M and no further increase at 50 μ M of LY294002. LT16 and LT23 were positive for *PIK3CA* mutations. However, there was no visible difference between their response to LY294002 and the other 4 samples (Figures 6.6 and 6.7). Looking at the fold proliferation responses of the six explants (Figure 6.7), all 6 showed a fold decrease of proliferation which was more evident at 10 μ M and 50 μ M of LY294002. Strangely, in 4 samples the fold proliferation difference seemed to be smaller at the middle dose of 20 μ M.

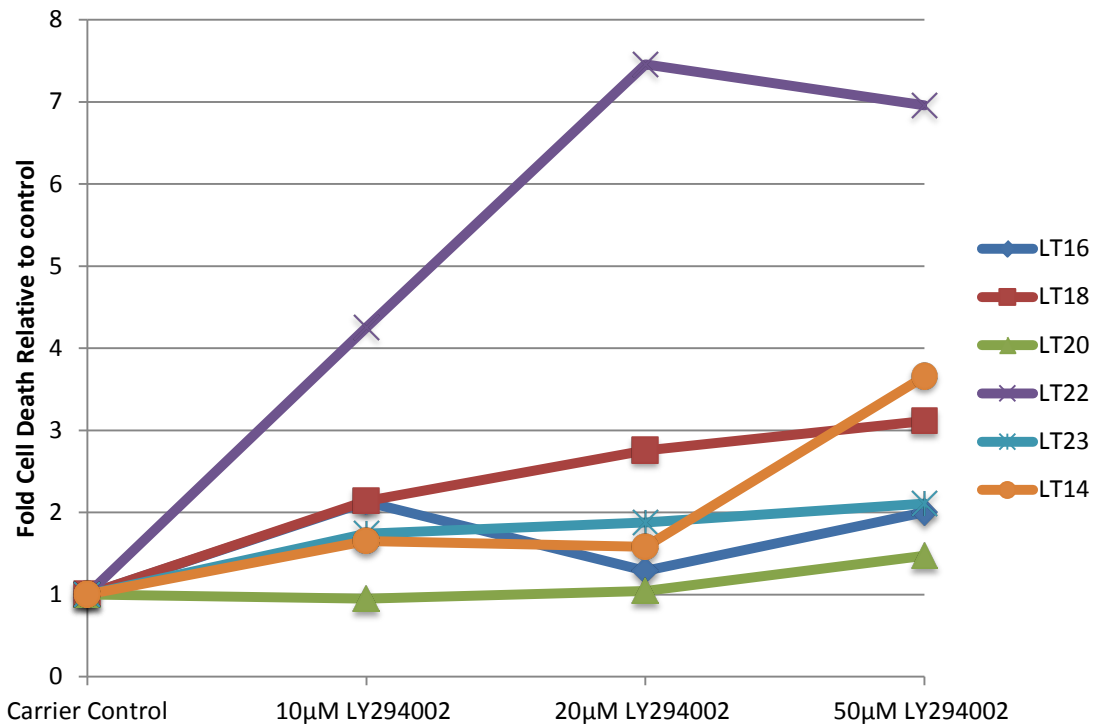


Figure 6.6. Fold cell death dose responses to LY294002 relative to control. The % Cell Death of tumour area of 6 NSCLC ex-vivo explant cultures as determined from cleaved PARP staining is shown. % cell death values from each sample in increasing LY294002 concentrations (10 µM, 20 µM and 50 µM) for 24 hours after an initial recovery of 16-20 hours were divided by each carrier control to determine the fold difference.

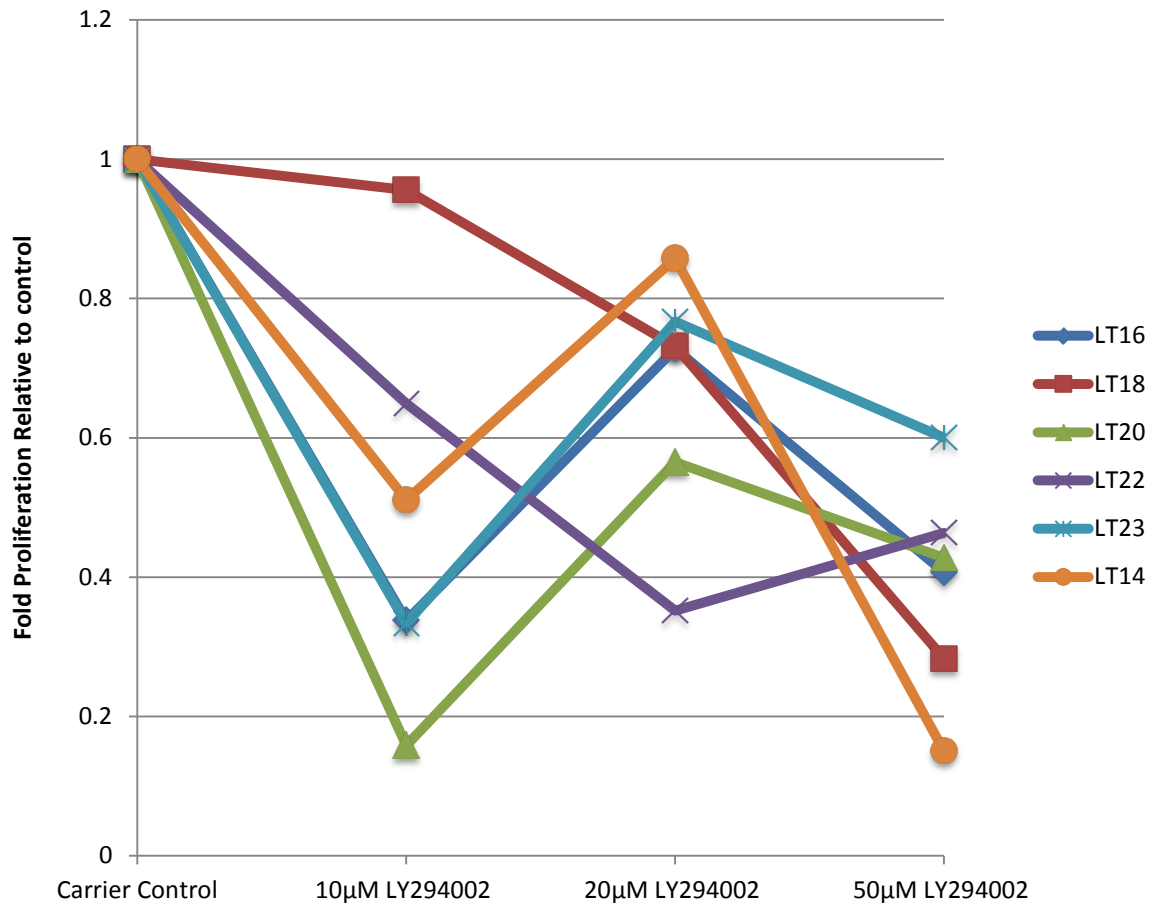


Figure 6.7. Fold proliferation dose responses to LY294002 relative to the carrier control. % Proliferation of tumour area of 6 NSCLC *ex-vivo* explant cultures as determined from Ki67 staining. The % Ki67 values from each sample in increasing LY294002 concentrations (10 µM, 20 µM and 50 µM) for 24 hours after an initial recovery of 16-20 hours were divided by each carrier control to determine the fold difference.

6.3.1.3 DOSE RESPONSES TO GDC-0941

Four *ex-vivo* NSCLC explants were treated with increasing doses of GDC-0941. The responses can be seen in Figure 6.8 for fold cell death and Figure 6.9 for fold proliferation. Three of the samples were squamous cell carcinomas and one was an adenocarcinoma. The latter, LT27, did not show evident fold cell death increase relative to the control (Figure 6.8). However, there was some reduction in proliferation which was higher at 10 µM of the drug (Figure 6.9). The other three squamous samples showed some fold increase of cell death relative to the control. LT88 showed a two fold increase at 5 µM, which went up

to three-fold at 10 μM but no increase in cell death was observed at the highest dose. The reduction in proliferation however, was evident in increasing concentrations of the drug. LT93 also showed increasing fold cell death at increasing concentrations of GDC-0941 and decreasing fold proliferation similarly. LT92 was positive for a *PIK3CA* mutation and showed the highest fold cell death response (6.5-fold increase) even at the lowest drug dose (Figure 6.8) suggesting GDC-0941 works better in selected samples which carry PI3K aberrations.

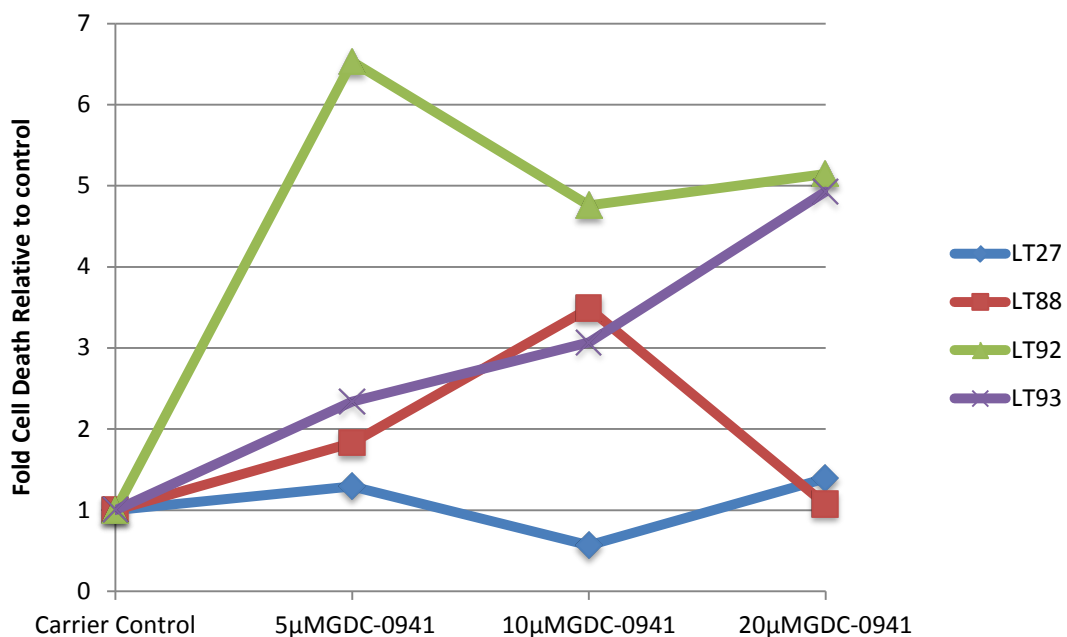


Figure 6.8. Fold cell death dose responses to GDC-0941 relative to control. The % Cell Death of tumour area of 4 NSCLC *ex-vivo* explant cultures as decided from cleaved PARP staining was analysed for samples treated with GDC-0941 concentrations (5 μM , 10 μM and 20 μM) for 24 hours after an initial recovery of 16-20 hours. Each sample was normalised to the carrier control.

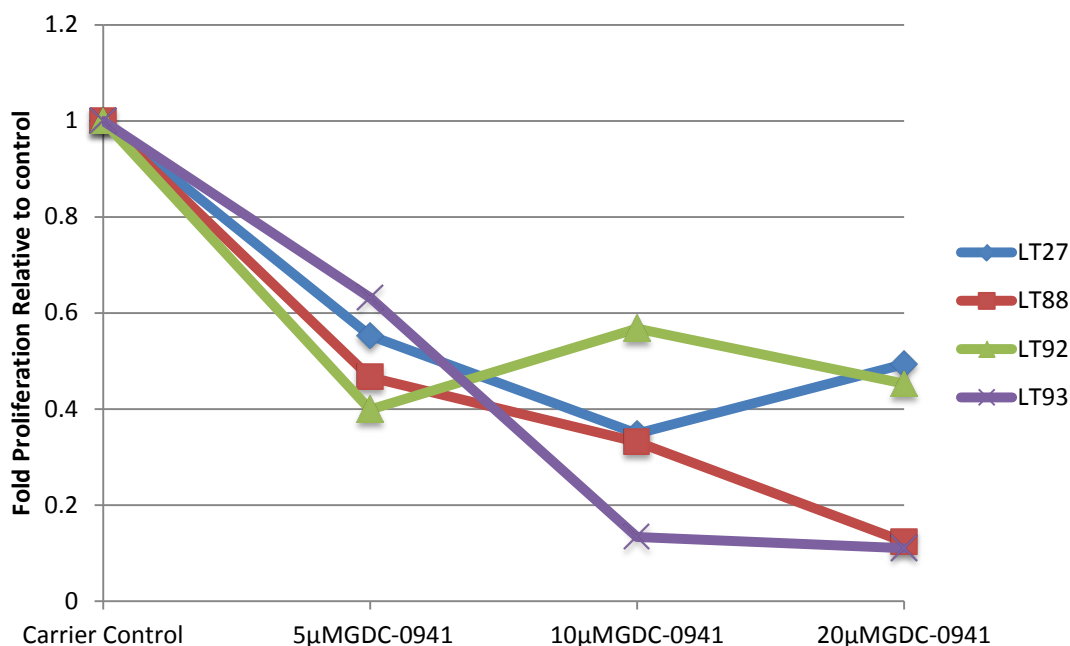


Figure 6.9. Fold proliferation dose responses to GDC-0941 relative to control. The % Proliferation of tumour area of 4 NSCLC *ex-vivo* explant cultures as decided from Ki67 staining was analysed for samples treated with GDC-0941 concentrations (5 μM, 10 μM and 20 μM) for 24 hours after an initial recovery of 16-20 hours. Each sample was normalised to the carrier control.

6.3.2 Targeting MEK

Seven *ex-vivo* NSCLC explant cultures were treated with increasing doses of PD184352. Unfortunately, we experienced a shortage of PD184352 and two samples therefore were treated with increasing doses of UO126.

6.3.2.1 EXAMPLE *PIK3CA* MUTANT CASE TREATED WITH PD184352

LT16 tested positively for the *PIK3CA* point mutation G1633A. LT16 showed a response to 5 μM and 20 μM PD184352 in compared to the carrier control in terms of cell death increase (Figure 6.10 and Figure 6.11). There was also a small reduction in proliferation with increasing concentrations of PD184352 in comparison to the carrier control (Figure 6.10 and Figure 6.11). LT16 had a very high p-ERK expression without any treatment (Figure 6.12 A). This increased p-ERK expression became less evident with treatment with 5, 10 and 20 μM of PD184352 (Figure 6.12 B, C and D), suggesting inhibition of the drug's target, MEK, with increasing doses.

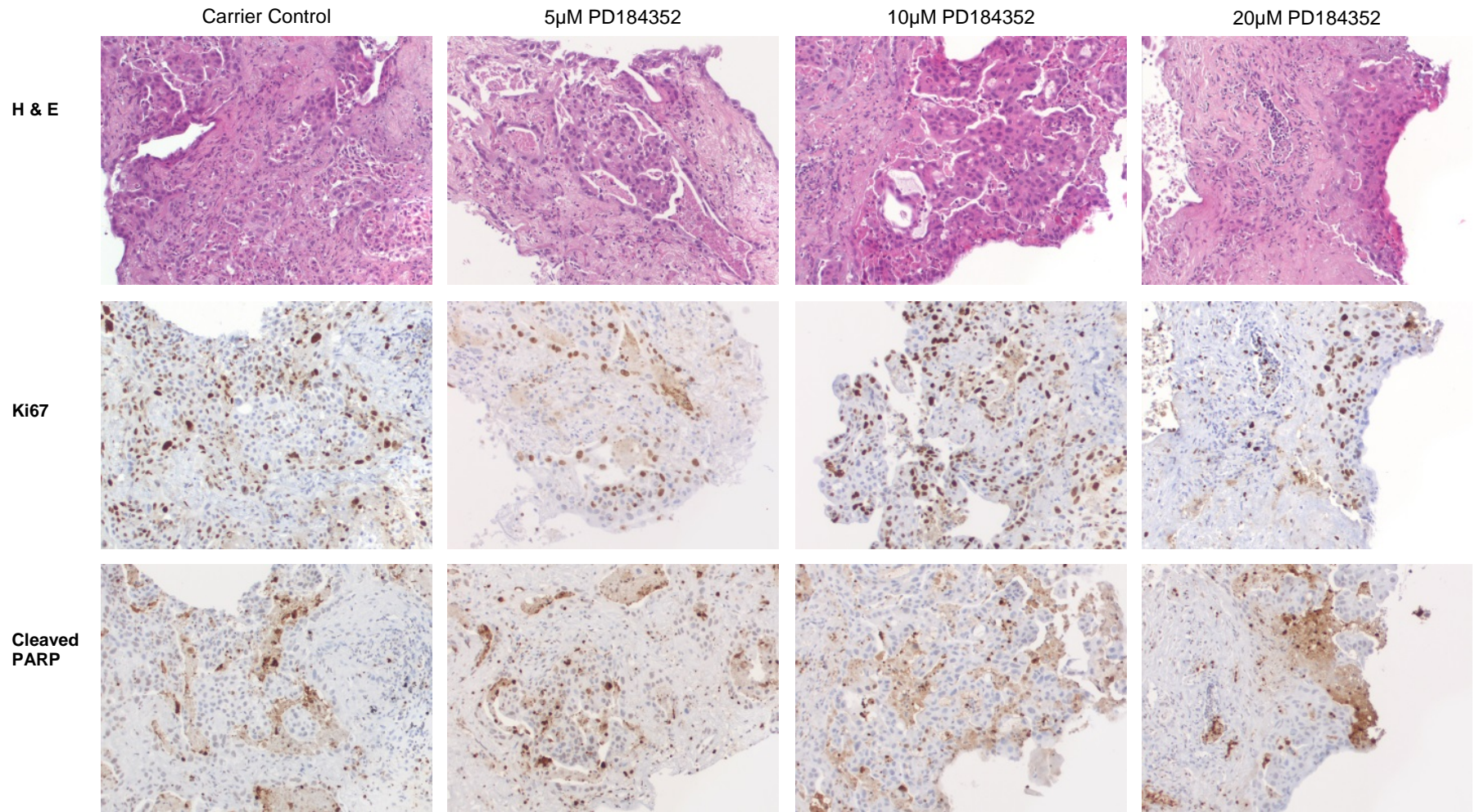


Figure 6.10. Representative images of corresponding areas of LT16 (*PIK3CA* mutation positive) in H&E staining, Ki67 staining (proliferation marker) and cleaved PARP staining (apoptosis marker).

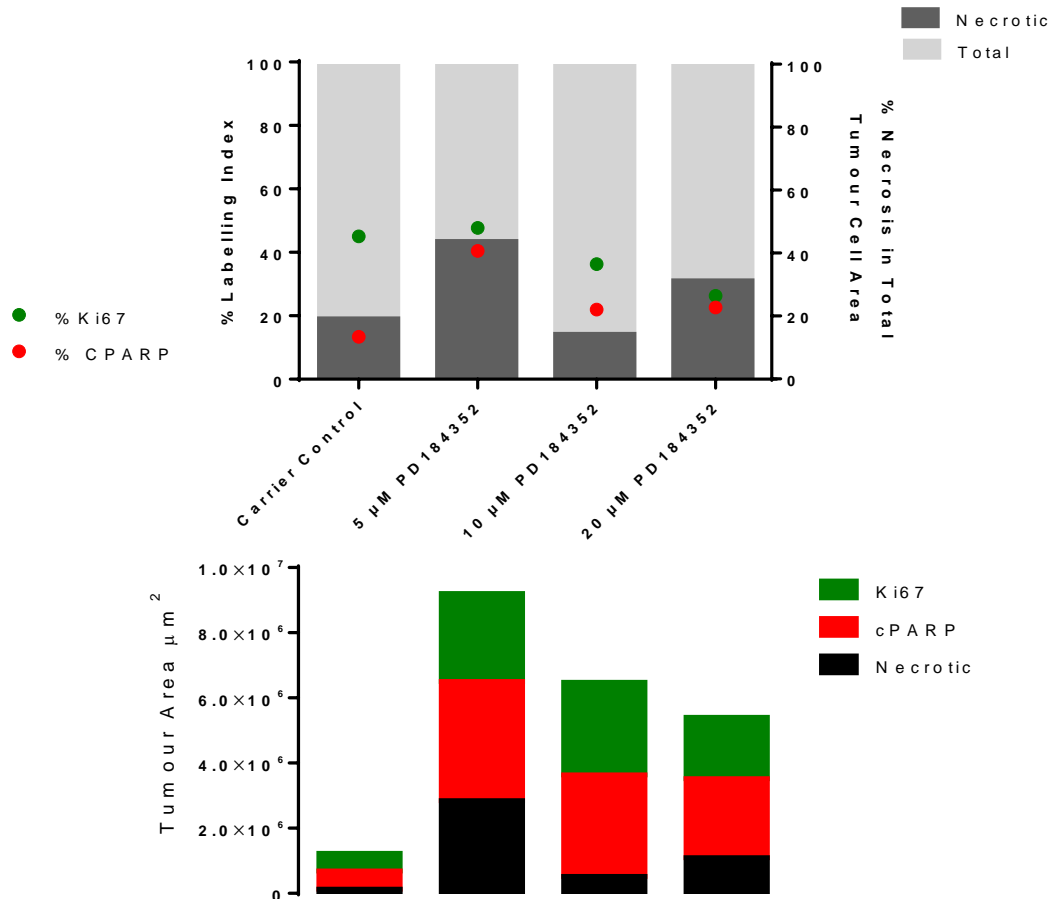


Figure 6.11. Dose response of LT16 (*PIK3CA* mutation positive) to PD184352. Upper graph. Each point represents an additive number which characterises all the staining from each slide and also takes into account the area of the tumour cells for each explant on the slide. The red dot represents the percentage of cells that have a nucleus stained with cleaved PARP out of all the tumour cells present in the slide and similarly the green dot represents the Ki67 labelling index. The dark grey bars behind show the percentage of the area that was undergoing secondary necrosis as decided by cleaved PARP leakage out of the total area (light grey). It shows the proliferation (Ki67-green) and the apoptosis (cPARP-red) or the secondary necrosis (dark grey) of LT16 undergoing culture with the carrier alone and with increasing PD184352 concentrations (5 μ M, 10 μ M and 20 μ M) for 24 hours after the initial recovery period. Lower graph. This graph represents the exact values of the tumour areas used for Ki67 analysis (green bar), cleaved PARP analysis (red bar) and secondary necrosis so we can compare each condition with the amount of tumour cells present.

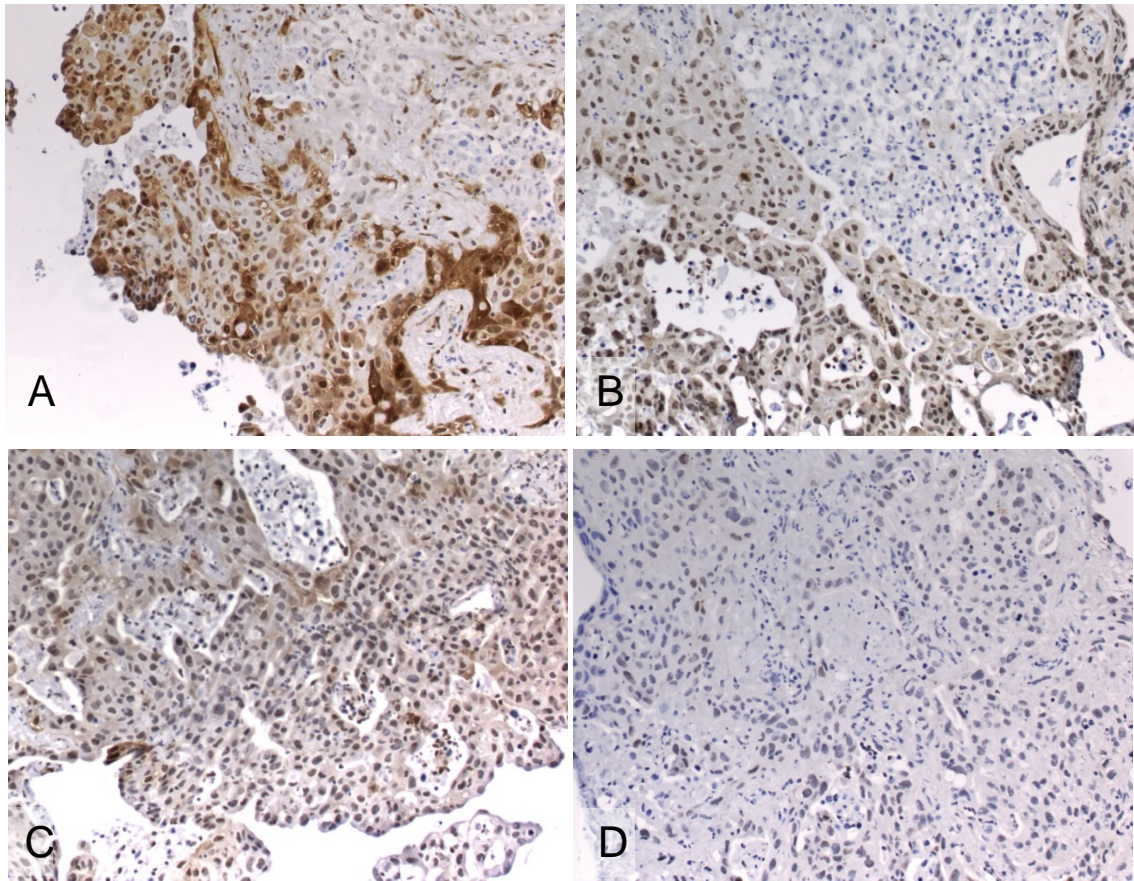


Figure 6.12. P-ERK staining of LT16 (*PIK3CA* mutation positive) in increasing concentrations of PD184352. A) P-ERK expression of the LT16 carrier control. P-Akt expression of LT16 treated with PD184352 B) 5 μ M, C) 10 μ M and D) 20 μ M of PD184352.

6.3.2.2 DOSE RESPONSES TO PD184352

Seven *ex-vivo* NSCLC explants were treated with increasing doses of PD184352. Five of the samples were squamous cell carcinomas and two were adenocarcinomas. The responses can be seen in Figure 6.13 for fold cell death and Figure 6.14 for fold proliferation. Most of the samples showed a very small response with cell death increases in increasing concentrations of the drug. LT92 which had a *PIK3CA* mutation, showed a near 7-fold increase of cell death at the highest PD184352 dose. Looking at the fold proliferation graph we can see some anomalous points which show increases of proliferation relative to the control in 3 samples. This probably arises from the variability of proliferation amongst different explants, as already mentioned in chapter 5.

Nevertheless decreases in proliferation are evident in the other 5 samples (Figure 6.14).

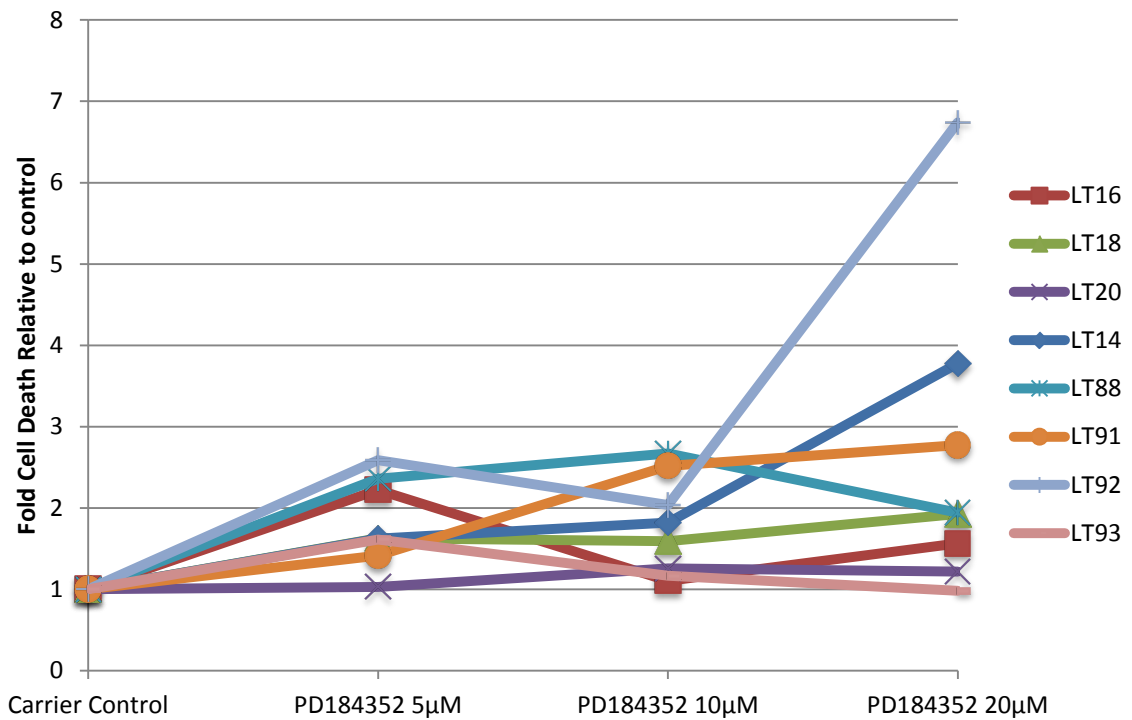


Figure 6.13. Fold cell death dose responses to PD184352 relative to control. The % cell death of tumour area of 7 NSCLC *ex-vivo* explant cultures as decided from cleaved PARP staining was analysed for samples treated with PD184352 concentrations (5 μM, 10 μM and 20 μM) for 24 hours after an initial recovery of 16-20 hours. Each sample was normalised to the carrier control.

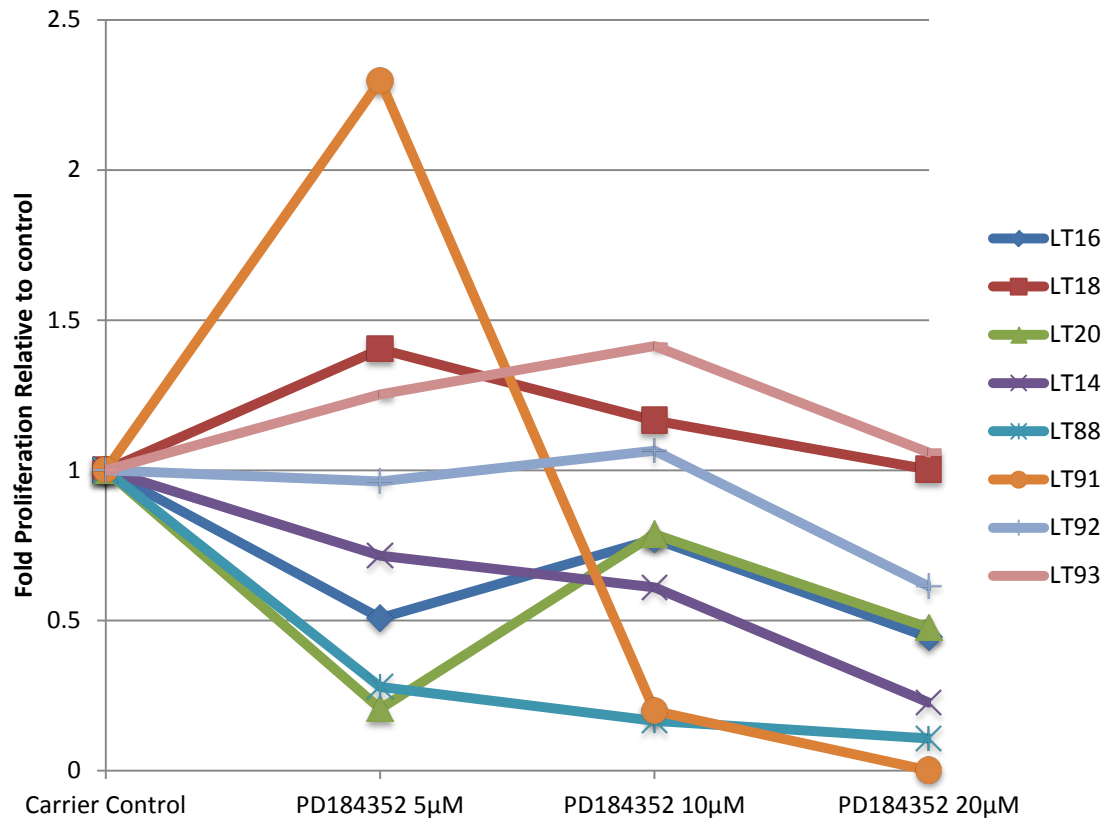


Figure 6.14. Fold proliferation dose responses to PD184352 relative to control. The % proliferation of tumour area of 7 NSCLC *ex-vivo* explant cultures as decided from Ki67 staining was analysed for samples treated with PD184352 concentrations (5 µM, 10 µM and 20 µM) for 24 hours after an initial recovery of 16-20 hours. Each sample was normalised to the carrier control.

6.3.2.3 DOSE RESPONSES TO UO126

Two *ex-vivo* adenocarcinoma explant cultures were treated with increasing doses of UO126 which is a MEK inhibitor routinely used in laboratory experiments but not very clinically relevant. The responses of LT22 and LT27 can be seen in Figure 15A for fold cell death and Figure 15B for fold proliferation. LT22 showed an increase of fold cell death relative to the control in increasing concentrations of UO126 while LT27 was not responding (Figure 15A). However, the decrease in proliferation in increasing concentrations of UO126 was more evident in LT27 than LT22 (Figure 15B).

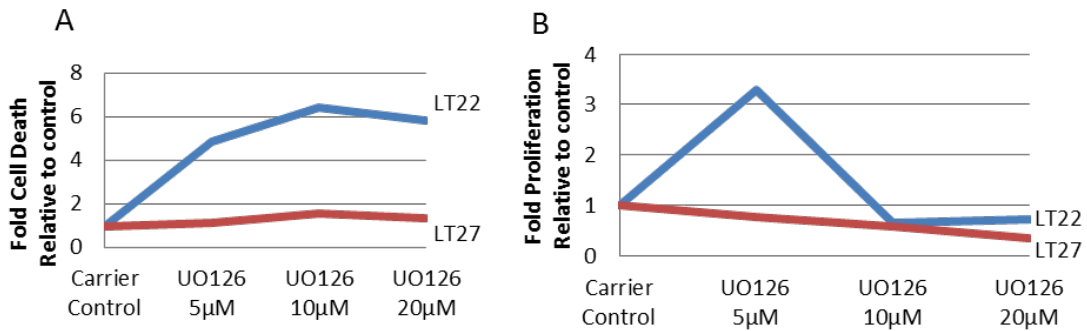


Figure 6.15. Fold cell death and fold proliferation to dose responses to UO126 relative to control. A) The % cell death of tumour area of 2 NSCLC *ex-vivo* explant cultures as decided from cleaved PARP staining was analysed for samples treated with UO126 concentrations (5 μ M, 10 μ M and 20 μ M) for 24 hours after an initial recovery of 16-20 hours. Each sample was normalised to the carrier control. B) The % proliferation of tumour area of 2 NSCLC *ex-vivo* explant cultures as decided from Ki67 staining was analysed for samples treated with UO126 concentrations (5 μ M, 10 μ M and 20 μ M) for 24 hours after an initial recovery of 16-20 hours. Each sample was normalised to the carrier control.

6.3.3. Inhibiting PI3K and MEK simultaneously

The ten *ex-vivo* NSCLC explants were also treated with combinations of PI3K and MEK inhibitors. Due to the availability of the drugs, four samples were treated with combinations of LY294002 and PD184352; three samples were treated with combinations of GDC-0941 and PD184352, and one sample was treated with LY294002 and UO126, another with GDC-0941 and UO126 and the last one with combinations of LY294002 and sorafenib.

6.3.3.1 EXAMPLE PIK3CA MUTANT CASE TREATED WITH COMBINATIONS OF LY294002 AND PD184352

LT16 tested positively for the *PIK3CA* point mutation G1633A. LT16 showed a better response to increasing concentrations of LY294002 in combination with PD184352 in comparison to the carrier control as measured by an increase of cell death (Figure 6.16 and Figure 6.17). The reduction in proliferation is also evident with combination treatments in comparison to the carrier control (Figure 6.16 and Figure 6.17).

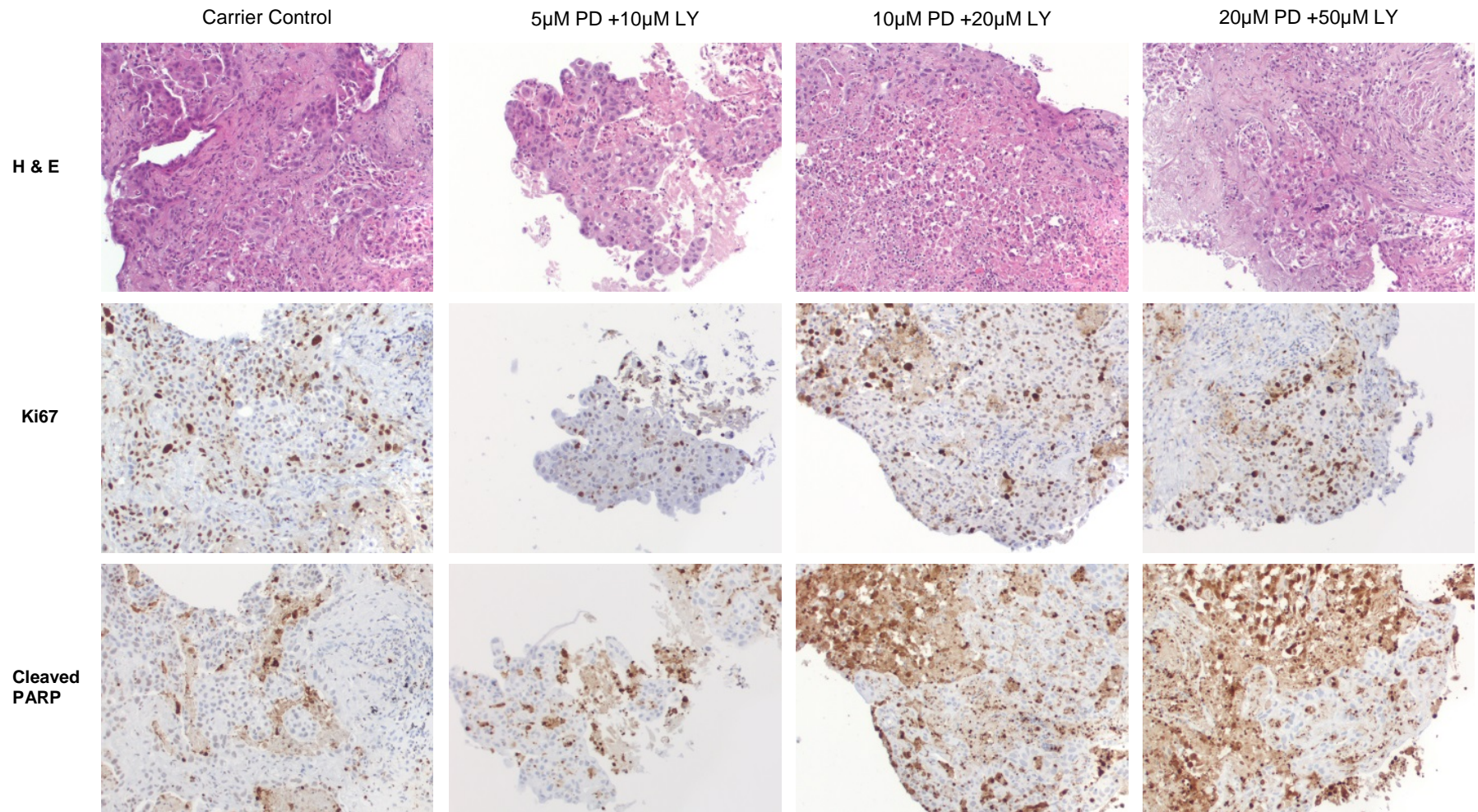


Figure 6.16. Representative images of corresponding areas of LT16 (*PIK3CA* mutation positive) in H&E staining, Ki67 staining (proliferation marker) and cleaved PARP staining (apoptosis marker).

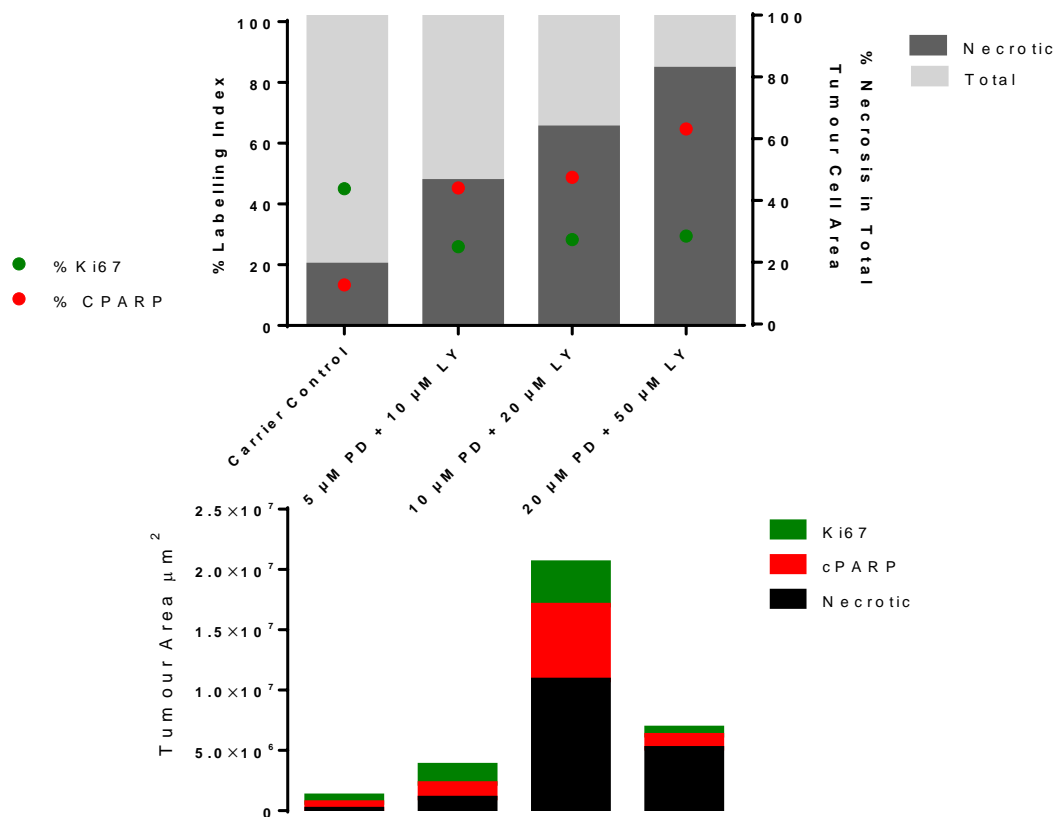


Figure 6.17. Dose responses of LT16 (*PIK3CA* mutation positive) to LY294002 in combination with PD184352. Upper graph. Each point represents an additive number which characterises all the staining from each slide and also takes into account the area of the tumour cells for each explant on the slide. The red dot represents the percentage of cells that have a nucleus stained with cleaved PARP out of all the tumour cells present in the slide and similarly the green dot represents the Ki67 labelling index. The dark grey bars behind show the percentage of the area that was undergoing secondary necrosis as decided by cleaved PARP leakage out of the total area (light grey). It shows the proliferation (Ki67-green) and the apoptosis (cPARP-red) or the secondary necrosis (dark grey) of LT16 undergoing culture with the carrier alone and with increasing PD184352 + LY294002 concentrations (5 μM PD +10 μM LY, 10 μM PD +20 μM LY and 20 μM PD +50 μM LY) for 24 hours after the initial recovery period. Lower graph. This graph represents the exact values of the tumour areas used for Ki67 analysis (green bar), cleaved PARP analysis (red bar) and secondary necrosis so we can compare each condition with the amount of tumour cells present.

6.3.3.2 DOSE RESPONSES TO LY294002 IN COMBINATION WITH PD184352

Four *ex-vivo* NSCLC explants were treated with increasing doses of LY294002 and PD184352. Two of these were adenocarcinomas and two were squamous cell carcinomas. The responses can be seen in Figure 6.18 A for fold cell death and Figure 6.18 B for fold proliferation. Three of the samples (LT16, LT18 and LT14) showed a high response with cell death increases in increasing concentrations and ki67 decreases similarly (Figure 6.18). LT20 only showed a small response at the highest concentration in terms of fold cell death increase. However, the fold proliferation went down in increasing concentrations of the drug combinations in all four samples.

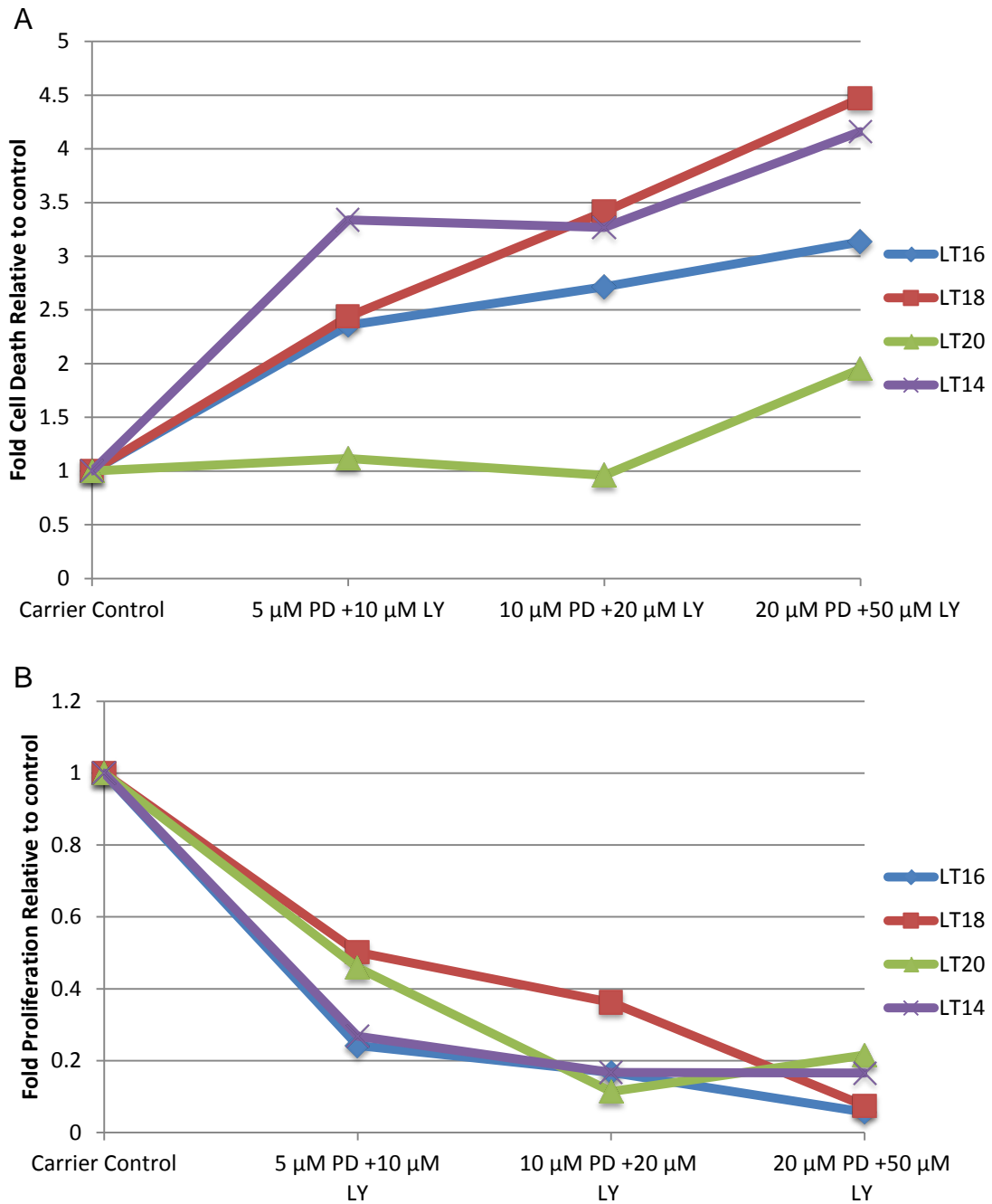


Figure 6.18 Fold cell death and proliferation dose responses to LY294002 in combination with PD184352 relative to control. A) The % cell death of tumour area of 4 NSCLC *ex-vivo* explant cultures as decided from cleaved PARP staining was analysed for samples treated with increasing PD184352 + LY294002 concentrations (5 μ M PD +10 μ M LY, 10 μ M PD +20 μ M LY and 20 μ M PD +50 μ M LY) for 24 hours after an initial recovery of 16-20 hours. Each sample was normalised to the carrier control. B) The % proliferation of tumour area of 4 NSCLC *ex-vivo* explant cultures as decided from Ki67 staining was analysed for samples treated with increasing PD184352 + LY294002 concentrations (5 μ M PD +10 μ M LY, 10 μ M PD +20 μ M LY and 20 μ M PD +50 μ M LY) for 24 hours after an initial recovery of 16-20 hours. Each sample was normalised to the carrier control.

6.3.3.3 DOSE RESPONSES TO GDC-0941 IN COMBINATION WITH PD184352

Three squamous cell carcinoma *ex-vivo* NSCLC explants were treated with increasing doses of GDC-0941 and PD184352. The responses can be seen in Figure 6.19A for fold cell death and Figure 6.19B for fold proliferation. All three samples showed response with cell death increases in increasing concentrations of the combination drugs and proliferation decreases similarly (Figure 6.19). LT92 which carried a *PIK3CA* mutation, showed the highest fold induction of cell death.

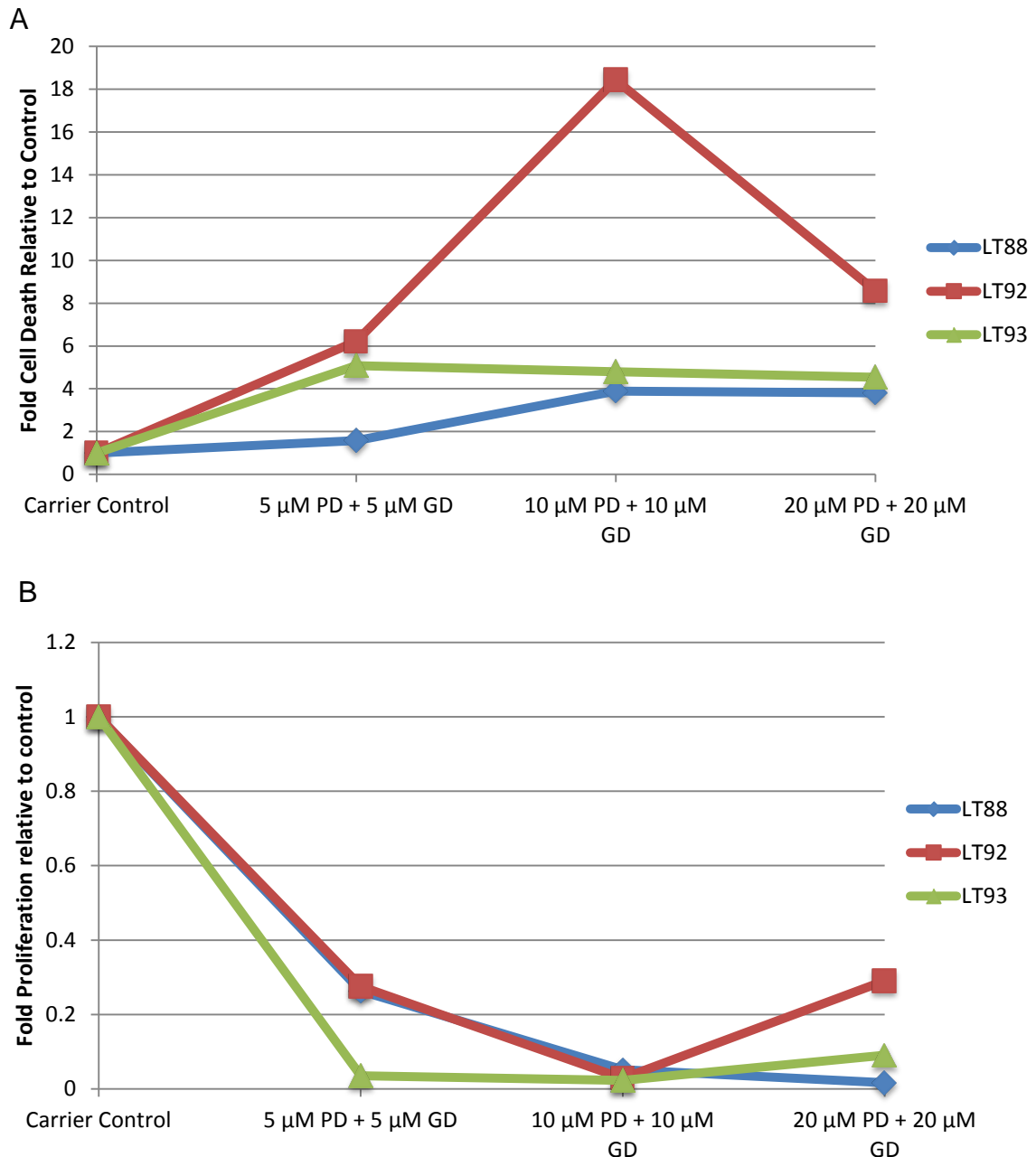


Figure 6.19 Fold cell death and proliferation dose responses to GDC-0941 in combination with PD184352 relative to control. A) The % cell death of tumour area of 3 NSCLC *ex-vivo* explant cultures as decided from cleaved PARP staining was analysed for samples treated with increasing PD184352 + GDC-0941 concentrations (5 μ M PD + 5 μ M GDC, 10 μ M PD + 10 μ M GDC and 20 μ M PD + 20 μ M GDC) for 24 hours after an initial recovery of 16-20 hours. Each sample was normalised to the carrier control. B) The % proliferation of tumour area of 3 NSCLC *ex-vivo* explant cultures as decided from Ki67 staining was analysed for samples treated with increasing PD184352 + GDC-0941 concentrations (5 μ M PD + 5 μ M GDC, 10 μ M PD + 10 μ M GDC and 20 μ M PD + 20 μ M GDC) for 24 hours after an initial recovery of 16-20 hours. Each sample was normalised to the carrier control.

6.4 Discussion

The responses of ten *ex-vivo* NSCLC explant cultures were tested after treatment with PI3K inhibitors (LY294002 in 6 samples and GDC-0941 in 4 samples) and MEK Inhibitors (PD184352 in 7 samples and UO126 in 2 samples) singly and in combination. The responses were variable. The average increase of cell death in LY294002 and PD184352 single treated samples was 2-fold. GDC-0941 single treatments showed 3-fold increases in 2 samples and one sample showed a 6-fold response. The same sample, LT92 which carried a *PIK3CA* mutation, also showed a high 6-fold response at the highest PD184352 single treatment, suggesting that correlation with genotype is important. In general however, most of the single treatments did not induce significant responses in the explants. The combination of PI3K and MEK inhibitors though, showed more promise since the fold induction of cell death and the fold decrease of proliferation was much higher, ranging from 4-fold to as high as 18-fold cell death increase. This high fold cell death increase is similar to samples treated with 50 μ M of Cisplatin (Chapter 5 section 5.3.2).

PD184352 (also known as CI-1040) was the first MEK inhibitor to proceed to clinical testing. A phase II clinical trial to assess its anti-tumour activity and safety in 67 patients with NSCLC, breast, colon and pancreatic cancer showed that the drug was generally well tolerated but did not demonstrate enough promise for further development (Rinehart *et al.*, 2004). Studies with other MEK inhibitors such as PD0325901 came to the conclusion that patients in future clinical trials with MEK inhibitors should be refined more carefully according to their genetics and that combinations with other inhibitors could be beneficial since MEK inhibitors only caused growth arrest on their own (Haura *et al.*, 2010).

This was highlighted in Phase II studies where it was seen that another MEK inhibitor, AZD6244, had clinical activity in patients with advanced NSCLC. However no advantage was observed from monotherapy over standard chemotherapy at least in an unselected population and it was proposed that further development of the drug in NSCLC should focus on *BRAF* or *RAS* mutation-positive patients and/or combination regimens (Hainsworth *et al.*, 2010). These observations are evident in our data as well since single

treatments with MEK inhibitors only showed minimal responses on the *ex-vivo* NSCLC explants compared to the fold inductions we observed with single treatment of 50 μ M Cisplatin, whereas combination treatments with PI3K inhibitors showed synergy and increases of cell death.

LY294002 was one of the first inhibitors of PI3K (Vlahos *et al.*, 1994) and has been widely used in the laboratory setting. However high levels of toxicity, poor pharmacological properties and lack of specificity prevented its progression to the clinic (Heavey *et al.*, 2014). In fact, LY294002 was found to inhibit a range of other substrates, such as mTOR, casein kinase 2, DNA-PK, GSK3 and several others suggesting its use to study PI3K signalling specifically should be questioned (Gharbi *et al.*, 2007).

GDC-0941 is a more selective inhibitor of class IA PI3Ks and has good pharmacological properties. A study using breast cancer cell lines and *in vivo* xenograft models found that models harbouring *PIK3CA* mutations, amplification of human epidermal growth factor receptor 2, or dual alterations in two pathway components were very sensitive to treatment with GDC-0941 (O'Brien *et al.*, 2010). However, several models that did not have these alterations also showed sensitivity to GDC-0941 (O'Brien *et al.*, 2010). For example, *PTEN* loss has been identified as a predictive biomarker of response to GDC-0941 (Heavey *et al.*, 2014).

In our study the response to either single treatment with PI3K inhibitors was correlated with *PIK3CA* mutation status only in one case out of the three *PIK3CA* mutant samples identified. However, the three explants were treated with different PI3K inhibitors. The sample that showed high response with single treatment was treated with the more potent GDC-0941 PI3K inhibitor, whereas the other two samples were treated with LY294002. They did show some response but they were no different to samples carrying none of the 10 mutations we tested. There are two possibilities; one is that LY294002 is not as good at targeting PI3K and the other one is that targeting PI3K alone in those two samples does not induce a massive response because they are not solely dependent on PI3K and there are also other drivers present.

What is evident from our study and published work is that monotherapies do not offer a great advantage to patients. Combination therapies work best and in this case the combination of a potent PI3K inhibitor such as GDC-0941 with a MEK inhibitor such as PD184352 shows promise.

Further *in vitro* data demonstrated that GDC-0941 synergizes with the MEK inhibitor U0126 in NSCLC cell lines to induce cell growth inhibition and apoptosis (Zou *et al.*, 2012). Several preclinical studies also showed that combinations between MEK and PI3K inhibitors work synergistically to reduce tumour burden. A preclinical study using NSCLC cell lines and xenograft models showed the combination of GDC-0941 with paclitaxel, erlotinib, or a MAPK inhibitor had greater effects on cell viability than PI3K inhibition alone (Spoerke *et al.*, 2012). Combined use of NVP-BEZ235 (a PI3K and mTOR inhibitor) and ARRY-142886 (MEK inhibitor) has also been shown to synergistically act in shrinking *KRAS*-driven murine lung cancers (Engelman *et al.*, 2008). Synergistic effects of concurrent blockade of PI3K and MEK pathways were also observed in pancreatic cancer preclinical models (Zhong *et al.*, 2013). Another study using a combination of AZD6244 (MEK inhibitor) and MK2206 (AKT inhibitor) showed a significant synergistic effect on tumour growth *in vitro* and *in vivo* and led to increased survival rates in mice bearing highly aggressive human lung tumours (Meng *et al.*, 2010).

In the clinical setting, a study investigated safety, efficacy, and correlations between tumour genetic alterations and clinical benefit in 236 patients with advanced cancers treated with drugs targeting PI3K and/or MAPK pathways in a Phase I setting (Shimizu *et al.*, 2012). They found that the dual inhibition of both pathways exhibited a favourable efficacy compared with inhibition of either pathway alone, at the expense however of greater toxicity (Shimizu *et al.*, 2012). Nevertheless, preclinical data investigating the combination of GDC-0941 and GDC-0973 (novel MEK inhibitor) both *in vitro* and *in vivo* showed that intermittent inhibition of the PI3K and MAPK pathway is sufficient for efficacy in *BRAF* and *KRAS* mutant cancer cells (Hoeflich *et al.*, 2012). Therefore, the toxicity of combination treatments observed in the previous mentioned clinical study, could potentially be reduced by alternating dosing of the inhibitors.

Our data demonstrate the utility of *ex-vivo* explant cultures for assessing *in situ* drug responses for targeted therapies. Our findings propose that the use of a combination of PI3K and MEK inhibitors could potentially provide a therapeutic improvement in the treatment of NSCLC. This is also evident in the literature with various studies proposing that concurrent inhibition of PI3K and MAPK pathways is an attractive cancer treatment.

7. ASSESSMENT OF RESPONSES TO NEW AGENTS: TARGETING NON-ONCOGENE ADDICTED CELL DEATH PATHWAYS

7.1 Introduction

After establishing the culture conditions of *ex-vivo* NSCLC explants and confirming the utility of the model to test drug responses of tumours to cisplatin and targeted therapies *in situ*, we wanted to use the model to assess the responses to agents targeting cell death pathways and combinations that could have therapeutic implications for the treatment of NSCLC.

Inhibition of apoptosis is one of the hallmarks of cancers and this allows cells that carry considerable genomic alterations to survive (Hanahan & Weinberg, 2000). Targeting the apoptotic machinery of tumour cells could potentially be used to treat cancer cells selectively. There are two apoptotic pathways; the intrinsic and the extrinsic pathway. The extrinsic pathway is activated through death receptor stimulation at the plasma membrane and subsequent formation of DISC and activation of caspases which leads to apoptosis. The intrinsic pathway is triggered through various conditions such as DNA damage and it signals through the mitochondria with cytochrome c release and the formation of the apoptosome leading to caspase activation.

We used recombinant TRAIL to induce the extrinsic cell death pathway and ABT-737 to induce the intrinsic cell death pathway in explants. ABT-737 is a BH3 mimetic which inhibits the anti-apoptotic proteins Bcl-2, Bcl-xL and Bcl-w, with a high affinity (Oltersdorf *et al.*, 2005). Synergistic interactions between ABT-737 and TRAIL have also been observed in tumour cell lines including NSCLC (Song *et al.*, 2008), so we wanted to test whether the combination gives a similar response on *ex-vivo* NSCLC explants. Another possibility we wanted to test was whether cisplatin enhances TRAIL or ABT-737 responses in the

explants. We tested the responses to TRAIL, ABT-737 and combinations with cisplatin in a total of 12 samples and the data are shown here.

7.2 Aims and Objectives

- Determine the responses of explants to TRAIL and ABT-737, singly and in combination, and in the presence and absence of cisplatin.
- Correlate responses to available clinical data on clinical trials with these agents in the literature.

7.3 Results

7.3.1 TRAIL responses in 12 samples

Twelve *ex-vivo* NSCLC explant cultures were treated with 1 µg/ml of TRAIL. The cleaved PARP and Ki67 staining of tumour cells were quantified for the 12 samples and normalised against each case's carrier control. From these 12 samples, 2 were atypical carcinoid tumours, 5 were adenocarcinomas and 5 were squamous cancers. The fold cell death responses of explants to TRAIL showed three groups (Figure 7.1): 1) One sample, LT22 showed a 4-fold increase of cell death, 2) Samples that showed a small fold increase (1.3 to 2-fold) relative to the control (LT20, LT83, LT27, LT23 and LT16) and 3) Samples that showed no fold increase of cell death and instead showed a small decrease (LT18, LT84, LT89, LT92, LT15 and LT88).

The fold proliferation responses showed that proliferation went down to varying degrees in the majority of samples (Figure 7.2). In LT89 and LT22 the proliferation seemed to be slightly increased (1.2 fold) compared to the control. This could again arise from variation of Ki67 staining between tumour areas in samples. However, it has been reported in the literature that TRAIL treatment could induce proliferation in TRAIL resistant tumours (Baader *et al.*, 2005;

Ehrhardt *et al.*, 2003). In LT22, however, a 4-fold increase of cell death was observed suggesting this is not the case.

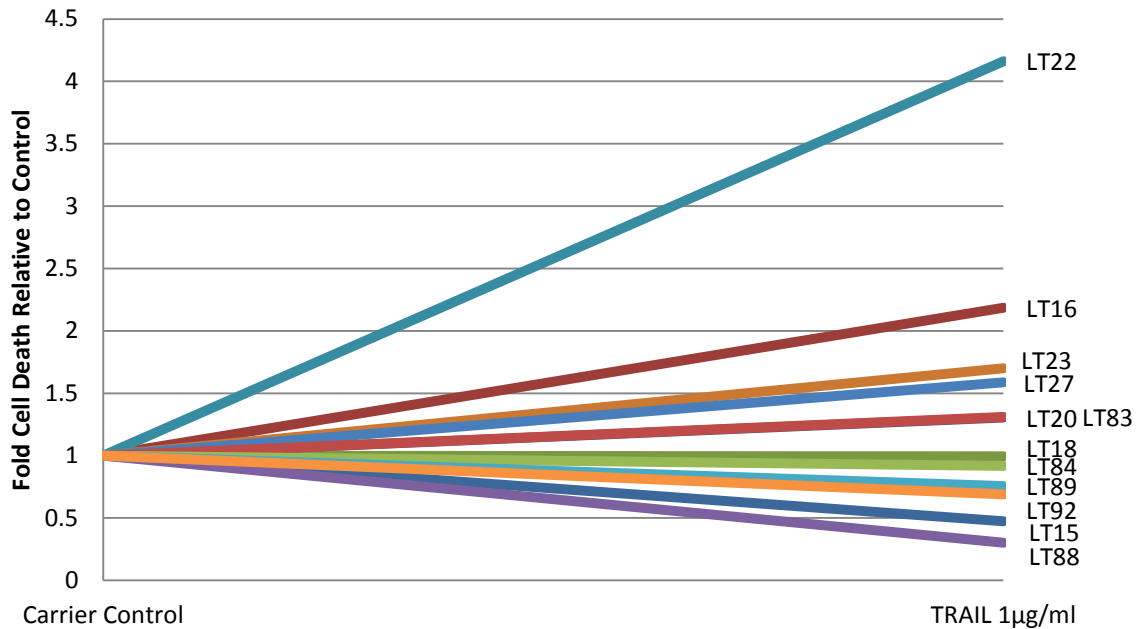


Figure 7.1. Fold Cell Death responses to 1 µg/ml of TRAIL relative to the carrier control. The % Cell Death of tumour area of 12 NSCLC *ex-vivo* explant cultures as determined from cleaved PARP staining after treatment with 1 µg/ml of TRAIL for 24 hours after an initial recovery of 16-20 hours were divided by each carrier control to calculate the fold difference.

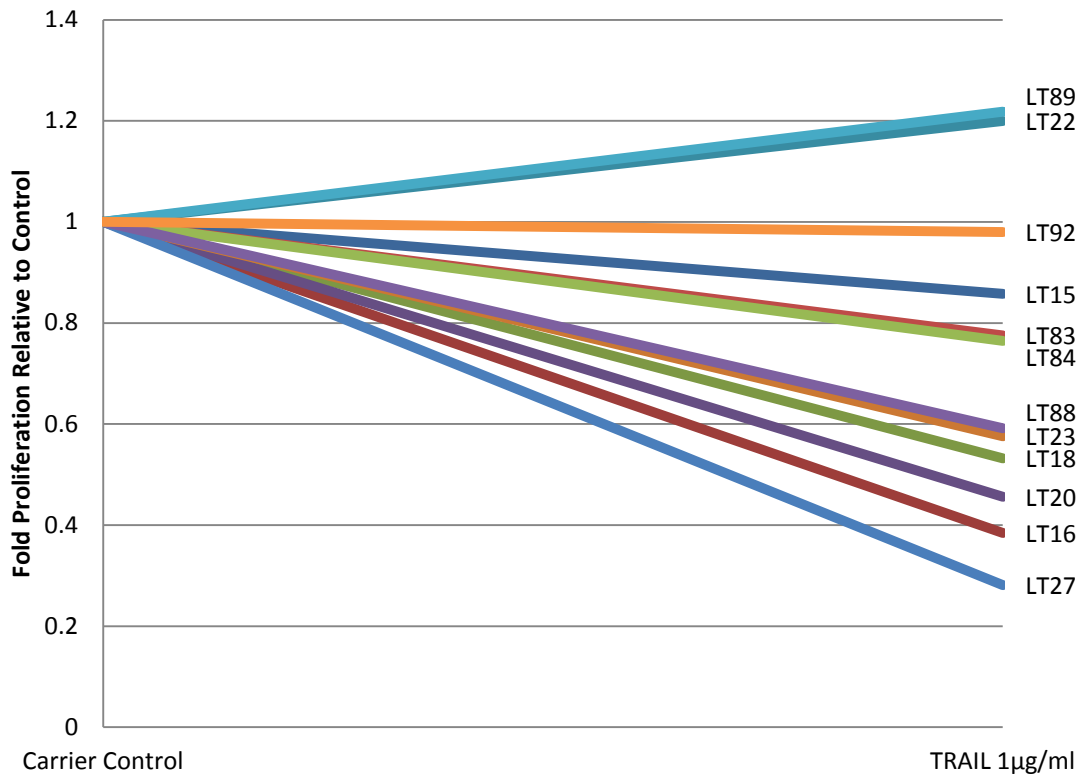


Figure 7.2. Fold Proliferation responses to 1 µg/ml of TRAIL relative to the carrier control. The % Proliferation of tumour area of 12 NSCLC *ex-vivo* explant cultures as determined from Ki67 staining after treatment with 1 µg/ml of TRAIL for 24 hours after an initial recovery of 16-20 hours were divided by each carrier control to calculate the fold difference.

7.3.2 TRAIL responses in combination with cisplatin in 12 samples

As shown in Figures 7.1 and 7.2 TRAIL treatment by itself was not very effective in the *ex-vivo* NSCLC explant cultures we tested. We wanted to see whether combination treatment with cisplatin would enhance the effect. We tested the responses of 1 µg/ml of TRAIL in combination with 50 µM cisplatin in the same 12 samples. The results of the fold cell death responses can be seen in Figure 7.3 and the fold proliferation in Figure 7.4. In the majority of cases TRAIL does not enhance the effect of treatment with 50 µM cisplatin alone (Figure 5.7) as the samples which were responsive to cisplatin showed approximately the same fold cell death increase with the addition of TRAIL suggesting the cell death effect is attributed to cisplatin sensitivity and TRAIL does not offer an advantage. In one case however, LT83, TRAIL seems to

synergise with cisplatin and induce 6-fold increase of cell death with the combination treatment whereas 4-fold cell death increase was observed with cisplatin alone (Figure 7.3). On the other hand, for LT22, addition of TRAIL produced the opposite effect and decreases 2-fold the cell death amount compared to 50 μ M cisplatin treatment alone.

For measurements of proliferation (Figure 7.4), most cases showed decrease with cisplatin treatment which remained constant with the addition of TRAIL. LT83 showed an additive effect with a greater decrease in proliferation with the combination treatment. A group of samples (LT15, LT89, LT27, LT23, and LT16) showed anomalous results with the proliferation going up and down with the different treatments. In the first 4 samples, combination of TRAIL and cisplatin increased the proliferation in comparison with cisplatin treatment alone, whereas in LT16 the proliferation seemed to be more decreased with TRAIL alone and TRAIL and cisplatin than cisplatin alone (Figure 7.4).

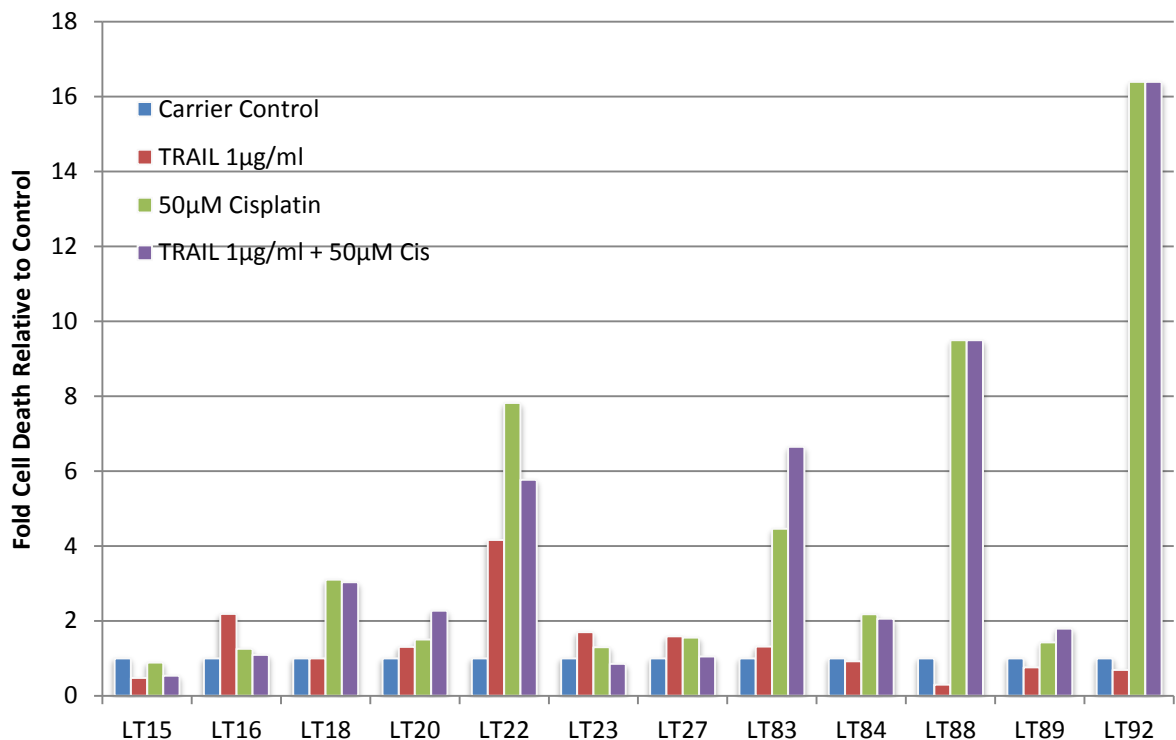


Figure 7.3. Fold Cell Death responses to 1 μ g/ml of TRAIL, 50 μ M Cisplatin and combination of the two relative to the carrier control. The % Cell Death of tumour area of 12 NSCLC *ex-vivo* explant cultures as determined from cleaved PARP staining after treatment with 1 μ g/ml of TRAIL, 50 μ M Cisplatin and TRAIL + cisplatin for 24 hours after an initial recovery of 16-20 hours were divided by each carrier control to calculate the fold difference.

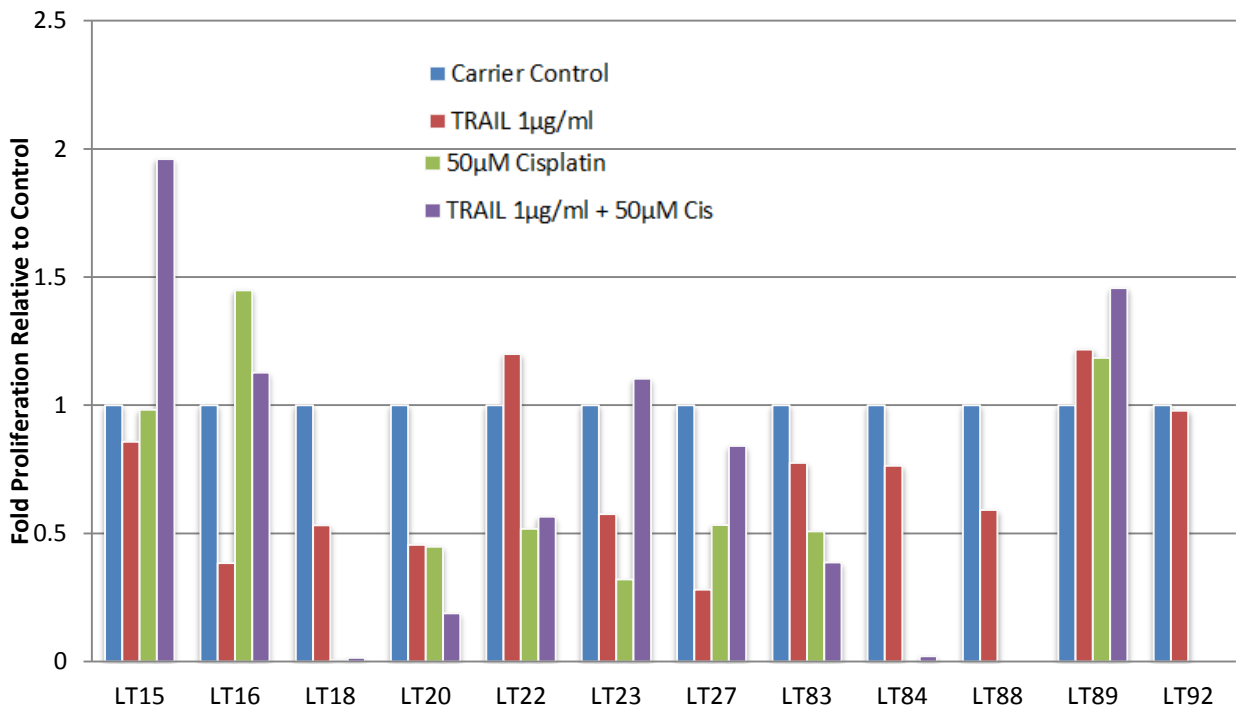


Figure 7.4. Fold Proliferation responses to 1 µg/ml of TRAIL, 50µM Cisplatin and combination of the two relative to the carrier control. The % Proliferation of tumour area of 12 NSCLC *ex-vivo* explant cultures as determined from Ki67 staining after treatment with 1 µg/ml of TRAIL, 50µM Cisplatin and TRAIL + cisplatin for 24 hours after an initial recovery of 16-20 hours were divided by each carrier control to calculate the fold difference.

7.3.4 Dose responses to ABT-737 in 10 samples

Ten *ex-vivo* NSCLC explant cultures were treated with 2 µM and 10 µM ABT-737. The cleaved PARP and Ki67 staining of tumour cells were quantified for the 10 samples and normalised against each case's carrier control. From these 10 samples, 1 was atypical carcinoid tumour, 5 were adenocarcinomas and 4 were squamous cancers. The responses in terms of fold cell death can be seen in Figure 7.5 and fold proliferation in Figure 7.6. The majority of the samples showed very little fold cell death increases (up to 2-fold) compared to the control in increasing concentrations of the drug. Two samples, LT22 and LT89, showed better dose responses which reached 7-fold and 6-fold at the highest ABT-737 dose respectively. The same can be broadly observed with the fold proliferation results. Most of the samples showed decreases in proliferation with increasing

ABT-737 doses. LT27 showed irregular results, with fold cell death decreasing at the highest dose and the fold proliferation increasing at the highest dose. This is highly unlikely. Looking at the tumour areas available for the analysis of the samples the 2 μM was double the tumour area compared to the 10 μM . It is possible that the results of the explants from 10 μM could be biased because of the smaller tumour area available for analysis.

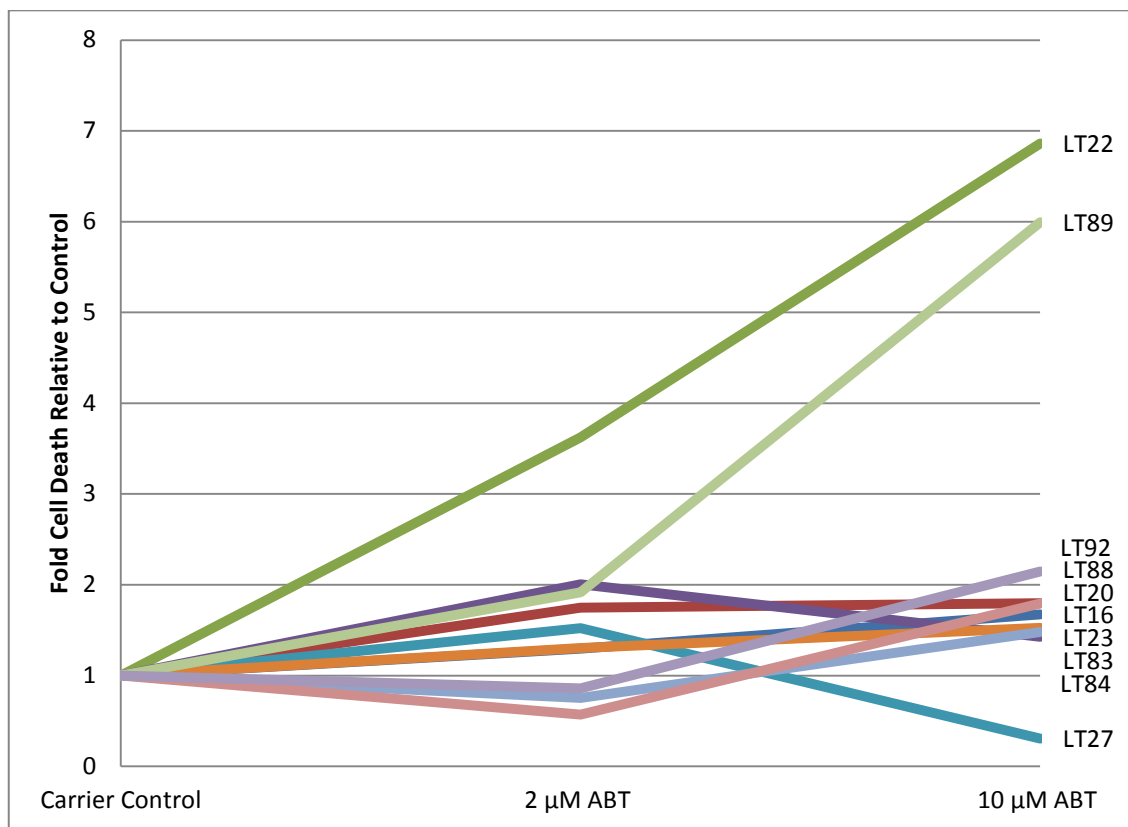


Figure 7.5. Fold Cell Death responses to increasing doses of ABT-737 relative to the carrier control. The % Cell Death of tumour area of 10 NSCLC *ex-vivo* explant cultures as determined from cleaved PARP staining after treatment with 2 μM and 10 μM ABT-737 for 24 hours after an initial recovery of 16-20 hours were divided by each carrier control to calculate the fold difference.

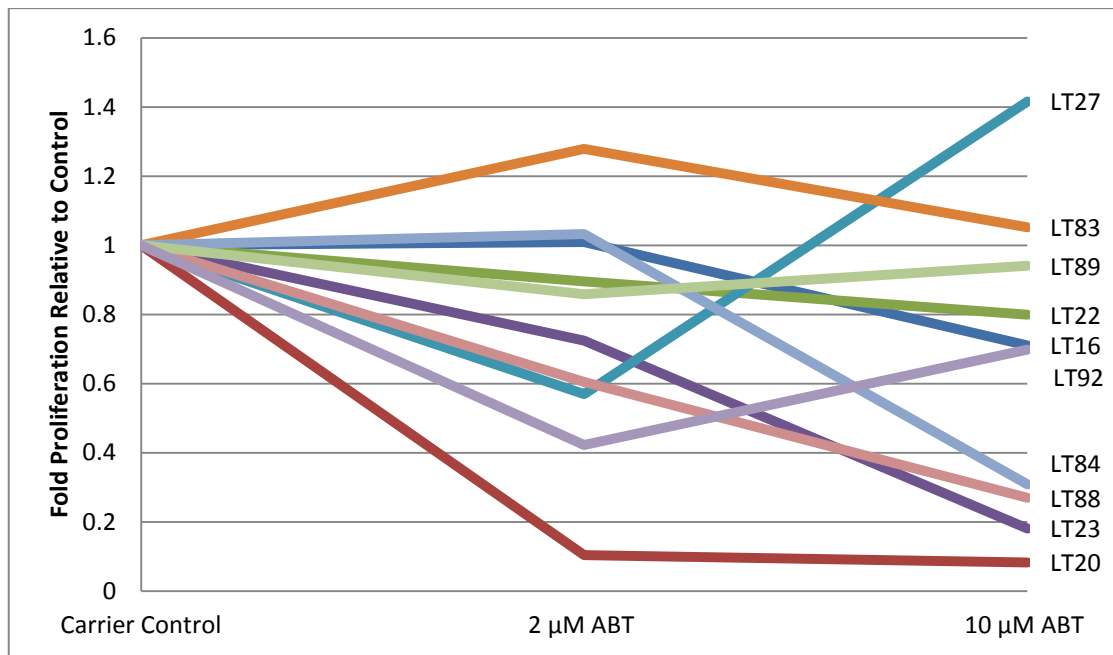


Figure 7.6. Fold Proliferation responses to increasing doses of ABT-737 relative to the carrier control. The % Proliferation of tumour area of 10 NSCLC *ex-vivo* explant cultures as determined from Ki67 staining after treatment with 2 μ M and 10 μ M ABT-737 for 24 hours after an initial recovery of 16-20 hours were divided by each carrier control to calculate the fold difference.

7.3.5 Dose responses to ABT-737 in combination with TRAIL in 10 samples

Next we wanted to see whether addition of TRAIL enhances the effect of ABT-737 treatment alone. The same ten explants were treated with combinations and the fold cell death results can be seen in Figure 7.7 and the fold proliferation in Figure 7.8. The combination of TRAIL with ABT-737 did not provide any advantage to the explants in comparison with ABT-737 alone in the majority of explants. LT22 and LT89 both responded with ABT-737 alone and in fact LT89 showed a smaller increase with the combination treatment. However, one case LT83 showed an additive effect between ABT-737 and TRAIL treatment with observed 4-fold cell death increase at the highest dose of the combination.

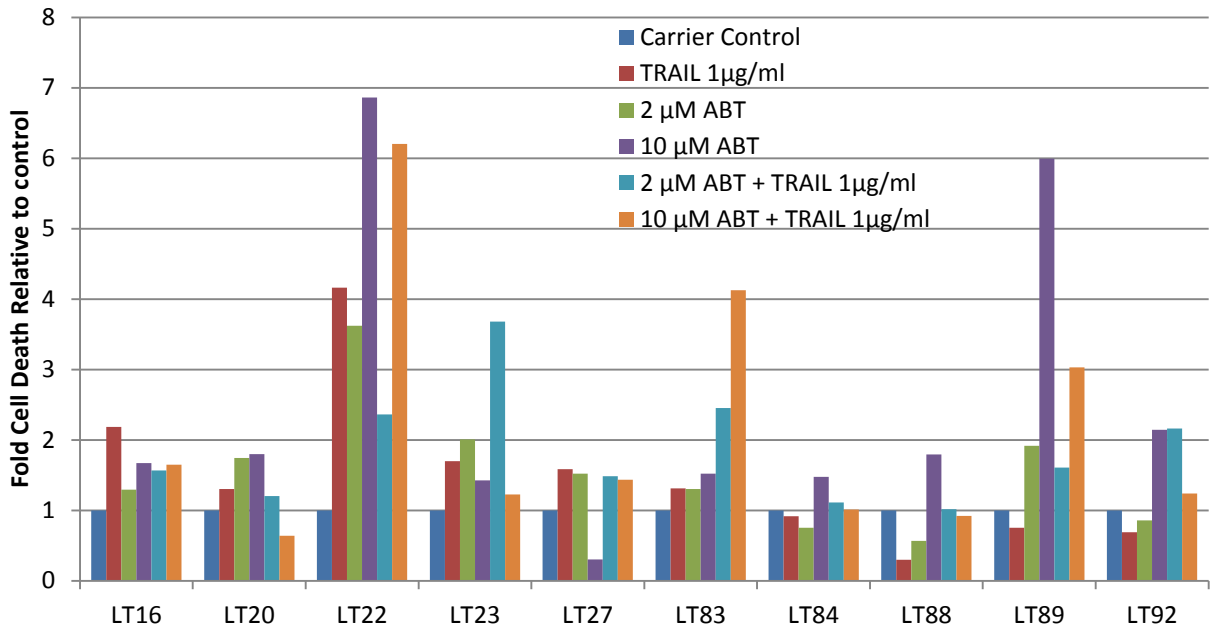


Figure 7.7. Fold Cell Death responses to increasing doses of ABT-737 in combination with TRAIL relative to the carrier control. The % Cell Death of tumour area of 10 NSCLC *ex-vivo* explant cultures as determined from cleaved PARP staining after treatment with 1 µg/ml of TRAIL, 2 µM and 10 µM ABT-737 in combination with 1 µg/ml of TRAIL for 24 hours after an initial recovery of 16-20 hours were divided by each carrier control to calculate the fold difference.

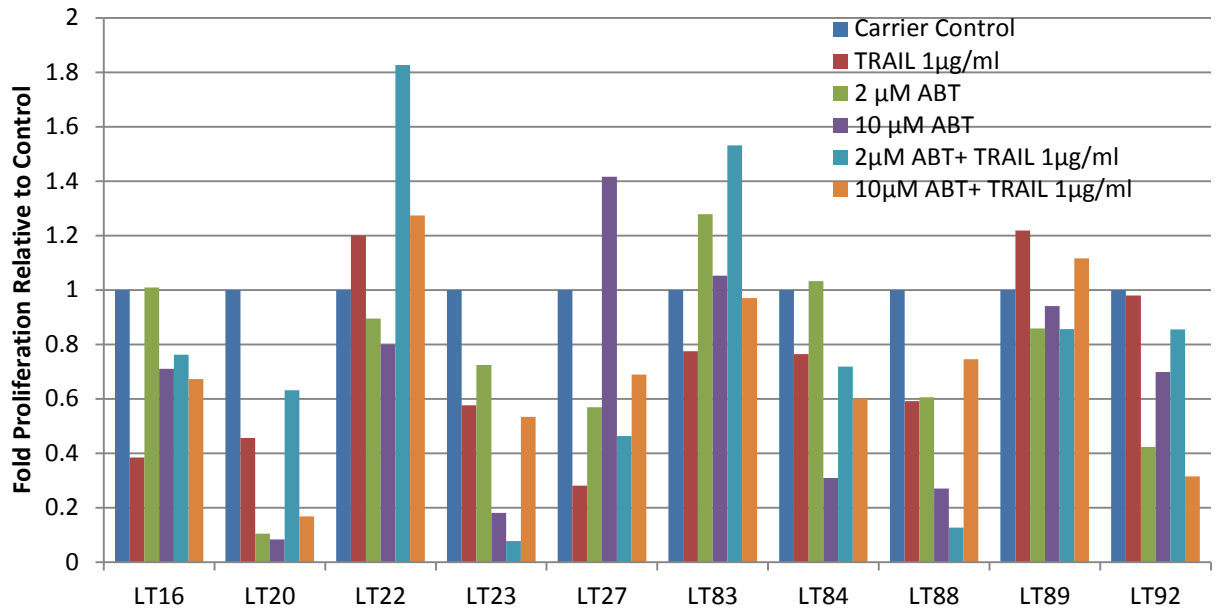


Figure 7.8. Fold Proliferation responses to increasing doses of ABT-737 in combination with TRAIL relative to the carrier control. The % Proliferation of tumour area of 10 NSCLC *ex-vivo* explant cultures as determined from Ki67 staining after treatment with 1 µg/ml of TRAIL, 2 µM and 10 µM ABT-737 in combination with 1 µg/ml of TRAIL for 24 hours after an initial recovery of 16-20 hours were divided by each carrier control to calculate the fold difference.

7.3.7 Dose responses to ABT-737 in combination with cisplatin in 4 samples

Finally, we wanted to test the response to ABT-737 in combination with 10 µM cisplatin. Due to time limitations we could only test this for 4 samples. The results of fold cell death can be seen in Figure 7.9 and fold proliferation in Figure 7.10. In three cases the single treatments or the combination did not show any visible response in fold cell death increases or fold proliferation. However in LT92 we saw a massive enhancement of cell death induction at increasing concentrations of the combination in comparison with each treatment alone (Figure 7.9).

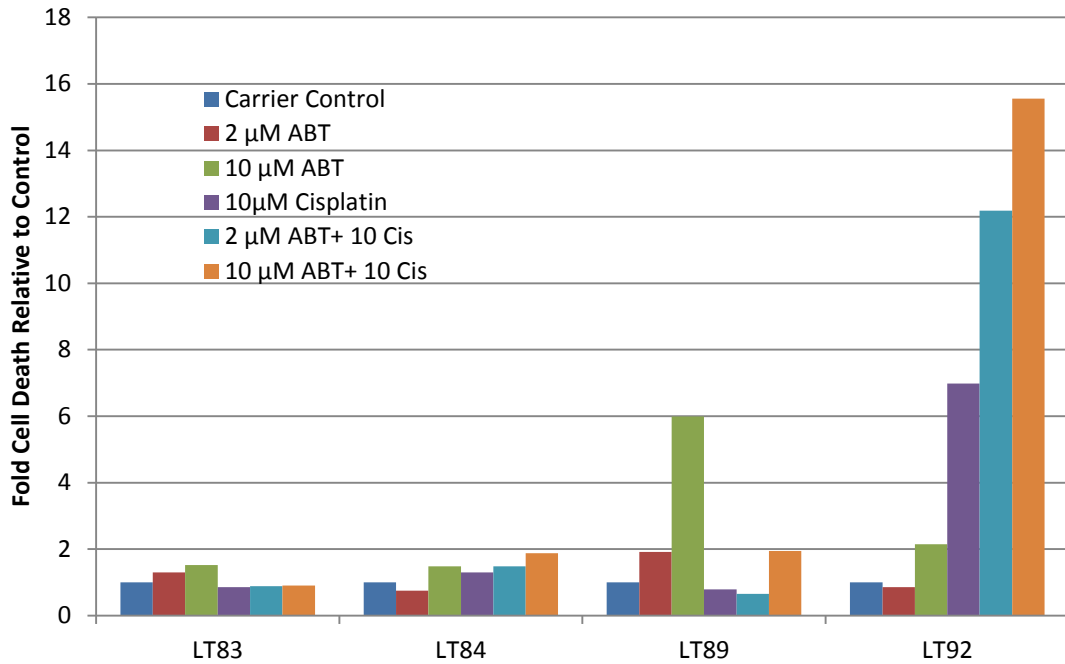


Figure 7.9. Fold Cell Death responses to 2 μ M and 10 μ M of ABT-737, 10 μ M cisplatin and combinations relative to the carrier control. The % Cell Death of tumour area of 10 NSCLC *ex-vivo* explant cultures as determined from cleaved PARP staining after treatment with 2 μ M and 10 μ M of ABT-737, 10 μ M cisplatin and combinations for 24 hours after an initial recovery of 16-20 hours were divided by each carrier control to see the fold difference.

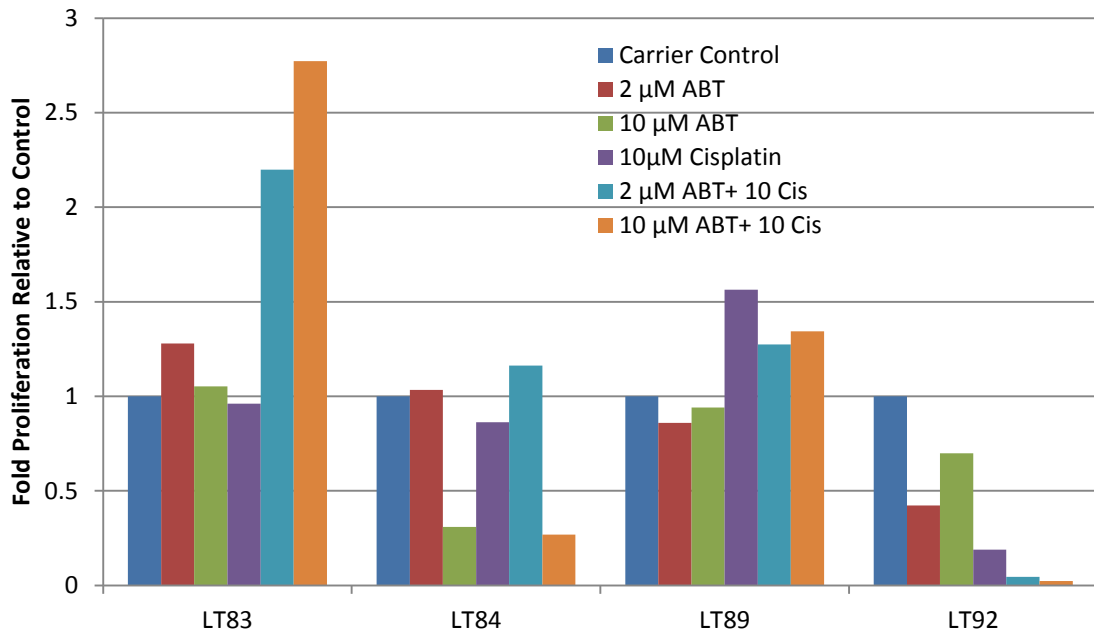


Figure 7.10. Fold Proliferation responses to 2 μ M and 10 μ M of ABT-737, 10 μ M cisplatin and combinations relative to the carrier control. The % Proliferation of tumour area of 10 NSCLC *ex-vivo* explant cultures as determined from Ki67 staining after treatment with 2 μ M and 10 μ M of ABT-737, 10 μ M cisplatin and combinations for 24 hours after an initial recovery of 16-20 hours were divided by each carrier control to see the fold difference.

7.4 Discussion

The responses of 12 *ex-vivo* NSCLC explant cultures were tested here for TRAIL and ABT-737 in the presence and absence of cisplatin. The general results of the treatments did not look very encouraging. The majority of the samples did not respond to the treatments even in combinations between the drugs. However, one sample LT22, showed response to TRAIL monotherapy (Figure 7.1). In another case, LT83, TRAIL seemed to synergise with cisplatin and induce more cell death with the combination treatment (Figure 7.3). Two samples, LT22 and LT89, showed good dose responses with ABT-737 treatment which reached 7-fold and 6-fold increase of cell death at the highest ABT-737 dose respectively (Figure 7.5). Only one case, LT83, showed an additive effect between ABT-737 and TRAIL treatment with an observed 4-fold cell death increase at the highest dose of the combination (Figure 7.7). The combination between ABT-737 and 10 μ M of cisplatin was only tested in four samples. Out of them, LT92, showed a massive enhancement of cell death induction at increasing concentrations of the combination in comparison with each treatment alone (Figure 7.9).

In vitro studies have shown that a number of cancer cell lines including NSCLC are sensitive to the cytostatic or cytotoxic effects of TRAIL monotherapy (Ashkenazi *et al.*, 1999; Stegehuis *et al.*, 2010). It has also been demonstrated that treatment of athymic mice with TRAIL shortly after tumour xenograft injection markedly reduced tumour incidence and that TRAIL treatment of mice bearing solid tumours induced tumour cell apoptosis, suppressed tumour progression, and improved survival (Ashkenazi *et al.*, 1999). Furthermore, in mice TRAIL showed synergism with chemotherapeutic drugs such as 5-fluorouracil causing substantial tumour regression or complete tumour ablation (Ashkenazi *et al.*, 1999). Additional experiments with orthotopic xenograft mouse models based on NCI-H460 NSCLC cell line showed that TRAIL administration alone inhibited growth of tumours by 60% compared to controls and when combined with Taxol plus carboplatin chemotherapy the growth inhibition was 97% (Jin *et al.*, 2004). They also showed similar results in an orthotopic lung tumour mouse model with apomab, a fully human monoclonal antibody that induces apoptosis via binding TRAIL-R2 (Jin *et al.*, 2008). Based

on all these promising preclinical studies, agents targeting TRAIL receptors, such as human recombinant TRAIL or agonistic monoclonal antibodies that target the functional TRAIL-R1 and TRAIL-R2 receptors, moved on to clinical testing.

A Phase II study of mapatumumab, a fully human agonistic monoclonal antibody which targets and activates the TRAIL receptor-1, in 32 heavily pre-treated patients with advanced NSCLC showed that no objective single agent activity of mapatumumab was demonstrated, but the drug was safe and well tolerated (Greco *et al.*, 2008). Nine patients (29%) however, had stable disease (Greco *et al.*, 2008). Similarly, in our study out of the twelve *ex-vivo* NSCLC explants tested with TRAIL treatment only one sample showed some response to single treatment with TRAIL. Further clinical studies focused on combinations with chemotherapy. A phase 1b Study of dulanermin (recombinant human Apo2L/TRAIL) in combination with paclitaxel, carboplatin, and bevacizumab (PCB) in patients with advanced Non-Squamous NSCLC showed promising results with one confirmed complete response and 13 confirmed partial responses and an overall response rate of 58% (Soria *et al.*, 2010). Nevertheless, the Phase II study which was done with 213 patients unfortunately concluded that the addition of dulanermin to PCB did not improve outcomes in unselected patients with previously untreated advanced or recurrent NSCLC (Soria *et al.*, 2011). Similar results were observed in another randomized phase 2 study of paclitaxel and carboplatin (PC) with or without conatumumab (a fully human monoclonal agonist antibody directed against TRAIL-R2) for first-line treatment of advanced NSCLC (Paz-Ares *et al.*, 2013). 172 patients randomised between treatments showed that although the drug was well tolerated, the addition of conatumumab to PC did not improve outcomes in unselected patients with previously untreated advanced NSCLC (Paz-Ares *et al.*, 2013). In our study we tested the responses of 12 *ex-vivo* NSCLC explant cultures to a combination of TRAIL and cisplatin and only one case showed increased cell death from the combination. Our observations broadly agree with the results of the clinical studies of either recombinant TRAIL or monoclonal antibodies targeting TRAIL receptors.

Neutralization of anti-apoptotic Bcl-2 family members (Bcl-2, Bcl-XL, Bcl-w, Mcl-1 and Bcl2A1) is required for apoptosis induction and has therefore made inhibitors of this family an attractive way to improve cancer therapy (Vogler *et al.*, 2009). Studies with ABT-737 (inhibitor of Bcl-2, Bcl-XL and Bcl-w) showed the drug to exhibit single agent killing of lymphoma and small-cell lung carcinoma lines in addition to patient-derived cells (Oltersdorf *et al.*, 2005). They also reported that in animal models, ABT-737 caused regression of established tumours and produced cures in a high percentage of the mice (Oltersdorf *et al.*, 2005). Oral administration of ABT-263 (the orally bioavailable improvement compound from ABT-737) alone induced complete tumour regression in xenograft models of small-cell lung cancer and acute lymphoblastic leukemia (Tse *et al.*, 2008). However in xenograft models of aggressive B-cell lymphoma and multiple myeloma ABT-263 exhibited modest or no single agent activity, but it significantly enhanced the efficacy of clinically relevant therapeutic regimens (Tse *et al.*, 2008).

In a phase I study of ABT-263 (aka Navitoclax) in patients with SCLC and other solid tumours from 47 patients, one patient with SCLC had a confirmed partial response lasting longer than 2 years, and eight patients with SCLC or carcinoid had stable disease (Gandhi *et al.*, 2011). However, in a further Phase II study of single-agent Navitoclax in patients with relapsed SCLC it was concluded that Bcl-2 targeting by navitoclax showed limited monotherapy activity against advanced and recurrent SCLC and that future studies should focus on combination therapies (Rudin *et al.*, 2012). In our study two samples out of ten showed good dose responses with ABT-737 treatment which reached 7-fold and 6-fold increase of cell death at the highest ABT-737 dose. When we combined ABT-737 with the chemotherapeutic drug cisplatin one out of four samples showed great enhancement of the response, further supporting the use of combinations between chemotherapy and BCL-2 inhibitors.

A combination of ABT-737 and TRAIL induced significant cell death in multiple cancer cell lines, including renal, prostate, and lung cancers, although each agent individually had little activity in these tumour cells (Song *et al.*, 2008). This synergy between ABT-737 and TRAIL was also observed in an *in vivo* glioblastoma model (Cristofanon & Fulda, 2012). In our study this combination

was tested in 10 *ex-vivo* NSCLC explants and only one case showed improved response. This combination has not been tested in the clinic yet.

The literature supports the use of TRAIL receptor targeting agents and BCL-2 inhibitors in improving cancer treatment. The generalised conclusion is that monotherapies provide very small if any advantage in cancer therapy. There are numerous studies examining different promising potential enhancers of TRAIL induced apoptosis such as the proteasome inhibitor bortezomib (Luster *et al.*, 2009; Voortman *et al.*, 2007), quercetin (Chen *et al.*, 2007), PI3K inhibitors (Bagci-Onder *et al.*, 2011) and trifluorothymidine (Azijli *et al.*, 2014). A further realisation is that drugs should be better selected according to the patients' tumour molecular characteristics. The *ex-vivo* NSCLC explant model we used points towards it being more predictive of patient outcome when comparing similar results with other *in vitro* studies or animal models. It could potentially be used to improve on the current preclinical models for lung cancer and other solid cancers and help the drug development process. It could also provide an *ex-vivo* way of personalising treatment to each patient to identify the best therapy for the individual.

8. SUMMARY AND CONCLUSIONS

Sixty patient samples were collected during the span of this project from consented patients undergoing lung surgery at Glenfield Hospital. 47% of the patients had adenocarcinomas, 40% had squamous cell carcinomas, 5% had large cell lung cancers and the remaining 8% had other histology. Reports for lung cancer in the UK as a whole, however, have shown slightly different figures with 27% being squamous cell carcinomas, 25% being adenocarcinomas, 23% being large cell lung cancers, 16% being SCLC and 7% categorised as other carcinomas (Walters et al., 2013). Thus, in Leicester we see significantly more adenocarcinomas, and less large cell carcinomas. This difference could be a result of the small population size of 60 patients.

Mutation analysis with qPCR in *KRAS*, *BRAF*, *PIK3CA* and *EGFR* identified *PIK3CA* mutations in 21% of the squamous cell carcinomas. In samples with adenocarcinoma histology, mutations of *KRAS* (14%), *PIK3CA* (11%) and *EGFR* (7%) were identified. *PIK3CA* mutation frequency was far higher amongst our cases that has been previously reported (Ji et al., 2011, Kawano et al., 2006, Okudela et al., 2007, Samuels et al., 2004) , however this could be a result of our small population study.

The main focus of this project was to establish a primary NSCLC *ex-vivo* explant culture system based on a previous breast cancer explant model established by Prof. MacFarlane's laboratory (Twiddy, D., et al., 2010-poster abstract) to test the efficacy of existing drugs as well as novel drug combinations.

Ex-vivo explant cultures were set-up for 34 out of the 60 NSCLC samples collected. Due to high necrosis and some technical problems, 21 *ex-vivo* NSCLC explants remained usable for full analysis with IHC. Thus there was an attrition rate of ~30% which needs to be borne in mind in utilising this platform further. However, current PhD students continuing to work with NSCLC explants report better quality of samples.

Six of 21 samples were used to determine the best conditions for explant culture. The best culture time was identified to be 24 hours after recovery as, at this time, the proliferation and viability was found to be better preserved compared to longer culture times. This should provide enough time to observe whether a drug treatment has a response or not and also maintains the tissue architecture intact. The effect of varying concentrations of FCS in the media was also studied. A positive trend for cell death with increasing FCS concentrations was observed amongst six samples. However, no significant differences were observed on proliferation. It was decided that 1% FCS was reasonable to use since most of the drug treatments were done in that concentration, consistent with the breast tumour studies. A moderate effect of cultivation was observed which is expected since the tumour samples are being taken out of their original environment and are subjected to vigorous cutting and changes of the original conditions.

Next, responses of *ex-vivo* NSCLC explants to cisplatin were tested at a range of concentrations (1, 10 and 50 μ M) for 10 samples and at the 50 μ M supra-pharmacological dose for a total of 19 samples. 2/10 samples showed response at 1 and 10 μ M cisplatin and 7/19 showed response at 50 μ M. None of the 7 patients from the responding explants have yet died, except one patient who died 20 days after the surgery suggesting complications that were probably not associated with chemotherapy. However, of the 12 resistance explants, two of these patients have died. Although these data are not statistically significant, it is interesting that only some of the cisplatin resistant patients have so far died.

The responses to cisplatin were also correlated to p53 IHC expression. IHC-mtp53 samples showed higher fold proliferation reductions and higher cell death differences compared to the control in response to cisplatin treatment than IHC-wtp53 samples agreeing with previous reports that patients who are IHC-mtp53 have greater responses to cisplatin than IHC-wtp53 (Tsao *et al.*, 2007; Cote *et al.*, 1997).

The responses of ten *ex-vivo* NSCLC explant cultures were tested after treatment with PI3K inhibitors (LY294002 in 6 samples and GDC-0941 in 4

samples) and MEK inhibitors (PD184352 in 7 samples and UO126 in 2 samples) singly and in combination. Our findings propose that the use of a combination of PI3K and MEK inhibitors, especially GDC-0941 and PD184352, could potentially provide a therapeutic improvement in the treatment of NSCLC. The responses were greater in the *PIK3CA* mutant samples. This is also evident in the literature with various studies proposing that concurrent inhibition of PI3K and MAPK pathways is an attractive cancer treatment.

The responses of 12 *ex-vivo* NSCLC explant cultures were tested here for TRAIL and ABT-737 in the presence and absence of cisplatin. TRAIL monotherapy or in combination with 50 μ M cisplatin did not induce responses in the explants tested except in 1/12 that showed moderate response. ABT-737 monotherapy showed response in 2/10 samples whereas ABT-737 in combination with TRAIL only showed an additive effect in 1/10 samples. These results were generally in agreement with clinical studies.

To conclude, we have shown here that the tissue architecture and tumour heterogeneity of individual NSCLC patients can be examined in an *ex-vivo* NSCLC explant culture system which maintains viability and proliferation in a short culture period of 24 hours + recovery (16-20hrs). Even though there is a moderate effect of cultivation, the *ex-vivo* NSCLC explant culture system can be used for assessing *in situ* drug responses. This model points towards being more predictive of patient outcome when comparing similar results with other *in vitro* studies or animal models. It could potentially be used to improve on the current preclinical models for lung cancer and other solid cancers and help the drug development process. It could also provide an *ex-vivo* way of personalising treatment to each patient to identify the best therapy for the individual.

It is unlikely that the *ex-vivo* NSCLC explant culture system described here could be adapted for high-throughput drug screening but is better applied to addressing specific questions on the *in situ* response of an anticancer agent. It is envisaged that this could have particular utility for assessing the effect of agents that target the tumour stroma for example anti-PD1 therapeutic antibodies or chemokine receptor inhibitors.

The analysis of the results was found to be very laborious and time-consuming since this was mainly done by hand. This should improve by introducing a slide scanner and specific software for accurately counting the staining and automation of the procedure. Another possibility would be to assess the cytotoxicity with Alamar Blue which is a dye that can be added to the culture medium, which can be sampled at various time-points for cytotoxicity measurements by fluorometry (Pirnia *et al.*, 2006).

Some interesting results have already been published using similar methods to explants (Pirnia *et al.*, 2006; Hoffman *et al.*, 1989; Vescio *et al.*, 1990; Furukawa *et al.*, 2000; Vaira *et al.*, 2010). However, different methodological and ethical restrictions limit the design of studies like these, despite their clinical relevance. Having a preclinical model which mimics the treatment outcomes of real patients more faithfully than other models such as cell lines and animal models should aid the drug development process and it could also provide a way of tailoring therapy to the individual. Before it could be incorporated as a routine platform, the next stage would be to undertake a study in which outcomes of explants are directly correlated with clinical outcomes. This was initially the purpose of the cisplatin study but it would take many months if not years to complete such an analysis so that statistically meaningful data is acquired.

APPENDIX

9.1 Ethics Documentation



Health Research Authority
National Research Ethics Service

NRES Committee North West - Haydock

North West Centre for Research Ethics Committees
3rd Floor - Barlow House
4 Minshull Street
Manchester
M1 3DZ

Tel: 0161 625 7819/7832
Fax: 0161 237 9427

13 June 2012

Professor Andrew Wardlaw
Professor of Respiratory Medicine
University of Leicester
Glenfield Hospital
Groby Road
Leicester
LE3 9QP

Dear Professor Wardlaw

Study title: Use of Tissue from Lung Resections to Investigate the Molecular and Functional Mechanisms of Human Lung Disease
REC reference: 07/MRE08/42
Amendment number: Substantial Amendment 3, 04-May-12
Amendment date: 04 May 2012

The above amendment was reviewed at the meeting of the Sub-Committee held on 12 June 2012.

Ethical opinion

The amendment (Substantial Amendment 3, 04-May-12) requested a number of changes to the approved Protocol and study documentation as follows:-

1. To remove references to AstraZeneca from the Protocol, and Participant Information Sheet and Consent Form as they are no longer involved in the study.
2. To make minor amendment to the 'background' section of the Protocol.
3. To make a number of minor clarifications and corrections of typographical errors
4. To make a number of minor changes to the Participant Information Sheet to make it more reader friendly.
5. To make amend the Consent Form to allow the Sponsor access to patient records.
6. To share anonymised samples and data with other ethically approved research studies and with other academic partners or industrial collaborators.
7. To extend the study end date to 31 June 2017.

It was noted that there was a typographical error in the stated end date of the study that should be corrected to read the 30 June 2017 instead of the 31 June 2017.

A Research Ethics Committee established by the Health Research Authority

The Sub-Committee identified no ethical issues with the proposed amendment.

The members of the Committee taking part in the review gave a favourable ethical opinion of the amendment on the basis described in the notice of amendment form and supporting documentation.

Approved documents

The documents reviewed and approved at the meeting were:

Document	Version	Date
Notice of Substantial Amendment (non-CTIMPs): Substantial Amendment 3, 04-May-12		04 May 2012
Protocol - tracked changes	2	04 May 2012
Protocol	2	04 May 2012
Participant Information Sheet: with tracked changes	3	04 May 2012
Participant Consent Form: with tracked changes	3	04 May 2012
Participant Information Sheet	3	04 May 2012
Participant Consent Form	3	04 May 2012
Data Collection Form	3	04 May 2012

Membership of the Committee

The members of the Committee who took part in the review are listed on the attached sheet.

R&D approval

All investigators and research collaborators in the NHS should notify the R&D office for the relevant NHS care organisation of this amendment and check whether it affects R&D approval of the research.

Statement of compliance

The Committee is constituted in accordance with the Governance Arrangements for Research Ethics Committees and complies fully with the Standard Operating Procedures for Research Ethics Committees in the UK.

07/MRE08/42:	Please quote this number on all correspondence
---------------------	-------------------------------------------------------

Yours sincerely



On behalf of:-

Professor Ravi S Gulati
Chair

E-mail: noel.graham@northwest.nhs.uk

Enclosures: List of names and professions of members who took part in the review

Copy to: R&D office for NHS care organisation at lead site:

Carolyn Maloney
R&D Manager
Research Office
Leicester General Hospital
Gwendolen Road
Leicester
LE5 4PW

DIRECTORATE OF RESEARCH & DEVELOPMENT

Research & Development Office
Leicester General Hospital
Gwendolen Road
Leicester
LE5 4PW

Director: Professor D Rowbotham

Assistant Director: Dr David Hetmanski

R&D Manager: Carolyn Maloney

Direct Dial: (0116) 258 8351

Fax No: (0116) 258 4226

18/06/2012

Professor Andrew Wardlaw
University of Leicester
Glenfield Hospital
Groby Road
Leicester
LE3 9QP

Dear Professor Andrew Wardlaw

Ref: UHL 10402

Title: Molecular and Functional Mechanisms of Human Lung Disease (plus sub studies)

Project Status: Project Approved

End Date: 30/06/2017

Thank you for submitting documentation for Substantial amendment **Number 3 Date 4th May 2012** for the above study.

I confirm that the amendment has the approval of the University Hospitals of Leicester NHS Trust R&D Department and may be implemented with immediate effect. The study End date has also been noted and extended to 30th June 2017.

The documents received are as follows:

Description	Version
Data Collection Form	V3 Date: 04.05.2012
PIS& ICF	V3 Date: 04.05.2012
Protocol	V2 Date: 04.05.2012

Please be aware that any changes to these documents after approval may constitute an amendment. The process of approval for amendments MUST be followed. Failure to do so may invalidate the approval of the study at this trust.

Please ensure that all documentation and correspondence relating to this amendment are filed appropriately in the relevant site file.

Yours sincerely



Carolyn Maloney
R&D Manager



Title: Creation of a Midlands Lung Tissue Consortium (MLTC) for the provision of lung resection tissue.

Hypothesis

The use of primary lung tissue as a source of material for studies into the pathogenesis of lung disease is more physiologically relevant than cell lines and animal tissue.

Objective:

To maximise the supply of lung tissue from resection material for use in research into lung disease by members of the MLTC.

Background:

Lung diseases including COPD, asthma, cancer and interstitial lung disease are common and cause considerable morbidity and mortality. Ideally research into lung disease should use material obtained from human lung. However lung tissue is difficult to obtain because it is dependent on invasive procedures such as lung surgery or fibre-optic bronchoscopy. As a result both academic research and the development of new drugs by the pharmaceutical industry often have to rely on cell lines or animal tissue which is a second best option because it lacks physiological relevance.

One source of fresh lung tissue is excess material from lung resections usually undertaken for carcinoma of the lung. In addition the 'normal' lung tissue can be compared with the malignant tissue for those with an interest in lung carcinoma. The lung tissue can be processed for histology or to obtain primary lung cells. These can include cells of the immune system (e.g. mast cells, T cells, eosinophils, neutrophils, alveolar macrophages) or structural cells (e.g type 1 and 2 pneumocytes, airway smooth muscle cells, fibroblasts, bronchial epithelium, and vascular endothelial cells). The immune cells need to be used within hours of resection whereas the structural cells can be cultured and stored for long periods. A wide variety of experiments can be performed on these cells depending on the interest of the investigator. Where appropriate the clinical status of the patient can be linked anonymously to the tissue so that the diagnosis and severity of disease can be related to the functional capacity of the cells.

The cardiothoracic unit at Glenfield Hospital in Leicester has an approximately fifteen-year history of using lung resection material for research into lung disease. During that time we have obtained and processed in the region of 700 lung specimens and in the region of thirty peer reviewed original papers have directly resulted from the use of lung resection material. In the last eleven years Leicester has had collaborations on studies relating to the pathogenesis of COPD which has involved the supply of lung tissue. This tissue has been used to investigate the relationship between pathology and function in patients undergoing lung volume reduction surgery (LVRS) and to help guide drug development. Birmingham Heartlands are also using lung resection material for their research programmes and Walsgrave Coventry have access to lung resection material and are keen to develop their research programmes.

In order to maximise the potential for research in the Midlands, Leicester entered into discussions with Birmingham Heartlands and Coventry Walsgrave about the possibility of establishing a consortium (MLTC) for the supply of lung tissue to members of the consortium to enhance their research programmes. These programmes differ in each of the centres with each needing different types of lung cells. As the research programmes are not resource competitive by maximising the use of lung tissue we can enhance the research programmes of all three centres. We will also be able to share expertise in lung processing and develop collaborative research projects where our research interests overlap.

07/MRE08/42
Protocol
Version 2, 04-May-12

Plan of Investigation

The Midlands Lung Tissue Consortium (MLTC)

The consortium has now been well established since 2007 and is made up of the participating centres noted above. Day to day running of the MLTC will be in the hands of a management board with representatives from each centre. The administration of the MLTC, in particular co-ordinating the provision of lung tissue will be undertaken by Leicester. Good communication between the centres in terms of the timing of the availability of the lung tissue will be essential to the success of the initiative.

Arrangements for the Supply and Processing of Lung Tissue

The broad outline will be the same for each centre with local variations.

Leicester:

This will broadly follow our current procedure. Patients undergoing lung resection will be asked for written informed consent to use their lung tissue (both malignant tissue and normal tissue at a distance from the tumour) for research purpose including sharing the tissue with our collaborators in the MLTC. Consent for the use of both the normal and malignant tissue as well as up to 50mls of blood will be obtained either by the doctor obtaining consent for the operation (usually a surgical SHO), a research nurse, study co-ordinator or clinical fellow involved in the research programme. When the lung is removed from the patient in theatre the nursing staff will check for the presence of consent. They will then contact the technician employed to harvest the lung tissue. The technician will collect the fresh unfixed lung tissue and take it to pathology where s(he) will dissect away the normal lung tissue from the malignant tissue. The remaining lung will then be placed in formalin and dealt with by the pathologists. The technician has been trained by the pathologists to do this 'cut up'. Where malignant tissue is required the cut up will be done by a pathologist or fully trained technician. The technician files the consent form and records the clinical details of the patient. The technician then codes the samples so that the tissue is dealt with anonymously by the research staff in a way that the clinical details can be linked to the patient if necessary. Only the technician, the research nurse or the principal investigator (Wardlaw) has access to the identity of the patient.

The technician will then take the lung tissue to the research laboratories where it is dealt with by the research staff depending on their immediate needs. Some of the lung will be transported between the hospitals either as whole lung, lung digests or single cell preparations. Where required some clinical details such as lung function, smoking history and diagnosis are provided to the research staff on an anonymous basis.

Birmingham Heartlands:

Consent will be obtained by the surgical SHO's or clinical research fellow as is the case for Leicester. In accordance with current agreed practice and ethical / trust approval, lung samples peripheral to the tumour specimen will be excised by the surgical team performing the lung resection. A mechanism for feedback to the pathologist about the resected lung is already in place. The clinical fellow will then file the consent form and record and code the patient details as described above for Leicester before handing the tissue over to the local research staff for processing or transporting the lung to Leicester by courier.

07/MRE08/42
Protocol
Version 2, 04-May-12

Coventry Walsgrave:

Consent will be obtained by the research nurse employed on the project. Suitable patients will be identified from the theatre lists. The nurse will also collect the lung from theatre, transport it to pathology where it will be cut up by the pathologist. S(he) will then record the details as above and arrange for the lung to be processed locally or transported by courier to Leicester.

Experimental Methodology

The way the lung is processed will depend on the current research priorities of the members of the MLTC. These will change over the course of the collaboration so it is not appropriate to describe specific experiments. Potentially we would aim to use all the lung cells for experiments ranging from immunological investigation through to gene expression analysis as well as high throughput screening of drug targets. Between us we have protocols for the isolation of most lung cell types and these will be shared between members of the MLTC. In some cases the tissue will be processed for immunohistochemistry and these samples will be stored in a manner appropriate to the embedding method used. In some cases structural cells will be cultured and stored in liquid nitrogen for thawing at a later date. Most of the experiments will involve normal tissue but in some cases we will want to use the malignant tissue either for immunohistochemistry, gene profiling or isolation of malignant and non-malignant cells for functional studies. In cases where malignant tissue is required this will only be done in close co-operation with the pathologist in the centre to make sure that the routine analysis of the sample is not compromised. For some experiments we will want to compare blood and lung cells from the same patient. Consent will be routinely obtained for blood (up to 50ml) to be taken as well as lung tissue as described above but this will only be acted upon in a small number of specific cases.

Numbers of Patients

It is anticipated based on the resection numbers in each centre that Leicester will source in the region of 60 useable lung samples a year, Walsgrave 40 and Birmingham 80. These figures may need to be adjusted based on experience.

9.2 Example patient sample sheet

Patient Sample Sheet

Lung Tumour Sample Number: 27

Ethics Project Title: Use of tissue from lung resections to investigate the molecular and functional mechanisms of human lung disease

LREC Ref:

Date of Operation: 27/07/11

Pathologist: Sally Muller, collected with Will Monteiro

Consent Given: Yes

Specific/Generic

Person attaining consent:

Patient Date of Birth: 59y 8m

Sex: M

Procedure: LLL

Tissue Tracking

Person/s processing tissue sample: Ellie Karekla

Total weight of sample:

Total weight of solid tissue: 4.3793 g

Total volume of holding media:

Total volume of bodily fluids:

Immunohistochemistry:

Total weight of sample to be used for slices:

Storage of tissue:

Total weight of sample to be used for PFFE for later analysis: ~1g

Total weight of sample to be used for DNA for later analysis: 135 mg

Total weight of sample to be used for RNA for later analysis: 641 mg

Total weight of sample to be used for protein for later analysis: 1430 mg

Disposal of tissue:

Total weight of sample disposed of on day of acquisition: none

Experimental Aims

Viability

Genotyping

Diffusion

Biochemical Assays

Long term cultures

Explants

Proliferation

Patient Sample Sheet

Sample taken to MM lab and processed by Ellie in the same days as operation.

A portion was taken for eventual generation of protein lysate using Kinase Assay Buffer.

The portion taken for RNA was stored in RNA Later at -20°C after 1 day at 4°C.

The portion taken for DNA was lysed in 0.05M Tris pH8/0.1% SDS buffer (+ 0.5mg/ml Proteinase K) for 3 hours at 65°C, cleaned with an equal volume of phenol/chloroform/IAA, washed in chloroform/IAA, precipitated with 100% ethanol (-20°C) and 1M NaCl, washed in 70% ethanol then air dried and resuspended in 250 µl TE and stored at 4°C.

Portion taken for explants was processed in MM lab by Ellie in the class II TC hood.

1 x 6 well processed for t_0

27 x 6 well processed and incubated in DMEM media plus 1% FCS+ 1%pen/strep

Samples harvested and processed for PFFE. They were fixed for ~20 hours in 4% PFA and then stored in cassettes in 70% EtOH. Processed for H&E and IHC in HP lab

Block numbers are as follows:

LT27-001: T = 0

LT27-002: 15hrs o/n + 24 hours untreated

LT27-003: 15hrs o/n + 24 hours untreated

LT27-004: 15hrs o/n + 24 hours control carrier alone (1.5µl DMSO)

LT27-005: 15hrs o/n + 24 hours control carrier alone (3µl DMSO)

LT27-006: 15hrs o/n + 24 hours control carrier alone (1.5µl DMF)

LT27-007: 15hrs o/n + 24 hours + 50 µM cisplatin in DMF (1.5 µl)

LT27-008: 15hrs o/n + 24 hours + 5 µM U0126 in DMSO (1.5 µl)

LT27-009: 15hrs o/n + 24 hours + 10 µM U0126 in DMSO (1.5 µl)

LT262-010: 15hrs o/n + 24 hours + 20 µM U0126 in DMSO (1.5 µl)

LT27-011: 15hrs o/n + 24 hours + 5 µM GDC-0941 in DMSO (1.5 µl)

LT27-012: 15hrs o/n + 24 hours + 10 µM GDC-0941 in DMSO (1.5 µl)

LT27-013: 15hrs o/n + 24 hours + 20 µM GDC-0941 in DMSO (1.5 µl)

Patient Sample Sheet

LT27-014: 15hrs o/n + 24 hours + 5 μ M U0126 in DMSO (1.5 μ l) + 5 μ M GDC-0941 in DMSO (1.5 μ l)

LT27-015: 15hrs o/n + 24 hours + 10 μ M U0126 in DMSO (1.5 μ l) + 10 μ M GDC-0941 in DMSO (1.5 μ l)

LT27-016: 15hrs o/n + 24 hours + 20 μ M U0126 in DMSO (1.5 μ l) + 20 μ M GDC-0941 in DMSO (1.5 μ l)

LT27-017: 15hrs o/n + 24 hours + 5 μ M U0126 in DMSO (1.5 μ l) + 5 μ M GDC-0941 in DMSO (1.5 μ l) + 50 μ M cisplatin in DMF (1.5 μ l)

LT27-018: 15hrs o/n + 24 hours + 10 μ M U0126 in DMSO (1.5 μ l) + 10 μ M GDC-0941 in DMSO (1.5 μ l) + 50 μ M cisplatin in DMF (1.5 μ l)

LT27-019: 15hrs o/n + 24 hours TRAIL 1 μ g/ml (1.5 μ l)

LT27-020: 15hrs o/n + 24 hours TRAIL 1 μ g/ml (1.5 μ l) + 50 μ M cisplatin in DMF (1.5 μ l)

LT27-021: 15hrs o/n + 24 hours TRAIL 2 μ g/ml (2 μ l)

LT27-022: 15hrs o/n + 24 hours 10 μ M ABT (1.5 μ l)

LT27-023: 15hrs o/n + 24 hours 2 μ M ABT (0.3 μ l)

LT27-024: 15hrs o/n + 24 hours 10 μ M ABT (1.5 μ l) + TRAIL 1 μ g/ml (1.5 μ l)

LT27-025: 15hrs o/n + 24 hours 2 μ M ABT (0.3 μ l) + TRAIL 1 μ g/ml (1.5 μ l)

LT27-026: 15hrs o/n + 24 hours 2 μ M TRAM-34 (0.3 μ l)

LT27-027: 15hrs o/n + 24 hours 10 μ M TRAM-34 (1.5 μ l)

LT27-028: 15hrs o/n + 24 hours 10 μ M TRAM-34 (3 μ l)

9.3 Summary table of all cases

Code	Date Taken	Age	Sex	Smoking History	Histopathology	Staging TNM	Mutations tested with qPCR probes	Positive mutations	Tumour Dimensions	Explants made/ Usable	P53 status**
LT1	11/03/2010	62	M	smoker	Adenosquamous carcinoma RUL	pT1, pN0, pMx, R0	PIK3CA, BRAF, KRAS, EGFR *	PIK3CA G1633A	26 x25 x 25 mm	NO	\
LT2	17/03/2010	73	F	ex-smoker	Squamous carcinoma	pT2, pN0, pMx, R0	PIK3CA, BRAF, KRAS, EGFR *	PIK3CA G1633A	35 x 21 x 38mm	YES/YES	\
LT3	22/03/2010	43	M	smoker	Combined small cell/ large cell neuroendocrine carcinoma	pT2, pN0, pMx, R0	PIK3CA, BRAF, KRAS, EGFR *		30x 15 x 10 mm	NO	\
LT4	24/03/2010	66	F	ex-smoker	Mixed acinar and micropapillary adenocarcinoma of RUL	pT4, pN1(mi), pM1, Rx	PIK3CA, BRAF, KRAS, EGFR *	KRAS 35G>T,C or A	40 x 58 x 48 mm	NO	\
LT5	24/03/2010	60	M	smoker	Squamous cell carcinoma	pT2, pN0, pMx, R0	PIK3CA, BRAF, KRAS, EGFR *		50 x 40 x 30 mm	NO	\
LT6	11/04/2010	81	M	ex-smoker	Squamous cell carcinoma	Debatable. At least pT2a, possibly pT3, pN2, R2	PIK3CA, BRAF, KRAS, EGFR *		19 x 16 x 26 mm	NO	\

LT7	07/05/2010	83	F	non-smoker	Squamous cell carcinoma	pT2a, pN0, pMx, R0	PIK3CA, BRAF, KRAS, EGFR *		35 mm maximum diameter	YES/NO	\
LT8	12/05/2010	52	M	ex-smoker 60 pack-years	Squamous cell carcinoma	pT3, pN1, pMx, R0	PIK3CA, BRAF, KRAS, EGFR *		55 mm maximum diameter		\
LT9	16/09/2010	65	F	ex-smoker	Adenocarcinoma		PIK3CA, BRAF, KRAS, EGFR *	KRAS 34G>T	8 mm maximum diameter	NO	\
LT10	27/09/2010	69	M	ex-smoker	Adenocarcinoma	pT3, pN0, pMx, R1	PIK3CA, BRAF, KRAS, EGFR *		45 x 35 x 20 mm	NO	\
LT11	07/10/2010	60	M	unknown	Metastatic colorectal carcinoma		PIK3CA, BRAF, KRAS, EGFR *		four fragments 4 mm max	NO	\
LT12	08/11/2010	74	M	unknown	Squamous cell carcinoma	pT2a, pN0, pMx, R0	PIK3CA, BRAF, KRAS, EGFR *		approx 40 mm	NO	\
LT13	15/11/2010	69	M	smoker	Adenocarcinoma	pT3, pN0, pMx, R1	PIK3CA, BRAF, KRAS, EGFR *		55 mm maximum diameter	NO	\
LT14	10/01/2011	65	F	unknown	Squamous cell carcinoma	pT1a, pN0, R0	PIK3CA, BRAF, KRAS, EGFR *		9 mm maximally	YES/YES	Mutant

LT15	31/01/2011	54	M	ex-smoker	Atypical carcinoid tumour	pT3, pN2,R2	PIK3CA, BRAF, KRAS, EGFR *		76 x 30 x 25 mm	YES/YES	WT
LT16	11/04/2011	69	F	ex-smoker	Acinar type adenocarcinoma	pT3, pN1, R0	PIK3CA, BRAF, KRAS, EGFR *	PIK3CA G1633A	86 x80 x55 mm	YES/YES	WT
LT17	24/05/2011	67	M	smoker	Squamous cell carcinoma	pT2b, pN0, pMX, R0	PIK3CA, BRAF, KRAS, EGFR *		50 x 70 x 60 mm	YES/NO	\
LT18	25/05/2011	84	M	ex-smoker	Squamous cell carcinoma	pT1b, pN0, R0	PIK3CA, BRAF, KRAS, EGFR *		29 x 25 x 25 mm	YES/YES	Mutant
LT19	31/05/2011	72	M	ex-smoker	Mixed acinar/papillary adenocarcinoma.	pT2a pN0 pMX RO	PIK3CA, BRAF, KRAS, EGFR *		40 x 35 x35 mm	YES/NO	\
LT20	20/06/2011	77	F	unknown	Separate parietal pleura and bronchial margin. One poorly differentiated adenocarcinoma. Second primary adenocarcinoma	First pT3 pN0 pMx Second PT1a, pN0, pMx R2	PIK3CA, BRAF, KRAS, EGFR *		70 x 75 x 55 mm	YES/YES	WT
LT21	27/06/2011	82	M	ex-smoker	Combined small cell carcinoma/ acinar predominant adenocarcinoma (extensive necrosis)	pT2b, pN1, pM1a	PIK3CA, BRAF, KRAS, EGFR *	PIK3CA G1633A	50 x 55 mm	YES/NO	\

LT22	29/06/2011	65	M	ex-smoker	Invasive lepidic predominant mucinous adenocarcinoma	pT2a, pN0, R0	PIK3CA, BRAF, KRAS, EGFR *		33 x 25 x 50 mm	YES/YES	WT
LT23	04/07/2011	81	M	ex-smoker	Squamous cell carcinoma with zones of necrosis	pT3,pN1,R0	PIK3CA, BRAF, KRAS, EGFR *	PIK3CA A3140G	90 x 70 x 50 mm	YES/YES	Mutant
LT24	25/07/2011	73	M	smoker	Centrally necrotic squamous cell carcinoma	pT2b,pN2, pMx, R0	PIK3CA, BRAF, KRAS, EGFR *		54 x 55 x 51 mm	YES/NO	\
LT25	25/07/2011	74	M	unknown	Squamous cell carcinoma	pT2b,pN0,pMX,R0	PIK3CA, BRAF, KRAS, EGFR *		40 x 38 x 65 mm	NO	\
LT26	27/07/2011	59	F	smoker	Adenocarcinoma	pT2b,pN0,pMX,R0	PIK3CA, BRAF, KRAS, EGFR *		50 x 58 x 50 mm	YES/NO	\
LT27	27/07/2011	60	M	never smoked	Adenocarcinoma	pT3, pN2, pMX,R0	PIK3CA, BRAF, KRAS, EGFR *		125 x 95 x 65 mm	YES/YES	Mutant
LT28	06/09/2011	83	F	ex-smoker	Squamous cell carcinoma	pT2b, pN1, pMX,R0	PIK3CA, BRAF, KRAS, EGFR *		52 x 45 x 35 mm	NO	\
LT29	14/09/2011	59	M	ex-smoker	Adenocarcinoma (partially necrotic)		PIK3CA, BRAF, KRAS, EGFR *		40 mm max	YES/NO	\
LT30	21/09/2011	79	M	ex-smoker	Adenocarcinoma predominant acinar pattern	pT2a,pN2,pMX,R0	PIK3CA, BRAF, KRAS, EGFR *		42 x 40 x 33 mm	YES/NO	\

LT31	28/09/2011	74	F		Squamous cell carcinoma	pT2a,N0,MX,R0	PIK3CA, BRAF, KRAS, EGFR *		40 x 45 x 40 mm	YES/YES	Mutant
LT32	05/10/2011	55	M	smoker	Solid type adenocarcinoma with areas of necrosis	pT2a,pN0,pMX,R0	PIK3CA, BRAF, KRAS, EGFR *		30 x 25 x 35 mm	YES/YES	WT
LT33	18/10/2011	79	F	ex-smoker	Pleomorphic carcinoma (with adenocarcinomatous components)	pT3, pN0, pMx, R0	PIK3CA, BRAF, KRAS, EGFR *		72 x 40 x 65 mm	YES/YES	WT
LT34	22/11/2011	65	F	ex-smoker	Lepidic type non mucinous adenocarcinoma	pT3,pN0,pMX, R0	PIK3CA, BRAF, KRAS, EGFR *		60 x 26 x 50 mm	YES/YES	Mutant
LT35	05/12/2011	77	M	smoker	Squamous cell carcinoma -shows extensive necrosis	pT2a,pN1,R0	PIK3CA, BRAF, KRAS, EGFR *	PIK3CA G1633A	approx 40 mm max	YES/NO	\
LT36	07/12/2011	61	M	unknown	Pleomorphic carcinoma /lepidic predominant adenocarcinoma	pT2,pN0,pMX,R0	PIK3CA, BRAF, KRAS, EGFR *	PIK3CA A3140G	31 x 30 x 25 mm	YES/YES	Mutant
LT37	11/01/2012	64	F	ex-smoker	Adenocarcinoma with predominant papillary architecture	pT2a, pN0,pMX,R0	PIK3CA, BRAF, KRAS, EGFR *		42 x 40 x 40 mm	YES/NO	\
LT38	01/02/2012	76	M	ex-smoker	Squamous cell carcinoma	pT2b,pN0,pMX,R0	PIK3CA, BRAF, KRAS, EGFR *	PIK3CA A3140G	65 x 20 x 25 mm	YES/YES	WT

LT39	06/02/2012	65	F	unknown	Large cell carcinoma NOS	ypT4,ypN1	PIK3CA, BRAF, KRAS, EGFR *		90 x 65 x 45 mm	NO	\
LT40	20/02/2012	62	M	ex-smoker	Large cell neuroendocrine carcinoma	pT2a,pN0,pMX,R0	PIK3CA, BRAF, KRAS, EGFR *		40 x 40 x 30 mm	NO	\
LT41	08/03/2012	50	F	smoker	Mucinous adenocarcinoma	pT3,pN2,pMX,R0	PIK3CA, BRAF, KRAS, EGFR *	EGFR L858R	120 x 90 x 80	NO	\
LT42	02/04/2012	73	F	ex-smoker	Squamous cell carcinoma	pT2a,pN1,pMX,R0	PIK3CA, BRAF, KRAS, EGFR *		27 x 32 x 30 mm	NO	\
LT43	25/04/2012	76	M	unknown	Squamous cell carcinoma	pT2b,pN1,pMX,R0	PIK3CA, BRAF, KRAS, EGFR *		45 x 55 x 35 mm	NO	\
LT44	14/05/2012	76	M	unknown	Non mucinous adenocarcinoma	pT2a,pN2,pMX,R0	PIK3CA, BRAF, KRAS, EGFR *		28 x 20 x 35 mm	NO	\
LT45	13/06/2012	57	F	smoker	Pleiomorphic carcinoma (adeno +spindle cell/sarcomatoid morphology)	pT2a,pN2,pMX,R0	PIK3CA, BRAF, KRAS, EGFR *		50 x 45 x 40 mm	NO	\
LT48	26/06/2012	78	F	never smoked	Adenocarcinoma	pT2b, pN0,pMX, R0	PIK3CA, BRAF, KRAS, EGFR *		55 x 40 x 30 mm	NO	\

LT49	26/06/2012	76	M	ex-smoker	Adenocarcinoma	pT2a, pN0,pMX, R0	PIK3CA, BRAF, KRAS, EGFR *	EGFR L858R	50 x 35 x 20 mm	NO	\
LT50	02/07/2012	77	F	smoker	Adenosquamous carcinoma	pT2a, pNx,pMX, R0	PIK3CA, BRAF, KRAS, EGFR *		45 x 33 x 30 mm	NO	\
LT51	04/07/2012	70	F	smoker	Adenocarcinoma	pT2b, pN1,pMX, Rx	PIK3CA, BRAF, KRAS, EGFR *	KRAS 34G>T, C or A	42 x 50 x 60 mm	NO	\
LT52	04/07/2012	74	M	ex-smoker	Squamous cell carcinoma	pT2a,pN1,pM1a,R0	PIK3CA, BRAF, KRAS, EGFR *		45 x 40 x 25 mm	NO	\
LT83	17/09/2013	70	M	ex-smoker	Acinar mucinous adenocarcinoma	pT2(pL1)b,pN1,pMX	PIK3CA, BRAF, KRAS, EGFR *	KRAS 34G>T, C or A	60 x 34 x 58 mm	YES/YES	WT
LT84	18/09/2013	75	F	smoker	Squamous cell carcinoma	R0	PIK3CA, BRAF, KRAS, EGFR *		45 x 30 x 48 mm	YES/YES	Mutant
LT86	23/09/2013	71	M	unknown	Acinar adenocarcinoma	pT2a,pN0,pMX,R0			35 x 34 x 24 mm	YES/NO	\
LT87	25/09/2013	71	F	smoker	NSCLC, favouring adenocarcinoma	pT3,pN0,R0			105 x84 x 43 mm	YES/NO	\
LT88	21/10/2013	68	F	unknown	Squamous cell carcinoma	at least pT1b,pN0,R0	PIK3CA, BRAF, KRAS *		23 x 18 x 24 mm	YES/YES	Mutant
LT89	30/10/2013	85	F	unknown	Atypical carcinoid tumour	pT2a,pN0,pMX,R0	PIK3CA, BRAF, KRAS *		25mm x 20x 15mm	YES/YES	WT

LT90	30/10/2013	75	F	unknown	Adenocarcinoma, mixed growth pattern	pT2(PL1),pN2b,pMX,R0			40 x 35 x 62 mm	YES/NO	\
LT91	06/11/2013	78	M	unknown	Squamous cell carcinoma	pT1b,pN0,pMX,pL0,R0	PIK3CA, BRAF, KRAS *		26 x 19 x 28 mm	YES/No	Mutant
LT92	11/11/2013	62	F	unknown	Squamous cell carcinoma	pT2b,pN1,pL1,R1	PIK3CA, BRAF, KRAS *	PIK3CA G1633A	67 mm max	YES/YES	Deleted
LT93	20/11/2013	78	M	unknown	Combined small cell carcinoma(predominantly squamous cell carcinoma with small area of small cell carcinoma)	pT2a,pN1,pMX,,R0	PIK3CA, BRAF, KRAS *		40 x 23 x 27 mm	YES/YES	\

REFERENCES

- Adjei, A.A., Cohen, R.B., Franklin, W., Morris, C., Wilson, D., Molina, J.R., Hanson, L.J., Gore, L., Chow, L., Leong, S., Maloney, L., Gordon, G., Simmons, H., Marlow, A., Litwiler, K., Brown, S., Poch, G., Kane, K., Haney, J., Eckhardt, S.G., 2008. Phase I pharmacokinetic and pharmacodynamic study of the oral, small-molecule mitogen-activated protein kinase kinase 1/2 inhibitor AZD6244 (ARRY-142886) in patients with advanced cancers. *Journal of Clinical Oncology: Official Journal of the American Society of Clinical Oncology*. 26, 2139-2146.
- Afonina, I., Zivarts, M., Kutyavin, I., Lukhtanov, E., Gamper, H., Meyer, R.B., 1997. Efficient priming of PCR with short oligonucleotides conjugated to a minor groove binder. *Nucleic Acids Research*. 25, 2657-2660.
- Alberg, A.J., Brock, M.V., Ford, J.G., Samet, J.M., Spivack, S.D., 2013. Epidemiology of lung cancer: Diagnosis and management of lung cancer, 3rd ed: American College of Chest Physicians evidence-based clinical practice guidelines. *Chest*. 143, e1S-29S.
- Almasan, A. & Ashkenazi, A., 2003. Apo2L/TRAIL: apoptosis signaling, biology, and potential for cancer therapy. *Cytokine & Growth Factor Reviews*. 14, 337-348.
- Amann, A., Zwierzina, M., Gameraith, G., Bitsche, M., Huber, J.M., Vogel, G.F., Blumer, M., Koeck, S., Pechriggl, E.J., Kelm, J.M., Hilbe, W., Zwierzina, H., 2014. Development of an innovative 3D cell culture system to study tumour--stroma interactions in non-small cell lung cancer cells. *PloS One*. 9, e92511.
- Ardizzoni, A., Boni, L., Tiseo, M., Fossella, F.V., Schiller, J.H., Paesmans, M., Radosavljevic, D., Paccagnella, A., Zatloukal, P., Mazzanti, P., Bisset, D., Rosell, R., CISCA (CISplatin versus CARboplatin) Meta-analysis Group, 2007. Cisplatin- versus carboplatin-based chemotherapy in first-line treatment of advanced non-small-cell lung cancer: an individual patient data meta-analysis. *Journal of the National Cancer Institute*. 99, 847-857.
- Ariyoshi, Y., Shimahara, M., Tanigawa, N., 2003. Study on chemosensitivity of oral squamous cell carcinomas by histoculture drug response assay. *Oral Oncology*. 39, 701-707.
- Ashkenazi, A., 2002. Targeting death and decoy receptors of the tumour-necrosis factor superfamily. *Nature Reviews Cancer*. 2, 420-430.
- Ashkenazi, A., Pai, R.C., Fong, S., Leung, S., Lawrence, D.A., Marsters, S.A., Blackie, C., Chang, L., McMurtrey, A.E., Hebert, A., DeForge, L., Koumenis, I.L., Lewis, D., Harris, L., Bussiere, J., Koeppen, H., Shahrokh, Z., Schwall, R.H., 1999. Safety and antitumor activity of recombinant soluble Apo2 ligand. *The Journal of Clinical Investigation*. 104, 155-162.
- Astashkina, A., Mann, B., Grainger, D.W., 2012. A critical evaluation of in vitro cell culture models for high-throughput drug screening and toxicity. *Pharmacology & Therapeutics*. 134, 82-106.
- Azijli, K., van Roosmalen, I.a.M., Smit, J., Pillai, S., Fukushima, M., de Jong, S., Peters, G.J., Bijnsdorp, I.V., Kruijff, F.a.E., 2014. The novel thymidylate synthase inhibitor

trifluorothymidine (TFT) and TRAIL synergistically eradicate non-small cell lung cancer cells. *Cancer Chemotherapy and Pharmacology*.

Baader, E., Toloczko, A., Fuchs, U., Schmid, I., Beltinger, C., Ehrhardt, H., Debatin, K.M., Jeremias, I., 2005. Tumor necrosis factor-related apoptosis-inducing ligand-mediated proliferation of tumor cells with receptor-proximal apoptosis defects. *Cancer Research*. 65, 7888-7895.

Bagci-Onder, T., Wakimoto, H., Anderegg, M., Cameron, C., Shah, K., 2011. A dual PI3K/mTOR inhibitor, PI-103, cooperates with stem cell-delivered TRAIL in experimental glioma models. *Cancer Research*. 71, 154-163.

Balsara, B.R., Pei, J., Mitsuuchi, Y., Page, R., Klein-Szanto, A., Wang, H., Unger, M., Testa, J.R., 2004. Frequent activation of AKT in non-small cell lung carcinomas and preneoplastic bronchial lesions. *Carcinogenesis*. 25, 2053-2059.

Barbie, D.A., Tamayo, P., Boehm, J.S., Kim, S.Y., Moody, S.E., Dunn, I.F., Schinzel, A.C., Sandy, P., Meylan, E., Scholl, C., Frohling, S., Chan, E.M., Sos, M.L., Michel, K., Mermel, C., Silver, S.J., Weir, B.A., Reiling, J.H., Sheng, Q., Gupta, P.B., Wadlow, R.C., Le, H., Hoersch, S., Wittner, B.S., Ramaswamy, S., Livingston, D.M., Sabatini, D.M., Meyerson, M., Thomas, R.K., Lander, E.S., Mesirov, J.P., Root, D.E., Gilliland, D.G., Jacks, T., Hahn, W.C., 2009. Systematic RNA interference reveals that oncogenic KRAS-driven cancers require TBK1. *Nature*. 462, 108-112.

Beck, J.T., Ismail, A., Tolomeo, C., 2014. Targeting the phosphatidylinositol 3-kinase (PI3K)/AKT/mammalian target of rapamycin (mTOR) pathway: An emerging treatment strategy for squamous cell lung carcinoma. *Cancer Treatment Reviews*.

Bendell, J.C., Rodon, J., Burris, H.A., de Jonge, M., Verweij, J., Birlle, D., Demanse, D., De Buck, S.S., Ru, Q.C., Peters, M., Goldbrunner, M., Baselga, J., 2012. Phase I, dose-escalation study of BKM120, an oral pan-Class I PI3K inhibitor, in patients with advanced solid tumors. *Journal of Clinical Oncology: Official Journal of the American Society of Clinical Oncology*. 30, 282-290.

Besse B, Soria J, Gomez-Roca C, et al. A phase Ib study to evaluate the PI3-kinase inhibitor GDC-0941 with paclitaxel (P) and carboplatin (C), with and without bevacizumab (BEV), in patients with advanced non-small cell lung cancer (NSCLC). *ASCO Meet Abstr* 2011;29:3044.

Bignell, G.R., Greenman, C.D., Davies, H., Butler, A.P., Edkins, S., Andrews, J.M., Buck, G., Chen, L., Beare, D., Latimer, C., Widaa, S., Hinton, J., Fahey, C., Fu, B., Swamy, S., Dalgliesh, G.L., Teh, B.T., Deloukas, P., Yang, F., Campbell, P.J., Futreal, P.A., Stratton, M.R., 2010. Signatures of mutation and selection in the cancer genome. *Nature*. 463, 893-898.

Black, a. & Morris, D., 2012. Personalized medicine in metastatic non-small-cell lung cancer: promising targets and current clinical trials. *Current Oncology (Toronto, Ont.)*. 19, S73-85.

Bland, J.M. & Altman, D.G., 1986. Statistical methods for assessing agreement between two methods of clinical measurement. *Lancet Oncology*. 1, 307-310.

Brandao, G.D.a., Brega, E.F., Spatz, a., 2012. The role of molecular pathology in non-small-cell lung carcinoma-now and in the future. *Current Oncology (Toronto, Ont.)*. 19, S24-32.

Bronte, G., Rizzo, S., La Paglia, L., Adamo, V., Siragusa, S., Ficorella, C., Santini, D., Bazan, V., Colucci, G., Gebbia, N., Russo, A., 2010. Driver mutations and differential sensitivity to targeted therapies: a new approach to the treatment of lung adenocarcinoma. *Cancer Treatment Reviews*. 36 Suppl 3, S21-9.

Buettner, R., Wolf, J., Thomas, R.K., 2013. Lessons learned from lung cancer genomics: the emerging concept of individualized diagnostics and treatment. *Journal of Clinical Oncology: Official Journal of the American Society of Clinical Oncology*. 31, 1858-1865.

Cancer Genome Atlas Research Network, Hammerman, P.S., Hayes, D.N., Wilkerson, M.D., Schultz, N., Bose, R., Chu, A., Collisson, E.A., Cope, L., Creighton, C.J., Getz, G., Herman, J.G., Johnson, B.E., Kucherlapati, R., Ladanyi, M., Maher, C.A., Robertson, G., Sander, C., Shen, R., Sinha, R., Sivachenko, A., Thomas, R.K., Travis, W.D., Tsao, M.S., Weinstein, J.N., Wigle, D.A., Baylin, S.B., Govindan, R., Meyerson, M., 2012. Comprehensive genomic characterization of squamous cell lung cancers. *Nature*. 489, 519-525.

Casaluce, F., Sgambato, A., Maione, P., Rossi, A., Ferrara, C., Napolitano, A., Palazzolo, G., Ciardiello, F., Gridelli, C., 2013. ALK inhibitors: a new targeted therapy in the treatment of advanced NSCLC. *Targeted Oncology*. 8, 55-67.

Chen, W., Wang, X., Zhuang, J., Zhang, L., Lin, Y., 2007. Induction of death receptor 5 and suppression of survivin contribute to sensitization of TRAIL-induced cytotoxicity by quercetin in non-small cell lung cancer cells. *Carcinogenesis*. 28, 2114-2121.

Chen, Z., Cheng, K., Walton, Z., Wang, Y., Ebi, H., Shimamura, T., Liu, Y., Tupper, T., Ouyang, J., Li, J., Gao, P., Woo, M.S., Xu, C., Yanagita, M., Altabef, A., Wang, S., Lee, C., Nakada, Y., Pena, C.G., Sun, Y., Franchetti, Y., Yao, C., Saur, A., Cameron, M.D., Nishino, M., Hayes, D.N., Wilkerson, M.D., Roberts, P.J., Lee, C.B., Bardeesy, N., Butaney, M., Chirieac, L.R., Costa, D.B., Jackman, D., Sharpless, N.E., Castrillon, D.H., Demetri, G.D., Janne, P.A., Pandolfi, P.P., Cantley, L.C., Kung, A.L., Engelman, J.A., Wong, K.K., 2012. A murine lung cancer co-clinical trial identifies genetic modifiers of therapeutic response. *Nature*. 483, 613-617.

Chinnaiyan, A.M., O'Rourke, K., Tewari, M., Dixit, V.M., 1995. FADD, a novel death domain-containing protein, interacts with the death domain of fas and initiates apoptosis. *Cell*. 81, 505-512.

Clavreul, A., Jean, I., Preisser, L., Chassevent, A., Sapin, A., Michalak, S., Menei, P., 2009. Human glioma cell culture: two FCS-free media could be recommended for clinical use in immunotherapy. *In Vitro Cellular & Developmental Biology. Animal*. 45, 500-511.

Cleary, J.M., Lima, C.M., Hurwitz, H.I., Montero, A.J., Franklin, C., Yang, J., Graham, A., Busman, T., Mabry, M., Holen, K., Shapiro, G.I., Uronis, H., 2014. A phase I clinical trial of navitoclax, a targeted high-affinity Bcl-2 family inhibitor, in combination with gemcitabine in patients with solid tumors. *Investigational New Drugs*.

Cohen, G.M., 1997. Caspases: the executioners of apoptosis. *The Biochemical Journal*. 326 (Pt 1), 1-16.

Cote, R.J., Esrig, D., Groshen, S., Jones, P.A., Skinner, D.G., 1997. P53 and Treatment of Bladder Cancer. *Nature*. 385, 123-125.

Cristofanon, S. & Fulda, S., 2012. ABT-737 promotes tBid mitochondrial accumulation to enhance TRAIL-induced apoptosis in glioblastoma cells. *Cell Death & Disease*. 3, e432.

Daniel, V.C., Marchionni, L., Hierman, J.S., Rhodes, J.T., Devereux, W.L., Rudin, C.M., Yung, R., Parmigiani, G., Dorsch, M., Peacock, C.D., Watkins, D.N., 2009. A primary xenograft model of small-cell lung cancer reveals irreversible changes in gene expression imposed by culture in vitro. *Cancer Research*. 69, 3364-3373.

Darlison, L., 2005. NICE guidelines for the diagnosis and treatment of lung cancer. *Nursing Times*. 101, 47-48.

Davies, H., Bignell, G.R., Cox, C., Stephens, P., Edkins, S., Clegg, S., Teague, J., Woffendin, H., Garnett, M.J., Bottomley, W., Davis, N., Dicks, E., Ewing, R., Floyd, Y., Gray, K., Hall, S., Hawes, R., Hughes, J., Kosmidou, V., Menzies, A., Mould, C., Parker, A., Stevens, C., Watt, S., Hooper, S., Wilson, R., Jayatilake, H., Gusterson, B.A., Cooper, C., Shipley, J., Hargrave, D., Pritchard-Jones, K., Maitland, N., Chenevix-Trench, G., Riggins, G.J., Bigner, D.D., Palmieri, G., Cossu, A., Flanagan, A., Nicholson, A., Ho, J.W., Leung, S.Y., Yuen, S.T., Weber, B.L., Seigler, H.F., Darrow, T.L., Paterson, H., Marais, R., Marshall, C.J., Wooster, R., Stratton, M.R., Futreal, P.A., 2002. Mutations of the BRAF gene in human cancer. *Nature*. 417, 949-954.

Dela Cruz, C.S., Tanoue, L.T., Matthay, R.A., 2011. Lung cancer: epidemiology, etiology, and prevention. *Clinics in Chest Medicine*. 32, 605-644.

Detterbeck, F.C., Boffa, D.J., Tanoue, L.T., 2009. The new lung cancer staging system. *Chest*. 136, 260-271.

Detterbeck, F.C., Postmus, P.E., Tanoue, L.T., 2013. The stage classification of lung cancer: Diagnosis and management of lung cancer, 3rd ed: American College of Chest Physicians evidence-based clinical practice guidelines. *Chest*. 143, e191S-210S.

Ding, L., Getz, G., Wheeler, D.A., Mardis, E.R., McLellan, M.D., Cibulskis, K., Sougnez, C., Greulich, H., Muzny, D.M., Morgan, M.B., Fulton, L., Fulton, R.S., Zhang, Q., Wendl, M.C., Lawrence, M.S., Larson, D.E., Chen, K., Dooling, D.J., Sabo, A., Hawes, A.C., Shen, H., Jhangiani, S.N., Lewis, L.R., Hall, O., Zhu, Y., Mathew, T., Ren, Y., Yao, J., Scherer, S.E., Clerc, K., Metcalf, G.A., Ng, B., Milosavljevic, A., Gonzalez-Garay, M.L., Osborne, J.R., Meyer, R., Shi, X., Tang, Y., Koboldt, D.C., Lin, L., Abbott, R., Miner, T.L., Pohl, C., Fewell, G., Haipek, C., Schmidt, H., Dunford-Shore, B.H., Kraja, A., Crosby, S.D., Sawyer, C.S., Vickery, T., Sander, S., Robinson, J., Winckler, W., Baldwin, J., Chirieac, L.R., Dutt, A., Fennell, T., Hanna, M., Johnson, B.E., Onofrio, R.C., Thomas, R.K., Tonon, G., Weir, B.A., Zhao, X., Ziaugra, L., Zody, M.C., Giordano, T., Orringer, M.B., Roth, J.A., Spitz, M.R., Wistuba, I.I., Ozenberger, B., Good, P.J., Chang, A.C., Beer, D.G., Watson, M.A., Ladanyi, M., Broderick, S., Yoshizawa, A., Travis, W.D., Pao, W., Province, M.A., Weinstock, G.M., Varmus, H.E., Gabriel, S.B., Lander, E.S., Gibbs, R.A., Meyerson, M., Wilson, R.K., 2008. Somatic mutations affect key pathways in lung adenocarcinoma. *Nature*. 455, 1069-1075.

Dingemans, A.C., Mellema, W.W., Groen, H.J.M., van Wijk, A., Burgers, S.A., Kunst, P.W.A., Thunnissen, E., Heideman, D.A.M., Smit, E.F., 2013. A Phase II Study of Sorafenib in Patients with Platinum-Pretreated, Advanced (Stage IIIb or IV) Non-Small Cell Lung Cancer with a KRAS Mutation. *Clinical Cancer Research*. 19, 743-751.

- Do, H., Salemi, R., Murone, C., Mitchell, P.L., Dobrovic, A., 2010. Rarity of AKT1 and AKT3 E17K mutations in squamous cell carcinoma of lung. *Cell Cycle*. 9, 4411-4412.
- Doll, R. & Hill, A.B., 1950. Smoking and carcinoma of the lung; preliminary report. *British Medical Journal*. 2, 739-748.
- Downward, J., 2008. Targeting RAS and PI3K in lung cancer. *Nature Medicine*. 14, 1315-1316.
- Drilon, A., Rekhtman, N., Ladanyi, M., Paik, P., 2012. Squamous-cell carcinomas of the lung: emerging biology, controversies, and the promise of targeted therapy. *The Lancet Oncology*. 13, e418-26.
- Dudley, D.T., Pang, L., Decker, S.J., Bridges, A.J., Saltiel, A.R., 1995. A synthetic inhibitor of the mitogen-activated protein kinase cascade. *Proceedings of the National Academy of Sciences of the United States of America*. 92, 7686-7689.
- Eastman, A., 1987. The formation, isolation and characterization of DNA adducts produced by anticancer platinum complexes. *Pharmacology & Therapeutics*. 34, 155-166.
- Ehrhardt, H., Fulda, S., Schmid, I., Hiscott, J., Debatin, K.M., Jeremias, I., 2003. TRAIL induced survival and proliferation in cancer cells resistant towards TRAIL-induced apoptosis mediated by NF-kappaB. *Oncogene*. 22, 3842-3852.
- Emmet, M., 2011. The TRAIL and Lung cancer. *Journal of Thoracic Oncology*. 6, 983-987.
- Endo, K., Konishi, A., Sasaki, H., Takada, M., Tanaka, H., Okumura, M., Kawahara, M., Sugiura, H., Kuwabara, Y., Fukai, I., Matsumura, A., Yano, M., Kobayashi, Y., Mizuno, K., Haneda, H., Suzuki, E., Iuchi, K., Fujii, Y., 2005. Epidermal growth factor receptor gene mutation in non-small cell lung cancer using highly sensitive and fast TaqMan PCR assay. *Lung Cancer (Amsterdam, Netherlands)*. 50, 375-384.
- Engelman, J.A., Chen, L., Tan, X., Crosby, K., Guimaraes, A.R., Upadhyay, R., Maira, M., McNamara, K., Perera, S.A., Song, Y., Chirieac, L.R., Kaur, R., Lightbown, A., Simendinger, J., Li, T., Padera, R.F., Garcia-Echeverria, C., Weissleder, R., Mahmood, U., Cantley, L.C., Wong, K.K., 2008. Effective use of PI3K and MEK inhibitors to treat mutant Kras G12D and PIK3CA H1047R murine lung cancers. *Nature Medicine*. 14, 1351-1356.
- Engelman, J.A. & Janne, P.A., 2008. Mechanisms of acquired resistance to epidermal growth factor receptor tyrosine kinase inhibitors in non-small cell lung cancer. *Clinical Cancer Research: An Official Journal of the American Association for Cancer Research*. 14, 2895-2899.
- Erdlenbruch, B., Nier, M., Kern, W., Hiddemann, W., Pekrun, A., Lakomek, M., 2001. Pharmacokinetics of cisplatin and relation to nephrotoxicity in paediatric patients. *European Journal of Clinical Pharmacology*. 57, 393-402.
- Favata, M.F., Horiuchi, K.Y., Manos, E.J., Daulerio, A.J., Stradley, D.A., Feeser, W.S., Van Dyk, D.E., Pitts, W.J., Earl, R.A., Hobbs, F., Copeland, R.A., Magolda, R.L., Scherle, P.A., Trzaskos, J.M., 1998. Identification of a novel inhibitor of mitogen-activated protein kinase kinase. *The Journal of Biological Chemistry*. 273, 18623-18632.

- Fennema, E., Rivron, N., Rouwkema, J., van Blitterswijk, C., de Boer, J., 2013. Spheroid culture as a tool for creating 3D complex tissues. *Trends in Biotechnology*. 31, 108-115.
- Florea, A.M. & Busselberg, D., 2011. Cisplatin as an anti-tumor drug: cellular mechanisms of activity, drug resistance and induced side effects. *Cancers*. 3, 1351-1371.
- Folkes, A.J., Ahmadi, K., Alderton, W.K., Alix, S., Baker, S.J., Box, G., Chuckowree, I.S., Clarke, P.A., Depledge, P., Eccles, S.A., Friedman, L.S., Hayes, A., Hancox, T.C., Kugendradas, A., Lensun, L., Moore, P., Olivero, A.G., Pang, J., Patel, S., Pergl-Wilson, G.H., Raynaud, F.I., Robson, A., Saghir, N., Salphati, L., Sohal, S., Ultsch, M.H., Valenti, M., Wallweber, H.J., Wan, N.C., Wiesmann, C., Workman, P., Zhyvoloup, A., Zvelebil, M.J., Shuttleworth, S.J., 2008. The identification of 2-(1H-indazol-4-yl)-6-(4-methanesulfonyl-piperazin-1-ylmethyl)-4-morpholin-4-yl-t hieno[3,2-d]pyrimidine (GDC-0941) as a potent, selective, orally bioavailable inhibitor of class I PI3 kinase for the treatment of cancer. *Journal of Medicinal Chemistry*. 51, 5522-5532.
- Forgacs, E., Biesterveld, E.J., Sekido, Y., Fong, K., Muneer, S., Wistuba, I.I., Milchgrub, S., Brezinschek, R., Virmani, A., Gazdar, A.F., Minna, J.D., 1998. Mutation analysis of the PTEN/MMAC1 gene in lung cancer. *Oncogene*. 17, 1557-1565.
- Freeman, a.E. & Hoffman, R.M., 1986. In vivo-like growth of human tumors in vitro. *Proceedings of the National Academy of Sciences of the United States of America*. 83, 2694-2698.
- Friday, B.B. & Adjei, A.A., 2008. Advances in targeting the Ras/Raf/MEK/Erk mitogen-activated protein kinase cascade with MEK inhibitors for cancer therapy. *Clinical Cancer Research: An Official Journal of the American Association for Cancer Research*. 14, 342-346.
- Fujita, Y., Hiramatsu, M., Kawai, M., Nishimura, H., Miyamoto, A., Tanigawa, N., 2009. Histoculture drug response assay predicts the postoperative prognosis of patients with esophageal cancer. *Oncology Reports*. 21, 499-505.
- Furukawa, T., Kubota, T., Hoffman, R.M., 1995. Clinical applications of the histoculture drug response assay. *Clinical Cancer Research*. 1, 305-311.
- Furukawa, T., Kubota, T., Tanino, H., Oura, S., Yuasa, S., Murate, H., Morita, K., Kozakai, K., Yano, T., Hoffman, R.M., 2000. Chemosensitivity of breast cancer lymph node metastasis compared to the primary tumor from individual patients tested in the histoculture drug response assay. *Anticancer Research*. 20, 3657-3658.
- Furukawa, T., Kubota, T., Watanabe, M., Takahara, T., Yamaguchi, H., Takeuchi, T., Kase, S., Kodaira, S., Ishibiki, K., Kitajima, M., 1992. High in vitro-in vivo correlation of drug response using sponge-gel-supported three-dimensional histoculture and the MTT end point. *International Journal of Cancer*. 51, 489-498.
- Gandhi, L., Camidge, D.R., Ribeiro de Oliveira, M., Bonomi, P., Gandara, D., Khaira, D., Hann, C.L., McKeegan, E.M., Litvinovich, E., Hemken, P.M., Dive, C., Enschede, S.H., Nolan, C., Chiu, Y.L., Busman, T., Xiong, H., Krivoshik, A.P., Humerickhouse, R., Shapiro, G.I., Rudin, C.M., 2011. Phase I study of Navitoclax (ABT-263), a novel Bcl-2 family inhibitor, in patients with small-cell lung cancer and other solid tumors. *Journal of*

Clinical Oncology : Official Journal of the American Society of Clinical Oncology. 29, 909-916.

Gautschi, O., Pauli, C., Strobel, K., Hirschmann, A., Printzen, G., Aebi, S., Diebold, J., 2012. A patient with BRAF V600E lung adenocarcinoma responding to vemurafenib. *Journal of Thoracic Oncology: Official Publication of the International Association for the Study of Lung Cancer*. 7, e23-4.

Gazdar, A.F., Gao, B., Minna, J.D., 2010. Lung cancer cell lines: Useless artifacts or invaluable tools for medical science? *Lung Cancer (Amsterdam, Netherlands)*. 68, 309-318.

Gerdes, J., Lemke, H., Baisch, H., Wacker, H.H., Schwab, U., Stein, H., 1984. Cell cycle analysis of a cell proliferation-associated human nuclear antigen defined by the monoclonal antibody Ki-67. *The Journal of Immunology*. 133, 1710-1715.

Gerdes, J., Schwab, U., Lemke, H., Stein, H., 1983. Production of a mouse monoclonal antibody reactive with a human nuclear antigen associated with cell proliferation. *International Journal of Cancer. Journal International Du Cancer*. 31, 13-20.

Gharbi, S.I., Zvelebil, M.J., Shuttleworth, S.J., Hancox, T., Saghir, N., Timms, J.F., Waterfield, M.D., 2007. Exploring the specificity of the PI3K family inhibitor LY294002. *The Biochemical Journal*. 404, 15-21.

Gilmartin, A.G., Bleam, M.R., Groy, A., Moss, K.G., Minthorn, E.A., Kulkarni, S.G., Rominger, C.M., Erskine, S., Fisher, K.E., Yang, J., Zappacosta, F., Annan, R., Sutton, D., Laquerre, S.G., 2011. GSK1120212 (JTP-74057) Is an Inhibitor of MEK Activity and Activation with Favorable Pharmacokinetic Properties for Sustained In Vivo Pathway Inhibition. *Clinical Cancer Research*. 17, 989-1000.

Gottlieb, T.M. & Oren, M., 1998. p53 and apoptosis. *Seminars in Cancer Biology*. 8, 359-368.

Govindan, R., Ding, L., Griffith, M., Subramanian, J., Dees, N.D., Kanchi, K.L., Maher, C.A., Fulton, R., Fulton, L., Wallis, J., Chen, K., Walker, J., McDonald, S., Bose, R., Ornitz, D., Xiong, D., You, M., Dooling, D.J., Watson, M., Mardis, E.R., Wilson, R.K., 2012. Genomic landscape of non-small cell lung cancer in smokers and never-smokers. *Cell*. 150, 1121-1134.

Greco, F.A., Bonomi, P., Crawford, J., Kelly, K., Oh, Y., Halpern, W., Lo, L., Gallant, G., Klein, J., 2008. Phase 2 study of mapatumumab, a fully human agonistic monoclonal antibody which targets and activates the TRAIL receptor-1, in patients with advanced non-small cell lung cancer. *Lung Cancer (Amsterdam, Netherlands)*. 61, 82-90.

Greenblatt, M.S., Bennett, W.P., Hollstein, M., Harris, C.C., 1994. Mutations in the p53 tumor suppressor gene: clues to cancer etiology and molecular pathogenesis. *Cancer Research*. 54, 4855-4878.

Gridelli, C., Peters, S., Sgambato, A., Casaluce, F., Adjei, A.a., Ciardiello, F., 2014. ALK inhibitors in the treatment of advanced NSCLC. *Cancer Treatment Reviews*. 40, 300-306.

Hainsworth, J.D., Cebotaru, C.L., Kanarev, V., Ciuleanu, T.E., Damyranov, D., Stella, P., Ganchev, H., Pover, G., Morris, C., Tzekova, V., 2010. A phase II, open-label, randomized study to assess the efficacy and safety of AZD6244 (ARRY-142886)

versus pemetrexed in patients with non-small cell lung cancer who have failed one or two prior chemotherapeutic regimens. *Journal of Thoracic Oncology: Official Publication of the International Association for the Study of Lung Cancer*. 5, 1630-1636.

Hanahan, D. & Weinberg, R.A., 2000. The hallmarks of cancer. *Cell*. 100, 57-70.

Hanahan, D. & Weinberg, R.A., 2011. Hallmarks of cancer: the next generation. *Cell*. 144, 646-674.

Hann, C.L., Daniel, V.C., Sugar, E.A., Dobromilskaya, I., Murphy, S.C., Cope, L., Lin, X., Hierman, J.S., Wilburn, D.L., Watkins, D.N., Rudin, C.M., 2008. Therapeutic efficacy of ABT-737, a selective inhibitor of BCL-2, in small cell lung cancer. *Cancer Research*. 68, 2321-2328.

Haura, E.B., Ricart, A.D., Larson, T.G., Stella, P.J., Bazhenova, L., Miller, V.A., Cohen, R.B., Eisenberg, P.D., Selaru, P., Wilner, K.D., Gadgeel, S.M., 2010. A phase II study of PD-0325901, an oral MEK inhibitor, in previously treated patients with advanced non-small cell lung cancer. *Clinical Cancer Research : An Official Journal of the American Association for Cancer Research*. 16, 2450-2457.

Hayashi, Y., Kuriyama, H., Umezu, H., Tanaka, J., Yoshimasu, T., Furukawa, T., Tanaka, H., Kagamu, H., Gejyo, F., Yoshizawa, H., 2009. Class III beta-tubulin expression in tumor cells is correlated with resistance to docetaxel in patients with completely resected non-small-cell lung cancer. *Internal Medicine (Tokyo, Japan)*. 48, 203-208.

Hayes, S.a., Hudson, A.L., Clarke, S.J., Molloy, M.P., Howell, V.M., 2014. From mice to men: GEMMs as trial patients for new NSCLC therapies. *Seminars in Cell & Developmental Biology*.

Heavey, S., O'Byrne, K.J., Gately, K., 2014. Strategies for co-targeting the PI3K/AKT/mTOR pathway in NSCLC. *Cancer Treatment Reviews*. 40, 445-456.

Hecht, S.S., 1999. Tobacco smoke carcinogens and lung cancer. *Journal of the National Cancer Institute*. 91, 1194-1210.

Heidorn, S.J., Milagre, C., Whittaker, S., Nourry, A., Niculescu-Duvas, I., Dhomen, N., Hussain, J., Reis-Filho, J.S., Springer, C.J., Pritchard, C., Marais, R., 2010. Kinase-dead BRAF and oncogenic RAS cooperate to drive tumor progression through CRAF. *Cell*. 140, 209-221.

Heist, R.S. & Engelman, J.A., 2012. SnapShot: non-small cell lung cancer. *Cancer Cell*. 21, 448.e2.

Heist, R.S., Sequist, L.V., Engelman, J.a., 2012. Genetic changes in squamous cell lung cancer: a review. *Journal of Thoracic Oncology: Official Publication of the International Association for the Study of Lung Cancer*. 7, 924-933.

Hengartner, M.O., 2000. The biochemistry of apoptosis. *Nature*. 407, 770-776.

Herbst, R.S. & Bunn, P.A., Jr, 2003. Targeting the epidermal growth factor receptor in non-small cell lung cancer. *Clinical Cancer Research: An Official Journal of the American Association for Cancer Research*. 9, 5813-5824.

Herbst, R.S., Heymach, J.V., Lippman, S.M., 2008. Lung cancer. *The New England Journal of Medicine*. 359, 1367-1380.

Heyer, J., Kwong, L.N., Lowe, S.W., Chin, L., 2010. Non-germline genetically engineered mouse models for translational cancer research. *Nature Reviews Cancer*. 10, 470-480.

Hidalgo, M., Bruckheimer, E., Rajeshkumar, N.V., Garrido-Laguna, I., De Oliveira, E., Rubio-Viqueira, B., Strawn, S., Wick, M.J., Martell, J., Sidransky, D., 2011. A pilot clinical study of treatment guided by personalized tumorgrafts in patients with advanced cancer. *Molecular Cancer Therapeutics*. 10, 1311-1316.

Hirai, H., Sootome, H., Nakatsuru, Y., Miyama, K., Taguchi, S., Tsujioka, K., Ueno, Y., Hatch, H., Majumder, P.K., Pan, B.S., Kotani, H., 2010. MK-2206, an allosteric Akt inhibitor, enhances antitumor efficacy by standard chemotherapeutic agents or molecular targeted drugs in vitro and in vivo. *Molecular Cancer Therapeutics*. 9, 1956-1967.

Hirsch, F.R., Varella-Garcia, M., Bunn, P.A., Jr, Di Maria, M.V., Veve, R., Bremmes, R.M., Baron, A.E., Zeng, C., Franklin, W.A., 2003. Epidermal growth factor receptor in non-small-cell lung carcinomas: correlation between gene copy number and protein expression and impact on prognosis. *Journal of Clinical Oncology: Official Journal of the American Society of Clinical Oncology*. 21, 3798-3807.

Hoang, T., Dahlberg, S.E., Schiller, J.H., Johnson, D.H., 2013. Does histology predict survival of advanced non-small cell lung cancer patients treated with platin-based chemotherapy? An analysis of the Eastern Cooperative Oncology Group Study E1594. *Lung Cancer (Amsterdam, Netherlands)*. 81, 47-52.

Hoeflich, K.P., Merchant, M., Orr, C., Chan, J., Den Otter, D., Berry, L., Kasman, I., Koeppen, H., Rice, K., Yang, N.Y., Engst, S., Johnston, S., Friedman, L.S., Belvin, M., 2012. Intermittent administration of MEK inhibitor GDC-0973 plus PI3K inhibitor GDC-0941 triggers robust apoptosis and tumor growth inhibition. *Cancer Research*. 72, 210-219.

Hoffman, R.M., Connors, K.M., Meerson-Monosov, A.Z., Herrera, H., Price, J.H., 1989. A general native-state method for determination of proliferation capacity of human normal and tumor tissues in vitro. *Proceedings of the National Academy of Sciences of the United States of America*. 86, 2013-2017.

Hoffman, R.M., 1993. In vitro assays for chemotherapy sensitivity. *Clinical Reviews in Oncology/Hematology*. 15, 99-111.

Huang, T., Karsy, M., Zhuge, J., Zhong, M., Liu, D., 2013. B-Raf and the inhibitors: from bench to bedside. *Journal of Hematology & Oncology*. 6, 30-8722-6-30.

Ihle, N.T. & Powis, G., 2010. Inhibitors of phosphatidylinositol-3-kinase in cancer therapy. *Molecular Aspects of Medicine*. 31, 135-144.

Ijijn, K., Ketola, K., Vainio, P., Halonen, P., Kohonen, P., Fey, V., Grafstrom, R.C., Perala, M., Kallioniemi, O., 2009. High-throughput cell-based screening of 4910 known drugs and drug-like small molecules identifies disulfiram as an inhibitor of prostate cancer cell growth. *Clinical Cancer Research: An Official Journal of the American Association for Cancer Research*. 15, 6070-6078.

Imielinski, M., Berger, A.H., Hammerman, P.S., Hernandez, B., Pugh, T.J., Hodis, E., Cho, J., Suh, J., Capelletti, M., Sivachenko, A., Sougnez, C., Auclair, D., Lawrence, M.S., Stojanov, P., Cibulskis, K., Choi, K., de Waal, L., Sharifnia, T., Brooks, A., Greulich, H., Banerji, S., Zander, T., Seidel, D., Leenders, F., Ansen, S., Ludwig, C., Engel-Riedel, W., Stoelben, E., Wolf, J., Goparju, C., Thompson, K., Winckler, W., Kwiatkowski, D., Johnson, B.E., Janne, P.A., Miller, V.A., Pao, W., Travis, W.D., Pass, H.I., Gabriel, S.B., Lander, E.S., Thomas, R.K., Garraway, L.A., Getz, G., Meyerson, M., 2012. Mapping the hallmarks of lung adenocarcinoma with massively parallel sequencing. *Cell*. 150, 1107-1120.

International Cancer Genome Consortium, Hudson, T.J., Anderson, W., Artez, A., Barker, A.D., Bell, C., Bernabe, R.R., Bhan, M.K., Calvo, F., Eerola, I., Gerhard, D.S., Guttmacher, A., Guyer, M., Hemsley, F.M., Jennings, J.L., Kerr, D., Klatt, P., Kolar, P., Kusada, J., Lane, D.P., Laplace, F., Youyong, L., Nettekoven, G., Ozenberger, B., Peterson, J., Rao, T.S., Remacle, J., Schafer, A.J., Shibata, T., Stratton, M.R., Vockley, J.G., Watanabe, K., Yang, H., Yuen, M.M., Knoppers, B.M., Bobrow, M., Cambon-Thomsen, A., Dressler, L.G., Dyke, S.O., Joly, Y., Kato, K., Kennedy, K.L., Nicolas, P., Parker, M.J., Rial-Sebbag, E., Romeo-Casabona, C.M., Shaw, K.M., Wallace, S., Wiesner, G.L., Zeps, N., Lichter, P., Biankin, A.V., Chabannon, C., Chin, L., Clement, B., de Alava, E., Degos, F., Ferguson, M.L., Geary, P., Hayes, D.N., Hudson, T.J., Johns, A.L., Kasprzyk, A., Nakagawa, H., Penny, R., Piris, M.A., Sarin, R., Scarpa, A., Shibata, T., van de Vijver, M., Futreal, P.A., Aburatani, H., Bayes, M., Botwell, D.D., Campbell, P.J., Estivill, X., Gerhard, D.S., Grimmond, S.M., Gut, I., Hirst, M., Lopez-Otin, C., Majumder, P., Marra, M., McPherson, J.D., Nakagawa, H., Ning, Z., Puente, X.S., Ruan, Y., Shibata, T., Stratton, M.R., Stunnenberg, H.G., Swerdlow, H., Velculescu, V.E., Wilson, R.K., Xue, H.H., Yang, L., Spellman, P.T., Bader, G.D., Boutros, P.C., Campbell, P.J., Flicek, P., Getz, G., Guigo, R., Guo, G., Haussler, D., Heath, S., Hubbard, T.J., Jiang, T., Jones, S.M., Li, Q., Lopez-Bigas, N., Luo, R., Muthuswamy, L., Ouellette, B.F., Pearson, J.V., Puente, X.S., Quesada, V., Raphael, B.J., Sander, C., Shibata, T., Speed, T.P., Stein, L.D., Stuart, J.M., Teague, J.W., Totoki, Y., Tsunoda, T., Valencia, A., Wheeler, D.A., Wu, H., Zhao, S., Zhou, G., Stein, L.D., Guigo, R., Hubbard, T.J., Joly, Y., Jones, S.M., Kasprzyk, A., Lathrop, M., Lopez-Bigas, N., Ouellette, B.F., Spellman, P.T., Teague, J.W., Thomas, G., Valencia, A., Yoshida, T., Kennedy, K.L., Axton, M., Dyke, S.O., Futreal, P.A., Gerhard, D.S., Gunter, C., Guyer, M., Hudson, T.J., McPherson, J.D., Miller, L.J., Ozenberger, B., Shaw, K.M., Kasprzyk, A., Stein, L.D., Zhang, J., Haider, S.A., Wang, J., Yung, C.K., Cross, A., Liang, Y., Gnaneshan, S., Guberman, J., Hsu, J., Bobrow, M., Chalmers, D.R., Hasel, K.W., Joly, Y., Kaan, T.S., Kennedy, K.L., Knoppers, B.M., Lowrance, W.W., Masui, T., Nicolas, P., Rial-Sebbag, E., Rodriguez, L.L., Vergely, C., Yoshida, T., Grimmond, S.M., Biankin, A.V., Bowtell, D.D., Cloonan, N., deFazio, A., Eshleman, J.R., Etemadmoghadam, D., Gardiner, B.A., Kench, J.G., Scarpa, A., Sutherland, R.L., Tempero, M.A., Waddell, N.J., Wilson, P.J., McPherson, J.D., Gallinger, S., Tsao, M.S., Shaw, P.A., Petersen, G.M., Mukhopadhyay, D., Chin, L., DePinho, R.A., Thayer, S., Muthuswamy, L., Shazand, K., Beck, T., Sam, M., Timms, L., Ballin, V., Lu, Y., Ji, J., Zhang, X., Chen, F., Hu, X., Zhou, G., Yang, Q., Tian, G., Zhang, L., Xing, X., Li, X., Zhu, Z., Yu, Y., Yu, J., Yang, H., Lathrop, M., Tost, J., Brennan, P., Holcatova, I., Zaridze, D., Brazma, A., Egevard, L., Prokhortchouk, E., Banks, R.E., Uhlen, M., Cambon-Thomsen, A., Viksna, J., Ponten, F., Skryabin, K., Stratton, M.R., Futreal, P.A., Birney, E., Borg, A., Borresen-Dale, A.L., Caldas, C., Foekens, J.A., Martin, S., Reis-Filho, J.S., Richardson, A.L., Sotiriou, C., Stunnenberg, H.G., Thoms, G., van de Vijver, M., van't Veer, L., Calvo, F., Birnbaum, D., Blanche, H., Boucher, P., Boyault, S., Chabannon, C., Gut, I., Masson-Jacquemier, J.D., Lathrop, M., Pauporte, I., Pivot, X., Vincent-Salomon, A., Tabone, E., Theillet, C., Thomas, G., Tost, J., Treilleux, I., Calvo, F., Bioulac-Sage, P., Clement, B., Decaens, T., Degos, F., Franco, D., Gut, I., Gut, M., Heath, S., Lathrop, M., Samuel, D., Thomas, G., Zucman-Rossi, J., Lichter, P.,

Eils, R., Brors, B., Korbel, J.O., Korshunov, A., Landgraf, P., Lehrach, H., Pfister, S., Radlwimmer, B., Reifemberger, G., Taylor, M.D., von Kalle, C., Majumder, P.P., Sarin, R., Rao, T.S., Bhan, M.K., Scarpa, A., Pederzoli, P., Lawlor, R.A., Delledonne, M., Bardelli, A., Biankin, A.V., Grimmond, S.M., Gress, T., Klimstra, D., Zamboni, G., Shibata, T., Nakamura, Y., Nakagawa, H., Kusada, J., Tsunoda, T., Miyano, S., Aburatani, H., Kato, K., Fujimoto, A., Yoshida, T., Campo, E., Lopez-Otin, C., Estivill, X., Guigo, R., de Sanjose, S., Piris, M.A., Montserrat, E., Gonzalez-Diaz, M., Puente, X.S., Jares, P., Valencia, A., Himmelbaue, H., Quesada, V., Bea, S., Stratton, M.R., Futreal, P.A., Campbell, P.J., Vincent-Salomon, A., Richardson, A.L., Reis-Filho, J.S., van de Vijver, M., Thomas, G., Masson-Jacquemier, J.D., Aparicio, S., Borg, A., Borresen-Dale, A.L., Caldas, C., Foekens, J.A., Stunnenberg, H.G., van't Veer, L., Easton, D.F., Spellman, P.T., Martin, S., Barker, A.D., Chin, L., Collins, F.S., Compton, C.C., Ferguson, M.L., Gerhard, D.S., Getz, G., Gunter, C., Gutmacher, A., Guyer, M., Hayes, D.N., Lander, E.S., Ozenberger, B., Penny, R., Peterson, J., Sander, C., Shaw, K.M., Speed, T.P., Spellman, P.T., Vockley, J.G., Wheeler, D.A., Wilson, R.K., Hudson, T.J., Chin, L., Knoppers, B.M., Lander, E.S., Lichter, P., Stein, L.D., Stratton, M.R., Anderson, W., Barker, A.D., Bell, C., Bobrow, M., Burke, W., Collins, F.S., Compton, C.C., DePinho, R.A., Easton, D.F., Futreal, P.A., Gerhard, D.S., Green, A.R., Guyer, M., Hamilton, S.R., Hubbard, T.J., Kallioniemi, O.P., Kennedy, K.L., Ley, T.J., Liu, E.T., Lu, Y., Majumder, P., Marra, M., Ozenberger, B., Peterson, J., Schafer, A.J., Spellman, P.T., Stunnenberg, H.G., Wainwright, B.J., Wilson, R.K., Yang, H., 2010. International network of cancer genome projects. *Nature*. 464, 993-998.

Jakobsen, J.N. & Sørensen, J.B., 2013. Clinical impact of ki-67 labeling index in non-small cell lung cancer. *Lung Cancer*. 79, 1-7.

Jänne, P.A., Shaw, A.T., Pereira, J.R., Jeannin, G., Vansteenkiste, J., Barrios, C., Franke, F.A., Grinsted, L., Zazulina, V., Smith, P., Smith, I., Crinò, L., 2013. Selumetinib plus docetaxel for KRAS-mutant advanced non-small-cell lung cancer: a randomised, multicentre, placebo-controlled, phase 2 study. *The Lancet Oncology*. 14, 38-47.

Ji, M., Guan, H., Gao, C., Shi, B., Hou, P., 2011. Highly frequent promoter methylation and PIK3CA amplification in non-small cell lung cancer (NSCLC). *BMC Cancer*. 11, 147.

Jin, G., Kim, M.J., Jeon, H., Choi, J.E., Kim, D.S., Lee, E.B., Cha, S.I., Yoon, G.S., Kim, C.H., Jung, T.H., Park, J.Y., 2010. PTEN mutations and relationship to EGFR, ERBB2, KRAS, and TP53 mutations in non-small cell lung cancers. *Lung Cancer (Amsterdam, Netherlands)*. 69, 279-283.

Jin, H., Yang, R., Fong, S., Totpal, K., Lawrence, D., Zheng, Z., Ross, J., Koeppen, H., Schwall, R., Ashkenazi, A., 2004. Apo2 ligand/tumor necrosis factor-related apoptosis-inducing ligand cooperates with chemotherapy to inhibit orthotopic lung tumor growth and improve survival. *Cancer Research*. 64, 4900-4905.

Jin, H., Yang, R., Ross, J., Fong, S., Carano, R., Totpal, K., Lawrence, D., Zheng, Z., Koeppen, H., Stern, H., Schwall, R., Ashkenazi, A., 2008. Cooperation of the agonistic DR5 antibody apomab with chemotherapy to inhibit orthotopic lung tumor growth and improve survival. *Clinical Cancer Research : An Official Journal of the American Association for Cancer Research*. 14, 7733-7740.

Jin, Z. & El-Deiry, W.S., 2005. Overview of cell death signaling pathways. *Cancer Biology & Therapy*. 4, 139-163.

Johnson, J.L., Pillai, S., Chellappan, S.P., 2012. Genetic and biochemical alterations in non-small cell lung cancer. *Biochemistry Research International*. 2012, 940405.

Kandioler, D., Stamatis, G., Eberhardt, W., Kappel, S., Zöchbauer-Müller, S., Kührer, I., Mittlböck, M., Zwrtek, R., Aigner, C., Bichler, C., Tichy, V., Hudec, M., Bachleitner, T., End, A., Müller, M.R., Roth, E., Klepetko, W., 2008. Growing clinical evidence for the interaction of the p53 genotype and response to induction chemotherapy in advanced non-small cell lung cancer. *The Journal of Thoracic and Cardiovascular Surgery*. 135, 1036-1041.

Kang, M.H. & Reynolds, C.P., 2009. Bcl-2 inhibitors: targeting mitochondrial apoptotic pathways in cancer therapy. *Clinical Cancer Research: An Official Journal of the American Association for Cancer Research*. 15, 1126-1132.

Kawano, O., Sasaki, H., Endo, K., Suzuki, E., Haneda, H., Yukiue, H., Kobayashi, Y., Yano, M., Fujii, Y., 2006. PIK3CA mutation status in Japanese lung cancer patients. *Lung Cancer (Amsterdam, Netherlands)*. 54, 209-215.

Kern, M.A., Hagg, A.M., Eiteneuer, E., Konze, E., Drebber, U., Dienes, H.P., Breuhahn, K., Schirmacher, P., Kasper, H.U., 2006. Ex vivo analysis of antineoplastic agents in precision-cut tissue slices of human origin: effects of cyclooxygenase-2 inhibition in hepatocellular carcinoma. *Liver International: Official Journal of the International Association for the Study of the Liver*. 26, 604-612.

Kerr, J.F., Wyllie, A.H., Currie, A.R., 1972. Apoptosis: a basic biological phenomenon with wide-ranging implications in tissue kinetics. *British Journal of Cancer*. 26, 239-257.

Khaled, W.T. & Liu, P., 2014. Cancer mouse models: Past, present and future. *Seminars in Cell & Developmental Biology*.

Kotsakis, A. & Georgoulas, V., 2010. Targeting epidermal growth factor receptor in the treatment of non-small-cell lung cancer. *Expert Opinion on Pharmacotherapy*. 11, 2363-2389.

Kumar, V., Abbas, A.K., Fausto, N. and Perkins, with illustrations by James A., 2005. *Robbins and Cotran pathologic basis of disease*. 7th ed. Philadelphia, Pa. ; London: Elsevier Saunders.

Lang, D.S., Droemann, D., Schultz, H., Branscheid, D., Martin, C., Ressmeyer, A.R., Zabel, P., Vollmer, E., Goldmann, T., 2007. A novel human ex vivo model for the analysis of molecular events during lung cancer chemotherapy. *Respiratory Research*. 8, 43.

Le Calvez Florence, Mukeria, A., Hunt, J.D., Kelm, O., Hung, R.J., Tanière, P., Brennan, P., Boffetta, P., Zaridze, D.G., Hainaut, P., 2005. TP53 and KRAS mutation load and types in lung cancers in relation to tobacco smoke: distinct patterns in never, former, and current smokers. *Cancer Research*. 65, 5076-5083.

Li, T., Kung, H.J., Mack, P.C., Gandara, D.R., 2013. Genotyping and genomic profiling of non-small-cell lung cancer: implications for current and future therapies. *Journal of Clinical Oncology: Official Journal of the American Society of Clinical Oncology*. 31, 1039-1049.

LoPiccolo, J., Blumenthal, G.M., Bernstein, W.B., Dennis, P.a., 2008. Targeting the PI3K/Akt/mTOR pathway: effective combinations and clinical considerations. *Drug*

Resistance Updates: Reviews and Commentaries in Antimicrobial and Anticancer Chemotherapy. 11, 32-50.

Luo, J., Emanuele, M.J., Li, D., Creighton, C.J., Schlabach, M.R., Westbrook, T.F., Wong, K.K., Elledge, S.J., 2009a. A genome-wide RNAi screen identifies multiple synthetic lethal interactions with the Ras oncogene. *Cell*. 137, 835-848.

Luo, J., Solimini, N.L., Elledge, S.J., 2009b. Principles of cancer therapy: oncogene and non-oncogene addiction. *Cell*. 136, 823-837.

Luster, T.A., Carrell, J.A., McCormick, K., Sun, D., Humphreys, R., 2009. Mapatumumab and lexatumumab induce apoptosis in TRAIL-R1 and TRAIL-R2 antibody-resistant NSCLC cell lines when treated in combination with bortezomib. *Molecular Cancer Therapeutics*. 8, 292-302.

Ma, X., Rousseau, V., Sun, H., Lantuejoul, S., Filipits, M., Pirker, R., Popper, H., Mendiboure, J., Vataire, A., Le Chevalier Thierry, Soria, J.C., Brambilla, E., Dunant, A., Hainaut, P., 2014. Significance of TP53 mutations as predictive markers of adjuvant cisplatin-based chemotherapy in completely resected non-small-cell lung cancer. *Molecular Oncology*. 8, 555-564.

Maira, S.M., Pecchi, S., Huang, A., Burger, M., Knapp, M., Sterker, D., Schnell, C., Guthy, D., Nagel, T., Wiesmann, M., Brachmann, S., Fritsch, C., Dorsch, M., Chene, P., Shoemaker, K., De Pover, A., Menezes, D., Martiny-Baron, G., Fabbro, D., Wilson, C.J., Schlegel, R., Hofmann, F., Garcia-Echeverria, C., Sellers, W.R., Voliva, C.F., 2012. Identification and characterization of NVP-BKM120, an orally available pan-class I PI3-kinase inhibitor. *Molecular Cancer Therapeutics*. 11, 317-328.

Mak, I.W., Evaniew, N., Ghert, M., 2014. Lost in translation: animal models and clinical trials in cancer treatment. *American Journal of Translational Research*. 6, 114-118.

Malaney, P., Nicosia, S.V., Davé, V., 2014. One mouse, one patient paradigm: New avatars of personalized cancer therapy. *Cancer Letters*. 344, 1-12.

Malanga, D., Scrima, M., De Marco, C., Fabiani, F., De Rosa, N., De Gisi, S., Malara, N., Savino, R., Rocco, G., Chiappetta, G., Franco, R., Tirino, V., Pirozzi, G., Viglietto, G., 2008. Activating E17K mutation in the gene encoding the protein kinase AKT1 in a subset of squamous cell carcinoma of the lung. *Cell Cycle (Georgetown, Tex.)*. 7, 665-669.

Mallon, R., Feldberg, L.R., Lucas, J., Chaudhary, I., Dehnhardt, C., Santos, E.D., Chen, Z., dos Santos, O., Ayril-Kaloustian, S., Venkatesan, A., Hollander, I., 2011. Antitumor efficacy of PKI-587, a highly potent dual PI3K/mTOR kinase inhibitor. *Clinical Cancer Research: An Official Journal of the American Association for Cancer Research*. 17, 3193-3203.

Marks, J.L., Gong, Y., Chitale, D., Golas, B., McLellan, M.D., Kasai, Y., Ding, L., Mardis, E.R., Wilson, R.K., Solit, D., Levine, R., Michel, K., Thomas, R.K., Rusch, V.W., Ladanyi, M., Pao, W., 2008. Novel MEK1 mutation identified by mutational analysis of epidermal growth factor receptor signaling pathway genes in lung adenocarcinoma. *Cancer Research*. 68, 5524-5528.

Marsit, C.J., Zheng, S., Aldape, K., Hinds, P.W., Nelson, H.H., Wiencke, J.K., Kelsey, K.T., 2005. PTEN expression in non-small-cell lung cancer: evaluating its relation to

tumor characteristics, allelic loss, and epigenetic alteration. *Human Pathology*. 36, 768-776.

Maund, S.L., Nolley, R., Peehl, D.M., 2014. Optimization and comprehensive characterization of a faithful tissue culture model of the benign and malignant human prostate. *Laboratory Investigation; a Journal of Technical Methods and Pathology*. 94, 208-221.

McCloskey, P., Balduyck, B., Van Schil Paul E, Faivre-Finn, C., O'Brien, M., 2013. Radical treatment of non-small cell lung cancer during the last 5 years. *European Journal of Cancer (Oxford, England : 1990)*. 49, 1555-1564.

McDermott, U., Iafrate, A.J., Gray, N.S., Shioda, T., Classon, M., Maheswaran, S., Zhou, W., Choi, H.G., Smith, S.L., Dowell, L., Ulkus, L.E., Kuhlmann, G., Greninger, P., Christensen, J.G., Haber, D.A., Settleman, J., 2008. Genomic alterations of anaplastic lymphoma kinase may sensitize tumors to anaplastic lymphoma kinase inhibitors. *Cancer Research*. 68, 3389-3395.

McDermott, U., Sharma, S.V., Dowell, L., Greninger, P., Montagut, C., Lamb, J., Archibald, H., Raudales, R., Tam, A., Lee, D., Rothenberg, S.M., Supko, J.G., Sordella, R., Ulkus, L.E., Iafrate, A.J., Maheswaran, S., Njauw, C.N., Tsao, H., Drew, L., Hanke, J.H., Ma, X.J., Erlander, M.G., Gray, N.S., Haber, D.A., Settleman, J., 2007. Identification of genotype-correlated sensitivity to selective kinase inhibitors by using high-throughput tumor cell line profiling. *Proceedings of the National Academy of Sciences of the United States of America*. 104, 19936-19941.

Meng, J., Dai, B., Fang, B., Bekele, B.N., Bornmann, W.G., Sun, D., Peng, Z., Herbst, R.S., Papadimitrakopoulou, V., Minna, J.D., Peyton, M., Roth, J.a., 2010. Combination treatment with MEK and AKT inhibitors is more effective than each drug alone in human non-small cell lung cancer in vitro and in vivo. *PloS One*. 5, e14124.

Minuti, G., D'Incecco, A., Cappuzzo, F., 2013. Targeted therapy for NSCLC with driver mutations. *Expert Opinion on Biological Therapy*. 13, 1401-1412.

Nakane, P.K. & Pierce, G.B., Jr, 1966. Enzyme-labeled antibodies: preparation and application for the localization of antigens. *The Journal of Histochemistry and Cytochemistry : Official Journal of the Histochemistry Society*. 14, 929-931.

Nardella, C., Lunardi, A., Patnaik, A., Cantley, L.C., Pandolfi, P.P., 2011. The APL paradigm and the "co-clinical trial" project. *Cancer Discovery*. 1, 108-116.

National Lung Screening Trial Research Team, Aberle, D.R., Adams, A.M., Berg, C.D., Black, W.C., Clapp, J.D., Fagerstrom, R.M., Gareen, I.F., Gatsonis, C., Marcus, P.M., Sicks, J.D., 2011. Reduced lung-cancer mortality with low-dose computed tomographic screening. *The New England Journal of Medicine*. 365, 395-409.

O'Brien, C., Wallin, J.J., Sampath, D., GuhaThakurta, D., Savage, H., Punnoose, E.a., Guan, J., Berry, L., Prior, W.W., Amler, L.C., Belvin, M., Friedman, L.S., Lackner, M.R., 2010. Predictive biomarkers of sensitivity to the phosphatidylinositol 3' kinase inhibitor GDC-0941 in breast cancer preclinical models. *Clinical Cancer Research: An Official Journal of the American Association for Cancer Research*. 16, 3670-3683.

Ohren, J.F., Chen, H., Pavlovsky, A., Whitehead, C., Zhang, E., Kuffa, P., Yan, C., McConnell, P., Spessard, C., Banotai, C., Mueller, W.T., Delaney, A., Omer, C., Sebolt-Leopold, J., Dudley, D.T., Leung, I.K., Flamme, C., Warmus, J., Kaufman, M., Barrett, S., Teclé, H., Hasemann, C.A., 2004. Structures of human MAP kinase kinase 1

(MEK1) and MEK2 describe novel noncompetitive kinase inhibition. *Nature Structural & Molecular Biology*. 11, 1192-1197.

Okudela, K., Suzuki, M., Kageyama, S., Bunai, T., Nagura, K., Igarashi, H., Takamochi, K., Suzuki, K., Yamada, T., Niwa, H., Ohashi, R., Ogawa, H., Mori, H., Kitamura, H., Kaneko, T., Tsuneyoshi, T., Sugimura, H., 2007. PIK3CA mutation and amplification in human lung cancer. *Pathology International*. 57, 664-671.

Oltersdorf, T., Elmore, S.W., Shoemaker, A.R., Armstrong, R.C., Augeri, D.J., Belli, B.A., Bruncko, M., Deckwerth, T.L., Dinges, J., Hajduk, P.J., Joseph, M.K., Kitada, S., Korsmeyer, S.J., Kunzer, A.R., Letai, A., Li, C., Mitten, M.J., Nettesheim, D.G., Ng, S., Nimmer, P.M., O'Connor, J.M., Oleksijew, A., Petros, A.M., Reed, J.C., Shen, W., Tahir, S.K., Thompson, C.B., Tomaselli, K.J., Wang, B., Wendt, M.D., Zhang, H., Fesik, S.W., Rosenberg, S.H., 2005. An inhibitor of Bcl-2 family proteins induces regression of solid tumours. *Nature*. 435, 677-681.

Ostrow, S., Egorin, M., Aisner, J., Bachur, N., Wiernik, P.H., 1980. High-dose cis-diamminedichloro-platinum therapy in patients with advanced breast cancer: pharmacokinetics, toxicity, and therapeutic efficacy. *Cancer Clinical Trials*. 3, 23-27.

Oxnard, G.R., Binder, A., Janne, P.a., 2013. New targetable oncogenes in non-small-cell lung cancer. *Journal of Clinical Oncology: Official Journal of the American Society of Clinical Oncology*. 31, 1097-1104.

Pal, S.K., Figlin, R.A., Reckamp, K., 2010. Targeted therapies for non-small cell lung cancer: an evolving landscape. *Molecular Cancer Therapeutics*. 9, 1931-1944.

Pampaloni, F., Reynaud, E.G., Stelzer, E.H., 2007. The third dimension bridges the gap between cell culture and live tissue. *Nature Reviews Molecular Cell Biology*. 8, 839-845.

Pao, W. & Girard, N., 2011. New driver mutations in non-small-cell lung cancer. *The Lancet Oncology*. 12, 175-180.

Papadimitrakopoulou, V., 2012. Development of PI3K / AKT / mTOR Pathway Inhibitors and Their Application in Personalized Therapy. *Journal of Thoracic Oncology*. 7, 1315-1326.

Parrish, A.R., Gandolfi, A.J., Brendel, K., 1995. Minireview Precision-Cut Tissue Slices: Applications in Pharmacology and Toxicology. *Life Sciences*. 57, 1887-1901.

Paz-Ares, L., Balint, B., de Boer, R.H., van Meerbeeck, J.P., Wierzbicki, R., De Souza, P., Galimi, F., Haddad, V., Sabin, T., Hei, Y.J., Pan, Y., Cottrell, S., Hsu, C.P., RamLau, R., 2013. A randomized phase 2 study of paclitaxel and carboplatin with or without conatumumab for first-line treatment of advanced non-small-cell lung cancer. *Journal of Thoracic Oncology: Official Publication of the International Association for the Study of Lung Cancer*. 8, 329-337.

Paz-Ares, L.G., Biesma, B., Heigener, D., von Pawel, J., Eisen, T., Bennouna, J., Zhang, L., Liao, M., Sun, Y., Gans, S., Syrigos, K., Le Marie, E., Gottfried, M., Vansteenkiste, J., Alberola, V., Strauss, U.P., Montegriffo, E., Ong, T.J., Santoro, A., 2012. Phase III, Randomized, Double-Blind, Placebo-Controlled Trial of Gemcitabine/Cisplatin Alone or With Sorafenib for the First-Line Treatment of Advanced, Nonsquamous Non-Small-Cell Lung Cancer. *Journal of Clinical Oncology*. 30, 3084-3092.

Peifer, M., Fernandez-Cuesta, L., Sos, M.L., George, J., Seidel, D., Kasper, L.H., Plenker, D., Leenders, F., Sun, R., Zander, T., Menon, R., Koker, M., Dahmen, I., Muller, C., Di Cerbo Vincenzo, Schildhaus, H., Altmuller, J., Baessmann, I., Becker, C., de Wilde, B., Vandesompele, J., Bohm, D., Ansen, S., Gabler, F., Wilkening, I., Heynck, S., Heuckmann, J.M., Lu, X., Carter, S.L., Cibulskis, K., Banerji, S., Getz, G., Park, K., Rauh, D., Grutter, C., Fischer, M., Pasqualucci, L., Wright, G., Wainer, Z., Russell, P., Petersen, I., Chen, Y., Stoelben, E., Ludwig, C., Schnabel, P., Hoffmann, H., Muley, T., Brockmann, M., Engel-Riedel, W., Muscarella, L.a., Fazio, V.M., Groen, H., Timens, W., Sietsma, H., Thunnissen, E., Smit, E., Heideman, D.a.M., Snijders, P.J.F., Cappuzzo, F., Ligorio, C., Damiani, S., Field, J., Solberg, S., Brustugun, O.T., Lund-Iversen, M., Sanger, J., Clement, J.H., Soltermann, A., Moch, H., Weder, W., Solomon, B., Soria, J., Validire, P., Besse, B., Brambilla, E., Brambilla, C., Lantuejoul, S., Lorimier, P., Schneider, P.M., Hallek, M., Pao, W., Meyerson, M., Sage, J., Shendure, J., Schneider, R., Buttner, R., Wolf, J., Nurnberg, P., Perner, S., Heukamp, L.C., Brindle, P.K., Haas, S., Thomas, R.K., 2012. Integrative genome analyses identify key somatic driver mutations of small-cell lung cancer. *Nature Genetics*. 44, 1104-1110.

Pennarun, B., Meijer, A., de Vries, E.G.E., Kleibeuker, J.H., Kruyt, F., de Jong, S., 2010. Playing the DISC: Turning on TRAIL death receptor-mediated apoptosis in cancer. *Biochimica Et Biophysica Acta (BBA) - Reviews on Cancer*. 1805, 123-140.

Pirnia, F., Frese, S., Gloor, B., Hotz, M.A., Luethi, A., Gugger, M., Betticher, D.C., Borner, M.M., 2006. Ex vivo assessment of chemotherapy-induced apoptosis and associated molecular changes in patient tumor samples. *Anticancer Research*. 26, 1765-1772.

Planchard D, Mazieres J, Riely GJ, et al. Interim results of phase II study BRF113928 of dabrafenib in BRAF V600E mutation--positive non-small cell lung cancer (NSCLC) patients. ASCO meeting 2013. *J Clin Oncol* 2013;31(Suppl):abstract 8009.

Pore, M.M., Hiltermann, T.J., Kruyt, F.A., 2010. Targeting apoptosis pathways in lung cancer. *Cancer Letters*.

Price, K.A., Azzoli, C.G., Krug, L.M., Pietanza, M.C., Rizvi, N.A., Pao, W., Kris, M.G., Riely, G.J., Heelan, R.T., Arcila, M.E., Miller, V.A., 2010. Phase II trial of gefitinib and everolimus in advanced non-small cell lung cancer. *Journal of Thoracic Oncology: Official Publication of the International Association for the Study of Lung Cancer*. 5, 1623-1629.

Raparia, K., Villa, C., DeCamp, M.M., Patel, J.D., Mehta, M.P., 2013. Molecular profiling in non-small cell lung cancer: a step toward personalized medicine. *Archives of Pathology & Laboratory Medicine*. 137, 481-491.

Reungwetwattana, T., Weroha, S.J., Molina, J.R., 2012. Oncogenic pathways, molecularly targeted therapies, and highlighted clinical trials in non-small-cell lung cancer (NSCLC). *Clinical Lung Cancer*. 13, 252-266.

Rinehart, J., Adjei, A.A., Lorusso, P.M., Waterhouse, D., Hecht, J.R., Natale, R.B., Hamid, O., Varterasian, M., Asbury, P., Kaldjian, E.P., Gulyas, S., Mitchell, D.Y., Herrera, R., Sebolt-Leopold, J.S., Meyer, M.B., 2004. Multicenter phase II study of the oral MEK inhibitor, CI-1040, in patients with advanced non-small-cell lung, breast, colon, and pancreatic cancer. *Journal of Clinical Oncology: Official Journal of the American Society of Clinical Oncology*. 22, 4456-4462.

Roberts, P.J., Stinchcombe, T.E., Der, C.J., Socinski, M.A., 2010. Personalized medicine in non-small-cell lung cancer: is KRAS a useful marker in selecting patients for epidermal growth factor receptor-targeted therapy? *Journal of Clinical Oncology: Official Journal of the American Society of Clinical Oncology*. 28, 4769-4777.

Romano, G., Acunzo, M., Garofalo, M., Di, G., Cascione, L., Zanca, C., Bolon, B., 2012. MiR-494 is regulated by ERK1/2 and modulates TRAIL-induced apoptosis in non-small-cell lung cancer through BIM down-regulation. *Proceedings of the National Academy of Sciences of the United States of America*. 109, 2-7.

Rosell, R., Carcereny, E., Gervais, R., Vergnenegre, A., Massuti, B., Felip, E., Palmero, R., Garcia-Gomez, R., Pallares, C., Sanchez, J.M., Porta, R., Cobo, M., Garrido, P., Longo, F., Moran, T., Insa, A., De Marinis, F., Corre, R., Bover, I., Illiano, A., Dansin, E., de Castro, J., Milella, M., Reguart, N., Altavilla, G., Jimenez, U., Provencio, M., Moreno, M.A., Terrasa, J., Munoz-Langa, J., Valdivia, J., Isla, D., Domine, M., Molinier, O., Mazieres, J., Baize, N., Garcia-Campelo, R., Robinet, G., Rodriguez-Abreu, D., Lopez-Vivanco, G., Gebbia, V., Ferrera-Delgado, L., Bombaron, P., Bernabe, R., Bearz, A., Artal, A., Cortesi, E., Rolfo, C., Sanchez-Ronco, M., Drozdowskyj, A., Queralt, C., de Aguirre, I., Ramirez, J.L., Sanchez, J.J., Molina, M.A., Taron, M., Paz-Ares, L., Spanish Lung Cancer Group in collaboration with Groupe Francais de Pneumo-Cancerologie and Associazione Italiana Oncologia Toracica, 2012. Erlotinib versus standard chemotherapy as first-line treatment for European patients with advanced EGFR mutation-positive non-small-cell lung cancer (EURTAC): a multicentre, open-label, randomised phase 3 trial. *The Lancet Oncology*. 13, 239-246.

Rosell, R., Moran, T., Queralt, C., Porta, R., Cardenal, F., Camps, C., Majem, M., Lopez-Vivanco, G., Isla, D., Provencio, M., Insa, A., Massuti, B., Gonzalez-Larriba, J.L., Paz-Ares, L., Bover, I., Garcia-Campelo, R., Moreno, M.A., Catot, S., Rolfo, C., Reguart, N., Palmero, R., Sanchez, J.M., Bastus, R., Mayo, C., Bertran-Alamillo, J., Molina, M.A., Sanchez, J.J., Taron, M., Spanish Lung Cancer Group, 2009. Screening for epidermal growth factor receptor mutations in lung cancer. *The New England Journal of Medicine*. 361, 958-967.

Rudin, C.M., Hann, C.L., Garon, E.B., Ribeiro de Oliveira, M., Bonomi, P.D., Camidge, D.R., Chu, Q., Giaccone, G., Khaira, D., Ramalingam, S.S., Ranson, M.R., Dive, C., McKeegan, E.M., Chyla, B.J., Dowell, B.L., Chakravarty, A., Nolan, C.E., Rudersdorf, N., Busman, T.A., Mabry, M.H., Krivoshik, A.P., Humerickhouse, R.A., Shapiro, G.I., Gandhi, L., 2012. Phase II study of single-agent navitoclax (ABT-263) and biomarker correlates in patients with relapsed small cell lung cancer. *Clinical Cancer Research: An Official Journal of the American Association for Cancer Research*. 18, 3163-3169.

Salphati, L., Pang, J., Plise, E.G., Chou, B., Halladay, J.S., Olivero, A.G., Rudewicz, P.J., Tian, Q., Wong, S., Zhang, X., 2011. Preclinical pharmacokinetics of the novel PI3K inhibitor GDC-0941 and prediction of its pharmacokinetics and efficacy in human. *Xenobiotica; the Fate of Foreign Compounds in Biological Systems*. 41, 1088-1099.

Samuels, Y., Wang, Z., Bardelli, A., Silliman, N., Ptak, J., Szabo, S., Yan, H., Gazdar, A., Powell, S.M., Riggins, G.J., Willson, J.K., Markowitz, S., Kinzler, K.W., Vogelstein, B., Velculescu, V.E., 2004. High frequency of mutations of the PIK3CA gene in human cancers. *Science (New York, N.Y.)*. 304, 554.

Sanders, H.R. & Albitar, M., 2010. Somatic mutations of signaling genes in non-small-cell lung cancer. *Cancer Genetics and Cytogenetics*. 203, 7-15.

- Sasaki, Y., Tamura, T., Eguchi, K., Shinkai, T., Fujiwara, Y., Fukuda, M., Ohe, Y., Bungo, M., Horichi, N., Niimi, S., 1989. Pharmacokinetics of (glycolate-0,0')-diammine platinum (II), a new platinum derivative, in comparison with cisplatin and carboplatin. *Cancer Chemotherapy and Pharmacology*. 23, 243-246.
- Sato, M., Shames, D.S., Gazdar, A.F., 2007. A Translational View of the Molecular Pathogenesis of Lung Cancer. *Journal of Thoracic Oncology*. 2, 327-343.
- Schmid, J.O., Dong, M., Haubeiss, S., Friedel, G., Bode, S., Grabner, A., Ott, G., Murdter, T.E., Oren, M., Aulitzky, W.E., van der Kuip, H., 2012. Cancer cells cue the p53 response of cancer-associated fibroblasts to cisplatin. *Cancer Research*. 72, 5824-5832.
- Schneider, C.A., Rasband, W.S., Eliceiri, K.W., 2012. NIH Image to ImageJ: 25 years of image analysis. *Nature Methods*. 9, 671-675.
- Scholl, C., Frohling, S., Dunn, I.F., Schinzel, A.C., Barbie, D.A., Kim, S.Y., Silver, S.J., Tamayo, P., Wadlow, R.C., Ramaswamy, S., Dohner, K., Bullinger, L., Sandy, P., Boehm, J.S., Root, D.E., Jacks, T., Hahn, W.C., Gilliland, D.G., 2009. Synthetic lethal interaction between oncogenic KRAS dependency and STK33 suppression in human cancer cells. *Cell*. 137, 821-834.
- Scoccianti, C., Vesin, A., Martel, G., Olivier, M., Brambilla, E., Timsit, J., Tavecchio, L., Brambilla, C., Field, J.K., Hainaut, P., the European Early Lung Cancer Consortium, 2012. Prognostic value of TP53, KRAS and EGFR mutations in nonsmall cell lung cancer: the EUELC cohort. *European Respiratory Journal*. 40, 177-184.
- Shames, D.S. & Wistuba, I.I., 2014. The evolving genomic classification of lung cancer. *The Journal of Pathology*. 232, 121-133.
- Shapiro G, LoRusso P, Kwak EL, et al. Clinical combination of the MEK inhibitor GDC-0973 and the PI3K inhibitor GDC-0941: a first-in-human phase Ib study testing daily and intermittent dosing schedules in patients with advanced solid tumors. *ASCO Meet Abstr* 2011;29:3005.
- Sharma, S.V., Bell, D.W., Settleman, J., Haber, D.A., 2007. Epidermal growth factor receptor mutations in lung cancer. *Nature Reviews.Cancer*. 7, 169-181.
- Sharma, S.V., Haber, D.a., Settleman, J., 2010. Cell line-based platforms to evaluate the therapeutic efficacy of candidate anticancer agents. *Nature Reviews.Cancer*. 10, 241-253.
- Shimizu, T., Tolcher, A.W., Papadopoulos, K.P., Beeram, M., Rasco, D.W., Smith, L.S., Gunn, S., Smetzer, L., Mays, T.a., Kaiser, B., Wick, M.J., Alvarez, C., Cavazos, A., Mangold, G.L., Patnaik, A., 2012. The clinical effect of the dual-targeting strategy involving PI3K/AKT/mTOR and RAS/MEK/ERK pathways in patients with advanced cancer. *Clinical Cancer Research : An Official Journal of the American Association for Cancer Research*. 18, 2316-2325.
- Siddik, Z.H., 2003. Cisplatin: mode of cytotoxic action and molecular basis of resistance. *Oncogene*. 22, 7265-7279.
- Silva, M.T., 2010. Secondary necrosis: The natural outcome of the complete apoptotic program. *FEBS Letters*. 584, 4491-4499.

Singh, B., Li, R., Xu, L., Poluri, A., Patel, S., Shaha, A.R., Pfister, D., Sherman, E., Goberdhan, A., Hoffman, R.M., Shah, J., 2002. Prediction of survival in patients with head and neck cancer using the histoculture drug response assay. *Head & Neck*. 24, 437-442.

Singh, M., Murriel, C.L., Johnson, L., 2012. Genetically engineered mouse models: closing the gap between preclinical data and trial outcomes. *Cancer Research*. 72, 2695-2700.

Siolas, D. & Hannon, G.J., 2013. Patient-derived tumor xenografts: transforming clinical samples into mouse models. *Cancer Research*. 73, 5315-5319.

Soda, M., Choi, Y.L., Enomoto, M., Takada, S., Yamashita, Y., Ishikawa, S., Fujiwara, S., Watanabe, H., Kurashina, K., Hatanaka, H., Bando, M., Ohno, S., Ishikawa, Y., Aburatani, H., Niki, T., Sohara, Y., Sugiyama, Y., Mano, H., 2007. Identification of the transforming EML4-ALK fusion gene in non-small-cell lung cancer. *Nature*. 448, 561-566.

Soldani, C. & Scovassi, A.I., 2002. Poly (ADP-ribose) polymerase-1 cleavage during apoptosis : An update. *Apoptosis : An International Journal on Programmed Cell Death*. 7, 321-328.

Solit, D.B., Garraway, L.A., Pratilas, C.A., Sawai, A., Getz, G., Basso, A., Ye, Q., Lobo, J.M., She, Y., Osman, I., Golub, T.R., Sebolt-Leopold, J., Sellers, W.R., Rosen, N., 2006. BRAF mutation predicts sensitivity to MEK inhibition. *Nature*. 439, 358-362.

Song, J.H., Kandasamy, K., Kraft, A.S., 2008. ABT-737 induces expression of the death receptor 5 and sensitizes human cancer cells to TRAIL-induced apoptosis. *The Journal of Biological Chemistry*. 283, 25003-25013.

Soria, J.C., Mark, Z., Zatloukal, P., Szima, B., Albert, I., Juhasz, E., Pujol, J.L., Kozielski, J., Baker, N., Smethurst, D., Hei, Y.J., Ashkenazi, A., Stern, H., Amler, L., Pan, Y., Blackhall, F., 2011. Randomized phase II study of dulanermin in combination with paclitaxel, carboplatin, and bevacizumab in advanced non-small-cell lung cancer. *Journal of Clinical Oncology: Official Journal of the American Society of Clinical Oncology*. 29, 4442-4451.

Soria, J.C., Smit, E., Khayat, D., Besse, B., Yang, X., Hsu, C.P., Reese, D., Wiezorek, J., Blackhall, F., 2010. Phase 1b study of dulanermin (recombinant human Apo2L/TRAIL) in combination with paclitaxel, carboplatin, and bevacizumab in patients with advanced non-squamous non-small-cell lung cancer. *Journal of Clinical Oncology: Official Journal of the American Society of Clinical Oncology*. 28, 1527-1533.

Spoerke, J.M., O'Brien, C., Huw, L., Koeppen, H., Fridlyand, J., Brachmann, R.K., Haverty, P.M., Pandita, A., Mohan, S., Sampath, D., Friedman, L.S., Ross, L., Hampton, G.M., Amler, L.C., Shames, D.S., Lackner, M.R., 2012. Phosphoinositide 3-kinase (PI3K) pathway alterations are associated with histologic subtypes and are predictive of sensitivity to PI3K inhibitors in lung cancer preclinical models. *Clinical Cancer Research: An Official Journal of the American Association for Cancer Research*. 18, 6771-6783.

Steelman, L.S., Chappell, W.H., Abrams, S.L., Kempf, R.C., Long, J., Laidler, P., Mijatovic, S., Maksimovic-Ivanic, D., Stivala, F., Mazzarino, M.C., Donia, M., Fagone, P., Malaponte, G., Nicoletti, F., Libra, M., Milella, M., Tafuri, A., Bonati, A., Basecke, J., Cocco, L., Evangelisti, C., Martelli, A.M., Montalto, G., Cervello, M., McCubrey, J.A.,

2011. Roles of the Raf/MEK/ERK and PI3K/PTEN/Akt/mTOR pathways in controlling growth and sensitivity to therapy-implications for cancer and aging. *Aging*. 3, 192-222.

Stegehuis, J.H., de Wilt, L.H. & M., de Vries, E.G.E., Groen, H.J., de Jong, S., Kruyt, F.a.E., 2010. TRAIL receptor targeting therapies for non-small cell lung cancer: current status and perspectives. *Drug Resistance Updates : Reviews and Commentaries in Antimicrobial and Anticancer Chemotherapy*. 13, 2-15.

Stratton, M.R., Campbell, P.J., Futreal, P.A., 2009. The cancer genome. *Nature*. 458, 719-724.

Tanahashi, M., Yamada, T., Moriyama, S., Suzuki, E., Niwa, H., 2008. [The effect of the histoculture drug response assay (HDRA) based perioperative chemotherapy for non-small cell lung cancer]. *Kyobu Geka - Japanese Journal of Thoracic Surgery*. 61, 26-30.

Tewari, M., Quan, L.T., O'Rourke, K., Desnoyers, S., Zeng, Z., Beidler, D.R., Poirier, G.G., Salvesen, G.S., Dixit, V.M., 1995. Yama/CPP32 β , a mammalian homolog of CED-3, is a CrmA-inhibitable protease that cleaves the death substrate poly(ADP-ribose) polymerase. *Cell*. 81, 801-809.

Tiwari, D., Brodie, S.A., Brandes, J.C., 2011. Targeted therapy of non-small-cell lung carcinoma. *Therapeutic Advances in Respiratory Disease*.

Tiwari, D., Brodie, S.a., Brandes, J.C., 2012. Targeted therapy of non-small-cell lung carcinoma. *Therapeutic Advances in Respiratory Disease*. 6, 41-56.

Toyooka, S., Tsuda, T., Gazdar, A.F., 2003. The TP53 gene, tobacco exposure, and lung cancer. *Human Mutation*. 21, 229-239.

Travis, W.D., Brambilla, E., Müller-Hermelink, H.K. and Harris C.C., eds, 2004. *Pathology and Genetics of Tumours of the Lung, Pleura, Thymus and Heart World Health Organization Classification of Tumours*. ISBN 92 83 22418 3: WHO.

Travis, W.D., Brambilla, E., Noguchi, M., Nicholson, A.G., Geisinger, K.R., Yatabe, Y., Beer, D.G., Powell, C.a., Riely, G.J., Van Schil Paul E, Garg, K., Austin, J.H.M., Asamura, H., Rusch, V.W., Hirsch, F.R., Scagliotti, G., Mitsudomi, T., Huber, R.M., Ishikawa, Y., Jett, J., Sanchez-Cespedes, M., Sculier, J., Takahashi, T., Tsuboi, M., Vansteenkiste, J., Wistuba, I., Yang, P., Aberle, D., Brambilla, C., Flieder, D., Franklin, W., Gazdar, A., Gould, M., Hasleton, P., Henderson, D., Johnson, B., Johnson, D., Kerr, K., Kuriyama, K., Lee, J.S., Miller, V.a., Petersen, I., Roggli, V., Rosell, R., Saijo, N., Thunnissen, E., Tsao, M., Yankelewitz, D., 2011. International association for the study of lung cancer/american thoracic society/european respiratory society international multidisciplinary classification of lung adenocarcinoma. *Journal of Thoracic Oncology : Official Publication of the International Association for the Study of Lung Cancer*. 6, 244-285.

Tsao, M., Aviel-Ronen, S., Ding, K., Lau, D., Liu, N., Sakurada, A., Whitehead, M., Zhu, C., Livingston, R., Johnson, D.H., Rigas, J., Seymour, L., Winton, T., Shepherd, F.A., 2007. Prognostic and Predictive Importance of p53 and RAS for Adjuvant Chemotherapy in Non-Small-Cell Lung Cancer. *Journal of Clinical Oncology*. 25, 5240-5247.

Tse, C., Shoemaker, A.R., Adickes, J., Anderson, M.G., Chen, J., Jin, S., Johnson, E.F., Marsh, K.C., Mitten, M.J., Nimmer, P., Roberts, L., Tahir, S.K., Xiao, Y., Yang, X.,

- Zhang, H., Fesik, S., Rosenberg, S.H., Elmore, S.W., 2008. ABT-263: a potent and orally bioavailable Bcl-2 family inhibitor. *Cancer Research*. 68, 3421-3428.
- Tsim, S., O'Dowd, C.A., Milroy, R., Davidson, S., 2010. Staging of non-small cell lung cancer (NSCLC): a review. *Respiratory Medicine*. 104, 1767-1774.
- Tsutsumi, Y., Serizawa, A., Kawai, K., 1995. Enhanced polymer one-step staining (EPOS) for proliferating cell nuclear antigen (PCNA) and Ki-67 antigen: application to intra-operative frozen diagnosis. *Pathology International*. 45, 108-115.
- Tuominen, V.J., Ruotoistenmaki, S., Viitanen, A., Jumppanen, M., Isola, J., 2010. ImmunoRatio: a publicly available web application for quantitative image analysis of estrogen receptor (ER), progesterone receptor (PR), and Ki-67. *Breast Cancer Research : BCR*. 12, R56.
- Twiddy, D., Naik, S., Mistry, R., Edwards, J., Walker, R.A., Cohen, G.M. and MacFarlane, M. (2010) A TRAIL-R1-selective Ligand selectively targets Primary Breast Tumour cells for Apoptosis. *Breast Cancer Res.*, 12 (Suppl 1): 17-18. Poster abstract only.
- Vaira, V., Fedele, G., Pyne, S., Fasoli, E., Zadra, G., Bailey, D., Snyder, E., Favarsani, A., Coggi, G., Flavin, R., Bosari, S., Loda, M., 2010. Preclinical model of organotypic culture for pharmacodynamic profiling of human tumors. *Proceedings of the National Academy of Sciences of the United States of America*. 107, 8352-8356.
- van der Kuip, H., Murdter, T.E., Sonnenberg, M., McClellan, M., Gutzeit, S., Gerteis, A., Simon, W., Fritz, P., Aulitzky, W.E., 2006. Short term culture of breast cancer tissues to study the activity of the anticancer drug taxol in an intact tumor environment. *BMC Cancer*. 6, 86.
- van Hennik, M.B., van der Vijgh, W.J., Klein, I., Elferink, F., Vermorken, J.B., Winograd, B., Pinedo, H.M., 1987. Comparative pharmacokinetics of cisplatin and three analogues in mice and humans. *Cancer Research*. 47, 6297-6301.
- Vansteenkiste, J., Solomon, B., Boyer, M., Wolf, J., Miller, N., Di Scala, L., Pylvaenaenen, I., Petrovic, K., Dimitrijevic, S., Anrys, B., Laack, E., 2011. Everolimus in combination with pemetrexed in patients with advanced non-small cell lung cancer previously treated with chemotherapy: a phase I study using a novel, adaptive Bayesian dose-escalation model. *Journal of Thoracic Oncology : Official Publication of the International Association for the Study of Lung Cancer*. 6, 2120-2129.
- Vermorken, J.B., van der Vijgh, W.J., Klein, I., Gall, H.E., Pinedo, H.M., 1982. Pharmacokinetics of free platinum species following rapid, 3-hr and 24-hr infusions of cis-diamminedichloroplatinum (II) and its therapeutic implications. *European Journal of Cancer & Clinical Oncology*. 18, 1069-1074.
- Vescio, R.a., Connors, K.M., Kubota, T., Hoffman, R.M., 1991. Correlation of histology and drug response of human tumors grown in native-state three-dimensional histoculture and in nude mice. *Proceedings of the National Academy of Sciences of the United States of America*. 88, 5163-5166.
- Vescio, R.a., Redfern, C.H., Nelson, T.J., Ugoretz, S., Stern, P.H., Hoffman, R.M., 1987. In vivo-like drug responses of human tumors growing in three-dimensional gel-supported primary culture. *Proceedings of the National Academy of Sciences of the United States of America*. 84, 5029-5033.

- Vescio, R.A., Connors, K.M., Youngkint, T., Bordint, G.M., Robbo, J.A., Umbreit, J.A.Y.N., li, R.M.H., 1990. Cancer biology for individualized therapy: Correlation of growth fraction index in native-state histoculture with tumor grade and stage. *Proceedings of the National Academy of Sciences of the United States of America*. 87, 691-695.
- Vivanco, I. & Sawyers, C.L., 2002. The phosphatidylinositol 3-Kinase AKT pathway in human cancer. *Nature Reviews.Cancer*. 2, 489-501.
- Vlahos, C.J., Matter, W.F., Hui, K.Y., Brown, R.F., 1994. A specific inhibitor of phosphatidylinositol 3-kinase, 2-(4-morpholinyl)-8-phenyl-4H-1-benzopyran-4-one (LY294002). *The Journal of Biological Chemistry*. 269, 5241-5248.
- Vogler, M., Dinsdale, D., Dyer, M.J., Cohen, G.M., 2009. Bcl-2 inhibitors: small molecules with a big impact on cancer therapy. *Cell Death and Differentiation*. 16, 360-367.
- Voortman, J., Resende, T.P., Abou El Hassan Mohamed a I, Giaccone, G., Kruyt, F.a.E., 2007. TRAIL therapy in non-small cell lung cancer cells: sensitization to death receptor-mediated apoptosis by proteasome inhibitor bortezomib. *Molecular Cancer Therapeutics*. 6, 2103-2112.
- Walczak, H., Miller, R.E., Ariail, K., Gliniak, B., Griffith, T.S., Kubin, M., Chin, W., Jones, J., Woodward, A., Le, T., Smith, C., Smolak, P., Goodwin, R.G., Rauch, C.T., Schuh, J.C., Lynch, D.H., 1999. Tumoricidal activity of tumor necrosis factor-related apoptosis-inducing ligand in vivo. *Nature Medicine*. 5, 157-163.
- Walters, S., Maringe, C., Coleman, M.P., Peake, M.D., Butler, J., Young, N., Bergstrom, S., Hanna, L., Jakobsen, E., Kolbeck, K., Sundstrom, S., Engholm, G., Gavin, A., Gjerstorff, M.L., Hatcher, J., Johannesen, T.B., Linklater, K.M., McGahan, C.E., Steward, J., Tracey, E., Turner, D., Richards, M.A., Rachet, B., ICBP Module 1 Working Group, 2013. Lung cancer survival and stage at diagnosis in Australia, Canada, Denmark, Norway, Sweden and the UK: a population-based study, 2004-2007. *Thorax*. 68, 551-564.
- Warth, A., Cortis, J., Soltermann, A., Meister, M., Budczies, J., Stenzinger, A., Goepfert, B., Thomas, M., Herth, F.J., Schirmacher, P., Schnabel, P.A., Hoffmann, H., Dienemann, H., Muley, T., Weichert, W., 2014. Tumour cell proliferation (Ki-67) in non-small cell lung cancer: a critical reappraisal of its prognostic role. *British Journal of Cancer*. 111, 1222-1229.
- Weir, B.a., Woo, M.S., Getz, G., Perner, S., Ding, L., Beroukhir, R., Lin, W.M., Province, M.a., Kraja, A., Johnson, L.a., Shah, K., Sato, M., Thomas, R.K., Barletta, J.a., Borecki, I.B., Broderick, S., Chang, A.C., Chiang, D.Y., Chirieac, L.R., Cho, J., Fujii, Y., Gazdar, A.F., Giordano, T., Greulich, H., Hanna, M., Johnson, B.E., Kris, M.G., Lash, A., Lin, L., Lindeman, N., Mardis, E.R., McPherson, J.D., Minna, J.D., Morgan, M.B., Nadel, M., Orringer, M.B., Osborne, J.R., Ozenberger, B., Ramos, A.H., Robinson, J., Roth, J.a., Rusch, V., Sasaki, H., Shepherd, F., Sougnez, C., Spitz, M.R., Tsao, M., Twomey, D., Verhaak, R.G.W., Weinstock, G.M., Wheeler, D.a., Winckler, W., Yoshizawa, A., Yu, S., Zakowski, M.F., Zhang, Q., Beer, D.G., Wistuba, I.I., Watson, M.a., Garraway, L.a., Ladanyi, M., Travis, W.D., Pao, W., Rubin, M.a., Gabriel, S.B., Gibbs, R.a., Varmus, H.E., Wilson, R.K., Lander, E.S., Meyerson, M., 2007. Characterizing the cancer genome in lung adenocarcinoma. *Nature*. 450, 893-898.

Wiley, S.R., Schooley, K., Smolak, P.J., Din, W.S., Huang, C.P., Nicholl, J.K., Sutherland, G.R., Smith, T.D., Rauch, C., Smith, C.A., 1995. Identification and characterization of a new member of the TNF family that induces apoptosis. *Immunity*. 3, 673-682.

Wilhelm, S.M., Carter, C., Tang, L., Wilkie, D., McNabola, A., Rong, H., Chen, C., Zhang, X., Vincent, P., McHugh, M., Cao, Y., Shujath, J., Gawlak, S., Eveleigh, D., Rowley, B., Liu, L., Adnane, L., Lynch, M., Auclair, D., Taylor, I., Gedrich, R., Voznesensky, A., Riedl, B., Post, L.E., Bollag, G., Trail, P.A., 2004. BAY 43-9006 Exhibits Broad Spectrum Oral Antitumor Activity and Targets the RAF/MEK/ERK Pathway and Receptor Tyrosine Kinases Involved in Tumor Progression and Angiogenesis. *Cancer Research*. 64, 7099-7109.

Wyllie, A.H., Kerr, J.F., Currie, A.R., 1980. Cell death: the significance of apoptosis. *International Review of Cytology*. 68, 251-306.

Yap, T.A., Yan, L., Patnaik, A., Fearen, I., Olmos, D., Papadopoulos, K., Baird, R.D., Delgado, L., Taylor, A., Lupinacci, L., Riisnaes, R., Pope, L.L., Heaton, S.P., Thomas, G., Garrett, M.D., Sullivan, D.M., de Bono, J.S., Tolcher, A.W., 2011. First-in-man clinical trial of the oral pan-AKT inhibitor MK-2206 in patients with advanced solid tumors. *Journal of Clinical Oncology: Official Journal of the American Society of Clinical Oncology*. 29, 4688-4695.

Yeh, T.C., Marsh, V., Bernat, B.A., Ballard, J., Colwell, H., Evans, R.J., Parry, J., Smith, D., Brandhuber, B.J., Gross, S., Marlow, A., Hurley, B., Lyssikatos, J., Lee, P.A., Winkler, J.D., Koch, K., Wallace, E., 2007. Biological characterization of ARRY-142886 (AZD6244), a potent, highly selective mitogen-activated protein kinase kinase 1/2 inhibitor. *Clinical Cancer Research: An Official Journal of the American Association for Cancer Research*. 13, 1576-1583.

Yokoyama, T., Kondo, M., Goto, Y., Fukui, T., Yoshioka, H., Yokoi, K., Osada, H., Imaizumi, K., Hasegawa, Y., Shimokata, K., Sekido, Y., 2006. EGFR point mutation in non-small cell lung cancer is occasionally accompanied by a second mutation or amplification. *Cancer Science*. 97, 753-759.

Yoshimasu, T., Oura, S., Hirai, I., Kokawa, Y., Okamura, Y., Furukawa, T., 2005. [Dose response curve of paclitaxel measured by histoculture drug response assay]. *Gan to Kagaku Ryoho [Japanese Journal of Cancer & Chemotherapy]*. 32, 497-500.

Yoshimasu, T., Oura, S., Hirai, I., Kokawa, Y., Sasaki, R., Honda, K., Tanino, H., Sakurai, T., Okamura, Y., 2003. [Histoculture drug response assay (HDRA) guided induction concurrent chemoradiotherapy for mediastinal node-positive non-small cell lung cancer]. *Gan to Kagaku Ryoho [Japanese Journal of Cancer & Chemotherapy]*. 30, 231-235.

Yoshimasu, T., Oura, S., Hirai, I., Tamaki, T., Kokawa, Y., Hata, K., Ohta, F., Nakamura, R., Kawago, M., Tanino, H., Okamura, Y., Furukawa, T., 2007. Data acquisition for the histoculture drug response assay in lung cancer. *The Journal of Thoracic and Cardiovascular Surgery*. 133, 303-308.

Zarogoulidis, K., Zarogoulidis, P., Darwiche, K., Boutsikou, E., Machairiotis, N., Tsakiridis, K., Katsikogiannis, N., Kougioumtzi, I., Karapantzos, I., Huang, H., Spyrtatos, D., 2013. Treatment of non-small cell lung cancer (NSCLC). *Journal of Thoracic Disease*. 5, S389-S396.

Zayed, A., Shoeib, T., Taylor, S.E., Jones, G.D.D., Thomas, A.L., Wood, J.P., Reid, H.J., Sharp, B.L., 2011. Determination of Pt–DNA adducts and the sub-cellular distribution of Pt in human cancer cell lines and the leukocytes of cancer patients, following mono- or combination treatments, by inductively-coupled plasma mass spectrometry. *International Journal of Mass Spectrometry*. 307, 70-78.

Zhang, X.C., Zhang, J., Li, M., Huang, X.S., Yang, X.N., Zhong, W.Z., Xie, L., Zhang, L., Zhou, M., Gavine, P., Su, X., Zheng, L., Zhu, G., Zhan, P., Ji, Q., Wu, Y.L., 2013. Establishment of patient-derived non-small cell lung cancer xenograft models with genetic aberrations within EGFR, KRAS and FGFR1: useful tools for preclinical studies of targeted therapies. *Journal of Translational Medicine*. 11, 168-5876-11-168.

Zhong, H., Sanchez, C., Spitzner, D., Plambeck-Suess, S., Gibbs, J., Hawkins, W.G., Denardo, D., Gao, F., Pufahl, R.a., Lockhart, A.C., Xu, M., Linehan, D., Weber, J., Wang-Gillam, A., 2013. Synergistic effects of concurrent blockade of PI3K and MEK pathways in pancreatic cancer preclinical models. *PLoS One*. 8, e77243.

Zhou, W., Ercan, D., Chen, L., Yun, C.H., Li, D., Capelletti, M., Cortot, A.B., Chirieac, L., Iacob, R.E., Padera, R., Engen, J.R., Wong, K.K., Eck, M.J., Gray, N.S., Janne, P.A., 2009. Novel mutant-selective EGFR kinase inhibitors against EGFR T790M. *Nature*. 462, 1070-1074.

Zhou, Y., Rideout, W.M., 3rd, Zi, T., Bressel, A., Reddypalli, S., Rancourt, R., Woo, J.K., Horner, J.W., Chin, L., Chiu, M.I., Bosenberg, M., Jacks, T., Clark, S.C., Depinho, R.A., Robinson, M.O., Heyer, J., 2010. Chimeric mouse tumor models reveal differences in pathway activation between ERBB family- and KRAS-dependent lung adenocarcinomas. *Nature Biotechnology*. 28, 71-78.

Zou, Z.Q., Zhang, L.N., Wang, F., Bellenger, J., Shen, Y.Z., Zhang, X.H., 2012. The novel dual PI3K/mTOR inhibitor GDC-0941 synergizes with the MEK inhibitor U0126 in non-small cell lung cancer cells. *Molecular Medicine Reports*. 5, 503-508.